

COSMOLOGY AND GRAVITATIONAL PHYSICS

The British Council
The Goethe Institute
Aristoteleion University of Thessaloniki
School of Physics
Astronomy Department

Editors:
Nikolaos K. Spyrou
Nikolaos Stergioulas
Christos Tsagas

THESSALONIKI 2006

Printed by

ΠΕΡΙΕΧΟΜΕΝΑ

	<i>Σελ. Page</i>
Πρόλογος	5
Κατάλογος Ομιλητών	7
Πρόγραμμα	9
Έναρξη	11
Ομιλίες	21
Επίλογος	185

CONTENTS

Preface
List of Speakers
Programme
Inaugural Ceremony
Talks
An Epilogue

ΠΡΟΛΟΓΟΣ

Κατά το διήμερο 15 και 16 Δεκεμβρίου 2005 του διεθνούς έτους Φυσικής-Einstein, το Εργαστήριο Αστρονομίας, σε συνεργασία με το Τμήμα Φυσικής της Σχολής Θετικών Επιστημών του Αριστοτέλειου Πανεπιστημίου και τα μορφωτικά ιδρύματα *British Council* και *Goethe Institut*, διοργάνωσε στην Θεσσαλονίκη το διεθνές εργασιακό συνέδριο με τίτλο *Cosmology and Gravitational Physics*. Το συνέδριο αυτό μπορεί να θεωρηθεί ως η τελευταία συνεισφορά-εκδήλωση του Τμήματος Φυσικής, μέσω του Εργαστηρίου Αστρονομίας, στους εορτασμούς του έτους Φυσικής-Einstein 2005, και έχει ως αντικειμενικό σκοπό την υποβοήθηση της πραγματοποίησης των μεταπτυχιακών σκοπών του Τμήματος Φυσικής με παρουσίαση διαλέξεων πρώτης γραμμής ενδιαφέροντος από Έλληνες, Βρετανούς και Γερμανούς ομιλητές. Ο ανά χείρας τόμος περιλαμβάνει τα πρακτικά του συνεδρίου αυτού.

Θεωρούμε υποχρέωσή μας να απευθύνουμε και από την θέση αυτή θερμές ευχαριστίες προς το Βρετανικό Συμβούλιο, το Ινστιτούτο Γκαίτε, τον Τομέα Αστροφυσικής, Αστρονομίας και Μηχανικής και το Τμήμα Φυσικής για την ουσιαστική συνεισφορά τους στον προγραμματισμό του συνεδρίου και την έκδοση των πρακτικών που περιλαμβάνονται σ' αυτόν τον τόμο.

Επίσης, ευχαριστούμε τους συναδέλφους μας στο Εργαστήριο Αστρονομίας, στον Τομέα Αστροφυσικής, Αστρονομίας και Μηχανικής και στο Τμήμα Φυσικής και τους συνεργαζόμενους μ' αυτούς νεότερους ερευνητές- ομιλητές, όπως και όλους τους εκτός Τμήματος Φυσικής ομιλητές για την πρόθυμη συμμετοχή τους στο συνέδριο.

Τέλος, επιθυμούμε να ευχαριστήσουμε την κ. Α. Τουλούμη για την βοήθειά της στην οργάνωση του συνεδρίου και την προετοιμασία αυτών των πρακτικών.

Θεσσαλονίκη, Δεκέμβριος 2006

Τα Μέλη της Επιστημονικής-Οργανωτικής Επιτροπής

Νικόλαος Κ. Σπύρου
Νικόλαος Χ. Στεργιούλας
Χρίστος Γ. Τσάγκας

KATAΛΟΓΟΣ ΟΜΙΛΗΤΩΝ-LIST OF SPEAKERS

<i>Barrow, J.</i>	DAMTP, Cambridge
<i>Challinor, A.</i>	Cavendish Laboratory, Cambridge
<i>Cotsakis, S.</i>	University of the Aegean
<i>Isliker, H.</i>	Aristoteleion University of Thessaloniki
<i>Kleidis, K.</i>	Aristoteleion University of Thessaloniki
<i>Kokkotas, K.</i>	Aristoteleion University of Thessaloniki
<i>Kouiroukidis, A.</i>	Aristoteleion University of Thessaloniki
<i>Nicolaidis, A.</i>	Aristoteleion University of Thessaloniki
<i>Papadopoulos, D.</i>	Aristoteleion University of Thessaloniki
<i>Paschalidis, V.</i>	University of Chicago
<i>Passamonti, A.</i>	Aristoteleion University of Thessaloniki
<i>Perivolaropoulos, L.,</i>	University of Ioannina
<i>Schaefer, G.</i>	University of Jena
<i>Siopis, Ch.</i>	University Libre de Bruxells
<i>Spyrou, N.K.</i>	Aristoteleion University of Thessaloniki
<i>Stavridis, A.</i>	Aristoteleion University of Thessaloniki
<i>Stergioulas, N.</i>	Aristoteleion University of Thessaloniki
<i>Tsagas, Ch.</i>	Aristoteleion University of Thessaloniki
<i>Tsinganos, K.</i>	National and Kapodistrian University of Athens
<i>Varvoglis, H.</i>	Aristoteleion University of Thessalonik
<i>Vlahos, L.</i>	Aristoteleion University of Thessaloniki

PROGRAMME

DAY 1 (Thursday, 15 December 2005)

Morning Session

- 09.30 - 10.00 *Welcome Ceremony* *AUTh, BC, and GI authorities*
- 10.00 -10.30 *ESA and Greece* *K. Tsinganos*
- 10.30 -11.00 *Coffee Break*
- 11.00 -12.00 *Probing Fundamental Physics with the CMB* *A. Challinor*
- 12.00 -13.00 *Large-Scale Cosmological Structures: A New Look* *N.K. Spyrou*
- 13.00 -15.30 *Lunch Break*

Afternoon Session

- 15.30 -16.00 *Magnetised Particle Dynamics in the Presence of Gravitational Waves* *L. Vlahos*
- 16.00 -16.30 *Exploring the Universe on the Back of a Gravitational Wave*
D. Papadopoulos
- 16.30 -17.00 *Stellar Dynamics in Scalar-Tensor Gravity* *K. Kokkotas*
- 17.00 -17.30 *Tea Break*
- 17.30 -18.00 *Cosmological Gravito-Magnetic Dynamos* *C. Tsagas*
- 18.00 -18.20 *Nonlinear Interaction of Gravitational Waves with Strongly Magnetized Plasmas* *H. Isliker*
- 18.20 -18.40 *Introducing Interactive Quadratic Gravity* *K. Kleidis*
- 18.40 -19.00 *MHD Modes of Magnetized Plasmas in Cosmology* *A. Kouroukidis*

DAY 2 (Friday, 16 December 2005)

Morning Session

- 09.00 -10.00 *Analytical Treatment of the Motions of Compact Binaries* G. Schaefer
- 10.00 -11.00 *Future Singularities and Completeness in Cosmology* S. Cotsakis
- 11.00 -11.30 Coffee Break
- 11.30 -12.30 *Cosmological Aspects of Varying Constants* J. Barrow
- 12.30 -13.30 *Repulsive Gravity and the Accelerating Universe* L. Perivolaropoulos
- 13.30 -15.30 Lunch Break

Afternoon Session

- 15.30 -16.00 *Aspects of Strong Gravity Physics* A. Nicolaidis
- 16.00 -16.30 *Modern Solar System Dynamics and the History of the Solar System* H. Varvoglis
- 16.30 -17.00 *Rotational Instabilities in Supermassive Stars: A New Way to Form Supermassive Black Holes* N. Stergioulas
- 17.00 -17.30 Tea Break
- 17.30 -17.50 *Coupling of Radial and Axial Non-Radial Oscillations of Compact Stars: Gravitational Waves From First-order Differential Rotation* A. Passamonti
- 17.50 -18.10 *Gravitational Waves From Tidal Interactions Between Black Holes and Neutron Stars* A. Stavridis
- 18.30-18.50 *Reliability of Supermassive Black Hole Mass Determinations from Stellar Dynamics* Ch. Siopis
- 18.10 -18.30 *Well-Posedness of the Cauchy Problem in 3+1 GR* V. Paschalidis
- 18.50 -19.00 *An Epilogue*
- 20.00 - *Goodbye Dinner*

ΕΝΑΡΧΗ - ΙΝΑΥΓΟΥΡΑΛ ΚΕΡΕΜΟΝΥ

*Εισαγωγή από τον Πρόεδρο της Οργανωτικής-Επιστημονικής Επιτροπής
Καθηγητή κ. Νικόλαο Κ. Σπύρου*

Αξιότιμε Κύριε Κοσμήτορα της ΣΘΕ,
Αξιότιμε Κύριε Πρόεδρε του Τμήματος Φυσικής,
Αξιότιμε Κύριε Διευθυντά του Τομέα Αστροφυσικής, Αστρονομίας και
Μηχανικής,
Αξιότιμοι Κύριοι Εκπρόσωποι του Βρετανικού Συμβουλίου Ελλάδας,
Αξιότιμοι Κύριοι Εκπρόσωποι του Ινστιτούτου Γκαίτε,
Κύριες και Κύριοι Συνάδελφοι,
Κύριες και Κύριοι,
Αγαπητές Φοιτήτριες, Αγαπητοί Φοιτητές, Μεταπτυχιακοί και Προπτυχιακοί

Καλημέρα σας,

Σας ευχαριστώ για την παρουσία σας εδώ σήμερα με την ευκαιρία αυτού του Εργασιακού Συνεδρίου, εκδήλωσης του Τμήματος Φυσικής του Πανεπιστημίου μας. Αυτή η εκδήλωση μπορεί να θεωρηθεί ως η τελευταία συνεισφορά του Τμήματος, μέσω του Εργαστηρίου Αστρονομίας, στους εορτασμούς του έτους Φυσικής- Einstein 2005.

Είναι ιδιαίτερη η ευχαρίστησή μου να καλωσορίσω όλους τους ομιλητές και ιδιαίτερα τους εκτός Θεσσαλονίκης και εκτός Ελλάδος συναδέλφους και να τους ευχαριστήσω για την άμεση και θετική ανταπόκρισή τους στην πρόσκλησή μας για συμμετοχή τους στο Συνέδριο αυτό, όπως και αυτούς, που δεν είναι λίγοι, οι οποίοι από μακριά συμμετέχουν με βάση τα θερμά μηνύματά τους.

Το Συνέδριο οργανωτικά βασίσθηκε στην από πολλών ετών συνεργασία του Εργαστηρίου Αστρονομίας και του Βρετανικού Συμβουλίου και συμπληρώθηκε από την άμεση ανταπόκριση του Ινστιτούτου Göthe της πόλης μας για επίσης συμμετοχή του. Συνεπώς, το Εργαστηριακό Συνέδριο αποτελεί μια πρώτης τάξεως ευκαιρία για να έλθουν σε επιστημονική επαφή Βρετανοί και Γερμανοί επιστήμονες με Έλληνες συναδέλφους τους και με αντικειμενικό σκοπό να δώσουν μια σειρά διαλέξεων προς τους μεταπτυχιακούς κυρίως, αλλά όχι μόνον, φοιτητές μας, βοηθώντας με τον τρόπο αυτό και προάγοντας τους διδακτικούς μεταπτυχιακούς σκοπούς του Τμήματος Φυσικής.

Η πραγματοποίηση του Συνεδρίου έγινε κατ' αρχήν δυνατή με βάση την οικονομική κάλυψη δύο Βρετανών συναδέλφων από το Βρετανικό Συμβούλιο και ενός από τα Ινστιτούτο Göthe.

Θεωρώ, λοιπόν, υποχρέωση μου, εκ μέρους της Επιστημονικής-Οργανωτικής Επιτροπής του Συνεδρίου αλλά και εκ μέρους του Εργαστηρίου Αστρονομίας, να ευχαριστήσω θερμά το Βρετανικό Συμβούλιο στο πρόσωπο του κ^{ov} James Carmichael, Deputy Country Examinations Manager του Βρετανικού Συμβουλίου. Ιδιαίτερος θέλω να ευχαριστήσω τις Επιστημονικές Υπευθύνους του Βρετανικού Συμβουλίου, κ^α Χρυσούλα Μελίδου του Γραφείου Θεσσαλονίκης και της κα Αναστασία Ανδρίτσου του Γραφείου Αθηνών, και για τον χρόνο και το συναίσθημα που αφιέρωσαν για το Συνέδριο αλλά και για αυτήν την συνεισφορά τους, για μία ακόμη φορά, στους μεταπτυχιακούς αντικειμενικούς σκοπούς του Τμήματος Φυσικής.

Στο πρόσωπο του Γενικού Διευθυντή του, κ^{ov} Karl-Heinz Thalmann, απευθύνω θερμές ευχαριστίες προς το Ινστιτούτο Γκαίτε Θεσσαλονίκης για την άμεση ανταπόκρισή του για συμμετοχή και οικονομική ενίσχυση του Συνεδρίου, στο πλαίσιο

των εορτασμών εφέτος για τα πεντηκοστά γενέθλια του Ινστιτούτου Γκαίτε Θεσσαλονίκης. Η συνεργασία της Επιστημονικής-Οργανωτικής Επιτροπής του Συνεδρίου με τον ίδιο και με την Υπεύθυνη Πολιτιστικού Προγράμματος του Ινστιτούτου Γκαίτε, κα Christina Biermann, υπήρξε καθ' όλα αποδοτική.

Τέλος, ευχαριστώ την Επιτροπή Ερευνών του Πανεπιστημίου μας για την οικονομική ενίσχυση του Συνεδρίου.

Ευχαριστώ τους συναδέλφους μου, μέλη ΔΕΠ στο Εργαστήριο Αστρονομίας, στον Τομέα Αστροφυσικής, Αστρονομίας και Μηχανικής και γενικότερα στο Τμήμα Φυσικής, οι οποίοι είναι επιβλέποντες της προδιδακτορικής εργασίας νέων ερευνητών-ομιλητών, διότι απεδέχθησαν την πρόσκλησή μας, ώστε οι ίδιοι αλλά και οι νέοι αυτοί ερευνητές να παρουσιάσουν τμήματα της πρόσφατης ερευνητικής εργασίας τους.

Θεωρώ και εγώ ότι ένα από τα πιο ενδιαφέροντα χαρακτηριστικά αυτού του Συνεδρίου είναι ότι θα μιλήσουν και νέοι επιστήμονες, αφού οι δύο απογευματινές συνεδριάσεις είναι αφιερωμένες σε υποψήφιους διδάκτορες και σε σχετικά νέους διδάκτορες στα πρώτα επιστημονικά βήματά τους. Ελπίζω ότι η παρουσία τους ενώπιον ενός διεθνούς ακροατηρίου ειδικών θα είναι μία ακόμη αποδοτική εμπειρία τους. Εξάλλου είναι γνωστό, ότι ο πρώτος ωφελούμενος από μια ομιλία είναι ο ίδιος ο ομιλητής, ιδιαίτερα ο νέος.

Οι πανεπιστημιακοί συντελεστές του σημερινού Σεμιναρίου είναι αρκετοί και οι ευχαριστίες προς αυτούς απαραίτητες. Έτσι, επιθυμώ να εκφράσω τις θερμές ευχαριστίες μου προς τον Πρόεδρο του Τμήματος Φυσικής, Καθηγητή κ. Στέργιο Λογοθετίδη (αλλά και τον προηγούμενο Πρόεδρο, Αναπληρωτή Καθηγητή κ. Δημήτριο Κυριάκο), το Διοικητικό Συμβούλιο του Τμήματος Φυσικής και, επίσης, τον Διευθυντή του Τομέα Αστροφυσικής, Αστρονομίας και Μηχανικής, Αναπληρωτή Καθηγητή κ. Α. Βλάχο, διότι αμέσως και με μεγάλη ευχαρίστηση έθεσαν το Σεμινάριο υπό την αιγίδα του Τμήματος και το ενίσχυσαν οικονομικά. Για δε την παντοειδή βοήθειά της προς το Συνέδριο πρέπει να ευχαριστήσω την Επιτροπή Εορτασμού του Έτους Φυσικής 2005, στο πρόσωπο του Προέδρου της, Αναπληρωτή Καθηγητή κ. Οδ. Βαλασιάδη.

Φυσικά, τις θερμές και ειλικρινείς ευχαριστίες μου για την αποδοτική συνεργασία μας, επιθυμώ να απευθύνω, και από αυτήν την θέση, στους συναδέλφους μου - μέλη της Επιστημονικής-Οργανωτικής του Συνεδρίου, και ιδιαίτερος στους δύο νεώτερους, Επίκουρους Καθηγητές κ.κ. Στεργιούλα και Τσάγκα, οι οποίοι επωμίσθηκαν και το μεγαλύτερο οργανωτικό βάρος του Συνεδρίου.

Όπως, ίσως, θα προσέξατε, ότι ο πρώτος ομιλητής του Συνεδρίου, ο συνάδελφος κ. Κανάρης Τσίγκανος, Καθηγητής του Τμήματος Φυσικής του Πανεπιστημίου Αθηνών, δεν θα μιλήσει για κάποιο κοσμολογικό θέμα αλλά για την ήδη αναπτυσσόμενη σχέση της χώρας μας με τον Ευρωπαϊκό Διαστημικό Οργανισμό (European Space Agency). Θεωρήσαμε μια τέτοια ομιλία επιβεβλημένη, με αντικειμενικό, ακριβές, σκοπό τη γενικότερη ενημέρωση για την προώθηση της σύνδεσης της χώρας μας με την ESA. Τον αγαπητό συνάδελφο κ. Τσίγκανο, ο οποίος είναι και Εθνικός Εκπρόσωπος της χώρας μας στην ESA, τον ευχαριστώ ιδιαίτερος για την άμεση αποδοχή της κάπως καθυστερημένης, σε σύγκριση με τους άλλους προσκεκλημένους ομιλητές, πρόσκλησή μας, και, μάλιστα παρά τις αυξημένες υποχρεώσεις του αυτήν την περίοδο, οι οποίες τον ανάγκασαν να κάνει στην Θεσσαλονίκη ένα ταξίδι, στην κυριολεξία, αστραπή.

Η ανταπόκριση των συναδέλφων-μελών ΔΕΠ σ' αυτήν την πρόσκληση συμμετοχής νέων επιστημόνων-ερευνητών επιβεβαιώνει την αναγκαιότητα διοργάνωσης

τέτοιων εκδηλώσεων που βοηθούν το έργο των μεταπτυχιακών τμημάτων. Είναι, πραγματικά, ευκολότερη από ό,τι φαίνεται η διοργάνωση τέτοιων εκδηλώσεων. Αυτό, βέβαια, δεν σημαίνει ότι θα έπρεπε να στηρίζομαστε πάντα στο Βρετανικό Συμβούλιο, και το Ινστιτούτο Γκαίτε, αν και πιστεύω ότι από πλευράς τους η διάθεση κατ' αρχήν συνεργασίας πάντοτε θα υπάρχει. Για μια τέτοια διοργάνωση αρκεί η διάθεση συνεννόησης και συντονισμού, ώστε, π.χ. εναλλακτικά μέσω ορισμένων ερευνητικών προγραμμάτων, να προσκληθεί ένας αριθμός συναδέλφων από το εξωτερικό σε συνδυασμό με ένα αριθμό ομιλητών από την χώρα μας. Στο σημείο αυτό σας θυμίζω, ότι τον Ιανουάριο 1997 το Εργαστήριο Αστρονομίας, το Μεταπτυχιακό Τμήμα Φυσικής Περιβάλλοντος και το Βρετανικό Συμβούλιο συνεργάστηκαν για την οργάνωση ενός ανάλογου σεμιναρίου μεταπτυχιακών διαλέξεων για αστρονομικά-περιβαλλοντικά προβλήματα, το οποίο θετικές εντυπώσεις και ότι, πιο πρόσφατα, μόλις προ διετίας, το Εργαστήριο Αστρονομίας και το Βρετανικό Συμβούλιο συνεργάστηκαν και πάλι για την οργάνωση μιας ενδιαφέρουσας Ημερίδας αναφερόμενης στους πιθανούς κινδύνους από γειτονικά ουράνια σώματα.

Όσον αφορά στο επιστημονικό περιεχόμενο αυτό καθ' εαυτό του σημερινού Σεμιναρίου, οι διαλέξεις των δυο πρωινών συνεδριών αναφέρονται σε σύγχρονα θέματα αστρονομικού-αστροφυσικού - κοσμολογικού ενδιαφέροντος. Εξάλλου, όπως και οι παρουσιάσεις των δυο απογευματινών συνεδριών από τους νέους και ελπιδοφόρους νέους ερευνητές μας, οι πρωινές διαλέξεις εκτείνονται σε πολλά θέματα Κοσμολογίας, Δυναμικής, Ηλιοσφαιρικής Φυσικής, Θεωρητικής Φυσικής, Γενικής Θεωρίας της Σχετικότητας και Σχετικιστικής Αστροφυσικής, όπου τον κυρίαρχο ρόλο παίζει το πεδίο βαρύτητας.

Πάντως, οι Ειδικότερες Θεματικές Περιοχές Διαλέξεων (από αστροφυσικού μέχρι καθαρά μαθηματικού περιεχομένου) περιλαμβάνουν, σε πολύ γενικές γραμμές, 1) *Ιδιότητες και κινήσεις σωμάτων μικρής μάζας, αστρικών ζευγών, αστρικών δυναμικών συστημάτων, κοσμολογικών δομών μεγάλης κλίμακας*, 2) *Διαστολή του Σύμπαντος, απωστική βαρύτητα, κύματα βαρύτητας, κοσμικά μαγνητικά πεδία και αλληλοσυσχετίσεις τους*, 3) *Ακτινοβολία μικροκυμάτων, μαθηματικές ανωμαλίες, μεταβλητές φυσικές σταθερές, έλεγχος θεμελιώδους Φυσικής*. Επομένως, με μια νοηματική ακρίβεια, χαρακτηριστική ενός Φυσικού, μπορεί να πει κανείς, ότι, θέματα σαν κι αυτά συνιστούν την πραγματική συνεισφορά στον Einstein, στο τέλος αυτού του εορταστικού γι' αυτόν έτους. Αυτό πρέπει να επισημανθεί, διότι, ιδίως εντός της χώρας μας, κατά τη διάρκεια αυτού του εορταστικού έτους ακούσαμε πάρα πολλά πράγματα για την Φυσική, αλλά, δυστυχώς, πολύ λιγότερα για τον Einstein και την Σχετικότητα.

Στο τέλος αυτής της Εισαγωγής, θα ήθελα να αναφέρω δύο σημαντικά γεγονότα αναφερόμενα στο Εργαστήριο Αστρονομίας-οργανωτή αυτού του Συνεδρίου. Το πρώτο είναι η βράβευση, με το βραβείο έρευνας Descartes της Ευρωπαϊκής Ένωσης, του συναδέλφου Καθηγητή κ. Ιωάννη-Χίου Σειραδάκη, Καθηγητή Παρατηρησιακής Αστρονομίας, για τη συνεισφορά του, ως μέλους της τετραεθνούς Ομάδας PULSE, στην παρατηρησιακή έρευνα των pulsars. Το δεύτερο είναι η τιμητική πρόσκληση προς τον συνάδελφο κ. Λουκά Βλάχο, Αναπληρωτή Καθηγητή Αστροφυσικής, από τη Διεθνή Αστρονομική Ένωση να συμμετάσχει, ως Reviewer, στις εργασίες της θεματικής ενότητας Cosmic Particle Acceleration: From Solar System to AGNs στην Πράγα τον Αύγουστο του 2006.

Πιστεύω ακράδαντα, ότι αυτά τα δύο γεγονότα αποτελούν απόδειξη της ποιότητας του έργου του επιτελούμενου στο Εργαστήριο Αστρονομίας, έργου που τιμά και τους δυο αγαπητούς συναδέλφους, αλλά και το Εργαστήριο Αστρονομίας και κατ' επέκταση το Τμήμα Φυσικής και το Πανεπιστήμιό μας.

Θεωρώντας ότι εκφράζω ολόκληρο το Εργαστήριο Αστρονομίας, συγχαίρω θερμά και τους δύο συναδέλφους μου και τους εύχομαι και εις ανώτερα.

And now a few words for our non Greek-speaking colleagues and guests.

Dear Colleagues and Guests,

Welcome to Thessaloniki and to our University.

On behalf of the Astronomy Department I wish to thank you for accepting our invitation and for being here with us today.

This Workshop is the last contribution, in a series of analogous contributions, of our Faculty of Physics, through our Astronomy Department, to the celebrations of the Physics-Einstein year 2005.

Also, this Workshop is not an international assembly, not an ambitious symposium, not a summer school; it is only a series of lectures on current, hot cosmological problems, addressed to mainly our post-graduate students, aiming to inform them on the frontiers of the astronomical cosmological science. As a physicist, I can express my strong belief that subjects exactly like the above constitute the real contribution to Einstein at the end of this celebrating year devoted to him and to his work. This has to be pointed out, since, especially in our country, during this celebrating year we heard a lot about Physics, but, unfortunately, only very few about Einstein and Relativity.

I wish to particularly emphasize that all the lecturers accepted immediately our invitation, and this is important if one into considers the various problems each one of them had to overcome. For all the above I thank them all warmly.

Our warm thanks go to the officials of the British Council in Athens and Thessaloniki, and of the Göthe Institut in Thessaloniki for their generous offer in financially supporting the Seminar, and for their kind spirit of collaboration, in both the Athens and the Thessaloniki offices, the Research Committee of our University and the General Secretariat for Research and Technology of the Ministry of Development for their financial support, all the University and the School of Physics authorities, and all my colleagues for their help, spirit of collaboration, contribution, and financial support .

Finally, I wish to recall that, beyond the senior lecturers, also predoctoral students and young Ph.D. holders will present parts of their recent research work in close interaction with the rest of the lecturers and all of you in the audience. I hope they will greatly profit from this interaction. The two afternoon sessions are devoted to our younger scientists-speakers.

I wish to our guests a pleasant stay in our city of Thessaloniki, the capital of Macedonia, Greece, and just before the beginning of the scientific part of the Workshop , I wish to ask the University, the British Council, and the Göthe Institute authorities to address the Workshop.

Πριν από το καθαρά επιστημονικό μέρος του Σεμιναρίου θα ήθελα να παρακαλέσω να απευθύνουν χαιρετισμό ο Πρόεδρος του Τμήματός της, Καθηγητής κ. Στ. Λογοθετίδης, ο Διευθυντής του Τομέα Αστροφυσικής, Αστρονομίας και Μηχανικής, Αναπληρωτής Καθηγητής κ. Λ. Βλάχος, ο κ. James Carmichael, Deputy Country Examinations Manager του Βρετανικού Συμβουλίου και ο κ. Karl-Heinz Thalmann, Γενικός Διευθυντής του Ινστιτούτου Γκαίτε Θεσσαλονίκης και, τέλος, ο Κοσμήτορας της Σχολής Θετικών Επιστημών, Καθηγητής κ. Α. Φιλιππίδης, ο οποίος και παρακαλείται να κηρύξει την έναρξη του Συνεδρίου.

*Χαιρετισμός του Προέδρου του Τμήματος Φυσικής ΣΘΕ/ΑΠΘ
Καθηγητή κ. Σ. Λογοθετίδη*

Αξιότιμοι Κυρίες και Κύριοι, Συνάδελφοι, Αγαπητές Φοιτήτριες, Αγαπητοί Φοιτητές,

Σας καλωσορίζουμε στην τελευταία από τις εκδηλώσεις του Τμήματος Φυσικής και του Πανεπιστημίου μας που οργανώθηκαν στο πλαίσιο του έτους Φυσικής 2005.

Το πλούσιο πρόγραμμα των εκδηλώσεων που οργάνωσε το Τμήμα Φυσικής είχε ως σκοπό να φέρει πλησιέστερα στη Φυσική τους Καθηγητές και τους Φοιτητές του Πανεπιστημίου μας αλλά και την κοινωνία της Βορείου Ελλάδος.

Χωρίς να θέλω να κάνω εδώ έναν απολογισμό, αναφέρω την διοργάνωση πολλών επιστημονικών ομιλιών στο Πανεπιστήμιο μας από συναδέλφους καθηγητές από την Ελλάδα και το εξωτερικό, μεγάλο αριθμό εκλαϊκευτικών ομιλιών και παρουσιάσεων κατά κύριο λόγο σε Γυμνάσια και Λύκεια της Βορείου Ελλάδας αλλά και σε επιστημονικούς και πολιτιστικούς συλλόγους.

Το Τμήμα Φυσικής άνοιξε τα εργαστήριά του και τα αμφιθέατρό του στο κοινό και εκατοντάδες συμπολίτες μας συμμετείχαν σ' αυτή μας την προσπάθεια. Τέλος, διοργανώθηκαν ημερίδες για τη αλληλοσύνδεση της Φυσικής με τις άλλες επιστήμες την Τεχνολογία και την παραγωγή.

Το Τμήμα Φυσικής μέσα από αυτή τη διαδικασία βγαίνει πιο ώριμο όχι μόνο επιστημονικά αλλά και κοινωνικά. Οι σχέσεις που οικοδομήθηκαν με άλλους επιστημονικούς, εκπαιδευτικούς, κοινωνικούς και παραγωγικούς φορείς θα σφυρηλατηθούν ακόμη περισσότερο με το πέρασμα του χρόνου με σκοπό πέραν της επιστημονικής και τη διαρκή συμμετοχή μας στο μορφωτικό και κοινωνικό γίγνεσθαι της Πόλης μας.

Η ημερίδα που ξεκινά σήμερα αποτελεί την τελευταία εκδήλωση για αυτή τη μνημειακή χρονιά. Το 2005 ονομάστηκε Έτος Φυσικής για να τιμηθεί ο πρωτοπόρος και θεμελιωτής της νεώτερης Φυσικής, ο Albert Einstein, του οποίου τα πέντε βασικά άρθρα το 1905 αποτέλεσαν την έναυση για την επανάσταση της Νεώτερης Φυσικής.

Οι εργασίες της ημερίδας αυτής επικεντρώνονται ακριβώς σ' αυτό που έκανε τον Einstein γνωστότερο στον κόσμο, τη Θεωρία της Σχετικότητας. Η Ειδική Θεωρία της Σχετικότητας το 1905 και η Γενική Θεωρία της Σχετικότητας το 1915 αποτελούν τις βασικές θεωρίες που εξηγούν το μακρόκοσμο της καθημερινότητας που ζούμε αλλά και εξηγούν το Σύμπαν που μας περιβάλλει.

Η Κοσμολογία και η Βαρύτητα γενικότερα αποτελούν πεδίο έντονης επιστημονικής έρευνας στις μέρες μας. Μας τροφοδοτούν καθημερινά με νέες και πολλές φορές εξωτικές ανακαλύψεις. Η αντίληψή μας για το Σύμπαν δεν είναι η ίδια με αυτή που μάθαινα όταν εγώ ήμουν φοιτητής αλλά ούτε καν και με αυτά που πιστεύαμε μόλις πέντε χρόνια πριν. Η μαζική ροή πληροφορίας από τα διάφορων τύπων τηλεσκόπια, μας εφοδιάζει καθημερινά με στοιχεία που επιβεβαιώνουν η καταρρίπτουν «χθεσινές» θεωρίες.

Ζούμε σε μια εποχή έντονης κινητικότητας σε ό,τι αφορά την αντίληψή μας για το Σύμπαν και το Τμήμα Φυσικής και ειδικότερα ο Τομέας Αστροφυσικής, Αστρονομίας και Μηχανικής συμμετέχει δυναμικά και πρωτοπόρα στην διεθνή προσπάθεια.

Αγαπητοί συνάδελφοι και φίλοι, περιμένουμε με ενδιαφέρον να παρακολουθήσουμε τα επιστημονικά νέα που φέρνετε και ευχόμαστε Καλή Επιτυχία στο συνέδριό σας και στην επιστημονική σας προσπάθεια.

*Χαιρετισμός του Διευθυντή του Τομέα Αστροφυσικής, Αστρονομίας και Μηχανικής
Αναπληρωτή Καθηγητή κ. Α. Βλάχου*

Dear Guests,
Dear Colleagues,

On behalf of the Section of Astrophysics, Astronomy and Mechanics, I would like to welcome all of you to this workshop, organized by our Department to honor the World Year of Physics.

As you probably know, many members of our Section are working on subjects relevant to the content of this meeting, so they will be speakers or reviewers in the next sessions. In the last years, our Section has taken many steps and made serious efforts to participate actively in research on Astrophysics, General Relativity and Cosmology, Observational Astrophysics and Non Linear Dynamics. Many of the Physics students chose to continue their studies in Astronomy and Astrophysics or Theoretical Physics and after their graduation continue as graduates in some of the world are renown Universities. Astrophysics, Cosmology and General Relativity are top priorities to most ambitious students in our department. A great number of post-doctoral researchers are working in our Section and more than ten research programs are currently conducted.

Recently Greece joined the European Space Agency and opened new paths for active research and Collaborations in a European setting. I believe that in the next years Space Physics will become a new research area for our Section.

I wish you, once again, a very successful meeting and we all hope to see you again in Thessaloniki soon.

*Χαιρετισμός του Deputy Country Examinations Manager
του Βρετανικού Συμβουλίου κ^ο James Carmichael*

Dear Mr Rector

Dear friends from the Physics Department

Esteemed guests,

Ladies and Gentlemen,

It is my great honour to welcome you all on behalf of the British Council and our Director Mr Desmond Lauder to this workshop we organise in collaboration with the Astronomy Department of the School of Physics at the Aristotle University of Thessaloniki.

This is not the first time we are working together with the Astronomy Department in building up an event. In fact our sincere friendship goes back many years ago with a number of very important and successful collaborations. “Possible Hazards from near Earth Objects” was the theme of our most recent collaboration. In this event, five UK specialists were invited to Thessaloniki to present the UK experience and discuss their views with their Greek counterparts in your Department as well as the wider informed audience. I would therefore like to thank the Department of Astronomy for this long lasting friendship, and just express the hope that this relationship has still a lot to offer in the years to come.

*Χαιρετισμός του Γενικού Διευθυντή του Ινστιτούτου Γκαίτε Θεσσαλονίκης
κ^ο Karl-Heinz Thalmann*

Magnificence,
dear Professor Spyrou,
dear participants of the workshop,
ladies and gentlemen,

On behalf of the Goethe-Institute Thessaloniki, I would like to wish you all a warm welcome. It's a great honour and pleasure for me to assist at the opening ceremony of the international scientific workshop „Cosmology and Gravitational Physics“, organized by the department of physics of the Aristoteles University of Thessaloniki in collaboration with the Goethe-Institute and the British Council in the framework of the World Year of Physics 2005.

The German side is represented by Professor Dr. Gerhard Schäfer of the Friedrich-Schiller-University in Jena. Professor Schäfer will arrive in Thessaloniki only in the afternoon, because he had a lecture last evening in Jena and will be present tomorrow.

2005 is the year where we are commemorating 50 years of Albert Einstein's death and 100 years of the publication of his theory of relativity.

The year, Albert Einstein died, was also the year of the foundation of the Goethe-Institute in Thessaloniki which belongs with the Institute in Athens to the oldest and most important ones in the world. And in October this year our Institute celebrated its 50th birthday.

I would like to thank Professor Spyrou and the department of physics for the good cooperation and preparation of the workshop and I wish you all good discussions and success in your work.

Thank you.

Χαιρετισμός του Κοσμήτορα ΣΘΕ/ΑΠΘ Καθηγητή κ. Α. Φιλιππίδη

Dear Chairman of the School of Physics
Mr. Chairman of the Organizing Committee
Dear Colleagues and Students, Ladies and Gentlemen,

It is my honour to welcome you at the Workshop on Cosmology and Gravitational Physics,

Colleagues of the Faculty of Sciences and mainly of the School of Physics, have made substantial efforts, both with national and international activities, to promote issues concerning Cosmology and Gravitational Physics, issues of vital importance to our history and environment.

I would like to express my sincere thanks to the Speakers – Colleagues from Universities of Cambridge, Chicago, Jena and Bruxells, also the Greek colleagues from Aegean University, Universities of Athens, Ioannina and Thessaloniki. My sincere thanks go also to the colleagues of the Department of Astrophysics, Astronomy and Mechanics for organizing this workshop.

Once again, welcome to our Faculty,

With my My best wishes for a successful workshop and for a pleasant stay in our city of the participants outside Thessaloniki, I gladly declare the opening of the Workshop.

Thank you

ΟΜΙΛΙΕΣ - TALKS

THE HELLENIC PARTICIPATION IN THE EUROPEAN SPACE AGENCY (ESA)*

Kanaris Tsinganos

Delegate to the ESA/SPC

Department of Physics, University of Athens

Panepistimiopolis GR-157 84 Zografos, Athens, Greece



1. ESA and Greece

ESA's role is to draw up the European space programme and carry it through. The Agency's projects are designed to find out more about the Earth, its immediate space environment, the solar system and the Universe, as well as to develop satellite-based technologies and services, and to promote European industries. ESA also works closely with space organizations outside Europe to share the benefits of space with the whole of mankind.

ESA was formed in 1975 and has currently 17 Member States : Austria, Belgium, Denmark, Finland, France, Germany, Greece, Ireland, Italy, Luxembourg, the Netherlands, Norway, Portugal, Spain, Sweden, Switzerland and the United Kingdom. Canada, Hungary and the Czech Republic also participate in some projects under cooperation agreements. As it can be seen from this list, not all member countries of the European Union are members of ESA and not all ESA Member States are members of the EU. ESA is an entirely independent organization although it maintains close ties with the EU through an ESA/EU Framework Agreement. The two organizations share a joint European strategy for space and together are developing a European space policy.

Cooperation between ESA and the Hellenic National Space Committee began in the early 1990s and in 1994 Greece signed its first cooperation agreement with ESA. This led to regular exchange of information, the award of fellowships, joint symposia, mutual

* Presented at the Workshop on *Cosmology and Gravitational Physics*, 15-16 December 2005, Thessaloniki, Greece, *Editors*: N. K. Spyrou, N. Stergioulas and C. G. Tsagas.

access to databases and laboratories, and studies on joint projects in fields of mutual interest. In September 2003 Greece formally applied to join ESA. Subsequent negotiations were followed in the summer of 2004 by the signing of an agreement on accession to the ESA Convention by Jean-Jacques Dordain, ESA Director General on behalf of ESA, and by D. Sioufas, the Greek Minister for Development and the Secretary General for Research and Technology Prof. I.Tsoukalas, on behalf of the Greek Government. Greece already participates in ESA's telecommunication and technology activities, and the Global Monitoring for Environment and Security Initiative. Following the ratification of the ESA Convention by the Greek Parliament, Greece has now become ESA's 16th Member State. The official announcement was made to the ESA Council on the 16th of March 2005 by the chairman of the ESA Council. Now, with the deposition of its instrument of ratification of the Convention for the establishment of ESA with the French Government on 9th of March 2005, Greece became the 16th full ESA Member State.

2. Structure of ESA

ESA's headquarters are in Paris (rue Mario Nikis, Cabronne) where policies and programmes are decided upon. In addition, ESA also has several centers in a number of European countries, each one of which has different responsibilities :

- ESTEC, the European Space Research and Technology Centre, the design hub for most ESA spacecraft and technology development, situated in Noordwijk, the Netherlands.
- ESOC, the European Space Operations Centre, responsible for controlling ESA satellites in orbit, situated in Darmstadt, Germany.
- EAC, the European Astronauts Centre, trains astronauts for future missions, situated in Cologne, Germany.
- ESRIN, the ESA Centre for Earth Observation, based in Frascati, near Rome in Italy. Its responsibilities include collecting, storing and distributing Earth Observation satellite data to ESA's partners, and acting as the Agency's information technology centre.

In addition, ESA has liaison offices in Belgium, the United States and Russia, a launch base in French Guiana and ground and tracking stations in various areas of the world. In February 2005 the total number of staff working for ESA numbered approximately 1907. These highly qualified people come from all the Member States and include scientists, engineers, information technology specialists and administrative personnel. Presently there are only a very few staff members of Greek origin working in ESA.

The ESA Council is the Agency's governing body and provides the basic policy guidelines within which the Agency develops the European space programme. Each Member State is represented on the Council and has one vote, regardless of its size or

financial contribution. The Agency is headed by a Director General who is elected by the Council every four years. The present Director General of ESA is Jean-Jacques Dordain.

Each individual research sector has its own Directorate that reports to the Director General. Thus, ESA's activities are divided into nine Directorates, each headed by a Director who reports directly to the Director General. These Directorates are:

- . Science Programmes
- . Earth Observation Programmes
- . Technical and Quality Management
- . Launcher Programmes
- . Human Spaceflight, Microgravity and Exploration Programmes
- . Resources Management
- . External Relations
- . EU and Industrial Programmes
- . Operations and Infrastructure

3. ESA funding

ESA's *mandatory* activities (space science programmes and the general budget) are funded by a financial contribution from all the Agency's Member States, calculated in accordance with each country's gross national product. In addition, ESA conducts a number of *optional* programmes. Individual countries decide in which optional programme they wish to participate and the amount they wish to contribute.

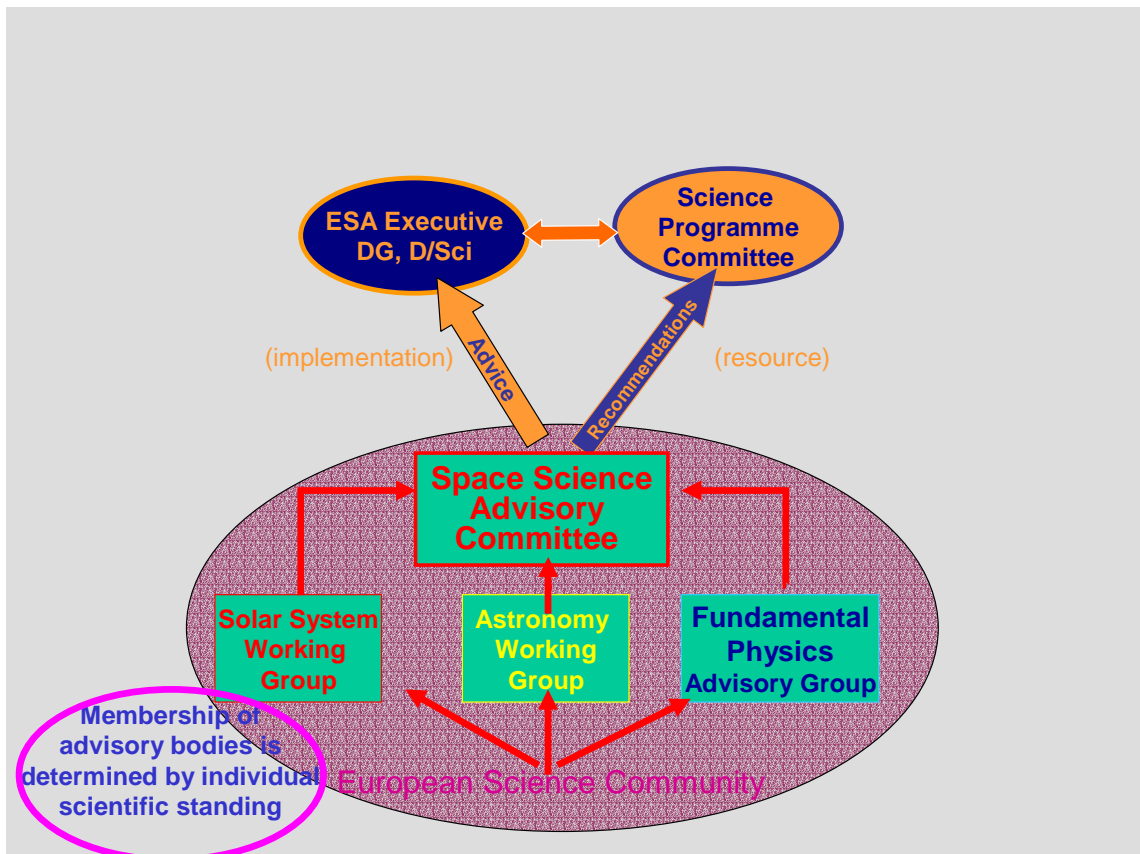
ESA's budget for 2005 was €2977 million. The agency operates on the basis of geographical return, i.e. it invests in each Member State, through industrial contracts for space programmes, an amount more or less equivalent to each country's contribution. The *mandatory* contribution from all member states is 371 million Euros, i.e., every citizen of an ESA Member State pays about 1 Euro per year. Thus, the total European per capita investment in space is very little. On average, every citizen of an ESA Member State pays, in taxes for a total expenditure on space, about the same as the price of a cinema ticket. In the United States, investment in civilian space activities is almost four times as much.

4. The Science Programme of ESA

The Science Programme is the only mandatory element of the ESA programme, and is therefore both a flagship and a symbol for the Agency. It enhances European capability in space science and applications, builds European industrial technical capacity, and brings together European national space programmes. ESA staff and contractors assemble and test new ESA scientific spacecraft at the European Space Research and Technology Centre (ESTEC), Noordwijk (The Netherlands). These will then be operated from ESA's European Space Operations Centre (ESOC) at Darmstadt in Germany. At

ESA headquarters, the Director of Science oversees policy and the overall shape of the science programme. ESA Science staff are also deployed elsewhere, for example in Spain, Germany, and the United States.

The present Director of Science (Programmes) is Prof. David Southwood. The scientific community is represented by three working groups : The Solar System Working Group, the Astronomy Working Group and the Fundamental Physics Advisory Group. Recently, Dr. I. Daglis was invited to become a member of ESA's Solar System Working Group for a period of three years (2006 to 2008). The recommendations of these three groups are finalized by the Space Science Advisory Committee, currently chaired by Prof. G. Bignami, which submits the scientific proposals for their final approval to the Science Programme Committee (SPC). Each Member State is also represented on the SPC with one vote, regardless of its size or financial contribution. The Hellenic Delegate in the SPC is the author of this article with Advisers Dr. V. Tritakis and Prof. Th. Karakostas.



(α) Early ESA missions

In the early period of ESA, 1968-1985, some 15 European spacecraft were launched on scientific missions to study a vast array of disciplines:

- Cosmic rays and solar X-rays (ESRO 1B & 2B) - 1 Oct 1969 and 17 May 1968
- Ionosphere and aurora (ESRO 1A) - 3 Oct 1968
- Solar wind (HEOS-1) - 5 Dec 1968
- Polar magnetosphere (HEOS-2) - 31 Jan 1972
- UV astronomy (TD-1) - 11 March 1972
- Ionosphere and solar particles (ESRO-4) - Nov 1972
- Gamma ray astronomy (COS-B) - 9 Aug 1975
- Magnetosphere (GEOS-1 & 2) - 20 Aug 1977 and 14 Jul 1978
- Magnetosphere and sun-Earth relations (ISEE-2) - 23 Oct 1977
- Ultraviolet astronomy (IUE) - 26 Jan 1978
- Cosmic x-rays (Exosat) - 26 May 1983

More recently, the ESA Giotto probe (launched in 1985) became the first spacecraft ever to meet two comets, Halley (1986) and Grigg-Skjellerup, (1992). Between 1989 (when it was launched) and 1993 the Hipparcos satellite collected data on the positions and movements of a million stars with the respective catalogues published in 1997. The infrared space observatory (ISO) was launched in 1995 and concluded its operation in 1998, giving the first detailed view and spectra of infrared celestial objects.

(β) ESA missions in operation

There are 15 ESA missions in operation today. The Hubble Space Telescope (1990), a long-term, space-based observatory whose observations are carried out in visible, infrared and ultraviolet light. In many ways Hubble has revolutionised modern astronomy, not only by being an efficient tool for making new discoveries, but also by driving astronomical research in general.

Ulysses (1990) developed in collaboration with NASA is the first mission to study the environment of space above and below the poles of the Sun. Its data have given scientists their first look at the variable effect that the Sun has on the space around it.

The solar observatory SoHO (1995) stationed 1.5 million kilometres away from the Earth, constantly watches the Sun, returning spectacular pictures and data of the storms that rage across its surface. SOHO's studies range from the Sun's hot interior, through its visible surface and stormy atmosphere, and out to distant regions where the wind from the Sun battles with a breeze of atoms coming from among the stars. The SOHO mission is a joint ESA/NASA project.

Cassini/Huygens (1997) also in collaboration with NASA is already in the Saturnian system. It will orbit Saturn for four years, making an extensive survey of the ringed planet and its moons. The ESA Huygens probe landed in January 2005 on the surface of

Titan, Saturn's largest moon. Data from Cassini and Huygens are offering us clues about how life began on Earth.

XMM-Newton (1999), the biggest science satellite ever built in Europe with its telescope mirrors are the most sensitive ever developed in the world, is detecting more X-ray sources than any previous satellite and is helping to solve many cosmic mysteries of the violent Universe, from what happens in and around black holes to the formation of galaxies in the early Universe. It is designed and built to return data for at least a decade.

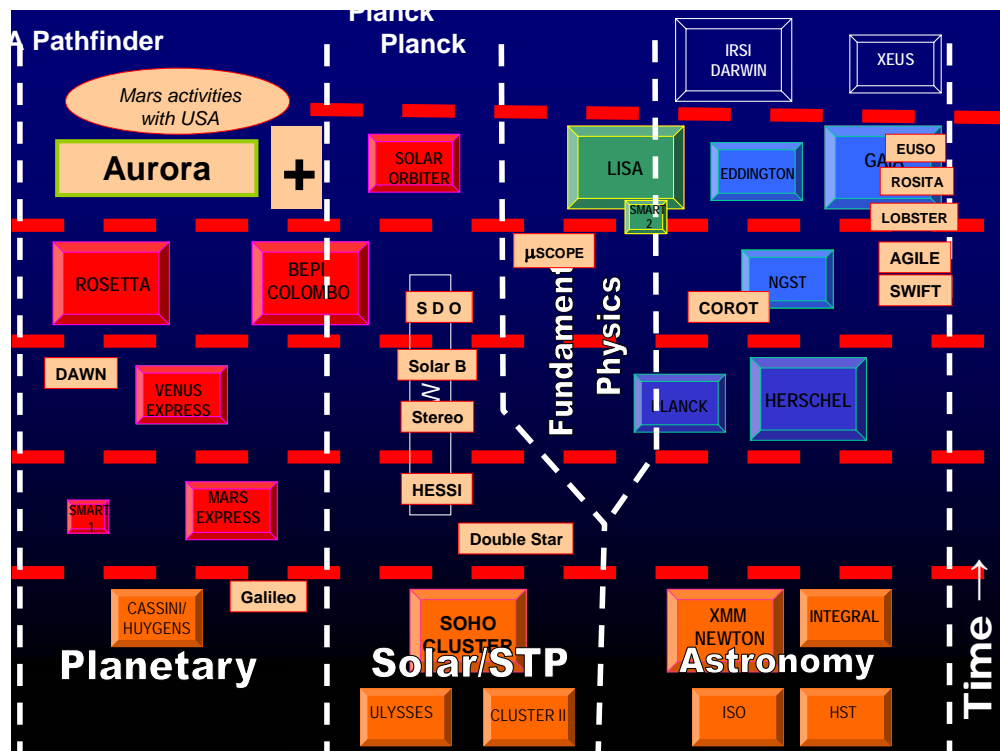
The second high-energy observatory is Integral (2002), observing a cosmos, full of violent phenomena and extreme energy in the γ -rays.

The mission Cluster (2000) is a collection of four spacecrafts flying in formation around Earth. They, in combination with the Double – Star (2003/2004) developed in collaboration with China, give us a stereoscopic view of the terrestrial magnetosphere and its interaction with the solar wind and relay the most detailed ever information about how the solar wind affects our planet in three dimensions. The solar wind can damage communications satellites and power stations on Earth. The original operation life-time of the Cluster mission ran from February 2001 to December 2005. However, in February 2005, ESA approved a mission extension from December 2005 to December 2009.

Mars Express (2003), Venus Express (2005) and SMART-1, (2003) are the first missions to our neighbouring planets and the moon. The SMART-1 mission in orbit around the Moon has had its scientific lifetime extended by ingenious use of its solar-electric propulsion system (or 'ion engine').

Finally, Rosetta, (2004) is the first mission ever to land on a comet and follow it in its orbit around the Sun. ESA's Rosetta spacecraft will be the first to undertake the long-term exploration of a comet at close quarters. It comprises a large orbiter, which is designed to operate for a decade at large distances from the Sun, and a small lander. Each of these carries a large complement of scientific experiments designed to complete the most detailed study of a comet ever attempted. After entering orbit around Comet 67P/Churyumov-Gerasimenko in 2014, the spacecraft will release a small lander onto the icy nucleus, then spend the next two years orbiting the comet as it heads towards the Sun. On the way to Comet Churyumov-Gerasimenko, Rosetta will receive gravity assists from Earth and Mars, and fly past main belt asteroids.

(γ) *ESA Missions under development*



5. The future science program of ESA : Cosmic Vision (2015-2025)

Space science is playing a prominent role in Europe’s space programme. It has been the core of European co-operation and success in space since the early 1960s. As ESA turns thirty years old, it continues a tradition of innovative thinking and long-term perspectives that form the basis for ESA's scientific programme. The Horizon 2000 long-term plan for space science, formulated 20 years ago (1984), is almost completed. Its successor, Horizon 2000+, approved ten years ago, comes now to fruition with a wealth of scientific satellites and space telescopes in orbit producing great results. In the first years of this new millennium, ESA is building its future in space science based on a ‘Cosmic Vision’. This is a way of looking ahead, building on a solid past, and working today to overcome the scientific, intellectual and technological challenges of tomorrow.

For this new *Cosmic Vision* programme, the scientific community was called upon to express its new ideas in April 2004 and did so by submitting more than 150 such novel ideas. ESA’s scientific advisory committees and working groups made a preliminary selection of themes, which were discussed in an open Workshop in Paris in September 2004 attended by about 400 members of the scientific and industrial communities. After an iteration with the Science Programme Committee (SPC) and its national delegations, the finally selected themes are addressing the following 4 questions:



1. What are the conditions for planet formation and the emergence of life?

- ***From gas and dust to stars and planets*** : Map the birth of stars and planets by peering into the highly obscured cocoons where they form.
- ***From exo-planets to biomarkers*** : Search for planets around stars other than the Sun, looking for biomarkers in their atmospheres, and image them.
- ***Life and habitability in the Solar system*** : Explore in situ the surface and subsurface of the solid bodies in the solar Systems most likely to host-or have hosted-life. Explore the environmental conditions that makes life possible

Candidate Projects are a Near – Infrared Nulling Interferometer, Mars Landers and Mars Sample Return, Far-Infrared Observatory, Solar Polar Orbiter, Terrestrial Planet Astrometric Surveyor, Europa Landers, Large Optical Interferometer.

2. How does the Solar System work?

- ***From the Sun to the edge of the Solar System***: Study the plasma and magnetic field environment around the Earth and around Jupiter, over the Sun's poles, and out to the Heliopause where the solar wind meets the interstellar medium.

- ***The giant planets and their environments*** : In situ studies of Jupiter, its atmosphere, internal structure and satellites
- ***Asteroids and other small bodies*** : Obtain direct laboratory information by analysing samples from a Near-Earth Object.

Candidate Projects are an Earth Magnetospheric Swarm, Solar Polar Orbiter, Jupiter Exploration Programme, Europa Lander, Orbiter and Jupiter probes, Near – Earth Object Sample Return, Interstellar Heliopause Probe.

3. What are the fundamental physical laws of the Universe?

- ***Explore the limits of contemporary physics*** : Use stable and weightless environment of space to search for tiny deviations from the standard model of fundamental interactions.
- ***The gravitational wave Universe*** : Make a Key step toward detecting the gravitational radiation background generated at the Big Bang.
- ***Matter under extreme conditions*** : Probe gravity theory in the very strong field environment of black holes and other compact objects, and the state of matter at supra-nuclear energies in neutron stars.

Candidate Projects are a Fundamental Physics Explorer Series, Large-Aperture X-ray Observatory, Deep Space Gravity Probe, Gravitational Wave Cosmic Surveyor, Space Detector for Ultra-High–Energy Cosmic Rays.

4. How did the Universe originate and what is it made of?

- ***The early Universe*** : Define the physical processes that led to the inflationary phase in the early Universe, during which a drastic expansion supposedly took place. Investigate the nature and origin of the Dark Energy that is accelerating the expansion of the Universe
- ***The Universe taking shape*** : Find the very first gravitationally-bound structures that were assembled in the Universe-precursors to today’s galaxies, groups and clusters of galaxies-and trace their evolution to the current epoch
- ***The evolving violent Universe*** : Trace the formation and evolution of the supermassive black holes at galaxy centres - in relation to galaxy and star formation – and the life cycles in matter in the Universe along its history

Candidate Projects are a Large-Aperture X-ray Observatory, Wide-Field Optical-Infrared Imager, All-sky Cosmic Microwave Background Polarisation Mapper, Far-Infrared Observatory, Gravitational Wave Cosmic Surveyor, Gamma-Ray Imaging Observatory (Credits: ESA).

6. Opportunities for ESA related science/technology work for Hellenic researchers

a) The first Call for Ideas for Hellenic participation to ESA programmes.

The Accession Agreement of Greece and ESA specifies transitional measures that will apply during a period of six years, starting from the date of accession (i.e., from 2005 to 2010). The transitional measures aim at adapting Greece's industry to the Agency requirements. An ESA-Greece Task Force was set-up in September 2005 which has a programmatic role and advises the Director General of ESA on the implementation of the transitional measures. Representatives from both ESA and the Hellenic Republic compose this Task Force. In the frame of these transitional measures contracts will be placed with Greek firms, institutions and universities. For this purpose the ESA-Greece Task Force has issued a first Call for Ideas¹. The proposal which the Greek community is invited to submit is a relatively simple one with a suggested overall maximum length of only 2-3 pages. The submitted ideas should cover activities that have a future potential in the frame of ESA activities or programmes (no "single-shot" activities will be considered), address specific niche markets (no competitive products available elsewhere in Europe or when a second source would be an asset), provide the resources to enable Greek industry/institutes to enter normal ESA procurement and finally foster the establishment of strong and long-term relations between Greek firms and well-established European space firms. The deadline for the submission was in February 2006.

b) Involvement in future Space missions within Horizon 2000+

Within the Horizon 2000+ programme there is still time for Hellenic scientists to participate in the preparation of several space missions. Such examples are the Herschel/Planck Observatory (launch in 2007, with involvement in the data analysis from one of its three instruments SPIRE, HIFI, PACS, for more information contact V. Charmandaris, Un. of Crete). The mission BepiColombo to the planet Mercury (launch in 2014, for more information contact I. Daglis NOA/ISARS), the astrometric satellite GAIA (launch 2012, for more information contact P. Niarchos or M. Kontizas, Un. of Athens), the mission Solar Orbiter (launch in 2015, for more information contact K. Tsinganos, Un. of Athens) and also the gravitational waves space interferometer LISA (launch 2015, for more information contact K. Kokkotas, AUTH).

c) Predoctoral ESA young graduate trainees (YGT)

ESA's Young Graduate Trainee (YGT) programme² offers recently graduated men and women, a one-year non-renewable training contract designed to give valuable work experience and to prepare for future employment in the space industry and/or research. Applicants should have just completed, or be in their final year, of a higher education course typically at Masters level and probably in a technical or scientific discipline at a university or equivalent institute. They should be fluent in either English or French. Contracts are for one year and non-renewable. ESA will provide a monthly salary. In 2003 the basic net salary for a single YGT ranged from €1930 to €2333 per month, depending on the establishment, including expatriation allowance. Also, a monthly expatriation allowance for those not resident in the country to which they are assigned,

¹ <http://www.astro.auth.gr/elaset/esa/>

² http://www.esa.int/SPECIALS/Careers_at_ESA/

plus an installation allowance upon arrival, travel expenses at the beginning and end of the contract and health cover under ESA's Social Security scheme. Towards the end of the training period, trainees are asked to submit a report on their activities and accomplishments achieved during the year.

d) Postdoctoral ESA research fellowships

ESA's *postdoctoral* research fellowship programmes³ aim to offer young scientists the possibility of carrying out research in a variety of disciplines related to space science, space applications or space technology. The Agency has an *internal* and an *external fellowship programme*, both for two years, with no possibility of an extension. ESA hosts approximately 20 external and 30 internal fellowships at any given time. Applicants must have recently attained their doctorate or be close to successfully completing studies in space science, space applications or techniques, or other fields closely connected to space activities. In the internal fellowship programme, fellows carry out their research topic under the supervision of one or more experienced scientists or engineers in one of the ESA establishments. Interested candidates should submit the *application form* that is available online. There is no specific closing date and applications may be submitted at any time during the year. In the external fellowship programme, the fellows work in a university, research institute or laboratory on a research topic related to the research activities of the Agency. The application should be sent directly to the relevant national delegation, who will forward it to ESA, by 31 March for the June selection and by 30 September for the December selection.

e) IKY fellowships for Space Physics

IKY started in the year 2006 new predoctoral fellowships for studies in the area of Space Physics, within the known frame of fellowships in Astronomy, Astrophysics, Relativity, Physics, etc. We hope that our scientific community will be mobilized to take soon advantage of the Hellenic participation to the Science programmes of ESA. The first indication of such a mobilization will be our response to the *Call for Ideas*. Secondly, we need to pursue a direct involvement in several ESA missions under development (Herschel/Planck, JWST, GAIA, BepiColombo, Solar Orbiter and LISA). As an example, we succeeded to convince ESA to issue an announcement for the employment of Greek software engineers in the upcoming (2007) ESA "cornerstone" Herschel/Planck observatory (see Dec. 2005 issue of the HelAS electronic newsletter). Similarly, Hellenic participation is needed at the level of PI or Co-I in specific mission instruments, or in the direct involvement for the analysis of related observations, in the upcoming ESA programmes. Finally, we should encourage Hellenic young researchers to apply for the various ESA related fellowships in order to get training and serve as links between ESA and the academic, research, industrial and technological sectors of Greece. All in all, it remains to be seen if the adventure of the Hellenic scientific and technological community in European space activities - something dated back thousands of years in mythology with the story of Daedalus and Icarus - will be fruitful and worth of our expectations.

³ http://www.esa.int/SPECIALS/Careers_at_ESA/SEM19DXO4HD_0.html

CONSTRAINING FUNDAMENTAL PHYSICS WITH THE COSMIC MICROWAVE BACKGROUND *

Anthony Challinor[†]

Astrophysics Group, Cavendish Laboratory, J. J. Thomson Avenue,
Cambridge, CB3 0HE, UK

Abstract

The temperature anisotropies and polarization of the cosmic microwave background (CMB) radiation provide a window back to the physics of the early universe. They encode the nature of the initial fluctuations and so can reveal much about the physical mechanism that led to their generation. In this contribution we review what we have learnt so far about early-universe physics from CMB observations, and what we hope to learn with a new generation of high-sensitivity, polarization-capable instruments.

1. Introduction

The cosmic microwave background (CMB) radiation has an almost perfect black-body spectrum with mean temperature 2.725 K (Mather et al 1994). Once corrected for a kinematic dipole due to our motion, the CMB is remarkably isotropic with fluctuations at the 10^{-5} level. These were first detected by the COBE satellite in 1992 (Smoot et al 1992) and have now been measured over three decades of scale by a combination of ground-based and balloon-borne experiments and the WMAP satellite (Bennett et al 2003). CMB photons were tightly coupled to matter in the early universe but propagated essentially freely after the primordial plasma recombined to form neutral atoms¹. For this reason, the CMB provides a snapshot of the spatial fluctuations on a spherical shell of comoving radius 14000 Mpc at redshift $z \sim 1000$ when the universe was only 400×10^3 years old. The small amplitude of these fluctuations [$O(10^{-5})$] means they are well described by linear perturbation theory and the physics of the CMB is thus very well understood.

The fluctuations on the last-scattering surface are believed to have resulted from primordial curvature fluctuations plausibly generated quantum mechanically during an inflationary phase in the first 10^{-35} seconds. These primordial fluctuations

*Presented at the Workshop on *Cosmology and Gravitational Physics*, 15-16 December 2005, Thessaloniki, Greece, *Editors*: N.K. Spyrou, N. Stergioulas and C.G. Tsagas.

[†]a.d.challinor@mrao.cam.ac.uk

¹Recent WMAP3 results indicate that around 10% of the photons re-scattered once the universe reionized around redshift 10.

are processed by gravitational instability and, on smaller scales, by the acoustic physics of the plasma which is supported by photon pressure. This makes the CMB anisotropy sensitive to the physics that initially produced the fluctuations and to the composition of the matter in the universe which affects the acoustic physics.

In this *contribution* we review what we have learnt from current CMB observations, with particular emphasis placed on constraints on fundamental physics and models of the early universe. We also look forward briefly to what might be learnt with more sensitive future observations, such as tighter constraints on the gravitational wave background predicted from inflation and sub-eV constraints on neutrino masses from weak gravitational lensing of the CMB.

2. CMB Physics

We begin with a brief review of the physics of the CMB temperature and polarization anisotropies. For more complete reviews see e.g. Hu & Dodelson (2001), Hu (2002) and Challinor (2005).

Consider a spatially-flat background universe linearly perturbed by density perturbations and gravitational waves. The metric can be taken to be $ds^2 = a^2(\eta)\{(1 + 2\psi)d\eta^2 - [(1 - 2\phi)\delta_{ij} + h_{ij}]dx^i dx^j\}$, where the Newtonian-like potentials ψ and ϕ describe the scalar (density) perturbations and the transverse, trace-free h_{ij} describes tensor perturbations (gravitational waves). In the absence of anisotropic stresses $\phi = \psi$. If we ignore scattering after the universe reionized, and approximate the last-scattering surface as sharp, the fractional temperature fluctuation along a line of sight $\hat{\mathbf{n}}$ has a scalar contribution

$$\Theta(\hat{\mathbf{n}}) = \Theta_0|_E + \psi|_E - \hat{\mathbf{n}} \cdot \mathbf{v}_b|_E + \int_E^R (\dot{\psi} + \dot{\phi}) d\eta, \quad (1)$$

and a tensor contribution

$$\Theta(\hat{\mathbf{n}}) = -\frac{1}{2} \int_E^R \dot{h}_{ij} \hat{n}^i \hat{n}^j d\eta. \quad (2)$$

Here, an overdot denotes a derivative with respect to conformal time η . Performing a spherical harmonic expansion of the anisotropies,

$$\Theta(\hat{\mathbf{n}}) = \sum_{lm} a_{lm} Y_{lm}(\hat{\mathbf{n}}), \quad (3)$$

the power spectrum is defined by $\langle a_{lm} a_{l'm'}^* \rangle = C_l^T \delta_{ll'} \delta_{mm'}$ where the angle brackets denote an ensemble average (or quantum expectation value). This form of the correlator follows from statistical isotropy and homogeneity. The quantity $l(l+1)C_l^T/2\pi$ is usually plotted and this gives the contribution to the mean-square anisotropy per $\ln l$.

The scalar anisotropies, equation (1), are sourced by fluctuations on the last-scattering surface at position E and an integral along the line of sight involving the evolution of the Weyl potential $\psi + \phi$. Regions of photon over-density have

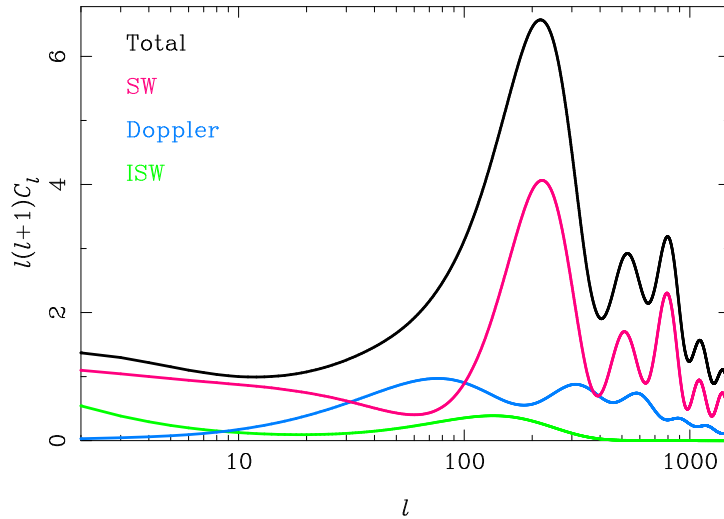


Figure 1. Scalar contributions to the temperature power spectrum from scale-invariant adiabatic initial fluctuations. At high l the contributions are (from top to bottom): total power (black); Sachs-Wolfe (magenta); Doppler (blue); and the integrated Sachs-Wolfe effect (green).

a positive intrinsic temperature fluctuation Θ_0 , but this is modified by the local gravitational potential $\psi|_E$ that the photon must climb out of at last scattering to give the observed anisotropy. There is a further contribution from the baryon peculiar velocity \mathbf{v}_b at the last-scattering event which Doppler blueshifts photons that scatter along the direction of motion. The last ‘integrated Sachs-Wolfe’ (ISW) term in equation (1) contributes to the large-angle fluctuations because of the decay of the gravitational potentials once dark energy dominates the expansion, and also on smaller scales due to evolution of the potentials around last scattering before the universe is fully matter dominated. The various contributions to the anisotropy power spectrum from scalar perturbations are shown in Fig. 1 for *adiabatic initial conditions* where the *relative* composition of the universe is initially the same everywhere. Such initial conditions are natural in inflation models with only a single field, but in models with multiple fields the initial conditions may include an *isocurvature* component where the relative composition fluctuates in space in such a way as not to perturb the curvature.

The initial curvature fluctuations are processed by gravitational and acoustic physics to determine the fluctuations on the last scattering surface. In particular, on scales above the photon mean free path, the radiation and baryons are tightly-coupled and the radiation is isotropic in the plasma rest-frame. In this limit, the intrinsic temperature fluctuation satisfies an oscillator equation (Hu & Sugiyama 1995)

$$\ddot{\Theta}_0 + \frac{\mathcal{H}R}{1+R}\dot{\Theta}_0 - \frac{1}{3(1+R)}\nabla^2\Theta_0 = 4\ddot{\phi} + \frac{4\mathcal{H}R}{1+R}\dot{\phi} + \frac{4}{3}\nabla^2\psi, \quad (4)$$

where $\mathcal{H} \equiv \dot{a}/a$ is the conformal Hubble parameter and $R \equiv 3\rho_b/(4\rho_\gamma)$ is the ratio of baryon to photon density. The sound speed in the plasma is $c_s^2 = 1/[3(1+R)]$ and is reduced from the value for a photon gas by the inertia of baryons. The oscillator

is damped by the Hubble drag on the baryons² and is driven by the gravitational potentials. A potential well accretes surrounding plasma until the induced pressure gradients balance the gravitational force. At this point $\Theta_0 = -(1 + R)\psi$ (ignoring evolution of the gravitational potentials) but the plasma is still infalling and doesn't turn around until a higher density. The amplitude of the oscillation about the midpoint is determined by the initial conditions and gravitational driving; for adiabatic initial conditions the plasma starts off over-dense in potential wells with $\Theta_0 = -\psi(0)/2$ for all wavelengths. This means that the oscillations of different Fourier modes all start off in phase, at an extrema, but the period of their subsequent oscillation is wavelength dependent. It follows that at the last-scattering surface different wavelengths will be caught at different phases of a cosine-like oscillation. Those wavelengths at an extremum at last scattering will give rise to a peak in the anisotropy power spectrum at a multipole $l \sim k/d_A(r_*)$, where $d_A(r_*)$ is the angular-diameter distance back to last scattering at comoving distance $r_* \approx 14$ Gpc.

The tensor anisotropies, equation (2), involve an integral of the metric shear h_{ij} which describes the local anisotropy in the expansion of the universe due to the presence of gravitational waves: CMB photons experience line-of-sight-dependent redshifts that imprint temperature anisotropies on the microwave sky. A cosmological background of gravitational waves is naturally produced during inflation from the vacuum fluctuations in the massless field h_{ij} (Starobinskii 1979); see Sec. 5. On scales larger than the Hubble radius, h_{ij} is constant but once a mode enters the Hubble radius it starts to oscillate with an amplitude that decays as a^{-1} . On scales $\lesssim 3^\circ$, i.e. $l \gtrsim 60$, the relevant gravitational waves at any distance back to last scattering are sub-Hubble and so the tensor signal is only appreciable on scales larger than this.

2.1 CMB Polarization

The other important CMB observable is its linear polarization (Rees 1968). The tightly-coupled description of the plasma given above breaks down for short wavelength modes, and universally as the mean-free path grows around recombination. As photons start to diffuse out of over-dense regions their density and velocity perturbations are damped which leads to an exponential damping tail in the anisotropy power spectrum (Silk 1968). However, a quadrupole anisotropy also starts to develop in the radiation and subsequent Thomson scattering generates linear polarization with an r.m.s. $\sim 5 \mu\text{K}$.

Linear polarization is described by Stokes parameters Q and U which measure the difference in intensity between two orthogonal polarizers (Q) and the same rotated by 45° . The Stokes parameters form the components of the polarization tensor \mathcal{P} which measures the (zero-lag) correlation of the electric field components in the radiation. They are therefore basis dependent but coordinate-independent fields can be derived by writing \mathcal{P} as a gradient (or electric) part and curl (or magnetic) part

²Expansion redshifts away the peculiar velocity of matter.

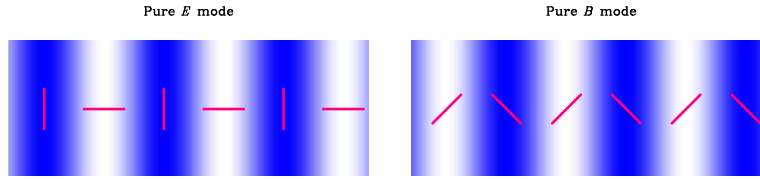


Figure 2. Polarization patterns for a pure E mode (left) and B mode (right) for a single Fourier mode on a flat patch of sky. In the basis defined by the wavevector, the E mode has vanishing U and the B mode vanishing Q .

(Kamionkowski, Kosowsky & Stebbins 1996; Zaldarriaga & Seljak 1996):

$$\mathcal{P}_{ab}(\hat{\mathbf{n}}) = \sum_{lm} \sqrt{\frac{(l-2)!}{(l+2)!}} \left(E_{lm} \nabla_{\langle a} \nabla_{b \rangle} Y_{lm}(\hat{\mathbf{n}}) + B_{lm} \epsilon^c_{\langle a} \nabla_{b \rangle} \nabla_c Y_{lm}(\hat{\mathbf{n}}) \right). \quad (5)$$

Here, the covariant derivatives are in the surface of the unit (celestial) sphere, angle brackets denote the symmetric, trace-free part and we have expanded the electric and magnetic parts in spherical harmonics. By way of example, Fig. 2 shows the polarization patterns for E and B modes that are locally plane waves. The E field behaves as a scalar under parity transformations but B is a pseudo-scalar. If parity-invariance is respected in the mean, there are only three additional non-vanishing power spectra: the E - and B -mode auto-correlations, C_l^E and C_l^B , and the cross-correlation of E with the temperature anisotropies C_l^{TE} . For linear scalar perturbations the B -mode polarization vanishes by symmetry, but gravitational waves produce E and B modes with approximately equal power (Kamionkowski et al 1996; Zaldarriaga & Seljak 1996; Hu & White 1997). This makes the large-angle B mode of polarization an excellent probe of primordial gravitational waves and several groups are now developing instruments with the aim of searching for this signal; see Sec. 6.

The temperature and polarization power spectra from density perturbations and gravitational waves are compared in Fig. 3. The gravitational wave amplitude is set to a value close to the current upper limit from the temperature anisotropies. Note that for scalar perturbations, C_l^E peaks at the troughs of C_l^T since the radiation quadrupole at last scattering is derived mostly from the plasma bulk velocity which oscillates $\pi/2$ out of phase with the intrinsic temperature. The polarization from density perturbations is maximised around $l \sim 1000$ which is related to the angle subtended by the photon mean-free patch around recombination. The ‘bump’ in the polarization spectra on large angles is due to reionization (Zaldarriaga 1997). Once the ultraviolet light from the first compact objects has reionized the intergalactic medium, the liberated electrons can re-scatter the CMB. This has the effect of damping the temperature and polarization spectra by $e^{-2\tau}$, where τ is the optical depth to Thomson scattering, on scales inside the horizon at that epoch. However, Thomson scattering of the quadrupole anisotropy that has now developed in the free-streaming radiation produces new large-angle polarization. The power in the reionization bump scales like τ^2 and the angular scale is related to the epoch of reionization. The high value $\tau = 0.17$ adopted in Fig. 3, favoured by the first-year WMAP data (Kogut et al 2003), is now at odds with the recent three-year WMAP

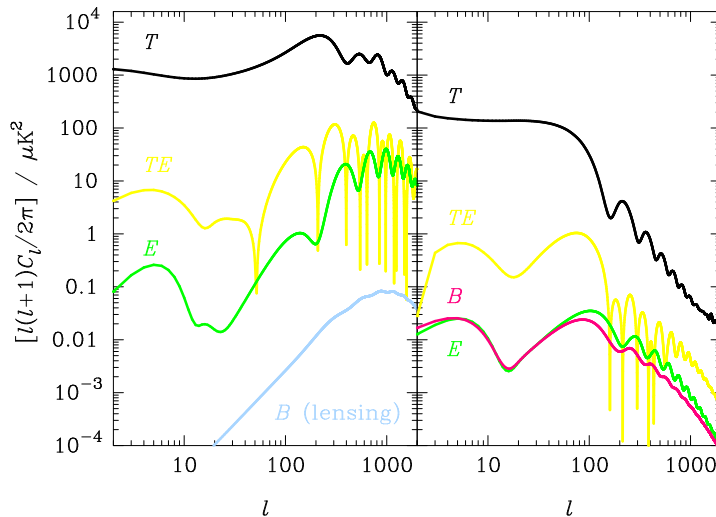


Figure 3. CMB temperature and polarization power spectra from scalar (left) and tensor perturbations (right) for a tensor-to-scalar ratio $r = 0.38$. The B -mode power generated by weak gravitational lensing is also shown.

data (Page et al 2006); see Sec. 4. Also shown in the figure is the non-linear B -mode signal generated by weak gravitational lensing of the primary E -mode polarization from density perturbations (Zaldarriaga & Seljak 1998; Lewis & Challinor 2006). We discuss this signal further in Sec. 6.

3. Current Observational Situation

Imaging the CMB temperature anisotropies is now a mature field. A number of complementary technologies have been deployed to map the CMB from frequencies of a few tens to hundreds of GHz. The remarkable full-sky maps from the WMAP satellite, most recently on the basis of three years of data (Hinshaw et al 2006), have a resolution up to 15 arcmin and are signal-dominated up to multipoles of a few hundred. The main cosmological information in the CMB images is encoded in their power spectra so in Fig. 4 we show a selection of recent measurements of the C_l^T taken from Jones et al (2005). The qualitative agreement with the theoretical expectation is striking, with the measurements clearly delimiting the first three acoustic peaks. As we discuss later, the agreement stands up to rigorous statistical analysis and has provided a very powerful means of constraining cosmological parameters and models. While the community awaits the high-sensitivity, full-sky results from the Planck satellite, due for launch in 2008, a number of groups are working to improve on ground-based measurements of the small angular scales inaccessible to WMAP.

Polarization measurements are less mature, with the first detection reported by DASI in 2002. Since that first detection, four further groups have published detections of E -mode polarization through its auto-correlation C_l^E . These measurements, also shown in Fig. 4, are still very noisy, but the qualitative agreement with the best-

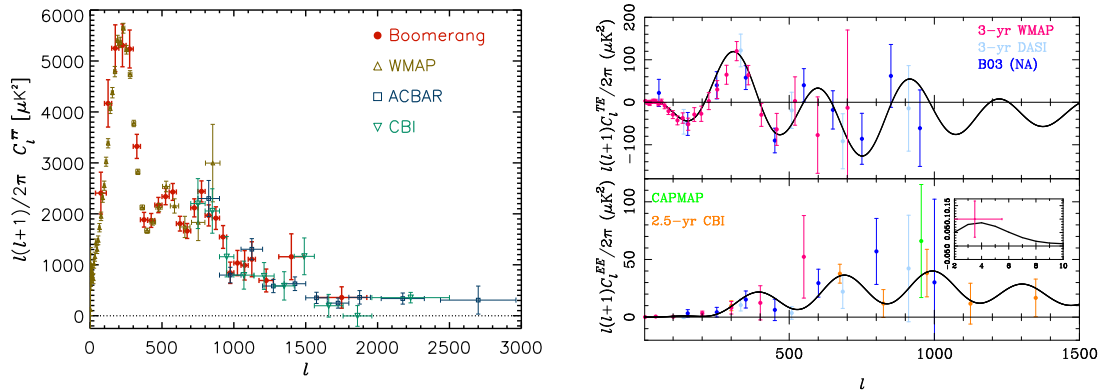


Figure 4. Recent CMB temperature (left) and polarization (right; C_l^{TE} top and C_l^E bottom) power spectra measurements. For polarization all measurements are plotted including WMAP3. The solid lines in the polarization plots are the theoretical expectation on the basis of the temperature data and an optical depth $\tau = 0.08$. The temperature plot, from Jones et al (2005), shows results from WMAP1 and a selection of ground and balloon-borne instruments. The recent WMAP3 data helps delimit the third acoustic peak in C_l^T further.

fit model to the temperature spectrum is striking. The cross-correlation C_l^{TE} has also been measured by several of these groups, and with the arrival of the third-year WMAP data the measurements are now quite precise for $l \lesssim 200$. As we discuss further in Sec. 6, several new high-sensitivity polarization-capable experiments are currently under construction and these have the ambition of measuring the B -mode power spectrum. At present only upper limits exist for C_l^B ; see Fig. 6. These instruments will also significantly improve on current measurements of C_l^E .

4. Major CMB Milestones and their Cosmological Implications

The current CMB data has confirmed a number of bold theoretical predictions, some of which pre-date the data by over thirty years. In this section we briefly describe these major milestones and discuss their implications for constraining the cosmological model.

4.1 Sachs-Wolfe Plateau and the Late-time ISW Effect

The large-angle temperature anisotropies are dominated by the Sachs-Wolfe effect, $\Theta_0 + \psi$, and the ISW effect (Sachs & Wolfe 1967). For adiabatic initial conditions, the combination $\Theta_0 + \psi$ reduces to $\psi/3$ on scales above the sound horizon at last scattering and so potential wells appear as cold regions. For a nearly scale-invariant spectrum of primordial curvature perturbations, we should have $l(l+1)C_l^T \approx \text{const.}$ on such scales. This plateau was first seen in the COBE data (Hinshaw et al 1996), and has since been impressively verified by WMAP. Departures from scale-invariance imply a slope to the $l(l+1)C_l^T$ spectrum on large

scales and this can be used to help constrain the spectral index n_s of the primordial spectrum; see Sec. 5. In practice, the large-angle data is not very constraining due to the large cosmic variance there, i.e. the fact we only have access to a sample of $2l + 1$ spherical harmonic modes at each l with which to estimate the variance of their population, C_l^T .

The late-time ISW effect, from the decay of the Weyl potential $\phi + \psi$ as dark energy dominates, contributes significantly on the largest angular scales. It is suppressed on smaller scales due to peak-trough cancellation in the integral along the line of sight and from the decay of the potential on sub-horizon scales during radiation domination. The late-time ISW adds incoherently with the Sachs-Wolfe contribution since at a give l they probe different linear scales. It is the only way to probe late-time growth of structure with linear CMB anisotropies (see Sec. 7 for an example of a non-linear probe), but this is hampered by large cosmic variance. The late-ISW effect produces a positive correlation between large-angle temperature fluctuations and tracers of the gravitational potential at redshifts $z \lesssim 1$. This was first detected by correlating the one-year WMAP data with the X-ray background and with the projected number density of radio galaxies (Boughn & Crittenden 2004), and has since been confirmed with several other tracers of large-scale structure. The correlation is sensitive to both the energy density in dark energy and any evolution with redshift. The ISW constraints on the former indicate $\Omega_\Lambda \sim 0.8$, consistent with other cosmological probes; see e.g. Cabre et al (2006). As yet there is no evidence for evolution but significant improvements can be expected from tomographic analyses of upcoming deep galaxy surveys.

4.2 Acoustic Peaks

The first three acoustic peaks are clearly resolved by the current temperature-anisotropy power spectrum. Corresponding oscillations are also apparent in the TE cross-correlation data and, at lower significance, in the EE power spectrum. For adiabatic models, the positions of the peaks are at the extrema of a cosine oscillation, giving $l \approx n\pi d_A(r_*)/r_s$ where $r_s \equiv \int_0^{\eta_*} c_s d\eta$ is the sound horizon at last scattering. The peak positions thus depend on the physical densities in matter $\Omega_m h^2$ and baryons $\Omega_b h^2$ through the sound horizon, and additionally through curvature and dark energy properties from the angular diameter distance. The same physics that gives rise to acoustic peaks in the CMB should produce oscillations in the matter power spectrum. These baryon oscillations were first detected in early 2005 in the clustering of the SDSS luminous red galaxy sample (Eisenstein et al 2005) and in the 2dF galaxy redshift sample (Cole et al 2005). Observing the connection between the fluctuations that produced the CMB anisotropies and those responsible for large-scale structure is an important test of the structure formation paradigm.

The relative heights of the acoustic peaks are influenced by baryon inertia, gravitational driving and photon diffusion. Baryons reduce the ratio of pressure to energy density in the plasma, shifting the midpoint of the oscillations to higher over-densities: $-(1 + R)\psi$. For adiabatic oscillations this enhances the 1st, 3rd

etc. (compressional) peaks over the 2nd, 4th etc. An additional effect comes from the gravitational driving term in equation (4) which initially resonantly drives the acoustic oscillations for the short wavelength modes that underwent oscillation during radiation domination. Increasing the matter density shifts matter-radiation equality to earlier times and the resonance is less effective for the low-order acoustic peaks. In combination, these two effects have allowed accurate measurements of the matter and baryon densities from the morphology of the acoustic peaks. From the three-year WMAP data alone, $\Omega_b h^2 = 0.0223^{+0.0007}_{-0.0009}$ and $\Omega_m h^2 = 0.127^{+0.007}_{-0.01}$ in flat, Λ CDM models (Spergel et al 2006). The baryon density implies a baryon-to-photon ratio $(6.10 \pm 0.2) \times 10^{-10}$ and predicts abundances for primordial deuterium, ^3He and ^4He that are consistent with observations. There is some tension between the low matter density favoured by WMAP3 and that favoured by tracers of large-scale structure, most notably weak gravitational lensing (Spergel et al 2006). Better measurements of the third and higher peaks will be very helpful here, and we look forward to sub-percent level precision in the determination of densities with the future Planck data³.

With the matter and baryon densities fixed by the morphology of the acoustic peaks, the acoustic oscillations become a standard ruler with which to measure $d_A(r_*)$, determined to be 13.7 ± 0.5 Gpc (Spergel et al 2003). The angular diameter distance depends on the Hubble parameter $H(z)$ and hence the composition of the universe. The dark energy model, curvature and sub-eV neutrino masses have no effect on the pre-recombination universe and they only affect the CMB through $d_A(r_*)$ and their large-scale clustering through the late-time ISW effect. The discriminatory power of the latter is limited by cosmic variance leading to the *geometric degeneracy* between curvature and dark energy (Efstathiou & Bond 1999). For example, closed models with no dark energy fit the WMAP data but imply a low Hubble constant and $\Omega_m h$ in conflict with other datasets. Using the Hubble Space Telescope (HST) measurement of H_0 , WMAP3 constrains the spatial sections of the universe to be very close to flat: $\Omega_K = -0.003^{+0.013}_{-0.017}$ and $\Omega_\Lambda = -0.78^{+0.035}_{-0.058}$ for cosmological constant models (Spergel et al 2006).

4.3 Damping Tail and Photon Diffusion

The acoustic oscillations in the photon-baryon plasma are exponentially damped at last scattering on comoving scales $\lesssim 30$ Mpc due to photon diffusion (Silk 1968). Furthermore, last scattering is not perfectly sharp: photons last scattered around recombination within a shell of thickness ~ 80 Mpc, and line of sight averaging through this shell also washes out anisotropy from small-scale fluctuations. We thus expect an exponential ‘damping tail’ in the temperature spectrum and this is seen in the ground and balloon-based data in the left plot in Fig. 4.

On scales $l > 2000$, the CBI, operating around 30 GHz, sees power in excess of that expected from the primary anisotropies at the 3σ level (Bond et al 2005). An

³<http://www.rssd.esa.int/index.php?project=Planck>

excess is also seen at smaller angular scales (centred on $l \sim 5000$) with the BIMA array operating at 28.5 GHz (Dawson et al 2006). Both analyses exclude point-source contamination as the source of the excess, suggesting instead that they are seeing a secondary contribution to the anisotropy from Compton up-scattering of CMB photons off hot gas in unresolved distant galaxy clusters. This explanation in terms of the Sunyaev-Zel'dovich (SZ) effect (Sunyaev & Zeldovich 1972) favours a variance in the matter over-density $\sigma_8 \approx 1$ (with 1σ errors at the 20% level), on the high side compared to inferences from current CMB and large-scale structure data (Spergel et al 2006). Optical follow-up of the BIMA fields shows no (anti-)correlation between galaxy over-densities and the anisotropy images, but the image statistics are consistent with SZ simulations. Data from the several high-resolution CMB experiments that will soon be operational should identify a definitive source for this excess small-scale power.

4.4 *E*-mode Polarization and *TE* Cross-Correlation

Current measurements of the *E*-mode polarization power spectrum and the cross-correlation with the temperature anisotropies are fully consistent with predictions based on the best-fit adiabatic model to the temperature anisotropies. This is an important test of the structure formation model: the polarization mainly reflects the plasma bulk velocities around recombination and these are consistent, via the continuity equation, with the density fluctuations that mostly seed the temperature anisotropies.

Apart from constraints on the reionization optical depth from large-angle polarization data (see Sec. 4.5), the power of the current polarization data for constraining parameters in adiabatic, Λ CDM models is rather limited. More important are the qualitative conclusions that we can draw from the data:

- The well-defined oscillations in C_l^{TE} further support the phase coherence of the primordial fluctuations, i.e. all modes with a given wavenumber oscillate in phase. This is a firm prediction of inflation models since then the fluctuations are produced in the growing mode and evolve passively, but is at odds with defect models.
- The (anti-)correlation between the polarization and temperature on degree scales (see Fig. 4) is evidence for fluctuations at last scattering that are outside the Hubble radius and are adiabatic (Peiris et al 2003). This is more direct, model-independent evidence for such fluctuations than from the temperature anisotropies since the latter could have been produced on these scales gravitationally all along the line of sight.
- The peak positions in polarization, as for the temperature, are in the correct locations for adiabatic initial conditions. Pre-WMAP3 analyses, combining CMB temperature and polarization with large-scale structure and nucleosynthesis priors on the baryon density, limit the contribution from isocurvature

initial conditions to the CMB power to be less than 30%, allowing for the most general correlated initial conditions (Dunkley et al 2005).

- That E -mode power peaks at the minima of the temperature power spectrum increases our confidence that the primordial power spectrum is a smooth function with no features ‘hiding’ on scales that reach a mid-point of their acoustic oscillation at last scattering (and so contribute very little to the temperature anisotropies).

4.5 Large-Angle Polarization from Reionization

The large-angle polarization generated by re-scattering at reionization was first seen in the TE correlation in the first-year WMAP data (Kogut et al 2003). This provided a broad constraint on the optical depth with mean $\tau = 0.17$ and prompted a flurry of theoretical activity to explain such early reionization. With the full polarization analysis of the three-year release (Page et al 2006), the reionization signal can be seen in the large-angle C_l^E spectrum (see the insert in the bottom right plot in Fig. 4). To obtain this spectrum required aggressive cleaning of Galactic foregrounds, using the 22.5-GHz (K-band) channel as a template for polarized synchrotron emission and a model for the contribution of polarized thermal dust emission, as well as a careful treatment of correlated noise in the noise-dominated polarization maps. However, the observation that the B -mode spectrum from the same analysis is consistent with zero suggests that residual foreground contamination is under control. On the basis of the EE spectrum alone, the WMAP team find $\tau = 0.10 \pm 0.03$, considerably lower than the best-fit to the one-year TE spectrum. The value from the improved three-year analysis sits much more comfortably with astrophysical reionization models.

5. CMB Constraints on Inflation

Inflation is a posited period of accelerated expansion in the early universe. It was originally proposed as a solution to a number of now-classic problems with Friedmann cosmologies, such as why the three-geometry is now so close to Euclidean and why the CMB temperature is so uniform given that points at last scattering subtending more than one degree today should never have been in causal contact (Guth 1981). In the inflationary picture, the observable universe is believed to derive from a small, causally-connected region that was inflated by at least 60 e-folds during a phase of accelerated expansion. One mechanism to realise inflation, which requires a violation of the weak energy condition, is with a scalar field ϕ — the inflaton — evolving slowly over a flat part of its interaction potential $V(\phi)$. It has proved difficult to realise inflation from (fundamental) field theory, and this has led to a plethora of phenomenological models in the literature. String-inspired approaches, in which the inflaton may emerge as one of the moduli fields in the low-energy

effective theory are also being actively pursued, e.g. Kachru et al (2003).

5.1 Inflationary Power Spectra

Inflation naturally predicts a universe that is very close to flat, consistent with the observed positions of the CMB acoustic peaks as discussed in Sec. 4. Significantly, it also naturally provides a causal mechanism for generating initial curvature fluctuations (Bardeen, Steinhardt & Turner 1983) and gravitational waves (Starobinskii 1979) with almost scale-invariant, power-law spectra. The mechanism is an application of semi-classical quantum gravity, in which the perturbations in the inflaton field and metric fluctuations are quantised on a classical background that is close to deSitter. Since the physical wavelength of a mode gets pushed outside the Hubble radius by the accelerated expansion, vacuum fluctuations initially deep inside the Hubble radius are stretched to cosmological scales and amplified during inflation. The spectra of the curvature perturbations and gravity waves can be approximated as power laws over the range of scales relevant for cosmology:

$$\mathcal{P}_{\mathcal{R}} \approx A_s (k/k_0)^{n_s-1} \quad , \quad \mathcal{P}_h \approx A_t (k/k_0)^{n_t} \quad , \quad (6)$$

where the amplitudes and spectral indices are given by [see e.g. Lidsey et al (1997) and references therein]

$$A_s = \frac{H^2}{\pi \epsilon m_{\text{Pl}}^2} \quad , \quad n_s - 1 = -4\epsilon + 2\eta \quad , \quad A_t \equiv r A_s = \frac{16H^2}{\pi m_{\text{Pl}}^2} \quad , \quad n_t = -2\epsilon \quad . \quad (7)$$

Here, H is the Hubble parameter during inflation evaluated when the mode k_0 exits the Hubble radius, i.e. when $k_0 = aH$, and ϵ and η are (Hubble) slow-roll parameters that depend on the evolution of H through inflation. The potential energy dominates the stress-energy of the scalar field during inflation, and in this limit H , ϵ and η are related to the potential $V(\phi)$ by

$$H^2 \approx \frac{8\pi}{3m_{\text{Pl}}^2} V \quad , \quad \epsilon \approx \frac{m_{\text{Pl}}^2}{16\pi} \left(\frac{V'}{V} \right)^2 \quad , \quad \eta \approx \frac{m_{\text{Pl}}^2}{8\pi} \left[\frac{V''}{V} - \frac{1}{2} \left(\frac{V'}{V} \right)^2 \right] \quad , \quad (8)$$

where primes denote derivatives with respect to the field ϕ . Equations (7) and (8) imply that the power spectrum of gravitational waves from slow-roll inflation depends only the energy density V . This is often expressed in terms of an *energy scale of inflation* $E_{\text{inf}} = V^{1/4}$, which gives a tensor-to-scalar ratio

$$r = 8 \times 10^{-3} (E_{\text{inf}}/10^{16} \text{ GeV})^4 \quad (9)$$

for a scalar amplitude $A_s = 2.36 \times 10^{-9}$. The four observables, A_s , A_t , n_s and n_t are not independent since they derive from three parameters, H , ϵ and η . This results in the leading-order slow-roll consistency relation $r = -8n_t$. Verifying this observationally would be a remarkable triumph for inflation, but the prospects are

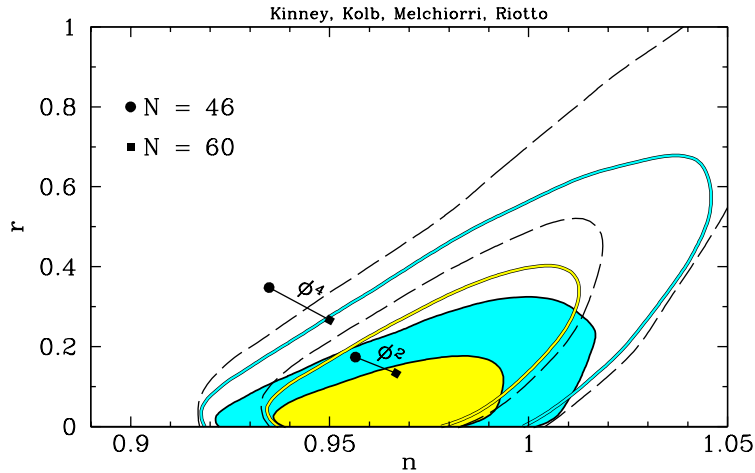


Figure 5. Constraints in the r - n_s plane for models with no running from Kinney et al (2006). Blue contours are 68% confidence regions and yellow are 95%. The filled contours are from combining WMAP3 and the SDSS galaxy survey; open are with WMAP3 alone. These results assume the HST prior on H_0 ; dropping this prior gives the dashed contours. The predictions for $V \propto \phi^2$ and ϕ^4 are shown assuming that modes with $k = 0.002 \text{ Mpc}^{-1}$ left the Hubble radius between 46 and 60 e-folds before the end of inflation.

poor even after accounting for the long lever-arm that a combination of CMB and direct detections could provide (Smith, Peiris & Cooray 2006).

Constraints in the r - n_s plane from WMAP3 and the SDSS galaxy survey are shown in Fig. 5, taken from Kinney et al (2006). The point $r = 0$ and $n_s = 1$ corresponds to inflation occurring at low energy with essentially no evolution in H (and hence a very flat potential); the gravitational waves are negligible and the curvature fluctuations have no preferred scale. This *Harrison-Zel'dovich* spectrum is clearly disfavoured by the data, but is not yet excluded at the 95% level. Attempts to pin down n_s with current CMB temperature data are still hampered by a degeneracy between n_s , A_s , the reionization optical depth τ and the baryon density (Lewis 2006). The WMAP3 measurement of τ from large-angle polarization helps considerably in breaking this degeneracy, and leads to a marginalised constraint of $n_s = 0.987^{+0.019}_{-0.037}$ in inflation-inspired models (Spergel et al 2006). The 95% upper limit on the tensor-to-scalar ratio from WMAP3 and SDDS is 0.28 for power-law spectra, thus limiting the inflationary energy scale $E_{\text{inf}} < 2.4 \times 10^{16} \text{ GeV}$. We see from Fig. 5 that large-field models with monomial potentials $V(\phi) \propto \phi^p$ are now excluded at high significance for $p \geq 4$.

Slow-roll inflation predicts that any running of the spectral indices with scale should be second-order in the slow-roll parameters, i.e. $O[(n_s - 1)^2]$. The CMB alone provides a rather limited lever-arm for measuring running, with current data having very little constraining power for $k > 0.05 \text{ Mpc}^{-1}$ (corresponding to $l \sim 700$). However, there is persistent, though not yet compelling, evidence for running from the CMB: WMAP3 alone gives $dn_s/d\ln k = -0.102^{+0.05}_{-0.043}$ (Spergel et al 2006), al-

lowing for gravitational waves. Running near this mean value would be problematic for slow-roll inflation models. The tendency for the CMB to favour large negative running is driven by the large-angle ($l \lesssim 15$) temperature data. A more definitive assessment of running must await independent verification of the large-scale spectrum from Planck and improved small-scale data from a combination of Planck and further ground-based observations. The current evidence for running weakens considerably when small-scale data from the Lyman- α forest (i.e. absorption lines in quasar spectra due to neutral hydrogen in the intergalactic medium) is included (Seljak, Slosar & McDonald 2006; Viel, Haehnelt & Lewis 2006). The Ly- α data probes the quasi-linear fluctuations on \sim Mpc scales at redshifts around 3, and is sensitive to the amplitude and slope of the matter power spectrum at these redshifts and scales. There is currently some tension between the amplitudes inferred from Ly- α and CMB, and this is worsened by inclusion of the negative running favoured by the CMB.

5.3 Non-Gaussianity and Inflation

There are further predictions of slow-roll inflation that are amenable to observational tests. The fluctuations from single-field models should be adiabatic and any departures from Gaussian statistics should be unobservably small. Gaussianity follows, in part, from the requirement of a flat potential and hence small self-interactions if inflation is to happen [see Bartolo et al (2004) for a recent review]. However, adiabaticity and Gaussianity can be violated in models with several scalar fields. An example of the latter is the curvaton model (Lyth & Wands 2002), which can produce a large correlated isocurvature mode and observably-large non-Gaussianity if the curvaton field decays before its energy density dominates that of radiation. As we have already noted, current data do allow a sizeable isocurvature fraction, but this is not favoured. In many models, the non-Gaussian curvature perturbation can be written as the sum of a Gaussian part plus the square of a Gaussian: symbolically

$$\mathcal{R} = \mathcal{R}_G + f_{\text{NL}}^{\mathcal{R}}(\mathcal{R}_G^2 - \langle \mathcal{R}_G^2 \rangle), \quad (10)$$

where, in general, $f_{\text{NL}}^{\mathcal{R}}$ is scale-dependent and the quadratic part is a convolution. Single-field slow-roll inflation predicts $f_{\text{NL}}^{\mathcal{R}} \sim O(\epsilon)$ (Maldacena 2003), but it can be much higher in alternative models. Observational constraints are usually expressed in terms of the f_{NL} appropriate to the gravitational potential ψ at last scattering. For $f_{\text{NL}}^{\mathcal{R}} \gg 1$, we have $f_{\text{NL}} \approx -5f_{\text{NL}}^{\mathcal{R}}/3$ since $O(1)$ non-linear corrections in the relation of the curvature to metric perturbation can then be ignored. The best constraints on a scale-independent f_{NL} are from an analysis of the three-point function of the three-year WMAP maps: $-54 < f_{\text{NL}} < 114$ at 95% confidence (Spergel et al 2006). Planck data should have sensitivity down to $f_{\text{NL}} \sim 5$ (Komatsu & Spergel 2001), but this is still too large to expect to see anything in simple inflation models.

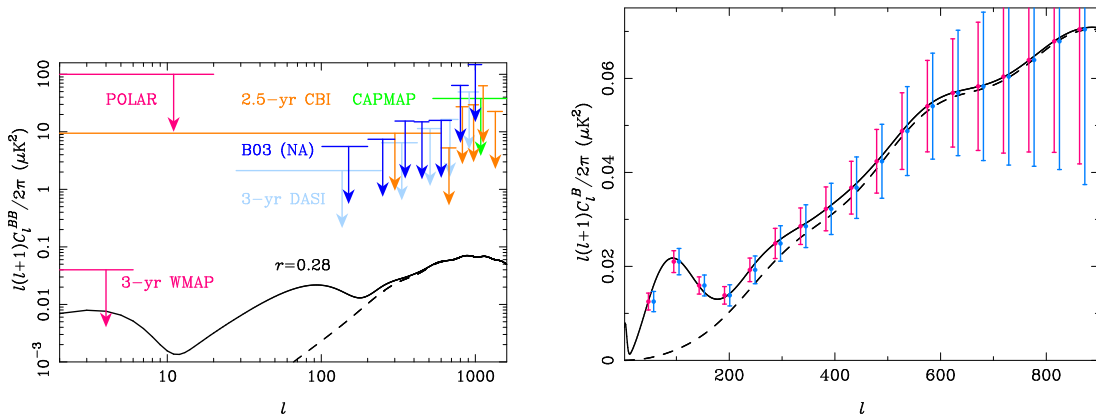


Figure 6. Left: current 95% upper limits on the the B -mode polarization power spectrum. The solid line is the theoretical prediction for a tensor-to-scalar ratio $r = 0.28$ — the current 95% limit from the temperature power spectrum and galaxy clustering (Spergel et al 2006) — while the dotted line is the contribution from weak gravitational lensing. Right: error forecasts for Clover after a two-year campaign observing 1000 deg² divided between four equal-area fields. Blue error bars properly account for E - B mixing effects due to the finite sky coverage while magenta ignore this. The tensor-to-scalar ratio is again $r = 0.28$.

6. Searching for Gravity Waves with the CMB

A detection of a Gaussian-distributed background of gravitational waves with cosmological wavelengths and a nearly scale-invariant (but red) spectrum would be seen by many as compelling evidence that inflation occurred. The amplitude of this background is directly related to the energy scale of inflation, and the near scale-invariance follows from the slow decrease in the Hubble parameter during inflation. Of course, a non-detection would not rule out inflation having happened at a low enough energy, but, importantly, a detection would rule out some alternative theories for the generation of the curvature perturbation, such as the cyclic model (Steinhardt & Turok 2002), that predict negligible gravity waves. The large-angle B mode of CMB polarization is a promising observable with which to search for the imprint of gravity waves since a detection would not be confused by linear curvature perturbations.

In Fig. 6 we show a compilation of current direct upper limits on the B -mode power spectrum. The solid curve is the theoretical spectrum, including the contribution from weak gravitational lensing, for $r = 0.28$ — the 95% upper limit inferred from WMAP3 temperature and E -mode data and SDSS galaxy clustering (Spergel et al 2006). Clearly, the direct measurements are not yet competitive, with at least a factor ten improvement in sensitivity required. The 2σ limit to determining r from ideal CMB temperature observations is 0.14 and this improves to 0.04 with E -mode data. Although the WMAP temperature data is already cosmic-variance limited on scales where gravity waves contribute, the constraints on r are considerably worse than $r = 0.14$ due to the uncertainties in other cosmological parameters. In principle, B -mode measurements of r can do much better as they are limited only by how well the lensing signal can be subtracted. Lensing reconstruction methods based on

the non-Gaussian action of lensing on the CMB have been proposed, e.g. Hu (2001), and with the most optimal methods $r \sim 10^{-6}$ may be achievable (Seljak & Hirata 2003). In practice, astrophysical foregrounds and instrumental systematic effects are likely to be a more significant obstacle.

A number of groups are now designing and constructing a new generation of CMB polarimeters that aim to be sensitive down to $r \sim 0.01$. These should be reporting data within the next five years, a timescale similar to the Planck satellite. The constraint $r < 0.28$ gives an r.m.s. gravity wave contribution < 200 nK to B -mode polarization. Detecting such signals requires instruments with many hundreds, or even thousands, of detectors, and demands exquisite control of instrumental effects and broad frequency coverage to deal with polarized Galactic foreground emission. With the exception of SPIDER, which will aim to survey around half of the sky, the surveys will each target small sky areas ($\lesssim 1000$ deg²) in regions of low foreground emission in total intensity. Despite this, removing foregrounds to the 10% level will likely be required to see a B -mode signal at $r = 0.01$. As an example of a next-generation instrument, we show in Fig. 6 projected errors on the B -mode power spectrum from the UK-led Clover experiment. Clover will have over 1200 superconducting detectors distributed over three scaled telescopes centred on 97, 145 and 225 GHz, each with better than 10-arcmin resolution. The instrument is planned to be deployed at the Chajnantor Observatory, Chile. The error forecasts in Fig. 6 are for a tensor-to-scalar ratio $r = 0.28$ for direct comparison with the adjacent plot of current upper limits. However, the Clover survey is optimised for smaller $r \sim 0.01$, and is designed to be limited on large scales by sample variance of the lens-induced B modes after two years of operation.

7. Other Physics in the CMB Fluctuations

Within the Λ CDM model, the major remaining CMB milestones are the detection of gravitational secondary effects (weak lensing and the non-linear ISW effect from collapsing structures), various scattering secondary effects from bulk velocities around and after the epoch of reionization, and the detection of B -mode polarization and (possibly) gravitational waves. A number of deep surveys at arcminute resolution will soon commence to study the temperature anisotropies at high l . Their main goal is to characterise the scattering secondaries, and hence learn more about the reionization history and morphology, and to detect the gravitational lensing effect in the temperature anisotropies. At the same time, high-sensitivity polarization surveys are being undertaken and these should also provide further valuable information on the weak-lensing effect. From the viewpoint of fundamental physics, the main interest in such small-scale observations is the possibility of using CMB lensing to determine neutrino masses and further constrain the dark-energy model. However, we should also be mindful of the possibility of serendipitous discovery of other physics in the small-scale CMB fields, such as the imprint of cosmic strings or primordial magnetic fields. We now discuss some of these briefly.

Cosmology has the potential to place constraints on the absolute neutrinos masses

rather than the (squared) differences from neutrino oscillations [see Lesgourgues & Pastor (2006) for a recent review]. The current constraint on the sum of neutrino masses from CMB, galaxy clustering and Lyman- α forest data is $\sum m_\nu < 0.17$ eV at 95% confidence (Seljak et al 2006). The implied sub-eV masses mean neutrinos are relativistic at recombination and their effect on the CMB is limited to late times. Changes they induce in the angular diameter distance are degenerate with dark energy and so, to constrain masses from the CMB alone, we need to look to gravitational lensing. Non-relativistic massive neutrinos increase the expansion rate over massless one impeding the growth of structure. This effect is cancelled on scales larger than the neutrino comoving Jeans' length (which decreases in time and is inversely proportional to the mass) by neutrino clustering, but on smaller scales the growth of fluctuations in the matter density is slowed. It is this suppression that allows the energy density (or sum of masses) of neutrinos to be constrained by small-scale tracers of matter clustering. The effect of neutrino masses on the power spectrum of the lensing deflections is scale dependent: no effect at low l but a reduction in power at high l . To exploit the effects of neutrino physics in CMB lensing, one must first attempt to reconstruct the underlying lensing deflection field from the lensed CMB fields. An accurate reconstruction requires high resolution and is greatly helped by polarization measurements once the sensitivity is high enough to image lens-induced B modes (Hu & Okamoto 2001; Seljak & Hirata 2003). Assuming a normal hierarchy of neutrino masses with two essentially massless⁴, Kaplinghat, Knox & Song (2003) estimated that the mass of the third should be measurable to an accuracy of 0.04 eV with a future polarization satellite mission. Errors of this magnitude are comparable to what should be achievable in the future with galaxy lensing, but with quite different potential systematic effects. It is an interesting result since atmospheric neutrino oscillations then imply that a detection of mass with the CMB *must* be possible at the 1σ level. Of course, the significance will be higher if the lightest neutrinos are not massless, or in the inverted hierarchy. Note that the latter is on the verge of being ruled out with the current cosmological constraints (Seljak et al 2006). It is also interesting to question whether CMB lensing will be able to tell us anything about individual masses rather than their sum? Taking differences from oscillation data at face value, the answer appears to be that dropping the assumption of degenerate masses would produce an improved fit to an idealised, cosmic-variance-limited reconstruction of the lensing power spectrum if $\sum m_\nu < 0.1$ eV (Slosar 2006). However, attempting to measure the mass differences with no prior from atmospheric oscillations is not possible because of degeneracies with other parameters and these severely degrade ones ability to measure $\sum m_\nu$ without mass priors.

The details of the dark-energy sector affect the primary CMB anisotropies only through the angular diameter distance and the late-time ISW effect. Using the former is plagued by degeneracies while the latter is hampered by cosmic variance. The effect of dark energy on CMB lensing is felt almost exclusively through the change in the expansion rate which is independent of scale. The different scale

⁴This combination has the smallest possible neutrino energy density and hence cosmological effect.

dependences from dark energy (say to changes in the equation of state parameter $w = p/\rho$) and massive neutrinos should allow them to be measured separately with the lensed CMB. Kaplinghat et al (2003) find a marginalised 1σ error on w of 0.18 from a future polarization satellite. Of course, tomography proper is not possible with the fixed source plane of the CMB (i.e. last scattering), and the CMB constraints on dark energy will not be competitive with future galaxy lensing and clustering (via baryon oscillations) surveys.

A significant feature of recent attempts to realise inflation in string/M-theory cosmology is the recognition that (local) cosmic strings may be produced generically at the end of brane inflation (Sarangi & Tye 2002). The details of the strings network (such as the spectrum of tensions and inter-commutation rates) depend on the details of the brane scenario, but the tensions $G\mu/c^4$ plausibly exceed 10^{-11} . Cosmic strings leave an imprint in the CMB temperature anisotropies due to string wakes stirring up the plasma prior to recombination, and from the integrated effect of rapidly moving strings crossing the line of sight (Kaiser & Stebbins 1984). Current data limits the contribution of local strings to the temperature power spectrum to be $\lesssim 10\%$, corresponding to $G\mu/c^4 < 2.7 \times 10^{-7}$ (Seljak et al 2006). Future high-resolution temperature data should improve this bound on the tension further, and searches for stringy non-Gaussian imprints in CMB maps should also help. As with the search for inflationary gravitational waves, B -mode polarization may prove to be the most promising observable for constraining strings. String networks excite scalar, vector and tensor perturbations and the latter two lead to B -mode polarization from the epoch of recombination and reionization. Many brane-inflation models predict a negligible gravity wave production *during* inflation in which case strings should be the dominant primordial source of B -mode polarization. Seljak & Slosar (2006) argue that B -mode measurements with a future polarization satellite may improve on current string constraints by an order of magnitude. The string signal peaks around $l \sim 1000$ and so the hope is that observations covering a range of scales should be able to separate it from primordial gravity waves and the lensing signal. However, further work is required to extend and test lensing reconstruction methods in the presence of a possible non-Gaussian string signal.

Finally, we note that there are statistically-significant anomalies in the large-angle temperature anisotropies, as imaged by COBE (Smoot 1992) and WMAP (Hinshaw 2003), that may signal departures from rotational invariance and/or Gaussianity; for a recent review and WMAP3 analysis, see Copi et al (2006) and references therein. Arguably most significantly, the $l \leq 6$ multipoles seem to favour a preferred axis about which they maximise the power concentrated in a single m mode (Land & Magueijo 2005). There are also significant correlations of the quadrupole and octupole ($l = 3$) with the ecliptic plane and the direction of the equinoxes and/or CMB dipole (Copi et al 2006). The significance of these anomalies is still under debate, as is their possible explanation. Suggestions include unidentified instrumental effects, residual foreground contamination, and effects of the local universe (Vale 2005), although it appears unlikely that the last two can be responsible (Cooray & Seto 2005). There have also been a number of suggestions that the large-angle anomalies may have a more fundamental origin, such as a topologically small universe (de

Oliveira-Costa et al 2004) or non-fluid dark energy (Battye & Moss 2006). Independent verification with the Planck data and improved analyses of further years of WMAP data should help with tracking down the source of these large-angle effects⁵.

8. Summary

Many of the bold predictions of CMB physics have now been impressively verified with a large number of independent observations. The large-scale Sachs-Wolfe effect, acoustic peak structure, damping tail, late-time integrated Sachs-Wolfe effect, E -mode polarization and the effect of reionization have all been detected. The large-scale anisotropies and the first three acoustic peaks have now been measured accurately and have yielded impressive constraints on cosmological parameters. The data is consistent with a very simple cosmological model with adiabatic primordial fluctuations, with an almost scale-free spectrum, evolving passively in a spatially-flat, Λ CDM universe.

Inflation continues to stand up to exacting comparisons with both CMB and tracers of matter clustering. Evidence for dynamics during inflation is emerging, most notably from the recent third-year WMAP data: models with scale-invariant curvature perturbations and no gravity waves are on the brink of being ruled out at 95% confidence. There are hints of a run in the spectral index in current CMB data at a level that would be problematic for many inflation models, but this is not corroborated by probes of the matter power spectrum on small scales (the Lyman- α forest). In the near future we can expect better measurements of the third acoustic peak in the temperature anisotropies and beyond. With Planck we can expect a per-cent level determination of the spectral index of curvature perturbations and a much more definitive assessment of running and any potential conflict with the small-scale matter power spectrum.

We look forward to improvements in E -mode polarization data and the better constraints this will bring on non-standard cosmological models such as those with a significant contribution from isocurvature fluctuations. On a similar timescale, a new generation of small-scale temperature experiments should constrain further the reionization history and its morphology, and detect the effect of weak gravitational lensing by large-scale structure in the CMB. Looking a little further ahead, a new generation of high-sensitivity polarization-capable instruments have the ambition of detecting the imprint of gravitational waves from inflation. They should be sensitive down to tensor-to-scalar ratios $r \sim 0.01$ — corresponding to an energy scale of inflation around 1.0×10^{16} GeV — and will place tight constraints on inflation models. There is also exciting secondary science that can be done with these instruments, such as lensing reconstruction which brings with it the promise of competitive constraints on neutrino masses from the CMB alone. Finally, there is always the hope of serendipitous discovery, such as the non-Gaussian signature of cosmic strings,

⁵The first-year WMAP data was already signal-dominated on large angular scales so further integration helps not by improving the signal-to-noise but by bettering our understanding of instrumental and foreground effects.

perhaps produced at the end of brane inflation, in small-scale temperature maps. These continue to be exciting times for CMB research.

Acknowledgements

AC thanks the Royal Society for a University Research Fellowship, the organisers for the invitation to attend this stimulating workshop and the British Council for sponsoring my attendance. Thanks also to Will Kinney and Bill Jones for permission to include their figures.

References

- Bardeen, J.M., Steinhardt, P.J., Turner, M.S., 1983, *Phys. Rev. D*, 28, 679
Battye, R.A., Moss, A., 2006, arXiv:astro-ph/0602377
Bartolo, N. et al, 2004, *Phys. Rept.*, 402, 103
Bennett, C.L. et al, 2003, *ApJS*, 148, 1
Bond, J.R. et al, 2005, *ApJ*, 626, 12
Bough, S., Crittenden, R., 2004, *Nature*, 427, 45
Cabre, A. et al, 2006, arXiv:astro-ph/0603690
Challinor, A., 2005, in *The Physics of the Early Universe*, E. Papantonopoulos (ed.),
Lect. Notes. Phys. 653, 71
Cole, S. et al, 2005, *MNRAS*, 362, 505
Cooray, A., Seto, N., 2005, *JCAP*, 12, 4
Copi, C. et al, 2006, arXiv:astro-ph/0605135
Dawson, K.S. et al, 2006, arXiv:astro-ph/0602413
Dunkley, J. et al, 2005, *Phys. Rev. Lett.*, 95, 261303
Eisenstein, D.J. et al, 2005, *ApJ*, 633, 560
Efstathiou, G., Bond, J.R., 1999, *MNRAS*, 304, 75
Guth, A.H., 1981, *Phys. Rev. D*, 23, 347
Hinshaw, G. et al, 1996, *ApJL*, 464, 17
Hinshaw, G. et al, 2006, arXiv:astro-ph/0603451
Hu, W., 2001, *ApJL*, 557, 79
Hu, W., 2002, *Ann. Phys.*, 303, 203
Hu, W., Sugiyama, N., 1995, *ApJ*, 444, 489
Hu, W., White, M., 1997, *Phys. Rev. D*, 56, 596
Hu, W., Dodelson, S., 2002, *Ann. Rev. Astron. Astrophys.*, 40, 171
Hu, W., Okamoto, T., 2002, *ApJ*, 574, 566
Jones, W.C. et al, 2005, arXiv:astro-ph/0507494
Kachru, S. et al, 2003, *JCAP*, 0310, 013
Kaiser, N., Stebbins, A., 1984, *Nature*, 310, 391
Kamionkowski, M., Kosowsky, A., Stebbins, A., 1997, *Phys. Rev. D*, 55, 7368
Kaplinghat, M., Knox, L., Song, Y.S., 2003, *Phys. Rev. Lett.*, 91, 241301
Kinney, W.H. et al, 2006, arXiv:astro-ph/0605338

Kogut, A. et al, 2003, ApJS, 148, 161
Komatsu, E., Spergel, D.N., 2001, Phys. Rev. D, 63, 063002
Land, K., Magueijo, J., 2005, Phys. Rev. Lett., 95, 071301
Lesgourgues, J., Pastor, S., 2006, arXiv:astro-ph/0603494
Lewis, A., 2006, arXiv:astro-ph/0603753
Lewis, A., Challinor, A., 2006, Phys. Rept., 429, 1
Lidsey, J.E. et al, 1997, Rev. Mod. Phys., 69, 373
Lyth, D.H., Wands, D., 2002, Phys. Lett. B, 524, 5
Maldacena, J., 2003, J. High Energy Phys., 5, 13
Mather, J.C. et al, 1994, ApJ, 420, 439
de Oliveira-Costa, A. et al, 2004, Phys. Rev. D, 69, 063516
Page, L. et al, 2006, arXiv:astro-ph/0603450
Peiris, H.V. et al, 2003, ApJS, 148, 213
Rees, M.J., 1968, ApJL, 153, 1
Sachs, R., Wolfe, A., 1967, ApJ, 147, 735
Sarangi, S., Tye, S.H.H., 2002, Phys. Lett. B, 536, 185
Seljak, U., Hirata, C.M., 2004, Phys. Rev. D, 69, 043005
Seljak, U., Slosar, A., 2006, arXiv:astro-ph/0604143
Seljak, U., Slosar, A., McDonald, P., 2006, arXiv:astro-ph/0604335
Silk, J., 1968, ApJ, 151, 459
Slosar, A., 2006, arXiv:astro-ph/0602133
Smith, T.L., Peiris, H.V., Cooray, A., 2006, arXiv:astro-ph/0602137
Smoot, G.F. et al, 1992, ApJL, 396, 1
Spergel, D.N. et al, 2003, ApJS, 148, 175
Spergel, D.N. et al, 2006, arXiv:astro-ph/0603449
Starobinskii, A.A., 1979, JETP Lett., 30, 682
Steinhardt, P.J., Turok, N., 2002, Science, 296, 1436
Sunyaev, R.A., Zeldovich, Y.B., 1972, Comm. Astrophys. Space Phys., 4, 173
Vale, C., 2005, arXiv:astro-ph/0509039
Viel, M., Haehnelt, M.G., Lewis, A., 2006, arXiv:astro-ph/0604310
Zaldarriaga, M., 1997, Phys. Rev. D, 55, 1822
Zaldarriaga, M., Seljak U., 1996, Phys. Rev. D, 55, 1830
Zaldarriaga, M., Seljak, U., 1998, Phys. Rev. D, 58, 023003

LARGE-SCALE COSMOLOGICAL STRUCTURES: A NEW LOOK *

N.K. Spyrou †

Astronomy Department, Aristoteleion University of Thessaloniki
541.24 Thessaloniki, Macedonia, Hellas (Greece)

Abstract

Current observational data suggest that the observable Universe differs very much from the simple picture of a collection of more or less widely separated galaxies or higher-order cosmological structures, and that the latter differ very much from their optical pictures. The constituting elements of the Universe and, plausibly, the Universe in its large scales, can quite satisfactorily be treated as continuous gravitational systems and, more specifically, bounded gravitating sources, preferably perfect-fluid sources. As predicted in the dynamical-equivalence approach in the case of a general-relativistic gravitating bounded perfect-fluid (magnetized or not), the isentropic hydrodynamical flows (and the properly defined hydromagnetic flows) are dynamically equivalent to the geodesic motions in a fully defined virtual perfect-fluid source. In the Newtonian theory of gravity, the generalized mass density producing the above generalized new geodesic motions can be either positive, or negative, or even vanish. This implies the possibility of a spatially increasing, or decreasing, or even vanishing acceleration, depending, beyond the internal physical characteristics of the source considered, on the distance from the center of the source as compared to the so-called inversion distance. In the interior of the source, the inversion distance, resulting from the vanishing of the generalized mass density, depends on the absolute temperature and chemical composition of the fluid source and on the mass of the central dark object, and it is the distance from the origin separating the regions of dominance of the attractive and repulsive gravity forces in the source. The extra ingredient to the generalized mass density, stemming from the source's internal physical characteristics, results in an extra, negative mass, the so-called internal mass, contributing to the geodesic motions in the source. As a consequence, a new picture emerges for any cosmological structure as a hot structure extending well beyond its conventional boundaries. For a supercluster of galaxies, the maximal linear dimensions of the supercluster and its matter's absolute temperature are evaluated, and are found to be in accordance with the fact that no third-order clusters of galaxies have been observed up to now. The importance of the Newtonian dynamical equivalence approach to other astrophysical and planetary phenomena and open problems is indicated.

*Presented at the Workshop on *Cosmology and Gravitational Physics*, 15-16 December 2005, Thessaloniki, Greece, *Editors*: N.K. Spyrou, N. Stergioulas and C.G. Tsagas.

†spyrou@astro.auth.gr

1. Observational Introduction and Motivation

According to many current observational data, the realistic picture and morphology of all astrophysical-cosmological structures differs greatly from their corresponding optical picture (For details see Spyrou 2001-2005 and references therein). Thus the morphology of galaxies is very different from the simple picture of spiral, elliptical, or, even irregular galaxies, in the sense that the galaxies (as well as the clusters of galaxies, and, possibly, the second-order clusters (superclusters) of galaxies) are almost spherically symmetric, very complex, practically continuous, and of much larger linear dimensions cosmological structures than previously assumed. The observable Universe differs very much from the simple picture of a collection of galaxies (or higher-order cosmological structures), in which the mutual distances of the neighboring members are much larger than their linear dimensions. Consequently, *the constituting elements of the Universe and, plausibly, the Universe in its large scales*, should preferably be treated as continuous gravitational systems and, more specifically, bounded, gravitating perfect-fluid sources, the physical-dynamical description of which is very well established in both the Newtonian and the general-relativistic levels. The Newtonian dynamical equivalence approach is briefly exposed in the next Section 2. In Section 3 we describe the possibility of attractive and repulsive gravity in the interior of a source like the above, and in Section 4 we examine the importance of the internal mass and the implications on the linear dimensions and structure of the fluid source-large scale cosmological structure. In Section 5 we present some cosmological applications. In the final Section 6 we conclude and discuss the possibility of planetary, astrophysical and cosmological perspectives of the Newtonian framework of the dynamical-equivalence approach.

2. Newtonian Dynamical Equivalence of Hydrodynamical Flows and Geodesics

In view of many current observational data and indications, it has been suggested (Kleidis and Spyrou 2000) that, in both the Newtonian and the general-relativistic theories of gravity, and at all the levels, namely, cosmological (Kleidis and Spyrou 2000; Spyrou 2001, 2002, 2003), galactic (Kleidis and Spyrou 2000; Spyrou 1997a,b, 1999, 2001, 2002; Spyrou and Kleidis 1999; Spyrou and Tsagas 2004), and stellar (Kleidis and Spyrou 2000; Spyrou 1997a,c; Spyrou 1999), it is possible to give to the equations of the hydrodynamical (and hydromagnetic) flow motions in the interior of a bounded gravitating perfect-fluid source the form of the equations of the geodesic motions in it. More precisely, applying the *equilibrium hydrodynamics hypothesis* for the isentropic flows, and assuming that along the flow lines the entropy is a group invariant, we can prove that the Euler equations for hydrodynamical flows can be written in the form of *Newton's equations* for the geodesic motions, namely,

$$\frac{d\bar{u}}{dt} = \bar{\nabla}V, \quad (1)$$

where the generalized (scalar) potential V is defined as

$$V = U - \left(\Pi + \frac{p}{\rho} \right). \quad (2)$$

In Eq. (1), which generalizes the standard Newtonian equations for the geodesic motions (the motions of a test particle)

$$\frac{d\bar{u}}{dt} = \bar{\nabla}U, \quad (3)$$

ρ , p , and Π are, respectively, the fluid source's rest-mass, isotropic pressure, and internal specific energy density, while the Newtonian gravitational potential U obeys the standard *Newtonian field equation (Poisson's Equation)*

$$\nabla^2 U = -4\pi G\rho, \quad (4)$$

with G being the universal constant of gravitation.

Moreover, in analogy to Eq. (4), the generalized mass-energy density, ρ_V , producing the potential V and, hence, the generalized geodesic equations of motion (1) is defined through the *Poisson-type field equation*

$$\nabla^2 V = -4\pi G\rho_V, \quad (5)$$

Direct consequence of Eqs. (4) and (5) is

$$\rho_V = \rho + \rho_i \quad (6)$$

where

$$\rho_i = \frac{1}{4\pi G} \nabla^2 \left(\Pi + \frac{p}{\rho} \right) = \frac{1}{4\pi G} \left[\bar{\nabla} \cdot \left(\frac{1}{\rho} \bar{\nabla} p \right) \right], \quad (7)$$

is the so-called *the internal-mass density* physically describing the contribution to the source of the generalized geodesic motions of the fluid source's all internal physical characteristics. Notice that Eq. (5) is a direct consequence of Eqs (2) and (4), and of the *equilibrium hydrodynamical hypothesis* for the isentropic flows.

It is obvious that the mass m_V , which corresponds to the density ρ_V producing the generalized potential V , is

$$m_V = \int_V \rho_V d^3x, \quad (8)$$

where V is the three-dimensional volume of the source considered. In view of Eqs. (6) and (8),

$$m_V = m + m_i, \quad (9)$$

namely, the mass m_V differs from the rest-mass (baryonic mass)

$$m = \int_V \rho d^3x, \quad (10)$$

by the inertial mass

$$m_i = \int_V \rho_i d^3x, \quad (11)$$

The astrophysical and cosmological significance of the above results lies in the fact that *the mass m_V (defined as the three-dimensional volume of the total density) determined at any moment with the aid of the geodesic motions is not m , which is produced by the potential U , as it is generally believed and applied, but m_V , which is produced by the generalized potential V , in which all the internal physical characteristics of the fluid source manifest themselves as sources of geodesic motions.* (For details and numerical data see Kleidis and Spyrou 2000, Spyrou 2002-2005b, and Spyrou and Tsagas 2004).

3. Attractive Gravity and Repulsive Gravity

Now we wish to remark that, unlike Eqs. (3) and (4) implying

$$\bar{\nabla} \cdot \left(\frac{d\bar{u}}{dt} \right) = \nabla^2 U = -4\pi G\rho < 0, \quad (12)$$

the generalized equations (1), (2), and (5) do not necessarily imply an inwards acceleration solely (namely, only attractive gravity), because

$$\bar{\nabla} \cdot \left(\frac{d\bar{u}}{dt} \right) = \bar{\nabla} \cdot (\bar{\nabla} V) = \nabla^2 V = -4\pi G\rho_V. \quad (13)$$

Therefore,

$$\nabla \cdot \left(\frac{d\bar{u}}{dt} \right) \begin{matrix} \leq \\ > \end{matrix} 0 \Leftrightarrow \rho_V \begin{matrix} \geq \\ < \end{matrix} 0 \quad (14)$$

or, equivalently,

$$\text{spatially decreasing } \frac{d\bar{u}}{dt} \text{ implies } \rho_V > 0 \quad (\nabla^2 V = -4\pi G\rho_V < 0); \quad (15)$$

$$\text{spatially non changing } \frac{d\bar{u}}{dt} \text{ implies } \rho_V = 0 \quad (\nabla^2 V = 0); \quad (16)$$

$$\text{spatially increasing } \frac{d\bar{u}}{dt} \text{ implies } \rho_V < 0 \quad (\nabla^2 V = -4\pi G\rho_V > 0) \quad (17)$$

and vice versa.

According to the above,

$$\rho_V > 0 \text{ implies dominance of inwards acceleration (attractive gravity);} \quad (18)$$

$$\rho_V = 0 \text{ implies non changing acceleration;} \quad (19)$$

$$\rho_V < 0 \text{ implies dominance of outwards acceleration (repulsive gravity...)} \quad (20)$$

The possible significance of the above results (12)-(20) in astrophysics and cosmology is that in the (Newtonian) context of the dynamical approach the possibility of repulsive gravity appears. Here we point out that it is rather straightforward to verify from the definition (7) for ρ_i , that, in realistic cases, ρ_i cannot be a constant or vanishing (See Spyrou, unpublshed) and, hence, ρ_V can have any sign, $\rho_V \lesseqgtr 0$, as stated above. Also, for a given form of the rest-mass density law and for the equation of state of the (spherically-symmetric) fluid source, the vanishing of ρ_V is an algebraic equation for the radial distance. The solution to this equation determines the so-called *inversion distance*. Details on the notion of the inversion distance in the case of a large-scale cosmological structure are given in the next Section.

4. Possible Cosmological Significance of the Internal - Mass Density: The Inversion Distance

In this Section we shall examine the relative importance of the rest-mass density, ρ , and the internal-mass density, ρ_i , in astronomical and cosmological structures, and its consequences. The rest-mass density distribution law to be used here is not arbitrary and stems from the well-known observation-based "universal profile" of Navarro, Frenk and White (1995; 1997) and the Hernquist (1991) profile (see also Dehnen 1995; Mcgough 2002; Syer and White 1998; and Zhao 1996) for the density distribution law of clusters of galaxies. So, in the case of a spherically symmetric source, we shall adopt a special case of the above profiles, namely, the *Plummer-type density* described by

$$\rho(r) = \rho_0 \left(1 + \frac{r^2}{r_0^2}\right)^{-n/2} \quad (r_0 > 0, \rho_0 > 0, n : \text{a positive integer}) \quad (21)$$

where r is the radial distance from the origin-centre of the source. Furthermore, we shall assume that the fluid source is described by a thermal equation of state of the form

$$p = k\rho, \quad k = \frac{k_B T}{\mu m_H}, \quad (22)$$

with m_H , T , μ , and k_B being, respectively, the mass of the atomic hydrogen, the absolute temperature of the source, the mean molecular weight of the material content of the source, and the Boltzmann constant.

Using Eqs. (21, for $n=3$) and (7) we find

$$\frac{-\rho_i}{\rho} = \alpha \frac{2 + z^2}{z}, \quad (23)$$

where

$$z = \left(1 + \frac{r^2}{r_0^2}\right)^{1/2} \geq \sqrt{2}, \quad (r \geq r_0) \quad (24)$$

and

$$\alpha = \frac{3k_B T}{\mu m_H} \frac{1}{4\pi G \rho_0 r_0^2}. \quad (25)$$

Then, first we notice that, by assumption,

$$r_0 = 3R_s = \frac{6GM_c}{c^2}, \quad (26)$$

where the mass M_c of the central object of the structure is approximated by

$$M_c = \frac{4}{3}\pi r_0^3 \rho(r = r_0) = \frac{4}{3}\pi r_0^3 \frac{\rho_0}{2^{3/2}}, \quad (27)$$

whence

$$4\pi G \rho_0 r_0^2 = \sqrt{2}c^2, \quad (28)$$

or

$$\rho_0 = 1.930 \times 10^{-9} (M_c/M_\odot)^2 \text{ gr} \cdot \text{cm}^{-3} \quad (29)$$

and

$$\alpha = \frac{3}{\sqrt{2}} \frac{k_B T}{\mu m_H c^2}. \quad (30)$$

Notice that, in the case of a supermassive black hole of mass $M_c \sim 10^9 m_\odot$, we find $r_0 \sim 10^{15}$ cm, whence the condition (28) implies $\rho_0 \sim 10^{-3}$ gr · cm⁻³, namely, about twenty orders of magnitude larger than the mass density of the Milky Way in the solar neighborhood ($\sim 10^{-24}$ gr · cm⁻³).

Then we notice that the condition

$$\frac{-\rho_i}{\rho} \underset{<}{\geq} 1 \quad (\text{equivalently, } 0 \underset{<}{\geq} \rho + \rho_i = \rho_V) \quad (31)$$

is equivalent to

$$\varphi(z) = z^2 - \frac{1}{\alpha}z + 2 \underset{<}{\geq} 0. \quad (32)$$

The discriminant

$$\Delta = \frac{1}{\alpha^2} - 8 \quad (33)$$

of the binomial $\phi(z)$ satisfies

$$\Delta \underset{<}{\geq} 0, \quad \text{when } T \underset{>}{\leq} T_{lim} \quad (34)$$

with

$$\frac{T_{lim}}{\mu} = \frac{m_H c^2}{6k_B} \sim 1.817 \times 10^{12} \text{ K} \quad (35)$$

Therefore

1. For $T \geq T_{lim}$ ($\Delta \leq 0$), $\varphi(x) > 0$, $\rho + \rho_i < 0$ (36)

2. For $T < T_{lim}$ ($\Delta > 0$), from the two solutions of the equation (32) only one (the largest ($z \geq \sqrt{2}$)) is acceptable, namely,

$$r = r_{inv} ; \frac{r_{inv}^2}{r_0^2} = \frac{1}{4} \left(\frac{1}{\alpha} + \left(\frac{1}{\alpha^2} - 8 \right)^{1/2} \right)^2 - 1 \quad (37)$$

such that

$$\text{a) If } r < r_{inv}, \text{ then } \rho + \rho_i > 0 \text{ (inwards acceleration or attractive gravity)} \quad (38)$$

$$\text{b) If } r = r_{inv}, \text{ then } \rho + \rho_i = 0 \text{ (non changing acceleration)} \quad (39)$$

$$\text{c) If } r > r_{inv}, \text{ then } \rho + \rho_i < 0 \text{ (outwards acceleration or repulsive gravity)} \quad (40)$$

In the special case $\Delta \gg 0$, namely, $T \ll T_{lim}$, which is believed to apply in almost all of the cosmological large-scale structures, Eqs. (37) and (24) reduce to, respectively,

$$\frac{r_{inv}}{r_0} = \frac{1}{\alpha} = \frac{\sqrt{2}}{3} \frac{\mu m_H c^2}{k_B T} \gg 1 \quad (41)$$

$$z_{inv} \sim \frac{r_{inv}}{r_0} \quad (42)$$

Representative values of the inversion distance, for various cosmological structures, and for reasonable values of T/μ , as given elsewhere (Spyrou, unpublished; see also next Section) are seen to be comparable to the currently accepted linear dimensions of the corresponding structure. Moreover, on simply physical grounds, we observe that, for increasing r , smaller than the inversion distance, the gravitational repulsion of the negative internal mass is smaller than the gravitational attraction of the positive rest-mass. The matter accelerates inwards and eventually reaches an equilibrium situation due to the action of some kind of pressure (here thermal pressure). At the inversion distance, the gravitational repulsion and gravitational attraction cancel each other. Beyond the inversion distance an inversion occurs, namely, the gravitational repulsion, described essentially by the quantity $-(\Pi + p/\rho)$, dominates over the gravitational attraction, and matter accelerates outwards up to the external boundaries of the source. Therefore, we conclude that, in general, mass, probably more dilute and hot, might exist also beyond the conventional limits of the structure. This means that the real dimensions of the structure might be much larger, than thought up to now. For the case of a supercluster of galaxies, this is examined in the next Section (For further details see Spyrou, unpublished).

5. Some Cosmological Applications

In this Section we present some applications of the above framework in the case of a supercluster of galaxies, which reveal/verify an emerging new picture of large-scale cosmological structures.

In the case of a typical supercluster of galaxies, Eq. (41) is written in the form

$$\frac{T_{(4)}}{\mu} = 1.476 \xi ; \quad \xi = \frac{M_{c(12)}}{r_{inv(100)}} \quad (43)$$

where T , M_c , and r_{inv} are measured in units of 10^4 K, $10^{12} M_\odot$, and 100 Mpc, respectively. Therefore, identifying the conventional dimensions of the supercluster with r_{inv} and assuming additionally that, for a supercluster of galaxies, $M_{c(12)} = 1$ (more generally, if $\xi = 1$), we find

$$\frac{T_{(4)}}{\mu} = 1.476. \quad (44)$$

Therefore, the absolute temperature of the *matter* in a supercluster of galaxies is of the order of 10^4 K.

As mentioned already, current observational data suggest, that matter-energy should exist beyond the conventional dimensions (inversion distance) of a structure. Obviously, outward motions beyond the inversion distance can exist provided that the thermal velocity at the inversion distance is larger than the escape velocity (parabolic velocity) at the inversion distance. An analytic treatment of the escape velocity at a point interior to a fluid source is given elsewhere (Spyrou, under preparation). Here we shall use for the escape velocity the approximate expression $2Gm_V(r)/r)^{1/2}$ which, however, is the dominant term and results in a value of the temperature in accordance to Eq. (44). Thus, since the thermal kinetic energy is $(3/2)k_B T$ and since, for $r \gg r_0$ (Spyrou 2004a),

$$m_V(r) = 4\pi\rho_0 r_0^3 \ln\left(\frac{r}{r_0}\right) - \frac{3k_B T}{G\mu m_H} r. \quad (45)$$

The above requirement reads

$$\frac{9k_B T}{\mu m_H} \leq 2\sqrt{2}c^2 \left[\frac{\ln\left(\frac{r}{r_0}\right)}{\left(\frac{r}{r_0}\right)} \right], \quad (46)$$

from which, for $\xi = 1$, we find

$$\frac{T_{(4)}}{\mu} \leq 19.352 \quad (47)$$

in accordance with Eq. (44).

Next, the outwards motions, beyond the inversion distance, will stop at the outer limits (real boundaries), r_{max} , of the structure, provided that, at r_{max} , the thermal velocity is smaller than the escape velocity there, . In the same way, as for the condition (46), we find

$$\frac{\ln\left(\frac{r_{max}}{r_0}\right)}{\left(\frac{r_{max}}{r_0}\right)} \geq \frac{9}{2\sqrt{2}} \frac{k_B}{m_H c^2} \frac{T}{\mu} \quad (48)$$

Hence, for $T/\mu = 1.476 \times 10^4$ K and $\xi = 1$, we find

$$\frac{r_{max}}{r_0} \leq 0.5192 \times 10^{10} \quad (49)$$

or, since, for a $10^{12} M_\odot$ central black hole

$$r_0 = 2.872 \times 10^{-7} \text{ Mpc} \quad (50)$$

we finally obtain

$$r_{max} \leq 0.49 \times 10^{10} \text{ lyr} \sim 0.49 \times \text{Dimensions of the observable universe}. \quad (51)$$

We conclude that only very few superclusters seem to be enough to comprise the whole observable Universe. Quite interestingly, this result is in accordance with and explains the fact that no third-order superclusters of galaxies are necessary (and so have not been observed up to now).

6. Conclusions

Motivated by a wealth of relevant observational data and based on the Newtonian dynamical equivalence approach, we presented some novel ideas concerning the structure of and motions in large-scale cosmological structures treated as continuous gravitating perfect-fluid sources. The introduced notion of the inversion distance permits the discrimination, inside the source, of regions of attracting and repulsive gravity, determines the true dimensions and temperature of the source, and reveals a totally new picture of the cosmological structures. In the case of a supercluster of galaxies the matter's temperature is of the order of 10^4 K and its true dimensions are approximately half the dimensions of the observable universe in agreement with the lack of observed third-order clusters of galaxies. Finally, we indicate here the possible importance of the dynamical equivalence approach in explaining interesting and currently open problems in planetary science e.g. the *Pioneer anomaly*, and in astrophysical-cosmological science e.g. the formation of jets. Problems like the above are currently under consideration.

References

- [1] Dehnen, W. 1995, MNRAS **274**, 919-932.
- [2] Hernquist, L. 1990, Ap. J. **356**, 359-364.
- [3] Kleidis, K., and Spyrou, N.K. 2000, Class. Quantum Grav. **17**, 2965-2982.
- [4] McGough, S.S. 2002, in *The Shapes of Galaxies and Their Dark Halos*, Yale University Workshop, Ed. P.Natarajan (World Scientific Publishing Pte. Ltd.) pp. 186-193.
- [5] Navarro, J.F., Frenk, C.S., and White, S.D.M. 1995, MNRAS **275**, 720-740.
- [6] Navarro, J.F., Frenk, C.S., and White, S.D.M. 1997., Ap. J. **490**, 493-508.
- [7] Spyrou, N.K. 1997a, in *The Physics of Ionized Gases* Proceedings of the 18th Summer School and International Symposium on the Physics of Ionized Gases (Kotor, Yugoslavia, 2-6 September 1996), eds. B.Vujicic, S. Djurovic and I.Puric, Institute of Physics, Novi Sad University, Yugoslavia, pp.417-446.

- [8] Spyrou, N.K. 1997b, in *The Earth and the Universe*, Volume in Honorem L. Mavrides, eds. G. Asteriadis, A. Bandellas, M. Contadakis, K. atsambalos, A. Papademetriou and I. Tziavos, Thessaloniki, Greece, pp. 277-291.
- [9] Spyrou, N.K. 1997c, *Facta Universitatis* **4**, 7-14.
- [10] Spyrou, N.K. 1999, in *Current Issues of Astronomical and Planetary Environmental Concern*, Proceedings of International Seminar (Thessaloniki, 6-7 April 1999) ed. N.K.Spyrou, Astronomy Department, Aristoteleion University of Thessaloniki, Thessaloniki, Greece, pp.23-35.
- [11] Spyrou, N.K. 2001 "Conformal Invariance and the Nature of Cosmological Structures", Invited Talk, Proceedings of *The Conference on Applied Differential Geometry-General Relativity*, and *The Workshop on Global Analysis, Differential Geometry, Lie Groups*, (Thessaloniki, 27 June-1July 2001) eds. G. Tsagas, C. Udriste, and D. Papadopoulos, pp. 101-107.
- [12] Spyrou, N.K 2002, "On the Determination of the Masses of Cosmological Structures" in *Modern Theoretical and Observational Cosmology*, Proceedings of the 2nd Hellenic Cosmology Meeting (Athens, 19-20 April 2001), eds. M.Plionis and S.Cotsakis, Kluwer Academic Publishers, Dordrecht, Vol. 276, pp.35-43.
- [13] Spyrou, N.K. 2003, "Conformal Dynamical Equivalence and the Cosmological Expansion of a Realistic Universe", in Proceedings of the *10th Conference Recent Developments in Gravity*, eds. K. Kokkotas and N. Stergioulas, Kluwer, Academic Publishers, Dordrecht, pp.90-96.
- [14] Spyrou, N.K. 2004a, "A Classical Treatment of the Dark-Matter and Flat-Rotation-Curves Problems", in Proceedings of the *6th Hellenic Astronomical Conference* (Penteli, Athens), September 2003, ed. P.G. Laskarides (and Editioning Office of the University of Athens), Athens, pp. 229-234.
- [15] Spyrou, N.K. 2004b, "A Classical Treatment of the Problems of Dark Energy, Dark Matter, and Accelerating Expansion", presented in Proceedings of the Conference *Recent Developments in Gravity (NEB) XI* (Mytilini, Lesvos, Hellas) 2-6 June 2004.
- [16] Spyrou, N.K. 2005a, *J. Phys. Conf. Ser.* **8**, 122-130.
- [17] Spyrou, N.K. 2005b, unpublished.
- [18] Spyrou, N.K. and Kleidis, K. 1999, "On the Nature of Nuclear Galactic Masses" in Proceedings of JENAM 1999, Samos.
- [19] Spyrou, N.K., and Tsagas, C.G. 2004, *Class. Quantum Grav.* **21**, 2435-2444.
- [20] Spyrou, N.K., and Tsagas,C.G 2006, in preparation.
- [21] Syer, D., and White, S.D.M.,1998, *MNRAS* **293**, 337-342.
- [22] Zhao,H.S., 1996, *MNRAS* **278**, 488-496.

MAGNETIZED PARTICLE DYNAMICS IN THE PRESENCE OF GRAVITATIONAL WAVES *

L. Vlahos [†]

Aristotle University of Thessaloniki,
Department of Physics, Section of Astrophysics, Astronomy and Mechanics,
Thessaloniki, 54124 Greece

Abstract

The non-linear interaction of a strong Gravitational Wave with the plasma during the collapse of a massive magnetized star to form a black hole, or during the merging of neutron star binaries (central engine) was investigated. Under certain conditions this coupling may result in an efficient energy space diffusion of particles. Superposition of many such short lived accelerators, embedded inside a turbulent plasma, may be the source for the observed impulsive short lived bursts. In several astrophysical events, gravitational pulses may accelerate the tail of the ambient plasma to very high energies and become the driver for many types of astrophysical bursts.

1. Introduction

The interaction of Gravitational Waves (GW) with the plasma and/or the electromagnetic waves propagating inside the plasma, has been studied extensively (DeWitt & Breme (1960); Cooperstock (1968); Zeldovich (1974); Gerlach (1974); Grishchuk & Polnarev (1980); Denisov (1978); Macdonald & Thorne (1982); Demianski (1985); Daniel & Tajima (1997); Brodin & Marklund (1999); Marklund, Brodin & Dunsby (2000); Brodin, Marklund & Dunsby (2000); Brodin, Marklund & Servin (2001); Servin et al. (2000); Servin, Brodin & Marklund (2001); Moortgat & Kuijpers (2003), Vlahos et al. (2004); Voyatzis et al. (2006)). All well known approaches for the study of the wave-plasma interaction have been used, namely the Vlasov-Maxwell equations (Macedo & Nelson (1982)), the MHD equations (Papadopoulos & Esposito (1981); Papadopoulos et al. (2001); Moortgat & Kuijpers (2003)) and the non-linear evolution of charged particles interacting with a monochromatic GW (Varvoglis & Papadopoulos (1992)). The Vlasov-Maxwell equations and the MHD equations were mainly used to investigate the linear coupling of the GW with the

*Presented at the Workshop on *Cosmology and Gravitational Physics*, 15-16 December 2005, Thessaloniki, Greece, *Editors*: N.K. Spyrou, N. Stergioulas and C.G. Tsagas.

[†]In collaboration with G. Voyatzis and D. Papadopoulos

normal modes of the ambient plasma, but the normal mode analysis is a valid approximation only when the GW is relatively weak and the orbits of the charged particles are assumed to remain close to the undisturbed ones. Several studies have also explored, using the weak turbulence theory, the non-linear wave-wave interaction of plasma waves with the GW (see Brodin et al. (2000)).

The strong nonlinear coupling of isolated charged particles with a coherent GW was studied using the Hamiltonian formalism (Varvoglis & Papadopoulos (1992); Kleidis, Varvoglis & Papadopoulos (1993); Kleidis et al. (1995)). The main conclusion of these studies was that the coupling between GW and an isolated charged particle gyrating inside a constant magnetic field can be very strong only if the GW is very intense. This type of analysis can treat the full non-linear coupling of the charged particle with the GW but loses all the collective phenomena associated with the excitation of waves inside the plasma and the back reaction of the plasma onto the GW.

Vlahos et al. (2004) re-investigate the non-linear interaction of an electron with a GW inside a magnetic field, using the Hamiltonian formalism. Their study is applicable at the neighborhood of the central engine (collapsing massive magnetic star, see Fryer, Holz & Hughes (2002); Dimmelmeier, Font & Muller (2002); Baumgarte & Shapiro (2003)) or during the final stages of the merging of neutron star binaries (Ruffert & Janka (1998); Shibata & Uryu (2002)). A strong but low frequency (10 KHz) GW can resonate with ambient electrons only in the neighborhood of magnetic neutral sheets and accelerates them to very high energies in milliseconds. Relativistic electrons travel along the magnetic field, escaping from the neutral sheet to the super strong magnetic field, and emitting synchrotron radiation. Vlahos et al. (2004) propose that the passage of a GW through numerous localized neutral sheets will create spiky sources which collectively produce the highly variable in time.

2. The Hamiltonian formulation of the GW-particle interaction

The motion of a charged particle in a curved space and in the presence of a magnetic field is described by a Hamiltonian, which, in a system of units $m = c = G = 1$, is given by

$$H(x^\alpha, p_\alpha) = \frac{1}{2}g^{\mu\nu}(p_\mu - eA_\mu)(p_\nu - eA_\nu) = \frac{1}{2}, \quad \alpha, \mu, \nu = 0, \dots, 3. \quad (1)$$

$g^{\mu\nu} = g^{\mu\nu}(x^\alpha)$ are the contravariant components of the metric tensor of the curved space and $A_\mu = A_\mu(x^\alpha)$ are the components of the vector potential of the magnetic field (Misner, Thorne & Wheeler (1973)). The variables p_α are the generalized momenta corresponding to the coordinates x^α , and their evolution with respect to the proper time τ is given by the canonical equations

$$\frac{dx^\alpha}{d\tau} = \frac{\partial H}{\partial p_\alpha}, \quad \frac{dp_\alpha}{d\tau} = -\frac{\partial H}{\partial x^\alpha}. \quad (2)$$

A constant magnetic field $\vec{B} = B_0\vec{e}_z$ is assumed and is produced by the vector

potential

$$A_0 = A_1 = A_3 = 0, \quad A_2 = B_0(x^1 + c_0), \quad c_0 : \text{const.}, \quad (3)$$

and that a GW propagates in a direction \vec{k} of angle θ with respect to the direction of the magnetic field. In that case the nonzero components of the metric tensor are (see Ohanian (1976); Papadopoulos & Esposito 1981) $g^{00} = 1$ and

$$\begin{aligned} g^{11} &= \frac{1-a \sin^2 \theta \cos \psi}{-1+a \cos \psi} & g^{22} &= \frac{-1}{1+a \cos \psi} \\ g^{33} &= \frac{1-a \cos^2 \theta \cos \psi}{-1+a \cos \psi} & g^{13} &= g^{31} = \frac{(-a/2) \sin 2\theta \cos \psi}{-1+a \cos \psi}, \end{aligned} \quad (4)$$

where a is the amplitude of the GW and $\psi = k_\mu x^\mu = \nu(\sin \theta x^1 + \cos \theta x^3 - x^0)$. The parameter ν is the relative frequency of the GW, i.e. $\nu = \omega/\Omega$, where $\Omega = eB_0/mc$ is the Larmor angular frequency. The scaling $eB_0 = 1$, thus $\Omega = 1$ is used.

In the above formalism, the coordinate x^2 is ignorable, so $p_2 = \text{const.}$. By setting the constant c_0 in Eq. (3) equal to p_2 we get an appropriate gauge that reduces by one degree of freedom the Hamiltonian (Eq. (1)), which takes the form

$$H = \frac{1}{2} \left(p_0^2 - \frac{1 - a s_\theta^2 \cos \psi}{1 - a \cos \psi} p_1^2 - \frac{1 - a c_\theta^2 \cos \psi}{1 - a \cos \psi} p_3^2 + \frac{2 a s_\theta c_\theta \cos \psi}{1 - a \cos \psi} p_1 p_3 - \frac{x_1^2}{1 + a \cos \psi} \right), \quad (5)$$

where we use the notation $c_\theta = \cos \theta$ and $s_\theta = \sin \theta$ for brevity. The canonical transformation of variables $(x^0, x^1, x^3, p_0, p_1, p_3) \rightarrow (\chi, q, \phi, I, p, J)$ is applied and the generating function used is

$$F(x^0, x^1, x^3, I, p, J) = x^0 I + x^1 p + \nu(s_\theta x^1 + c_\theta x^3 - x^0) J. \quad (6)$$

The relation between the old and the new variables is given by the equations

$$\begin{aligned} \chi &= x^0, & I &= p_0 + p_3/c_\theta \\ q &= x^1, & p &= p_1 - (s_\theta/c_\theta)p_3 \\ \phi &= \nu(s_\theta x^1 + c_\theta x^3 - x^0) & J &= p_3/(c_\theta s_\theta). \end{aligned} \quad (7)$$

In the new variables the Hamiltonian (Eq. (5)) takes the form

$$H = \frac{1}{2} \left(I^2 - 2I\nu J - 2s_\theta \nu J p - \frac{1 - a s_\theta^2 \cos \phi}{1 - a \cos \phi} p^2 - \frac{q^2}{1 + a \cos \phi} \right). \quad (8)$$

Since the variable χ is ignorable, I is a constant of motion and Eq. (8) can be studied as a system of two degrees of freedom, where I is a parameter. The variables q and p are associated with the gyro-motion. H is of mod(2π) with respect to the angle-variable ϕ and the variable J is related linearly with the energy $\gamma = (1 - \nu^2)^{-1/2}$ of the particles according to the equation

$$\gamma = I - \nu J. \quad (9)$$

The equations of motion are

$$\begin{aligned} \dot{q} &= -s_\theta \nu J - \frac{1 - a s_\theta^2 \cos \phi}{1 - a \cos \phi} p & \dot{p} &= \frac{q}{1 + a \cos \phi} \\ \dot{\phi} &= -\nu I - s_\theta \nu p & \dot{J} &= \frac{a}{2} \left(\frac{q^2}{(1 + a \cos \phi)^2} - \frac{c_\theta^2 p^2}{(1 - a \cos \phi)^2} \right) \sin \phi, \end{aligned} \quad (10)$$

where the dot means derivative with respect to the proper time τ . Furthermore, Eq.(8) can be written as a perturbed Hamiltonian in the usual way, i.e.

$$H = H_0 + aH_1 + a^2H_2 + \dots, \quad (11)$$

where

$$H_m = -(c_\theta^2 p^2 + (-1)^m q^2) \cos^m \phi, \quad m \geq 1 \quad (12)$$

are the perturbation terms and

$$H_0 = \frac{1}{2}(I^2 - 2I\nu J - 2s_\theta\nu Jp) - \frac{1}{2}(p^2 + q^2) \quad (13)$$

is the integrable part of the system that describes the unperturbed helical motion of the particle in the flat space. Considering action-angle variables $(J_1, J_2, \phi_1, \phi_2)$, Eq.(13) takes the form

$$H_0(J_1, J_2) = \frac{I}{2} - I\nu J_1 + \frac{s_\theta^2 \nu^2}{2} J_1^2 - J_2, \quad (14)$$

where $\phi_1 = \phi, J_1 = J$ and

$$J_2 = \frac{1}{2\pi} \oint pdq = \frac{1}{2}(I^2 - 2I\nu J + s_\theta^2 \nu^2 J^2 - 1), \quad \phi_2 = \arcsin\left(\frac{\pm q}{\sqrt{2J_2}}\right).$$

Therefore, the unperturbed system is isoenergetically non-degenerate for $\theta \neq 0$ (Arnol'd, Kozlov & Neishtadt (1987)) and the gyro motion of the particles is represented by trajectories that twist invariant tori with angular frequencies $\omega_1 = \partial H_0 / \partial J_1$ and $\omega_2 = \partial H_0 / \partial J_2$. The periodic or quasi-periodic evolution of the trajectories depends on whether the rotation number, defined by

$$\rho = \frac{\omega_1}{\omega_2} = \nu I - s_\theta^2 \nu^2 J_1 = \nu(c_\theta^2 I + s_\theta^2 \gamma), \quad (15)$$

is rational or irrational, respectively.

Most of the invariant tori will persist with the presence of the perturbation introduced by the GW, if the amplitude is sufficiently small, according to the KAM theorem (Arnol'd et al. (1987)). The orbits of the particles remain close to the unperturbed ones but their projection on the $x^1 - x^2$ plane is not exactly circular and periodic. Close to the resonant tori, where ρ is rational, the Poincaré-Birkhoff theorem applies; a finite number of pairs of stable and unstable periodic trajectories survive, producing locally a pendulum like topology in phase space (Sagdeev, Usikov & Zaslavsky (1988)).

Since the system is of two degrees of freedom, we can study its evolution by using the Poincaré sections $P_S = \{(\phi, \gamma), q = 0, H = 1/2\}$ choosing specific sets of the parameters a, I, ν and θ . In the numerical calculations, which will follow, we set $I = 1$. For the unperturbed system ($a = 0$) the sections show invariant curves $\gamma = \text{const}$. For $a \neq 0$ some typical examples are shown in Fig.1.

For small values of a (Fig.1a), the invariant curves are perturbed slightly and only close to the most significant resonances their deformation becomes noticeable.

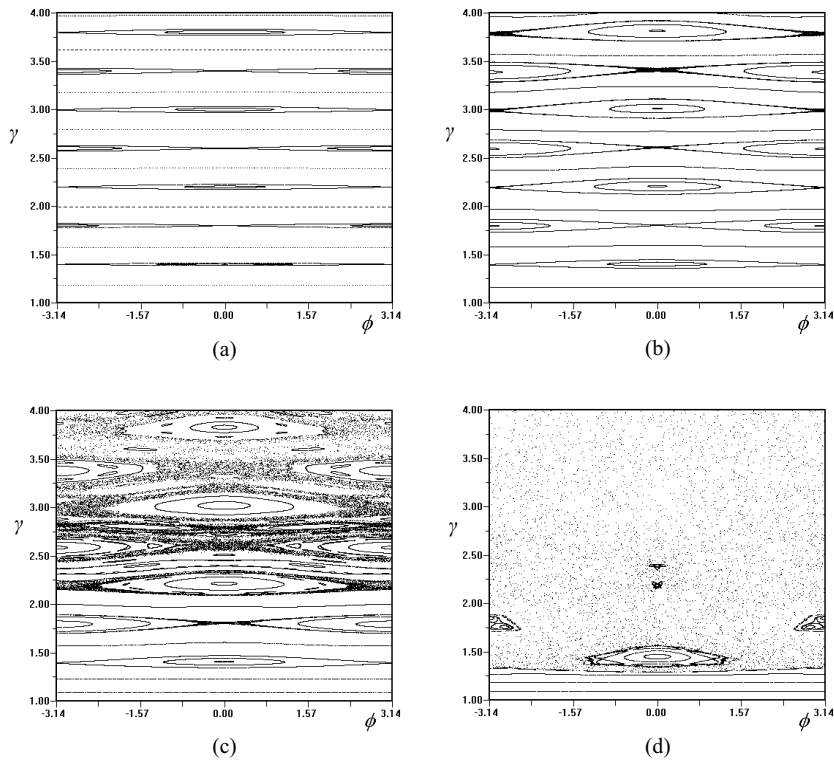


Figure 1: Typical Poincaré sections on the plane (ϕ, γ) of the perturbed system for $\nu = 5, \theta = 45^\circ$ and a) $a = 0.001$ b) $a = 0.01$ c) $a = 0.02$ and d) $a = 0.1$.

Increasing further the perturbation parameter a , the width of the resonances increases and homoclinic chaos becomes more obvious close to the hyperbolic fixed points (Fig.1b). The existence of invariant curves, which confine the resonant regions, guarantees the bounded variation of the particle's energy ($\Delta\gamma = O(\sqrt{a})$) for the chaotic trajectories.

When the amplitude a exceeds a critical value a_c , overlapping of resonances takes place and large chaotic regions are generated (Fig.1c) (see also Chirikov (1979)). Particles with initial energy γ greater than a critical value γ_c may follow a chaotic orbit which diffuse to regions of higher energy, and this will lead them to very high energies in short time scales. For relatively large values of $a_c \ll a < 1$, the islands of regular motion, which survive from the resonance overlapping, are gradually destroyed and chaos extends down to relatively low energy particles (Fig.1d). The chaotic part of the phase space will be called “the chaotic sea”.

The dynamics, presented by the Poincare sections in Fig.1, is typical for the majority of parameter values. Generally, the critical values a_c and γ_c determine the conditions for possible chaotic diffusion. The dynamics of the charged particles shows some exceptional characteristics when the frequency of the GW is comparable to the Larmor frequency of the unperturbed motion, particularly when $1 \leq \nu < 3$. For such parameter values, stochastic behavior will appear when $\gamma = 1$ and for sufficiently large perturbation values large chaotic regions are generated and diffusion, even for particles with very low initial energies, will be possible. An

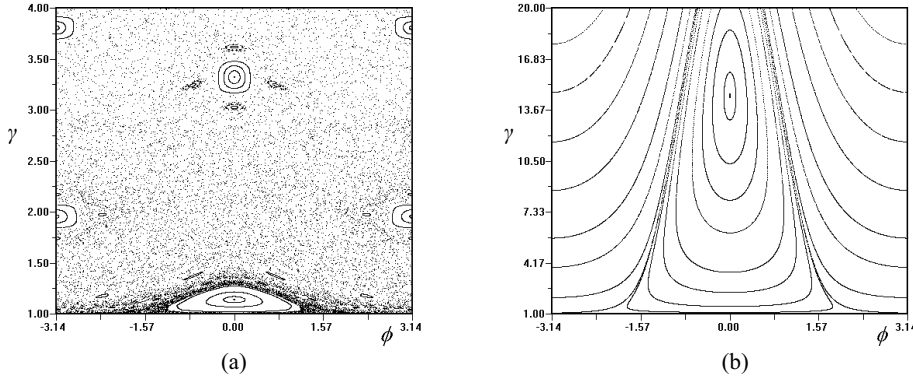


Figure 2: Poincaré sections on the plane (ϕ, γ) a) $a = 0.2, \nu = 2, \theta = 45^\circ$ b) $a = 0.2, \nu = 1, \theta = 5^\circ$.

example is shown in Fig.2a.

The evolution of the particles changes character when the direction of propagation of the GW is almost parallel to \vec{B} . In this case, chaos disappears, and the particles undergo large energy oscillations. As it is shown in Fig. 2b, a particle, starting even from rest ($\gamma \approx 1$), will be driven regularly to high energies ($\gamma > 20$) and returns back to its initial energy in an almost periodic way. In a realistic, non infinite system, several particles may escape from the interaction with the GW before returning back to low energies. At $\theta = 0$ the system is integrable and the energy of the particles shows regular slow oscillations with an amplitude proportional to a (see Voyatzis et al. (2006) for details).

3. Chaotic diffusion and particle acceleration

In the previous section, we showed that chaotic diffusion is possible for $a \geq a_c$ and for the particles with $\gamma \geq \gamma_c$. Such conditions are necessary but not sufficient for acceleration, since islands of regular motion may be present inside the wide chaotic region (see for example Fig. 2).

In Fig. 3a the evolution of γ along a temporarily trapped chaotic orbit ($\gamma < \gamma_c$) and an orbit which undergoes fast diffusion is shown, using $a = 0.02$. In Fig. 3b we plot the orbit of a particle which on the average is not gaining energy and the average rate of energy gain of 200 particles. The diffusion rate of the particles in the energy space is initially fast but for time $t > 5000$ it starts to slow down. The time t is normalized with the gyro period $2\pi/\Omega$. We study next the evolution of an energy distribution $N(\gamma, t = 0)$ of electrons interacting with the GW. In Fig. 4a we follow the evolution of 3×10^4 particles forming initially a cold energy distribution $N(\gamma, t = 0) \sim \delta(\gamma - 3)$, where δ is the Dirac delta function i.e. all particles have the same initial energy $\gamma = 3$. A large spread in their energy is achieved in short time scales, and for $t = 1000$, a non-thermal tail extending up to $\gamma = 100$ is formed.

We repeat the same analysis, assuming that the initial distribution is the tail ($v > V_{the}$, where V_{the} is the ambient thermal velocity) of a Maxwellian distribution

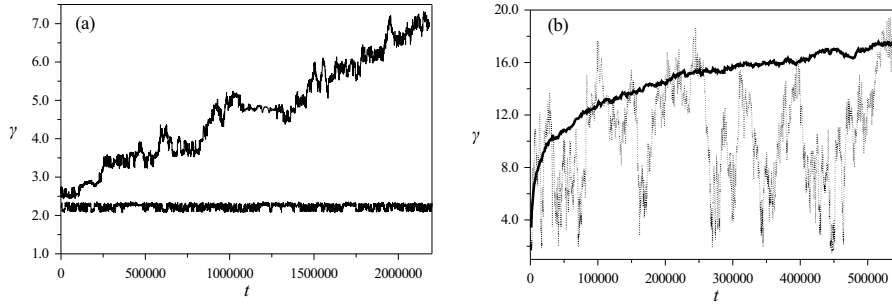


Figure 3: a) The evolution of γ along a trapped in a magnetic island chaotic orbit for $\gamma(0) = 2.2, \phi(0) = \pi$ and along a diffusive one for $\gamma(0) = 2.6, \phi(0) = 0$ ($a = 0.02, \theta = 45^\circ, \nu = 5$) b) The evolution of γ along a strongly chaotic orbit (dotted line) and its average value (solid line) along 200 trajectories starting with $\gamma(0) = 2.0$ and a randomly selected $\phi(0)$ ($a = 0.1, \theta = 45^\circ, \nu = 5$). The time is normalized with the gyro-period ($2\pi/\Omega$).

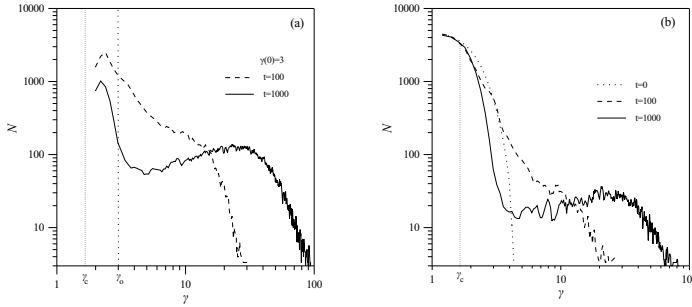


Figure 4: The evolution of an energy distribution. a) The initial distribution (dotted line) consists of 3×10^4 particles having $\gamma(t = 0) = 3$. b) The initial distributions is Maxwellian, as it is shown by the dotted curve. Only particles in the tail of the Maxwellian with $\gamma > \gamma_c$ will be accelerated. The parameters used in both studies are $a = 0.5, \nu = 20$ and $\theta = 30^\circ$.

(Fig.4b). The distribution of the high energy particle form a long non-thermal tail analogously to the results reported in Fig.(4a).

The mean energy diffusion as a function of time is plotted in Fig. ??a for a particular set of parameters, and it has the general form

$$\langle \gamma \rangle \sim t^d. \quad (16)$$

From a large number of calculations, we find that the energy spread in time follow a normal diffusion ($d = 0.5$) in energy space but as α increases (see Fig. ??b), the interaction becomes super-diffusive ($d \geq 0.5$) in energy space. This allows electrons to spread fast in energy space and explains the efficient coupling between the GW and the plasma.

4. Discussion and Summary

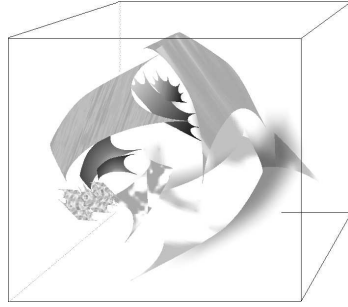


Figure 5: A schematic representation of the thin three dimensional magnetic null sheets appearing spontaneously and fill densely a driven turbulent magnetized plasma

Vlahos et al. (2005) propose a new mechanism for efficient particle acceleration around strong and impulsive sources of GW using the estimates presented above for the strong interaction of GW with electrons. They assume that in the atmosphere of the central engine a turbulent magnetic field will be formed. Inside this complex magnetic topology, a distribution of 3-D magnetic neutral sheets (magnetic null surfaces) (see Fig. 5)

The GW passing through magnetic neutral sheets and claim that the GW will enhance dramatically the acceleration process inside the neutral sheet, causing very intense bursts. We can now list several characteristics of the bursty emission driven by the model proposed above:

- A fraction of the energy carried by the orbital energy of the neutron stars at merger will go to the the GW and a portion of this energy will be transferred to the high energy electrons.
- The topology of the magnetic field varies from event to event, so every burst has its own characteristics.
- The superposition of many small scale localized sources produces a fine time structure on the burst.
- The superposition of null surfaces with a power law distribution of the acceleration lengths will result in a power law energy distribution for the accelerated electrons and an associated synchrotron radiation emitted by the relativistic electrons.
- The decay of the amplitude of the GW and/or the lack of magnetic neutral sheets away from the central engine will mark the end of the burst, but not necessarily the end of other types of bursts since the cooling of the ambient turbulent plasma has a much longer time scale.

On the basis of these findings, we propose that pulsed GW emitted from the central engine will interact with the ambient plasma in the vicinity of the magnetic

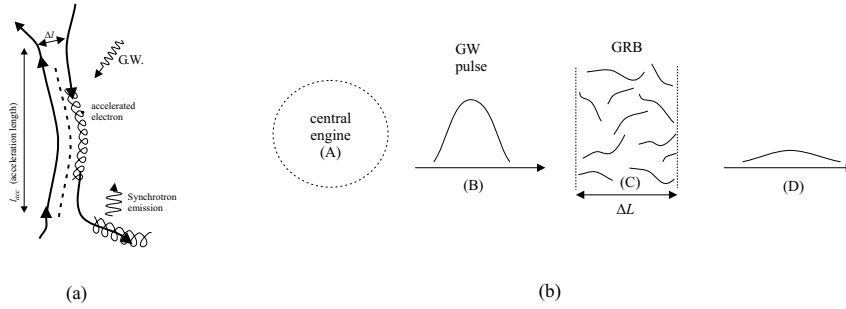


Figure 6: (a) The propagation of a GW through a magnetic neutral sheet accelerates electrons very efficiently. Relativistic electrons stream away from the accelerator and emit a pulse of synchrotron radiation when they reach the super strong magnetic fields. The dashed line represents the magnetic field null surface and ℓ_{acc} is the acceleration length. (b) A collection of magnetic neutral sheets is formed inside the turbulent atmosphere (region C) of the central engine (region A). A GW pulse propagating away from the central engine and passing through the region C will form numerous γ -ray spikes by accelerating particles near the magnetic null surfaces. The superposition of these spikes form a short lived burst. The total burst duration is approximately 100s ($\Delta T \sim \Delta L/c$) but it is composed by many short spikes lasting less than a second (ℓ/c). The GW pulse will become very weak and the density of the magnetic null surfaces will drop dramatically in the region D, and this will mark the end of the burst.

neutral sheets formed naturally inside externally driven turbulent MHD plasmas. Magnetic neutral sheets have characteristic lengths $\ell \sim 10^7 - 10^8$ cm and are short lived 3-D surfaces. Although these structures are efficient accelerators, we are emphasizing in this article only the role of the GW passing through these surfaces since we focus our attention on the very strong and bursty sources. The GW passing through the neutral sheets will accelerate electrons to very high energies (see Fig. 6). Relativistic electrons escape from the magnetic neutral sheets radiating synchrotron emission as soon as they reach the very strong magnetic fields.

A detailed model for the interaction of GW with turbulent MHD plasma is currently under study, and we hope to develop an even more efficient energy transfer from the GW to the plasma e.g by triggering the interaction (percolation) of many null sheets during the passage of the GW. We hope that this may lead us to an alternative scenario for the still unresolved questions related with the acceleration mechanism in the atmosphere of the central engines and the physical processes behind the X-ray and GRB.

Acknowledgements.

This research has been supported in part by a grant (PYTHAGORAS I) from the Ministry of Education of Greece.

References

- Arnol'd, V. I., Kozlov V. V., & Neishtadt, A. I., 1987, in *Dynamical Systems III*, ed. V. I. Arnol'd (Berlin: Springer), 116
- Baumgarte, T. W., & Shapiro, S. L., 2003, *ApJ*, 585, 930
- Brodin, G., & Marklund, M., 1999, *Phys. Rev. Lett.*, 82, 3012
- Brodin, G., Marklund, M., & Dunsby, P. K. S., 2000, *Phys. Rev. D*, 62, 104008
- Brodin, G., Marklund, M., & Servin, M., 2001, *Phys. Rev. D*, 63, 124003
- Chirikov, B. V., 1979, *Phys. Rep.* 52, 264
- Cooperstock, F. I., 1968, *Ann. Phys.*, 47, 173
- Daniel, J., & Tajima, T., 1997), *Phys. Rev. D*, 55, 5193
- Demianski, M., 1985, *Relativistic Astrophysics* (Oxford: Pergamon)
- Denisov, V. I., 1978, *Soviet. Phys.-JETP*, 42,209
- DeWitt, B. S., & Breheme, R. W., 1960, *Ann. Physics*, 9, 220
- Dimmelmeier, H., Font, A. J., & Muller, E., 2002, *A&A*, 393, 523
- Fryer, C. L., Holz, D. E., & Hughes, S. T., 2002, *ApJ*, 565, 430
- Gerlach, U. H., 1974, *Phys. Rev. Lett.* 32, 1023
- Grishchuk, L. P., & Polnarev, A. G., 1980, in *General Relativity and Gravitation: One Hundred Years after the Birth of Einstein*, Vol. 2, ed. A. Held (New York: Plenum Press), 393
- Kleidis, K., Varvoglis, H., & Papadopoulos, D., 1993, *A&A*, 275, 309
- Kleidis, K., et al., 1995, *A&A*, 294, 313
- Macdonald, D., & Thorne, K. S., 1982, *MNRAS*, 198, 345
- Macedo, P. G., & Nelson, A. G., 1982, *Phys. Rev. D*, 28, 2382
- Marklund, M., Brodin, G., & Dunsby, P. K. S., 2000, *ApJ*, 536, 875
- Misner, C. W., Thorne, K. S., & Wheeler, J. A., 1973, *Gravitation* (San Francisco: Freeman)
- Moortgat, J., & Kuijpers, J., 2003, *A&A*, 402, 905
- Ohanian, H. C., 1976, *Gravitation and Spacetime* (New York: Norton)
- Papadopoulos, D., & Esposito, F., 1981, *pJ*, 248, 783
- Papadopoulos, D., et al., 2001), *A&A*, 377, 701
- Ruffert, M., & Janka, H. T., 1998, *A&A*, 338, 535
- Sagdeev, R. Z., Usikov, D. A., & Zaslavsky, G. M., 1988, *Nonlinear Physics* (New York: Harwood)
- Servin, M., et al., 2000, *Phys. Rev. E*, 62, 8493
- Servin, M., Brodin, G., & Marklund, M., 2001, *Phys. Rev. D*, 64, 024013
- Shibata, M., & Uryu, K., 2002, *Prog. Theor. Phys.*, 107, 265
- Varvoglis, H., & Papadopoulos, D., 1992, *A&A* 261, 664
- Vlahos, L., Voyatzis, G., & Papadopoulos, D., 2004, *ApJ*, 604, 297
- Voyatzis, G.; Vlahos, L.; Ichtiaroglou, S. & Papadopoulos, D., 2006, *Physics Lett. A*, 352, 261.
- Zeldovich, Y. B., 1974, *Soviet. Phys.-JETP*, 38, 652

EXPLORING THE UNIVERSE ON THE BACK OF A GRAVITATIONAL WAVE *

K. Kleidis^{1,2} † and D. B. Papadopoulos¹ ‡

¹ Department of Physics, Aristotle University of Thessaloniki,
54124, Thessaloniki, Greece

² Department of Civil Engineering, Technological Education Institute of Serres,
62124, Serres, Greece

Abstract

The indirect interaction between cosmological gravitational waves (CGWs) and the surrounding matter content is considered, along with the evolution of the Universe from the inflationary epoch to the matter dominated era. Focusing on the power spectrum of the relic gravitational radiation, we arrive at a simple formula which relates the spectral index with the evolutionary period at which a CGW enters the horizon.

1. Introduction

The so-called cosmological gravitational waves (CGWs) represent small-scale perturbations to the Universal metric tensor (Weinberg 1972). Since gravity is the weakest of the four known forces, these metric corrections decouple from the rest of the Universe at very early times, presumably at the Planck epoch (Maggiore 2000). Their subsequent propagation is governed by the spacetime curvature (Misner et al 1973), encapsulating in the field equations the inherent coupling between relic GWs and the Universal matter content; the latter being responsible for the background gravitational field (Grishchuk and Polnarev 1980).

A GW background of cosmological origin is expected to be isotropic, stationary and unpolarized (Allen 1997). Therefore, its main property will be its frequency spectrum. Along with the propagation of relic GWs, the Universe experiences a number of (phase) transitions, mostly due to non-gravitational physics. The question that arises now is, if there are any imprints (of the various modifications in the spacetime dynamics) left on the spectrum of the CGWs during their journey from the inflationary epoch to the matter-dominated era. Provided that these imprints

*Presented at the Workshop on *Cosmology and Gravitational Physics*, 15-16 December 2005, Thessaloniki, Greece, *Editors*: N.K. Spyrou, N. Stergioulas and C.G. Tsagas.

†kleidis@astro.auth.gr

‡papadop@astro.auth.gr

can be detected at the present epoch, CGWs would be a powerful tool to study Universal evolution.

The intensity of a GW background is characterized by the dimensionless quantity (Carr 1980)

$$\Omega_{gw} = \frac{1}{\rho_c} \frac{d\rho_{gw}}{d(\ln k)} = \frac{1}{\rho_c} k \frac{d}{dk} \left[\frac{1}{2G} \int_0^\infty k^4 |\alpha(k, t)|^2 dk \right] \quad (1)$$

where, ρ_{gw} is the energy-density of the GW background, spatially averaged over several wavelengths, $\alpha(k, t)$ is the corresponding time-dependent amplitude, k is the coordinate wave-number and ρ_c is the present value of the critical energy-density for closing the Universe. In order to understand the effect of the GW background on a detector, we need to think in terms of amplitudes and therefore, it is convenient to express the *logarithmic spectrum* (1) in the form

$$\frac{d\rho_{gw}}{d(\ln k)} = \frac{1}{2G} k^2 \delta_h^2(k) \quad (2)$$

where,

$$\delta_h^2(k) = k^3 |\alpha(k, t)|^2 \quad (3)$$

is the *power spectrum* (Mukhanov et al 1992), also referred to as the *characteristic amplitude* $h_c^2(k)$ (Maggiore 2000), which is a dimensionless quantity representing a characteristic value of the amplitude per unit of a logarithmic frequency interval. Clearly, in order to determine the spectrum of relic gravitational radiation one should first determine $\alpha(k, t)$ in curved spacetime. The safest way to do so, is to evaluate a family of solutions to the corresponding equation of propagation.

In the present article we consider a plane polarized gravitational wave (in the transverse-traceless gauge) propagating in a spatially flat Friedmann - Robertson - Walker (FRW) model. This model appears to interpret adequately the observational data related to the known thermal history of the Universe and therefore, it seems to be the most appropriate candidate for the curved background needed for this study. Accordingly, we arrive at a simple formula for the power spectrum of relic gravitational radiation, which relates the spectral index with the evolutionary period at which a CGW has entered the horizon.

2. Gravitational waves in curved spacetime

The far-field propagation (i.e. away from the source) of a weak CGW ($|h_{\mu\nu}| \ll 1$) in a curved, non-vacuum spacetime, is determined by the differential equations (Misner et al 1973)

$$h_{\mu\nu;\alpha}^{\alpha} - 2\mathcal{R}_{\alpha\mu\nu\beta} h^{\alpha\beta} = 0 \quad (4)$$

under the gauge choice

$$(h^{\alpha\beta} - \frac{1}{2}g^{\alpha\beta}h)_{;\beta} = 0 \quad (5)$$

which brings the linearized Einstein equations into the form (4). In Eqs (4) and (5), Greek indices refer to the four-dimensional spacetime, $\mathcal{R}_{\alpha\mu\nu\beta}$ is the Riemann curvature tensor of the background metric, h is the trace of $h_{\mu\nu}$ and the semicolon denotes covariant derivative. A linearly polarized plane GW propagating in a spatially flat FRW cosmological model, is defined by the expression (Allen 1997)

$$ds^2 = c^2 dt^2 - R^2(t)(\delta_{ik} + h_{ik})dx^i dx^k \quad (6)$$

where, Latin indices refer to the three-dimensional spatial section, δ_{ik} is the Kronecker symbol and the dimensionless scale factor $R(t)$ is a solution to the Friedmann equations, with matter-content in the form of a perfect fluid. Introducing the so-called *conformal time* coordinate, as

$$\eta = \int \frac{dt}{R(t)} \quad , \quad 0 < \eta < \infty \quad (7)$$

the CGW equation of propagation reads (Grishchuk 1975)

$$h''_{ik} + 2\frac{R'}{R}h'_{ik} + \delta^{lm}h_{ik,lm} = 0 \quad (8)$$

where, a prime denotes differentiation with respect to η and the comma denotes spatial derivative. To decompose Eq (8), we represent the metric corrections h_{ik} in the form

$$h_{ik}(\eta, x^j) = \alpha(k, \eta) \varepsilon_{ik} e^{ik_j x^j} = \frac{h(\eta)}{R(\eta)} \alpha \varepsilon_{ik} e^{ik_j x^j} \quad (9)$$

where, $h(\eta)$ is the time-dependent part of the modes, k_j is the co-moving wave-vector, α is the dimensionless amplitude of the CGW and ε_{ik} is the corresponding polarization tensor. Combination of Eqs (8) and (9) results in a differential equation for the evolution of the time-dependent part of the modes

$$h'' + (k^2 c^2 - \frac{R''}{R})h = 0 \quad (10)$$

To solve Eq (10), one needs an evolution formula for the cosmological model under consideration. In terms of the conformal time, the spatially flat FRW model considered, is a solution to the Friedmann equation

$$\left(\frac{R'}{R^2}\right)^2 = \frac{8\pi G}{3} \rho(\eta) \quad (11)$$

with matter-content in the form of a perfect fluid, $T_{\mu\nu} = \text{diag}(\rho c^2, -p, -p, -p)$, which obeys the conservation law

$$\rho' + 3\frac{R'}{R}(\rho + \frac{1}{c^2}p) = 0 \quad (12)$$

and the equation of state

$$p = \left(\frac{m}{3} - 1\right) \rho c^2 \quad (13)$$

where, $\rho(\eta)$ and $p(\eta)$ represent the matter density and the pressure, respectively. The linear equation of state (13) covers most of the matter-components considered to drive the evolution of the Universe, such as quantum vacuum ($m = 0$), gas of strings ($m = 2$), dust ($m = 3$), radiation ($m = 4$) and Zel'dovich ultra-stiff matter ($m = 6$). For each component, the continuity equation (12) yields

$$\rho = \frac{M_m}{R^m} \quad (14)$$

where, M_m is an integration constant, representing the *total density* attributed to the m -th component. On the other hand, a mixture of these components obey (Bleyer et al 1991)

$$\rho = \sum_m \frac{M_m}{R^m} \quad (15)$$

where, now, Eq (12) holds for every matter-component separately. In this case, M_m represent the amount of the m -th component in the mixture and may vary asymptotically. Accordingly, for $M_m \rightarrow \infty$, the m -th component dominates over the others, while, for $M_m \rightarrow 0$, the m -th component is negligible in the composition of the mixture.

3. The power spectrum of relic gravitational radiation

In the case of an one-component fluid, the Friedmann equation reads

$$R^{\frac{m}{2}-2} R' = \left(\frac{8\pi G}{3} M_m\right)^{1/2} \quad (16)$$

admitting two families of exact solutions:

- For the gas of strings ($m = 2$)

$$R(\eta) \sim \exp\left(\sqrt{\frac{8\pi G}{3} M_2} \eta\right) \quad (17)$$

- For all the other types of matter-content ($m \neq 2$)

$$R(\tau) = \left(\frac{\tau}{\tau_m}\right)^{\frac{2}{m-2}} \quad (18)$$

where, the time-parameter τ is linearly related to the corresponding conformal one, by $\tau = \frac{m-2}{2} \eta$ and we have set $\tau_m = \left(\frac{8\pi G}{3} M_m\right)^{-1/2}$. Notice that, for $m = 0$ (De Sitter inflation) and $0 < \eta < \infty$, one obtains $-\infty < \tau < 0$.

In accordance, we obtain two families of solutions regarding the temporal evolution of a CGW in curved spacetime:

- Inserting Eq (17) into Eq (10) we obtain the temporal evolution of a CGW in a string-dominated Universe

$$h'' + (k^2 c^2 - \frac{8\pi G}{3} M_2)h = 0 \Rightarrow h_2(k, \eta) = \sqrt{\eta} H_{1/2}^{(1,2)}(\omega\eta) \quad (19)$$

where, $H_{1/2}^{(1,2)}$ denotes a linear combination of the Hankel's functions of the first and the second kind, of order 1/2 and

$$\omega^2 = k^2 c^2 - \frac{8\pi G}{3} M_2 \quad (20)$$

is the constant frequency of the CGW.

- Similarly, inserting Eq (18) into Eq (10) one obtains the temporal evolution of a CGW within the context of the inflationary and/or the standard model scenario

$$h'' + (k_*^2 c^2 - 2[\frac{4-m}{(m-2)^2}] \frac{1}{\tau^2})h = 0 \Rightarrow h_m(k_*, \tau) = \sqrt{\tau} H_{|\nu|}^{(1,2)}(k_* c\tau) \quad (21)$$

where, in this case, a prime denotes derivative with respect to τ , $k_* = \frac{2}{m-2}k$, so that $k_* c\tau = kc\eta$ and the Hankel's functions order is

$$\nu = \frac{1}{2}(\frac{m-6}{m-2}) \quad (22)$$

(e.g. see Gradshteyn and Ryzhik 1965, Eq 8.491.5, p. 971). Therefore, different evolutionary periods admit different Hankel's functions.

With these solutions at hand, we may now examine the resulting power spectrum which can reveal a great deal of information on the physical conditions of the Universe at the time the CGWs have entered the horizon, i.e when the *physical wavelength* (λ_{ph}) of the wave becomes of the order of the Universal circumference

$$\lambda_{ph} \leq 2\pi\ell_H \Rightarrow \frac{2\pi}{k}R(\tau) \leq 2\pi\frac{c}{H} \Rightarrow k_*c\tau \geq 1 \Rightarrow kc\eta \geq 1 \quad (23)$$

Since a string-dominated Universe does not seem likely (Hindmarsh and Kibble 1995), in what follows, we confine ourselves within the inflationary and/or the standard model scenario, in which, the power spectrum is written in the form

$$\delta_h \sim k^{3/2} \tau^\nu |H_{|\nu|}^{(1,2)}(k_*c\tau)| \quad (24)$$

We define the *spectral index* as

$$n = \frac{k}{\delta_h(k)} \frac{d\delta_h(k)}{dk} \quad (25)$$

and taking into account the asymptotic properties of the Hankel functions (Lebedev 1972), we consider the following cases:

- A CGW is *well-outside* the horizon: In this case, we have $\lambda_{ph} \gg \ell_H$ and $k_*c\tau \rightarrow 0$. Accordingly, the power spectrum results in

$$\delta_h(k) \sim k^{\frac{3}{2}-|\nu|} \tau^{\nu-|\nu|} \quad (26)$$

and the spectral index is given by

$$n = \frac{3}{2} - |\nu| \quad (27)$$

In the case of inflationary expansion ($m = 0$), as well as during the matter-dominated epoch ($m = 3$) we obtain $n = 0$, i.e. the CGW spectrum is *flat*, as it has already been predicted by many authors (e.g. see Mukhanov et al 1992, Allen 1997). On the other hand in the radiation-dominated epoch ($m = 4$) one is left with the Harrison - Zel'dovich slope, where $n = 1$ and $\delta_h \sim k$.

- A CGW is *well-inside* the horizon: In this case, $\lambda_{ph} \ll \ell_H$ and $k_*c\tau \rightarrow \infty$. Accordingly, the power spectrum reads

$$\delta_h \sim k \tau^{\nu-\frac{1}{2}} \quad (28)$$

and the spectral index is constant ($n = 1$) for every m , yielding the Harrison - Zel'dovich slope (a not unexpected result) (e.g. see Mukhanov et al 1992).

- Finally, when the CGW enters the horizon one admits $\lambda_{ph} \simeq \ell_H \Rightarrow k_*c\tau \simeq 1$, thus obtaining

$$\delta_h \sim k^{\frac{3}{2}-\nu} \left| H_{|\nu|}^{(1,2)}(1) \right| \quad (29)$$

In this case, the Hankel's function is independent of k and, therefore, the spectral index reads

$$n = \frac{m}{m-2} \quad (30)$$

Eq (30) decomposes to

- $n = 0$ (a flat spectrum) in the inflationary regime ($m = 0$)
- $n = 2$ ($\delta_h \sim k^2$) in the radiation-dominated epoch ($m = 4$)
- $n = 3$ ($\delta_h \sim k^3$) in the matter-dominated epoch ($m = 3$)

Therefore, knowledge of the spectral index allows us to determine the value of m which, in turn, determines the form of the matter-energy content of the Universe at the time the CGW has entered the horizon

$$m = \frac{2n}{n-1} \quad (31)$$

In this sense, a possible detection of CGWs can result in a powerful tool for exploring the Universe, even more powerful than the CMRB.

Acknowledgements

This research has been supported by the Greek Ministry of Education, through the PYTHAGORAS program.

References

- Allen B, 1997, *The stochastic gravity-wave background: Sources and detection*, in: Marck J A and Lassota J P (eds) *Les Houches School on Astrophysical Sources of Gravitational Waves*, Cambridge University Press, Cambridge
- Bleyer U, Liebscher D E and Polnarev A G, 1991, *Class Quantum Grav* **8**, 477
- Carr B J, 1980, *A & A* **89**, 6
- Gradshteyn I S and Ryzhik I M, 1965, *Tables of Integrals, Series and Products*, Academic Press, New York
- Grishchuk L P, 1975, *Sov Phys JETP* **40**, 409
- Grishchuk L P and Polnarev A G, 1980, *Gravitational Waves and their Interaction with Matter and Fields*, in: Held A (ed) *General Relativity and Gravitation - One Hundred Years After the Birth of Albert Einstein*, Plenum, New York
- Hindmarsh M B and Kibble T W B, 1995, *Rep Prog Phys* **58**, 477
- Lebedev NN, 1972, *Special Functions and their Applications*, Dover New York
- Maggiore M, 2000, *Phys Rep* **331**, 283
- Misner C W, Thorne K S and Wheeler J A, 1973, *Gravitation*, Freeman, San Francisco
- Mukhanov V F, Feldman H A and Brandenberger R H, 1992, *Phys Rep* **215**, 203
- Weinberg S, 1972, *Gravitation and Cosmology*, Wiley, New York

STELLAR DYNAMICS IN SCALAR-TENSOR GRAVITY *

K.D. Kokkotas [†] and H. Sotani [‡]

Department of Physics, Aristotle University of Thessaloniki, Thessaloniki 54124, Greece

Abstract

We study perturbations of relativistic stars in scalar-tensor theory of gravity and examine the effects of the scalar field on the corresponding oscillation spectrum. Scalar waves which might be produced from such oscillations can be a unique probe for the theory, but their detectability is questionable if the radiated energy is small. However we show that there is no need for a direct observation of scalar waves: the shift in the gravitational wave spectrum could unambiguously signal the presence of a scalar field.

1. Introduction

Scalar-tensor theories of gravity are an alternative or generalization of Einstein's theory of gravity, where in addition to the tensor field a scalar field is present. The theory has been proposed in its earlier form about half century ago [1, 2, 3], and it is a viable theory of gravity for a specific range of the coupling strength of the scalar field to gravity [4, 5]. Actually, the existence of scalar fields is crucial (e.g. in inflationary and quintessence scenarios) to explain the accelerated expansion phases of the universe. Experimentally, the existence of a scalar field has not yet been probed, but a number of experiments in the weak field limit of general relativity set severe limits on the existence and coupling strengths of scalar fields [6].

A basic assumption is that the scalar and gravitational fields φ and $g_{\mu\nu}$ are coupled to matter via an "effective metric" $\tilde{g}_{\mu\nu} = A^2(\varphi)g_{\mu\nu}$. The Fierz-Jordan-Brans-Dicke [1, 2, 3] theory assumes that the "coupling function" has the form $A(\varphi) = \alpha_0\varphi$, i.e., it is characterized by a unique free parameter $\alpha_0^2 = (2\omega_{\text{BD}} + 3)^{-1}$, and all its predictions differ from those of general relativity by quantities of order α_0^2 [7]. Solar system experiments set strict limits in the value of the Brans-Dicke parameter ω_{BD} , i.e., $\omega_{\text{BD}} > 40000$, which suggests a very small $\alpha_0^2 < 10^{-5}$ (see [6]).

In the early 1990s, based on a simplified version of scalar tensor theory where $A(\varphi) = \alpha_0\varphi + \beta\varphi^2/2$, Damour and Esposito-Farese [7, 8] found that for certain values of the coupling parameter β the stellar models develop some strong field

*Presented at the Workshop on *Cosmology and Gravitational Physics*, 15-16 December 2005, Thessaloniki, Greece, *Editors*: N.K. Spyrou, N. Stergioulas and C.G. Tsagas.

[†]kokkotas@auth.gr

[‡]sotani@astro.auth.gr

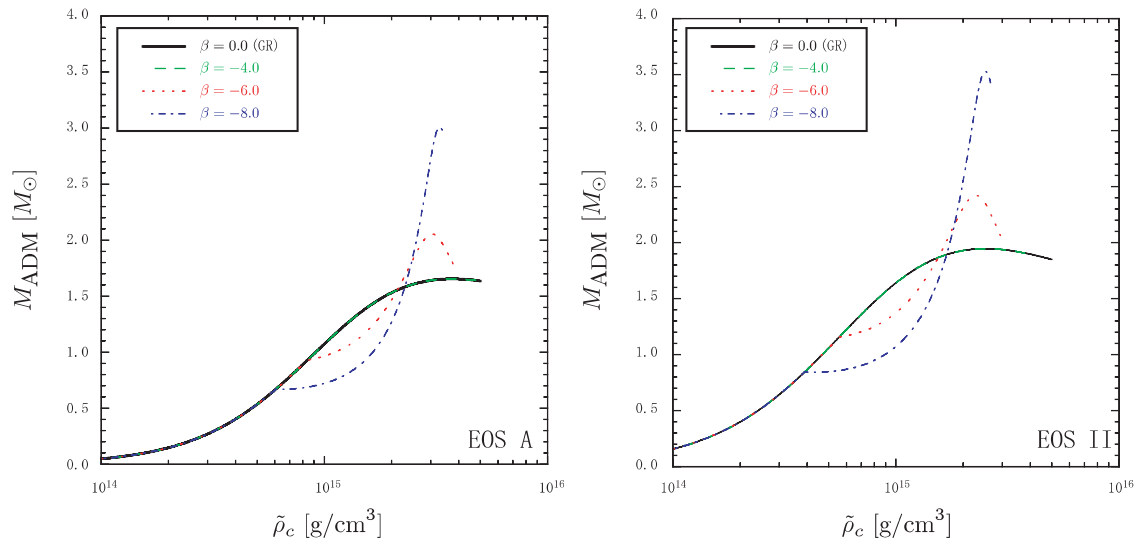


Figure 1: *Stellar models with $\beta=0, -4, -6$ and -8 are shown. The left column corresponds to models for the EOS A while in the right to models for EOS II. The effect of the scalar field is apparent for $\rho_c \geq 5 \times 10^{14}$ gr/cm³. In both panels, the general relativistic stellar models are shown by a solid line (GR).*

effects which induce significant deviations from general relativity. This sudden deviation from general relativity for specific values of the coupling constants has been named “spontaneous scalarization”. Harada [9] studied in more detail models of non-rotating neutron stars in the framework of the scalar-tensor theory and he reported that “spontaneous scalarization” is possible for $\beta < -4.35$.

Recently, we have examined the possibility to obtain the information for the presence of the scalar field via gravitational wave observations of oscillating neutron stars [10, 11]. The effect of the scalar field on the fluid perturbations, i.e., f and p modes has been examined in [10] (in the Cowling approximation, i.e., no spacetime perturbations). In [11] the effect of the scalar field on the spacetime perturbations (w modes) has been studied.

2. Stellar models in scalar-tensor theory

In this section we study neutron star models in scalar-tensor theory of gravity with one scalar field. This is a natural extensions of Einstein’s theory, in which gravity is mediated not only by a second rank tensor (the metric tensor $g_{\mu\nu}$) but also by a massless long-range scalar field φ . The action is given by [4]

$$S = \frac{1}{16\pi G_*} \int \sqrt{-g_*} (R_* - 2g_*^{\mu\nu} \varphi_{,\mu} \varphi_{,\nu}) d^4x + S_m [\Psi_m, A^2(\varphi)g_{*\mu\nu}], \quad (1)$$

where all quantities with asterisks are related to the “Einstein metric” $g_{*\mu\nu}$, then R_* is the curvature scalar for this metric and G_* is the bare gravitational coupling

constant. Ψ_m represents collectively all matter fields, and S_m denotes the action of the matter represented by Ψ_m , which is coupled to the ‘‘Jordan-Fierz metric tensor’’ $\tilde{g}_{\mu\nu}$. The field equations are usually written in terms of the ‘‘Einstein metric’’, but all non-gravitational experiments measure the ‘‘Jordan-Fierz’’ or ‘‘physical metric’’. The ‘‘Jordan-Fierz metric’’ is related to the ‘‘Einstein metric’’ via the conformal transformation, $\tilde{g}_{\mu\nu} = A^2(\varphi)g_{*\mu\nu}$. Hereafter, we denote by a tilde quantities in the ‘‘physical frame’’. From the variation of the action S we get the field equations in the Einstein frame

$$G_{*\mu\nu} = 8\pi G_* T_{*\mu\nu} + T_{*\mu\nu}^{(\varphi)} \quad \text{and} \quad \nabla_*^\mu \nabla_{*\mu} \varphi = -4\pi G_* \alpha(\varphi) T_*, \quad (2)$$

where $T_{*\mu\nu}^{(\varphi)}$ is the energy-momentum of the massless scalar field and $T_*^{\mu\nu}$ is the energy-momentum tensor in the Einstein frame. It is apparent that $\alpha(\varphi)$ is the only field-dependent function which couples the scalar field with matter, for $\alpha(\varphi) = 0$ the theory reduces to general relativity. Finally, the law of energy-momentum conservation $\tilde{\nabla}_\nu \tilde{T}_\mu{}^\nu = 0$ is transformed into

$$\nabla_{*\nu} T_{*\mu}{}^\nu = \alpha(\varphi) T_* \nabla_{*\mu} \varphi, \quad (3)$$

In this paper, we adopt the same form of conformal factor $A(\varphi)$ as in Damour and Esposito-Farese [7], which is

$$A(\varphi) = e^{\frac{1}{2}\beta\varphi^2}, \quad (4)$$

i.e., $\alpha(\varphi) = \beta\varphi$ where β is a real number. In the case $\beta = 0$ this scalar-tensor theory reduces to general relativity.

Here we model the neutron stars as self-gravitating perfect fluid of cold degenerate matter in equilibrium.

3. Basic Perturbation Equations

In this section we present the equations describing perturbations of the spacetime, scalar field, and fluid in a spherically symmetric background. The equations we provide describe the non-radial oscillations of spherically symmetric neutron stars in scalar-tensor theories. We assume, in the physical frame, using the Regge-Wheeler gauge [12], the following form of the perturbed metric tensor

$$\tilde{h}_{\mu\nu} = \tilde{h}_{\mu\nu}^{(-)} + \tilde{h}_{\mu\nu}^{(+)}, \quad (5)$$

where $\tilde{h}_{\mu\nu}^{(-)}$ denotes the *axial* (or *odd parity*) part of metric perturbations and $\tilde{h}_{\mu\nu}^{(+)}$ denotes the *polar* (or *even parity*) part of metric perturbations.

Following the previous definitions the perturbed metric tensor $h_{*\mu\nu}$ in the Einstein frame has the form:

$$h_{*\mu\nu} = \frac{1}{A^2} \tilde{h}_{\mu\nu} - \frac{2}{A} g_{*\mu\nu} \delta A \quad (6)$$

where $\delta A \equiv A\beta\varphi\delta\varphi$ is the perturbation of the conformal factor A and $\delta\varphi$ is the perturbation of the scalar field, where $\delta\varphi$ is a function of t and r only. The above

definition of $h_{*\mu\nu}$ will be used to derive the perturbation equations: in other words, we will work out the perturbations in the Einstein frame and we will transform back to the physical frame whenever we need it.

The perturbation equations will be derived by taking the variation of eqns (2)

$$\delta G_{*\mu\nu} = 8\pi G_* \delta T_{*\mu\nu} + \delta T_{*\mu\nu}^{(\varphi)} \quad \text{and} \quad \delta(\nabla_*^\mu \nabla_{*\mu} \varphi) = -4\pi G_* \delta[\alpha(\varphi) T_*]. \quad (7)$$

The components of $\delta T_{*\mu\nu}^{(\varphi)}$ are expressed as linear combinations of $\delta\varphi$ and $\tilde{h}_{\mu\nu}$.

4. Results and Discussion

The spectrum of an oscillating neutron star is directly related to its parameters, mass, radius and EOS [13, 14, 15]. As we have seen in Section II the presence of the scalar field on the background star is influencing both the mass and the radius, while in the way that it enters in the equilibrium equations it has a role of an extra pressure term, i.e., it seems to alter the actual EOS. As before we will restrict our study only two equations of state, i.e., EOS A and EOS II.

The oscillation frequencies of the various types of modes have been derived using two complementary techniques. One way is to assume a harmonic time dependence of the perturbation functions, e.g., $W(t, r) = e^{i\omega t} W(r)$ and transform the problem into a boundary value one. Alternatively, we can just use time evolution of the perturbation equations and by Fourier transformations of the derived time-series one can get the characteristic oscillation frequencies [10, 11].

First, we will examine the effect of the scalar factor β on the frequency and especially whether the “spontaneous scalarization” can be traced in the spectrum. A discontinuous change in a system, as one varies its parameters, signals a catastrophic behavior and the so called “spontaneous scalarization” [7] is related to it. In order to study this effect we constructed a sequence of stellar models with $M_{ADM} = 1.4M_\odot$ by varying β , where M_{ADM} is ADM mass.

The idea of a gravitational wave asteroseismology [14, 15] was based on empirical relations that can be drawn for the relation of the stellar parameters to the eigenfrequencies of an oscillating neutron star. These empirical relations were derived by taking into account data for a dozen or more EOS, and it was shown that through these relations one can extract the stellar parameters by analyzing the gravitational wave signal of an oscillating neutron star. The easiest relation to be understood on intuitive physical grounds is the one between the fundamental oscillation mode the f mode and the average density. This relation emerges naturally by combining the time that a perturbation needs to propagate across the star and the sound speed, this boils down to a linear relation between the period of oscillation and the average density or the star or better $\omega^2 \sim M/R^3$. According to [14] the empirical relation between the f mode frequency and the average density of typical neutron stars is

$$f_{f\text{-mode}}(\text{kHz}) \approx 0.78 + 1.63 \left(\frac{M}{1.4M_\odot} \right)^{1/2} \left(\frac{R}{10\text{km}} \right)^{-3/2}. \quad (8)$$

Almost, all EOS follow this empirical relation (including the two EOS used in this article) for the case of general relativity. This observation suggests a unique way in

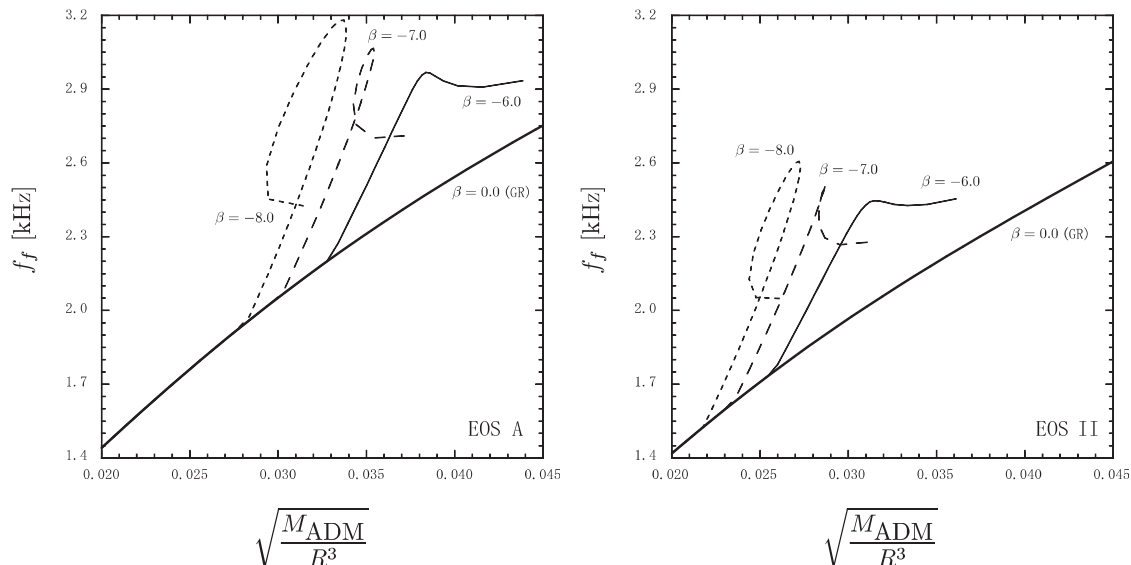


Figure 2: The frequency of the f mode as function of the averaged density $(M_{\text{ADM}}/R^3)^{1/2}$ of the star (notice that $f_f = \omega_f/2\pi$). The thick solid line corresponds to the values of the mode for $\beta = 0.0$ (GR) while we also show the effect of the scalar field for three values of the scalar parameter β (-6 , -7 , and -8). The left panel corresponds to EOS A and the right panel to EOS II.

estimating the average density of a star via its f mode frequency, and it can be a very good observational test for the neutron stars in scalar-tensor theories.

In Figure 2 we draw the frequency as function of the averaged density. The introduction of a scalar field even in moderate central densities alters completely the behavior of the f mode for both EOS. The frequencies grow considerably faster as functions of the average density, for $\beta < -4.35$, and the three examples that we have chosen ($\beta = -6$, -7 , and -8) show exactly this behavior. The change is quite dramatic even for typical neutron stars with average density. Depending on the value of the parameter β they become 30 – 50% larger than those of a general relativistic neutron star. This can be an observable effect, since the detection of frequencies are higher than those expected from a typical neutron star, would signal in a unique way the presence of a scalar field.

The results of the two methods we described briefly earlier agree very well, providing a good consistency check on our calculations. In Figure 3 we present the eigenvalues for different stellar models derived for EOS A and II. Our results suggest that the presence of a spontaneous scalarization can be inferred from the w modes emitted by a newly born, oscillating neutron star. The modes that might be relevant for gravitational wave detectors are the lowest w modes [17]. The w_{II} modes [18] damp out roughly twice as fast as the w modes, but having lower frequencies they could also be relevant for detection by Earth-based interferometers. The higher-frequency w modes (w_2 , w_3 , w_4 , ...) are difficult, if not impossible to detect. In the study of w modes as a tool for asteroseismology [13, 14, 16, 15] it

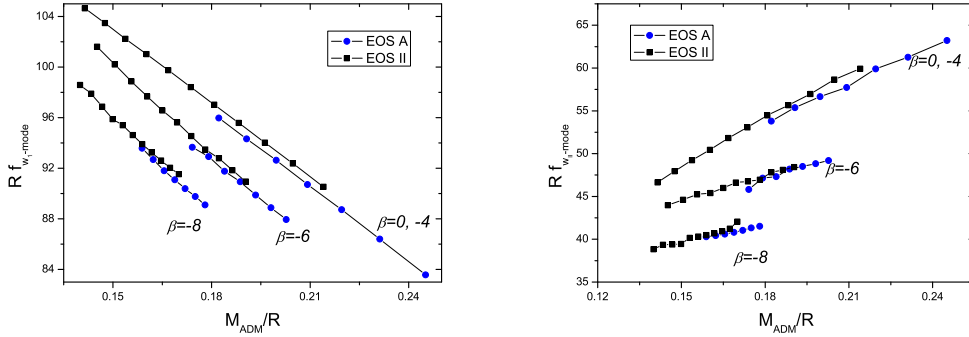


Figure 3: The w_1 modes (left panel) and the w_{II} modes (right panel) for EOS A and II and for values of $\beta = 0, -4, -6$, and -8 .

has been suggested that a proper normalization for $Re(\omega)$ is to multiply it with the radius R of the star and to scale it as a function of the compactness M/R . This phenomenological argument has been recently verified analytically by Tsui and Leung [19]. Introducing $f = Re(\omega)/2\pi$, it is clear that Rf scales linearly as function of the compactness M/R . This applies both to w_{II} and w_1 modes (and even to the higher overtones). The linear relations that can be derived from Figure 3 are

$$f_{w_1\text{-mode}}(\text{kHz}) = \frac{1}{R} \left(\alpha_1 - \beta_1 \frac{\bar{M}}{R} \right) \quad \text{and} \quad f_{w_{II}\text{-mode}}(\text{kHz}) = \frac{1}{R} \left(\alpha_{II} + \beta_{II} \frac{\bar{M}}{R} \right), \quad (9)$$

where the constants $\alpha_1, \beta_1, \alpha_{II}$ and β_{II} are fitting factors given [11].

Another reason why it is harder to detect high-damped quasinormal modes such as the w_{II} modes for compact stars is that the effective amplitude scales as the square root of the number of oscillations [15]. Typically we can hardly observe more than 2 – 3 cycles for highly damped quasinormal modes of black-holes and for the w_{II} modes of compact stars. Spontaneous scalarization might help in this direction. The reason is that the damping time of the w_{II} mode for stars with $\beta < -4.35$ is significantly longer than for typical stars in general relativity. The reason is that the presence of a scalar field increases the maximum mass of the stars and their compactness. Since the damping scales with compactness, the w_{II} modes live considerably longer. On the contrary, the damping times of the w_1 modes become shorter as the compactness increases [11].

For the study of the stellar oscillations in scalar theory of gravity we conclude that the presence of a scalar field affects the equilibrium model, and consequently the oscillation spectrum. The scalar field perturbations couple with the polar perturbations of the spacetime and fluid, but they don't couple with the axial perturbations. Since the spacetime modes of polar and axial perturbations have the same qualitative behavior, we have chosen to study the effect of the scalar field on the axial perturbations.

The results show that in the presence of spontaneous scalarization, a scalar field

reduces the oscillation frequency of the w_1 modes by about 10% (i.e. by about 1kHz). The decrease in frequency for the w_{II} modes is about 25% the frequency of (i.e., about 1.5 kHz). The effect on the damping time is even more pronounced. The damping rate of w_{II} modes can decrease by as much as 30%, while it can increase by as much as 50% for the w_1 modes. Detectors operating at these high frequencies are under development. Through a detection of the w mode spectrum, they could provide a unique proof for the existence of scalar fields with $\beta < -4.35$.

Acknowledgements

This work is supported by the Pythagoras I program, the European Program ILIAS and the Marie-Curie grant FP6-021979.

References

- [1] M.Fierz Helv. Phys. Acta **29**, 128 (1956).
- [2] P. Jordan Z.Phys. **157**, 112 (1959).
- [3] C. Brans and R. H. Dicke, Phys. Rev. **124**, 925 (1961).
- [4] T. Damour and G. Esposito-Farèse, Class. Quantum Grav. **9**, 2093 (1992).
- [5] C. M. Will, *Theory and Experiment in Gravitational Physics* (Cambridge University Press, Cambridge, England 1993).
- [6] G.Esposito-Farese gr-qc/0402007.
- [7] T. Damour and G. Esposito-Farèse, Phys. Rev. Lett. **70**, 2220 (1993).
- [8] T. Damour and G. Esposito-Farèse, Phys. Rev. D **54**, 1474 (1996).
- [9] T. Harada, Phys. Rev. D **57**, 4802 (1998).
- [10] H. Sotani and K. D. Kokkotas, Phys. Rev. D, **70**, 084026 (2004).
- [11] H. Sotani and K. D. Kokkotas, Phys. Rev. D, **71**, 124038 (2005).
- [12] T. Regge and J. A. Wheeler Phys. Rev. **108**, 1063 (1957)
- [13] N. Andersson, K.D. Kokkotas, Phys. Rev. Letters, **77**, 4134 (1996).
- [14] N. Andersson, K.D. Kokkotas, MNRAS, **299**, 1059 (1998).
- [15] K. D. Kokkotas, T. A. Apostolatos and N. Andersson, MNRAS, **320** , 307 (2001).
- [16] H. Sotani, K. Kohri and T. Harada, Phys. Rev. D, **69**, 084008 (2004).
- [17] K.D.Kokkotas and B.F.Schutz MNRAS **255**, 119 (1992).

[18] M. Leins, H-P. Nollert and M. H. Soffel *Phys.Rev. D*, **48**, 3467 (1993)

[19] L. K. Tsui and O. T. Leung *MNRAS* **357** 1029 (2005)

GEOMETRICAL GENERATION OF COSMIC MAGNETIC FIELDS WITHIN STANDARD ELECTROMAGNETISM *

Christos G. Tsagas^{1†} and Alejandra Kandus^{3‡}

¹Department of Physics, Aristotle University of Thessaloniki, Thessaloniki 54124, Greece

³LATO-DCET, Universidade Estadual de Santa Cruz, Rodovia Ilhéus-Itabuna km 16 s/n
Salobrinho CEP-05508-900, Ilhéus - BA, Brazil

Abstract

We study the evolution of cosmological magnetic fields in FRW models with curved spatial sections and outline a geometrical mechanism for their superadiabatic amplification on large scales. The mechanism operates within standard electromagnetic theory and applies to FRW universes with open spatial sections. We discuss the general relativistic nature of the effect and show how it modifies the adiabatic magnetic evolution by reducing the depletion rate of the field. Assuming a universe that is only marginally open today (i.e. for $1 - \Omega_0 \sim 10^{-2}$), we estimate the main features of the superadiabatically amplified residual field and find that is of astrophysical interest.

Key-words: Cosmology, Magnetic Fields

1. Introduction

Magnetic fields appear everywhere in the universe [1]. Despite this and the numerous scenarios of magnetogenesis the origin of cosmic magnetism remains a mystery [2]. These scenarios are generally classified into those arguing for a late (post-recombination) magnetic generation and those advocating a primordial origin for the fields. Early magnetogenesis is attractive because it makes the ubiquity of large-scale magnetic fields in the universe easier to explain. Inflation seems the plausible candidate for producing the primordial fields, as it naturally leads to large-scale phenomena from subhorizon microphysics. The main obstacle is that any magnetic field that survives inflation is so drastically diluted that it can never seed the galactic dynamo. The reason is the ‘adiabatic’, a^{-2} decay of the field (a is the scale factor of the universe). This is attributed to the conformal invariance of standard

*Presented at the Workshop on *Cosmology and Gravitational Physics*, 15-16 December 2005, Thessaloniki, Greece, *Editors*: N.K. Spyrou, N. Stergioulas and C.G. Tsagas.

[†]email address: tsagas@astro.auth.gr

[‡]e-mail address: kandus@uesc.br

electromagnetism and to the conformal flatness of the Friedmann-Robertson-Waler (FRW) models. Strictly speaking, however, this is only true in FRW spacetimes with flat spatial sections.

The usual way of modifying the $B \propto a^{-2}$ law is by breaking away from standard electromagnetic theory. Turner and Widrow did this by introducing to their Lagrangian an extra coupling between the Maxwell field and the curvature of the spatially flat FRW spacetime [3]. The conformal invariance and the gauge invariance of Maxwell's equations were lost as a result, but a new magneto-curvature term appeared in the magnetic wave equation. The immediate consequence was a superadiabatic-type amplification of the primordial field. To be precise, superhorizon-sized magnetic fields, evolving in a poorly conducting inflationary universe, decayed as a^{-1} [3]. Since then, many scenarios of early magnetic amplification have appeared in the literature (e.g. see [4]).

Here we discuss a conventional interaction between the electromagnetic and the gravitational field, which so far has been sparsely studied in cosmology. This is the natural, general relativistic coupling between electromagnetism and space-time geometry that emerges from the vector nature of the Maxwell field and from the geometrical approach of Einstein's theory (e.g. see [5, 6]). Our mechanism operates primarily on magnetic fields coherent on the largest subcurvature scales of a spatially open FRW universe, which asymptotically approaches flatness as it undergoes a period of inflationary expansion. The result is that these fields decay as a^{-1} , a rate considerably slower than the adiabatic a^{-2} law. Then, assuming that $1 - \Omega \sim 10^{-2}$ today, we find that a residual field of approximately 10^{-35} G on a comoving length of $\sim 10^4$ Mpc [6]. This is much stronger than any other large-scale field obtained by conventional methods. Moreover, in a dark-energy dominated universe, seeds field of 10^{-35} G lie within the broad galactic dynamo requirements [7].

2. Superadiabatic Magnetic Amplification in FRW Universes

Consider a large-scale magnetic field B_a and introduce the rescaled *magnetic flux* variable $\mathcal{B}_a = a^2 B_a$. Also, adopt the decomposition $\mathcal{B}_a = \mathcal{B}_{(n)} Q_a^{(n)}$, with $Q_a^{(n)}$ being the standard vector harmonics, and use conformal instead of proper time. The wave-equation of the field, linearised around a FRW background with curved spatial sections, reads [5, 6]

$$\mathcal{B}_{(n)}'' + n^2 \mathcal{B}_{(n)} = -2k \mathcal{B}_{(n)}. \quad (1)$$

Here n is the comoving wavenumber of the mode, $k = 0, \pm 1$ is the curvature index of the background 3-space and a prime indicates conformal time derivatives (see [5, 6] for details). The above closely resembles Eq. (2.15) in [3]. The similarity is in the presence of a curvature related source term in both expressions. The difference is that here the magneto-curvature term is a natural general relativistic effect. No new physics has been introduced and standard electromagnetism still holds. For $k = 0$ Eq. (1) reduces to the well known Minkowski-space expression, which leads to the adiabatic $B_a \propto a^{-2}$ decay for the field. When $k = +1$ the compactness of the space guarantees that B_a still drops as a^{-2} despite the presence of the magneto-curvature

term [6]. However, for $k = -1$ and on the largest subcurvature scales we obtain

$$B = \mathcal{C}_1 (1 - e^{2\eta}) a^{-1} + \mathcal{C}_2 e^{-\eta} a^{-2}, \quad (2)$$

with \mathcal{C}_1 and \mathcal{C}_2 constants [6]. Thus, in a spatially open FRW universe and near the curvature scale the dominant magnetic mode never depletes faster than a^{-1} . This means an effective superadiabatic amplification of the field due to curvature effects alone (see [6] for details). Note that at the onset of inflation subcurvature scales are in causal contact if the universe is sufficiently open (e.g. $\Omega < 0.1$ will suffice). On wavelengths larger than the curvature scale the depletion rate of the field is even slower. As $n \rightarrow 0$, for example, we find that $B_a \propto a^{\sqrt{2}-2}$. It should be noted, however, that these supercurvature scales lie always outside the horizon.

3. The Amplified Residual Field

Following [3], the energy density of the n -th magnetic mode as it crosses outside the horizon is $\rho_B = (M/m_{Pl})^4 \rho$, where $\rho \simeq M^4$ is the total energy density of the universe and m_{Pl} is the Planck mass. When $B_a \propto a^{-2}$ we have [3]

$$\rho_B = B^2/8\pi \sim 10^{-104} \tilde{\lambda}_{Mpc}^{-4} \rho_\gamma, \quad (3)$$

at the end of inflation. Note that ρ_γ is the radiation energy density and $\tilde{\lambda}$ is the comoving scale of the field (in Mpc and normalized so that $\tilde{\lambda}$ is the physical scale today). The situation changes if during inflation the field decays as a^{-1} instead of following the adiabatic a^{-2} -law. For a direct comparison, it helps to follow the analysis of [3]. Consider a typical GUT-scale inflationary scenario with $M \sim 10^{17}$ GeV and reheating temperature $T_{RH} \sim 10^9$ GeV. Then, for $B_a \propto a^{-2}$, the energy density stored in a given magnetic mode at the end of inflation is [6]

$$\rho_B \sim 10^{-90} M^{8/3} T_{RH}^{-2/3} \tilde{\lambda}_{Mpc}^{-2} \rho_\gamma \sim 10^{-51} \tilde{\lambda}_{Mpc}^{-2} \rho_\gamma, \quad (4)$$

instead of (3). After inflation the high conductivity of the plasma is restored. This ensures that $B \propto a^{-2}$ and consequently that the ratio $r = \rho_B/\rho_\gamma \sim 10^{-51} \tilde{\lambda}_{Mpc}^{-2}$ remains fixed. If $1 - \Omega_0$ is of the order of 10^{-2} , as it appears to be today [8], the current curvature length is $(\lambda_k)_0 = (\lambda_H)_0 / \sqrt{1 - \Omega_0} \sim 10^4$ Mpc (see [6] for further details). By substituting this scale into expression (4) we find that $r = \rho_B/\rho_\gamma \sim 10^{-59}$, which corresponds to a magnetic field with current strength around 10^{-35} G. The latter is within the lower values required for large scale galactic dynamo to operate in a dark-energy dominated universe [7].

4. Discussion

Although all three of the FRW spacetimes are conformally flat they are clearly not the same. Their different geometries are manifested by the fact that, while for $k = 0$ the conformal factor is the cosmological scale factor, in the other two cases it is not.

Thus, the conformal flatness of the Friedmann models does not a priori guarantee the adiabatic $B_a \propto a^{-2}$ -law in all FRW universes. By allowing for curved spatial sections, we showed the presence of an extra curvature-related source term in the magnetic wave equation. When $k = -1$, this meant that large-scale fields evolving through a period of inflationary expansion decay as a^{-1} instead of a^{-2} . As a result, primordial magnetic fields coherent on the largest subcurvature scales could survive an epoch of inflation and still be strong enough to sustain the dynamo process.

If the universe is marginally open today, our mechanism allows for a simple, viable and rather efficient amplification of large-scale primordial magnetic fields to strengths that can seed the galactic dynamo. Even if the universe is not open, however, this study still provides a clear counter example to the widespread perception that the superadiabatic magnetic amplification on FRW backgrounds is impossible unless standard electromagnetism is violated.

References

- [1] P.P. Kronberg, Rep. Prog. Phys. **57**, 325 (1994); R. Beck, A. Brandenburg, D. Moss, A.A. Sukurov and D. Sokoloff, Annu. Rev. Astron. Astrophys. **34**, 155 (1996); J.-L. Han and R. Wielebinski, Chin. J. Astron. Astrophys. **2**, 293 (2002)
- [2] K. Enqvist, Int. J. Mod. Phys. D **7**, 331 (1998); D. Grasso and H. Rubinstein, Phys. Rep. **348**, 163 (2001); L.M. Widrow, Rev. Mod. Phys. **74**, 775 (2002); M. Giovannini, Int. J. Mod. Phys. D **13**, 391 (2004)
- [3] M.S. Turner and L. Widrow, Phys. Rev. D **37**, 2743 (1988).
- [4] B. Ratra, Astrophys. J. Lett. **391**, L1 (1992); A.D. Dolgov, Phys. Rev. D **48**, 2499 (1993); E.A. Calzetta, A. Kandus and F.D. Mazzitelli, Phys. Rev. D **57**, 7139 (1998); O. Bertolami and D.F. Mota, Phys. Lett. B **455**, 96 (1999); A.C. Davis, K. Dimopoulos, T. Prokopec and O. Törnkvist, Phys. Lett. B **501**, 165 (2001)
- [5] C.G. Tsagas, Class. Quantum Grav. **22**, 393 (2005)
- [6] C.G. Tsagas and A. Kandus, Phys. Rev. D **71**, 123506 (2005).
- [7] A.-C. Davis, M. Lilley and O. Törnkvist, Phys. Rev. D **60**, 021301 (1999)
- [8] M. Tegmark et al. (the SSDS collaboration), Phys. Rev. D **69**, 103501 (2004).

NONLINEAR INTERACTION OF GRAVITATIONAL WAVES WITH STRONGLY MAGNETIZED PLASMAS *

H. Isliker †

Section of Astrophysics, Astronomy and Mechanics, Department of Physics,
University of Thessaloniki, GR 54006 Thessaloniki, Greece

Abstract

We study the interaction of a gravitational wave (GW) with a plasma that is strongly magnetized. The GW is considered a small disturbance, and the plasma is modeled by the general relativistic analogue of the induction equation of ideal MHD and the single fluid equations. The system is specified to the case of Cartesian coordinates and a constant background magnetic field. The equations are derived without neglecting any of the non-linear interaction terms, and the non-linear equations are integrated numerically. We find that for strong magnetic fields of the order of 10^{15} G the GW excites electromagnetic plasma waves very close to the magnetosonic mode, and a large amount of energy is absorbed from the GW by the electromagnetic oscillations. The energization of the plasma takes place on fast time scales of the order of milliseconds.

1. Introduction

Gravitational waves (GW) can carry a large amount of energy near the sources where they are generated (e.g. Kokkotas 2004). They tend not to interact much with matter under normal conditions, it has been shown though in a number of articles (e.g. Ignat'ev 1995, Brodin & Marklund 1999, Brodin et al. 2000, Servin et al. 2000, Papadopoulos et al. 2001, Servin & Brodin 2003, Moortgat & Kuijpers 2003, Källberg et al. 2004, Moortgat & Kuijpers 2004) that GWs excite various kinds of plasma waves, the more efficient, the stronger the background magnetic field is and the more tenuous the plasma is. Most of these studies are analytical and the equations describing the GW-plasma interaction were linearized. The GW-plasma interaction is a totally non-linear effect, and there is so-far no conclusive answer to the question of how much energy can be absorbed by a plasma from a GW.

Here, we study the GW-plasma interaction in its full non-linearity, solving the non-linear system of equations numerically. Our main interest is in the amount

*Presented at the Workshop on *Cosmology and Gravitational Physics*, 15-16 December 2005, Thessaloniki, Greece, *Editors*: N.K. Spyrou, N. Stergioulas and C.G. Tsagas.

†isliker@helios.astro.auth.gr

of energy absorbed by the plasma from the GW and in the kind of plasma waves excited by the GW, and we focus on the case of very strong magnetic fields of the order of 10^{15} G.

In Sec. 2, we introduce the basic equations and specify the one dimensional model, and in Sec. 3, numerical results are presented. Sec. 4 contains the conclusions.

2. Basic equations

The GW is considered as a small amplitude perturbation of the otherwise flat spacetime, and we assume it to be + polarized and to propagate along the z -direction, so that the metric has the form $g_{ab} = \text{diag}(-1, 1 + h, 1 - h, 1)$, with $h(z, t) \ll 1$ the amplitude of the GW (Hartle 2003). Our aim is to express the final equations in terms of the potentially observable quantities (electric field \vec{E} , magnetic field \vec{B} , 3-velocity \vec{V} of the fluid, and rest-mass density ρ), which can either be defined in a Local Inertial Frame (LIF) or in an orthonormal (ON) frame (ONF) (Hartle 2003). Here, we use the ONF, because it is a global frame, and it can be shown that the ONF in our case is locally equivalent to a LIF when applying the particular coordinate transformation given in Landau & Lifshitz (1981). Indices of quantities in the ONF carry a hat in the following. The transformation from and to the ONF is given by the transformation matrix $(\mathbf{e}_{\hat{a}})^b = \text{diag}\left(1, \frac{1}{\sqrt{1+h}}, \frac{1}{\sqrt{1-h}}, 1\right)$ and its inverse $(\mathbf{e}^{\hat{a}})_b$. Here, $\mathbf{e}_{\hat{a}}$ are the ON basis vectors, and $(\mathbf{e}_{\hat{a}})^b$ are their coordinates in the coordinate base. The metric in the ONF is of flat spacetime form, $\eta_{\hat{a}\hat{b}} = \text{diag}(-1, 1, 1, 1)$, and also 4-vectors and tensors take the same form as in flat space-time, the effects of curvature appear only through the covariant derivatives. The covariant derivatives in the ONF are denoted by $;$ in the following, and they are calculated with the use of the Ricci rotation coefficients (Landau & Lifshitz 1981).

We assume an ideal conducting fluid, so that the electric field is given by the ideal Ohm's law, $0 = F^{\hat{a}\hat{b}}u_{\hat{b}}/c$, which in the ONF takes the usual form, $0 = \hat{\gamma}\left(\vec{E} + \frac{1}{c}\vec{V} \times \vec{B}\right)$, with $\hat{\gamma} = 1/\sqrt{1 - \vec{V}^2/c^2}$, $u^{\hat{a}}$ the 4-velocity, $u^{\hat{a}} = \hat{\gamma}(c, V_x, V_y, V_z)$, and c the speed of light, and $F^{\hat{a}\hat{b}}$ Faraday's field tensor. The evolution of the magnetic field is determined by the Maxwell's equation, $F_{\hat{a}\hat{b};\hat{c}} + F_{\hat{b}\hat{c};\hat{a}} + F_{\hat{c}\hat{a};\hat{b}} = 0$ (Landau & Lifshitz 1981). The electromagnetic (EM) energy momentum tensor is defined as $T_{(EM)}^{\hat{a}\hat{b}} = \frac{c^2}{4\pi}\left(F^{\hat{a}\hat{c}}F_{\hat{c}}^{\hat{b}} - \frac{1}{4}\eta^{\hat{a}\hat{b}}F^{\hat{c}\hat{d}}F_{\hat{c}\hat{d}}\right)$, and for the fluid, we have the energy momentum tensor $T_{(fl)}^{\hat{a}\hat{b}} = Hu^{\hat{a}}u^{\hat{b}} + \eta^{\hat{a}\hat{b}}pc^2$, where H is the enthalpy and p the pressure (Landau & Lifshitz 1981). We assume an ideal and adiabatic fluid, so that $H = \rho c^2 + \frac{p}{\Gamma-1} + p$, with Γ the adiabatic index. The total energy momentum tensor $T^{\hat{a}\hat{b}} = T_{(fl)}^{\hat{a}\hat{b}} + T_{(EM)}^{\hat{a}\hat{b}}$ yields the momentum and energy equations $T^{\hat{a}\hat{b}}_{;\hat{b}} = 0$ (Landau & Lifshitz 1981). Continuity is expressed by $(\rho u^{\hat{a}})_{;\hat{a}} = 0$. The evolution of the GW is determined by the linearized Einstein equation, where we take the back-reaction of the plasma onto the GW into account, $-\partial_{tt}h + c^2\vec{\nabla}^2h = -\frac{1}{2}\frac{16\pi G}{c^4}(\delta T_{xx} - \delta T_{yy})$, where δT_{xx} , δT_{yy}

are the non-background, fluctuating parts of the components T_{xx} , T_{yy} of the total energy momentum tensor, and G is the gravitational constant (Hartle 2003). To close the system of equations, we assume an adiabatic and isentropic equation of state, $p = K\rho^\Gamma$, with K a constant.

2.1 The model

We focus on the excitation of MHD modes which propagate in the z -direction, parallel to the propagation direction of the GW and perpendicular to the background magnetic field $\vec{B}_0 = B_0\mathbf{e}_{\hat{x}}$. We let consequently $\vec{B}\|\mathbf{e}_{\hat{x}}$, $\vec{E}\|\mathbf{e}_{\hat{y}}$, and $\vec{V}\|\mathbf{e}_{\hat{z}}$, and all variables depend spatially only on z . In specifying the general equations to this particular geometry, (i) we express all 4-vector and tensor components through the potentially observable B_x , V_z , and ρ ; (ii) we expand the covariant derivatives; (iii) we keep all non-linear terms, no approximations are thus made (except for the linearized Einstein equation). In this way, we are led to a system of non-linear, coupled, partial differential equations in a spatially 1-D geometry: With the electric field E_y from Ohm's law, $E_y = -\frac{1}{c}V_zB_x$, Faraday's equation is fully expanded to

$$\partial_t B_x = c\partial_z E_y + \frac{1}{2}B_x \frac{\partial_t h}{1-h} - \frac{1}{2}cE_y \frac{\partial_z h}{1-h}. \quad (1)$$

Expansion of the z -component of the momentum equation yields

$$\begin{aligned} \partial_t q_{\hat{z}} + \partial_z \left[\left(q_{\hat{z}} - \frac{c}{4\pi} (-E_y B_x) \right) V_z \right] + \partial_z \left[\frac{c^2}{8\pi} (B_x^2 + E_y^2) \right] + c^2 \partial_z p \\ + \frac{c}{8\pi} B_x (cB_x + E_y V_z) \frac{\partial_z h}{(1+h)} - \frac{c}{8\pi} E_y (cE_y + B_x V_z) \frac{\partial_z h}{(1-h)} \\ - q_{\hat{z}} (\partial_t h + V_z \partial_z h) \frac{h}{1-h^2} = 0, \end{aligned} \quad (2)$$

where we defined the new momentum variable $q_{\hat{z}}$ as $q_{\hat{z}} := HV_z\hat{\gamma}^2 + \frac{c}{4\pi}(-E_y B_x)$. The continuity equation takes the form

$$\partial_t D + \partial_z(DV_z) - (D\partial_t h + DV_z\partial_z h) \frac{h}{1-h^2} = 0, \quad (3)$$

with the new density variable $D := \hat{\gamma}\rho$. The GW evolves according to

$$\partial_{tt} h = c^2 \partial_{zz} h + \frac{2G}{c^2} (E_y^2 - (B_x^2 - B_0^2)) + \frac{16\pi G}{c^2} (p - p_0)h, \quad (4)$$

where the background magnetic field B_0 and background pressure $p_0 = K\rho_0^\Gamma$ have been subtracted.

3. Numerical Solution

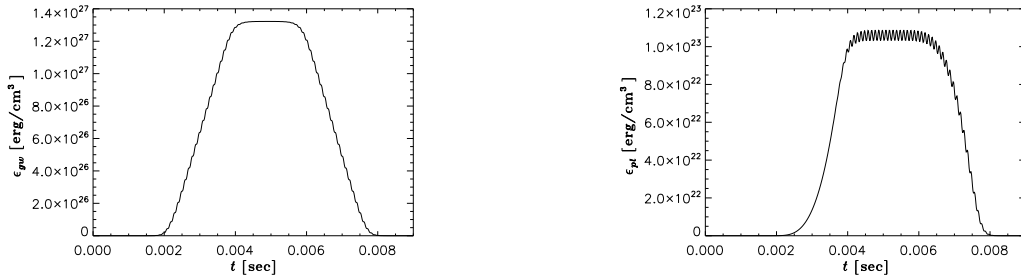


Figure 1: *Left: Average energy density $\epsilon_{gw}(t)$ of the GW as a function of time. — Right: Mean total energy density $\epsilon_{pl}(t)$ of the plasma as a function of time.*

We solve the GW-plasma system of equations applying a pseudo-spectral method that is based on Chebyshev polynomials (see e.g. Fornberg 1998). The basic principle is that all the spatially dependent variables are expanded in terms of Chebyshev polynomials, which allows to calculate the spatial derivatives, so that the original partial differential equations turn into a set of coupled, non-linear ordinary differential equations. Time stepping is then done with the method of lines, using a fourth order Runge-Kutta method with adaptive step-size control. The one-dimensional grid along the z -direction consists of 256 grid-points and corresponds to a physical domain along the z -axis of length $L = 5.4 \cdot 10^7$ cm. The sampling time step Δt is set to $\Delta t = T_{gw}/14$, with $T_{gw} = 1/f_{gw}$ and f_{gw} the GW frequency.

We assume a background magnetic field B_0 of 10^{15} G, a background density $\rho_0 = 10^{-14}$ g cm $^{-3}$, and an adiabatic index $\Gamma = 4/3$. The GW has as boundary condition at the left end z_L of the box $h(z_L, t) = h_0(t) \cos(k_{gw}z_L - \omega_{gw}t)$, so that a monochromatic plane wave is entering the box. The amplitude h_0 rises within roughly 1 ms from 0 to 10^{-4} , at which value it stays constant for about 3 ms where after it decays to 0 again. The GW frequency is set to $f_{gw} = 5$ kHz, and the GW dispersion relation is of the form $2\pi f_{gw} = \omega_{gw} = k_{gw}c$, with k_{gw} the wave-number of the GW. At the right edge z_R of the box, we apply non-reflecting boundary conditions to $h(z_R, t)$, and B_x , V_z , and ρ have free outflow boundary conditions at both edges of the box.

The total mean energy density ϵ_{pl} in the plasma at a given time t is numerically determined as

$$\epsilon_{pl}(t) = \left[\frac{1}{8\pi} \int E_y(z, t)^2 dz + \frac{1}{8\pi} \int (B_x(z, t) - B_0)^2 dz + \frac{1}{2} \int \rho(z, t) v_z(z, t)^2 dz \right] \frac{1}{L} \quad (5)$$

with L the size of the system — note that we subtract the constant background magnetic field B_0 in order to take into account only the energy that is in the wave motion. Fig. 1 shows $\epsilon_{pl}(t)$ and the mean energy density $\epsilon_{gw}(t)$ of the GW as a function of time, where $\epsilon_{gw}(t) = \frac{c^2}{32\pi G} \omega_{gw}^2 \bar{h}(t)^2$, with $\bar{h}(t)$ the mean instantaneous amplitude of the GW oscillation, defined as the root mean square average over the entire simulation box (Hartle 2003).

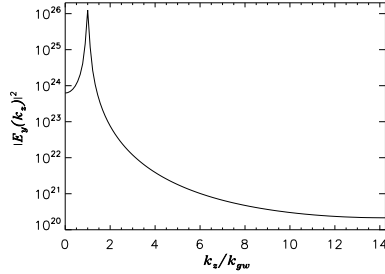


Figure 2: *Spatial Fourier transform* $|\hat{E}_y(k_z, t)|^2$ *of* $E_y(z, t)$ *at a fixed time* $t = 0.00545$ *s.*

In Fig. 1 then and at maximum GW amplitude, the energy density of the GW amounts to $\epsilon_{gw} = 1.3 \times 10^{27}$ erg/cm³. Once the GW enters the system, the plasma starts to absorb energy from the GW, and in roughly 2 ms, slightly delayed in the beginning but finally in parallel with the GW reaching its maximum energy, the absorption has reached its maximum, the energy density in the plasma is roughly 10^{23} erg/cm³. The absorbed energy is a fraction 10^{-4} of the GW energy density, so that the back-reaction onto the GW is not yet important. The GW excites wave motions in the plasma that travel with the GW and whose amplitudes increase linearly towards the out-flowing edge of the box. When the GW leaves the system, the energy in the plasma decays almost together with the GW amplitude, i.e. the excited waves propagate out of the simulation box. The fluid motions remain non-relativistic, so that our non-relativistic estimate of the kinetic energy is justified.

The waves excited in E_y , B_x , and V_z have wave-number k_z and frequency ω that cannot be distinguished from k_{gw} and ω_{gw} within the numerical precision of the simulation, see Fig. 2. The relativistic Alfvén speed $u_A^2 = B_0^2 / (4\pi\rho_0 + B_0^2/c^2)$ is very close to the speed of light, so that the excited plasma modes are indistinguishable from magneto-sonic modes. In particular, we do not find any harmonics to be excited.

In a parametric study, we found that the energy absorbed by the plasma is proportional to B_0^2 and to h_0^2 . Varying ρ_0 in the range 10^{-20} g/cm³ $\leq \rho_0 \leq 10^5$ g/cm³, it turned out that the absorbed energy is independent of the value of the matter density ρ_0 . The absorbed energy density is furthermore proportional to ω_{gw}^2 , as we verified by varying the frequency in the kHz range. It also seems that the time for the plasma needed to reach the maximum level of energy absorption is related to the time needed for the GW to cross the box, L/c , which equals 0.002 sec for the case considered here.

We can summarize our numerical findings for the total energy E_{pl} absorbed by a plasma that interacts with a GW along a length L as follows,

$$E_{pl} = 3.4 \times 10^7 \left(\frac{L}{1 \text{ cm}} \right)^3 \left(\frac{A_{eff}}{1 \text{ cm}^2} \right) \left(\frac{B_0}{10^{15} \text{ G}} \right)^2 \left(\frac{h_0}{10^{-4}} \right)^2 \left(\frac{f_{gw}}{5 \text{ kHz}} \right)^2 \text{ erg}, \quad (6)$$

and E_{pl} is independent of ρ_0 (A_{eff} is the area through which the GW is incident).

4. Conclusion

Our results show that strongly magnetized plasmas, with magnetic fields of the order of 10^{15} Gauss, are efficient absorbers of GW energy, largely irrespective of the plasma density, and with an absorption time-scale of the order of milli-seconds. The excited plasma modes are of the magnetosonic type, with phase-velocity that numerically is indiscernible from the speed of light, and no harmonics are found to be excited. The damping of the GWs is still relatively weak, even for the very strong magnetic fields considered here. The results concerning the plasma energetics are summarized in the scaling law of Eq. (6) and they imply that GWs may be the energy source for secondary, very energetic phenomena in the vicinity of strongly magnetized stars.

Acknowledgments: This work was supported by the Greek Ministry of Education through the PYTHAGORAS program. We thank K. Kokkotas, J. Moortgat, D. Papadopoulos, N. Stergioulas, and J. Ventura for helpful discussions.

References

- Brodin, G., Marklund, M., Phys. Rev. Lett. **82**, 3012 (1999).
Brodin, G., Marklund, M., Dunsby, P. K. S., Phys. Rev. D **62**, 104008 (2000).
Duez, M.D., Liu, Y.T., Shapiro, S.L., Stephens, B.S., arXiv:astro-ph/0503420, (2005).
Fornberg, B., *A Practical Guide to Pseudospectral Methods*, Cambridge, (1998).
Hartle, J.B, *Gravity*, San Francisco (Addison Wesley), (2003).
Ignat'ev, Yu.G., Gravitation and Cosmology, Vol. 1, No. 04, pp. 287 – 300 (1995).
Källberg, A., Brodin, G., Bradley, M., Phys. Rev. D **70**, 044014 (2004)
Kokkotas, K.D., Class. Quantum Grav. **21**, S501 (2004).
Landau, L. D. and Lifshitz, E.M., *The Classical Theory of Fields*, 4th ed., Oxford, (1984)
Moortgat, J., Kuijpers, J., Astron. & Astrophys. **402**, 905 (2003).
Moortgat, J., Kuijpers, J., Phys. Rev. D **70**, 3001 (2004)
Papadopoulos, D., Stergioulas, N., Vlahos, L., Kuijpers, J., Astron. & Astrophys. **377**, 701 (2001)
Servin, M., Brodin, G., Phys. Rev. D **68**, 044017 (2003).
Servin, M., Brodin, G., M. Bradley, and Marklund, M, Phys. Rev. E **62**, 8493 (2000)
Thorne, K.S., Blandford, R.D., *Applications of Classical Physics*, Chap. 26, (2004)
(<http://www.pma.caltech.edu/Courses/ph136/yr2004/>)

INTRODUCING QUADRATIC GRAVITY *

K. Kleidis^{1,2†}

¹ Department of Physics, Aristotle University of Thessaloniki,
54124, Thessaloniki, Greece

² Department of Civil Engineering, Technological Education Institute of Serres,
62124, Serres, Greece

Abstract

A novel approach in the semiclassical interaction of gravity with a quantum scalar field is considered, to guarantee the renormalizability of the energy-momentum tensor in a multi-dimensional curved spacetime. According to it, a self-consistent coupling between the square curvature term \mathcal{R}^2 and the quantum field is introduced. The subsequent interaction discards any higher-order derivative terms from the gravitational field equations, but, in the expense, it introduces a *geometric source* term in the wave equation for the quantum field. Unlike the conformal coupling case, this term does not represent an additional "mass" and, therefore, the quantum field interacts with gravity in a generic way and not only through its mass (or energy) content.

Key-words: Quantum gravity - semiclassical theory - gravity quintessence

1. Introduction

In the last few decades there has been a remarkable progress in understanding the quantum structure of the non-gravitational fundamental interactions (Nanopoulos 1997). On the other hand, so far, there is no quantum framework consistent enough to describe gravity itself (Padmanabhan 1989), leaving string theory as the most successful attempt towards this direction (Green et al 1987, Polchinsky 1998, Schwarz 1999). Within the context of General Relativity (GR), one usually resorts to perturbations' approach, where string theory predicts corrections to the Einstein equations. Those corrections originate from higher-order curvature terms arising in the string action, but their exact form is not yet being fully explored (Polchinsky 1998).

A self-consistent mathematical background for *higher-order gravity theories* was formulated by Lovelock (1971). According to it, the most general gravitational

*Presented at the Workshop on *Cosmology and Gravitational Physics*, 15-16 December 2005, Thessaloniki, Greece, *Editors*: N.K. Spyrou, N. Stergioulas and C.G. Tsagas.

†kleidis@astro.auth.gr

Lagrangian reads

$$\mathcal{L} = \sqrt{-g} \sum_{m=0}^{n/2} \lambda_m \mathcal{L}^{(m)} \quad (1)$$

where λ_m are constant coefficients, n denotes the spacetime dimensions, g is the determinant of the metric tensor and $\mathcal{L}^{(m)}$ are functions of the Riemann curvature tensor \mathcal{R}_{ijkl} and its contractions \mathcal{R}_{ij} and \mathcal{R} , of the form

$$\mathcal{L}^{(m)} = \frac{1}{2^m} \delta_{i_1 \dots i_{2m}}^{j_1 \dots j_{2m}} \mathcal{R}_{j_1 j_2 \dots}^{i_1 i_2 \dots} \mathcal{R}_{j_{2m-1} j_{2m}}^{i_{2m-1} i_{2m}} \quad (2)$$

where Latin indices refer to the n -dimensional spacetime and $\delta_{i_1 \dots i_{2m}}^{j_1 \dots j_{2m}}$ is the generalized Kronecker symbol. In Eq (2), $\mathcal{L}^{(1)} = \frac{1}{2} \mathcal{R}$ is the Einstein-Hilbert (EH) Lagrangian, while $\mathcal{L}^{(2)}$ is a particular combination of quadratic terms, known as the Gauss-Bonnett (GB) combination, since in four dimensions it satisfies the functional relation

$$\frac{\delta}{\delta g^{\mu\nu}} \int \sqrt{-g} \left(\mathcal{R}^2 - 4\mathcal{R}_{\mu\nu} \mathcal{R}^{\mu\nu} + \mathcal{R}_{\mu\nu\kappa\lambda} \mathcal{R}^{\mu\nu\kappa\lambda} \right) d^4x = 0 \quad (3)$$

corresponding to the GB theorem (Kobayashi and Nomizu 1969). In Eq (3), Greek indices refer to four-dimensional coordinates. Introducing the GB term into the gravitational Lagrangian will not affect the four-dimensional field equations at all. However, within the context of the perturbations' approach mentioned above, the most important contribution comes from the GB term (Mignemi and Stewart 1993). As in four dimensions it is a total divergence, to render this term dynamical, one has to consider a higher-dimensional background or to couple it to a scalar field.

The idea of a multi-dimensional spacetime has received much attention as a candidate for the unification of all fundamental interactions, including gravity, in the framework of *super-gravity* and *super-strings* (Appelquist et al 1987, Green et al 1987). In most higher-dimensional theories of gravity, the extra dimensions are assumed to form, at the present epoch, a compact manifold (*internal space*) of very small size compared to that of the three-dimensional visible space (*external space*) and therefore they are unobservable at the energies currently available (Green et al 1987). This so-called *compactification* of the extra dimensions may be achieved, in a natural way, by adding a square-curvature term ($\mathcal{R}_{ijkl} \mathcal{R}^{ijkl}$) in the EH action of the gravitational field (Müller-Hoissen 1988). In this way, the higher-dimensional theories are closely related to those of non-linear Lagrangians and their combination probably yields a natural generalization of GR.

In the present paper, we explore this generalization, in view of the renormalizable energy-momentum tensor which acts as the source of gravity in the (semiclassical) interaction between the gravitational and a quantum matter field. In particular:

We discuss briefly how GR is modified by the introduction of the renormalizable energy-momentum tensor first recognized by Calan et al (1970), on the rhs of the field equations. Introducing an analogous method, we explore the corresponding implications as regards a multi-dimensional higher-order gravity theory. We find that, in this case, the action functional, describing the semi-classical interaction of a quantum scalar field with the classical gravitational one, is being further modified

and its variation with respect to the quantum field results in an inhomogeneous Klein-Gordon equation, the source term of which is purely geometric ($\sim \mathcal{R}^2$).

2. A Quadratic Interaction

Conventional gravity in n -dimensions implies that the dynamical behavior of the gravitational field arises from an action principle involving the EH Lagrangian

$$\mathcal{L}_{EH} = \frac{1}{16\pi G_n} \mathcal{R} \quad (4)$$

where, $G_n = GV_{n-4}$ and V_{n-4} denotes the volume of the internal space, formed by some extra spacelike dimensions. In this framework, we consider the semi-classical interaction between the gravitational and a massive quantum scalar field $\Phi(t, \vec{x})$ to the lowest order in G_n . The quantization of the field $\Phi(t, \vec{x})$ is performed by imposing canonical commutation relations on a hypersurface $t = \text{constant}$ (Isham 1981)

$$\begin{aligned} [\Phi(t, \vec{x}), \Phi(t, \vec{x}')] &= 0 = [\pi(t, \vec{x}), \pi(t, \vec{x}')] \\ [\Phi(t, \vec{x}), \pi(t, \vec{x}')] &= i\delta^{(n-1)}(\vec{x} - \vec{x}') \end{aligned} \quad (5)$$

where, $\pi(t, \vec{x})$ is the momentum canonically conjugate to the field $\Phi(t, \vec{x})$. The equal-time commutation relations (5) guarantee the local character of the quantum field theory under consideration, thus attributing its time-evolution to the classical gravitational field equations (Birrell and Davies 1982).

In any local field theory, the corresponding energy-momentum tensor is a very important object. Knowledge of its matrix elements is necessary to describe scattering in a relatively-weak external gravitational field. Therefore, in any quantum process in curved spacetime, it is desirable for the corresponding energy-momentum tensor to be *renormalizable*; i.e. its matrix elements to be cut-off independent (Birrell and Davies 1982). In this context, it has been proved (Callan et al 1970) that the functional form of the renormalizable energy-momentum tensor involved in the semi-classical interaction between the gravitational and a quantum field in n -dimensions, should be

$$\Theta_{ik} = T_{ik} - \frac{1}{4} \frac{n-2}{n-1} [\Phi^2_{;ik} - g_{ik} \square \Phi^2] \quad (6)$$

where, the semicolon stands for covariant differentiation (∇_k), $\square = g^{ik} \nabla_i \nabla_k$ is the d' Alembert operator and

$$T_{ik} = \Phi_{,i} \Phi_{,k} - g_{ik} \mathcal{L}_{mat} \quad (7)$$

is the *conventional* energy-momentum tensor of an (otherwise) free massive scalar field, with Lagrangian density of the form

$$\mathcal{L}_{mat} = \frac{1}{2} [g^{ik} \Phi_{,i} \Phi_{,k} - m^2 \Phi^2] \quad (8)$$

It is worth noting that the tensor (6) defines the same n -momentum and Lorentz generators as the conventional energy-momentum tensor.

It has been shown (Callan et al 1970) that the energy-momentum tensor (6) can be obtained by an action principle, involving

$$S = \int [f(\Phi)\mathcal{R} + \mathcal{L}_{mat}] \sqrt{-g} d^n x \quad (9)$$

where, $f(\Phi)$ is an arbitrary, analytic function of $\Phi(t, \vec{x})$, the determination of which can be achieved by demanding that the rhs of the field equations resulting from Eq (9) is given by Eq (6). Accordingly,

$$\frac{\delta S}{\delta g^{ik}} = 0 \Rightarrow \mathcal{R}_{ik} - \frac{1}{2} g_{ik} \mathcal{R} = -8\pi G_n \Theta_{ik} = -\frac{1}{2f} (T_{ik} + 2f_{;ik} - 2g_{ik} \square f) \quad (10)$$

To lowest order in G_n , one obtains (Callan et al 1970)

$$f(\Phi) = \frac{1}{16\pi G_n} - \frac{1}{8} \frac{n-2}{n-1} \Phi^2 \quad (11)$$

Therefore, in any *linear Lagrangian gravity theory*, the interaction between a quantum scalar field and the classical gravitational one is determined through Hamilton's principle involving the action scalar

$$S = \int \sqrt{-g} \left[\left(\frac{1}{16\pi G_n} - \frac{1}{8} \frac{n-2}{n-1} \Phi^2 \right) \mathcal{R} + \mathcal{L}_{mat} \right] d^n x \quad (12)$$

On the other hand, both super-string theories (Candelas et al 1985, Green et al 1987) and the one-loop approximation of quantum gravity (Kleidis and Papadopoulos 1998), suggest that the presence of quadratic terms in the gravitational action is *a priori* expected. Therefore, in connection to the semi-classical interaction previously stated, the question that arises now is, what the functional form of the corresponding *renormalizable* energy-momentum tensor might be, if the simplest quadratic curvature term, \mathcal{R}^2 , is included in the description of the classical gravitational field. To answer this question, by analogy to Eq (9), we may consider the action principle

$$\frac{\delta}{\delta g^{ik}} \int \sqrt{-g} [f_1(\Phi)\mathcal{R} + \alpha f_2(\Phi)\mathcal{R}^2 + \mathcal{L}_{mat}] d^n x = 0 \quad (13)$$

where, both $f_1(\Phi)$ and $f_2(\Phi)$ are arbitrary, polynomial functions of Φ . Eq (13) yields

$$\mathcal{R}_{ik} - \frac{1}{2} g_{ik} \mathcal{R} = -\frac{1}{2F} [T_{ik} + 2F_{;ik} - 2g_{ik} \square F + \alpha g_{ik} f_2(\Phi) \mathcal{R}^2] \quad (14)$$

where, the function F stands for the combination

$$F = f_1(\Phi) + 2\alpha \mathcal{R} f_2(\Phi) \quad (15)$$

For $\alpha = 0$ and to the lowest order in G_n (but to every order in the coupling constants of the quantum field involved), we must have

$$\mathcal{R}_{ik} - \frac{1}{2} g_{ik} \mathcal{R} = -8\pi G_n \Theta_{ik} \quad (16)$$

where, Θ_{ik} [given by Eq (6)] is the renormalizable energy-momentum tensor first recognized by Calan et al (1970). In this respect, we obtain $f_1(\Phi) = f(\Phi)$, i.e. a function quadratic in Φ [see Eq (11)]. Furthermore, on dimensional grounds regarding Eq (14), we expect that

$$F \sim \Phi^2 \quad (17)$$

and, therefore, $\alpha\mathcal{R}f_2(\Phi) \sim \Phi^2$, as well. However, we already know that $\mathcal{R} \sim [\Phi]$, as indicated by Whitt (1984), something that leads to $f_2(\Phi) \sim \Phi^{-1}$ and in particular,

$$F(\Phi) = \frac{1}{16\pi G_n} - \frac{1}{8} \frac{n-2}{n-1} [\Phi^2] + 2\alpha\mathcal{R}\Phi \quad (18)$$

In Eq (18), the coupling parameter α encapsulates any arbitrary constant that may be introduced in the definition of $f_2(\Phi)$. Accordingly, the action describing the semi-classical interaction of a quantum scalar field with the classical gravitational one up to the second order in curvature tensor, is being further modified and is written in the form

$$S = \int \sqrt{-g} \left[\left(\frac{1}{16\pi G_n} - \frac{1}{2} \xi_n \Phi^2 \right) \mathcal{R} + \alpha \mathcal{R}^2 \Phi + \mathcal{L}_{mat} \right] d^n x \quad (19)$$

where

$$\xi_n = \frac{1}{4} \frac{n-2}{n-1} \quad (20)$$

is the so-called *conformal coupling* parameter (Birrell and Davies 1982). In this case, the associated gravitational field equations (14) result in

$$\mathcal{R}_{ik} - \frac{1}{2} g_{ik} \mathcal{R} = -8\pi G_n (\Theta_{ik} + \alpha S_{ik}) \quad (21)$$

where

$$S_{ik} = g_{ik} \mathcal{R}^2 \Phi \quad (22)$$

The rhs of Eq (21) represents the "new" renormalizable energy-momentum tensor. Notice that, as long as $\alpha \neq 0$, this tensor contains the extra "source" term S_{ik} . In spite the presence of this term, the generalized energy-momentum tensor still remains renormalizable. This is due to the fact that, the set of the quantum operators $\{\Phi, \Phi^2, \square\Phi\}$ is closed under renormalization, as it can be verified by straightforward power counting (see Callan et al 1970).

Eq (22) implies that the quadratic curvature term (i.e. pure global gravity) acts as a source of the quantum field Φ . Indeed, variation of Eq (19) with respect to $\Phi(t, \vec{x})$ leads to the following quantum field equation of propagation

$$\square\Phi + m^2\Phi + \xi_n \mathcal{R}\Phi = \alpha \mathcal{R}^2 \quad (23)$$

that is, an inhomogeneous Klein-Gordon equation in curved spacetime. It is worth pointing out that, in Eq (19), the generalized coupling constant α remains dimensionless (and this is also the case for the corresponding action) only as long as

$$n = 6 \quad (24)$$

¹In fact, $[\mathcal{R}] \sim [\Phi]^{\frac{4}{n-2}}$ and, therefore, $f_2 \sim \Phi^{2\frac{n-4}{n-2}}$. In order to render the coupling constant α dimensionless, one should consider $n = 6$. Hence, $f_2 \sim \Phi$ only in six dimensions.

thus indicating the appropriate spacetime dimensions for the semi-classical theory under consideration to hold, without introducing any additional arbitrary length scales.

Summarizing, a self-consistent coupling between the square curvature term \mathcal{R}^2 and the quantum field $\Phi(t, \vec{x})$ should be introduced in order to yield the "correct" renormalizable energy-momentum tensor in non-linear gravity theories. The subsequent *quadratic interaction* discards any higher-order derivative terms from the gravitational field equations, but it introduces a *geometric source* term in the wave equation for the quantum field. In this case, unlike the *conventional* conformal coupling ($\sim \mathcal{R}\Phi^2$), the quantum field interacts with gravity not only through its mass (or energy) content ($\sim \Phi^2$), but, also, in a more generic way ($\mathcal{R}^2\Phi$).

Acknowledgements

This research has been supported by the Greek Ministry of Education, through the PYTHAGORAS program.

References

- Appelquist T, Chodos A and Freund P, 1987, *Modern Kaluza-Klein Theories*, Addison-Wesley, Menlo Park, CA
- Birrell N D and Davies P C W, 1982, *Quantum Fields in Curved Space*, Cambridge University Press, Cambridge
- Calan C G, Coleman S and Jackiw R, 1970, *Ann Phys* **59**, 42
- Candelas P, Horowitz G T, Strominger A and Witten E, 1985, *Nucl Phys B* **258**, 46
- Green M B, Schwartz J H and Witten E, 1987, *Superstring Theory*, Cambridge University Press, Cambridge
- Isham C J, 1981, "Quantum Gravity - an overview", in *Quantum Gravity: a Second Oxford Symposium*, ed C J Isham, R Penrose and D W Sciama, Clarendon, Oxford
- Kleidis K and Papadopoulos D B, 1998, *Class Quantum Grav* **15**, 2217
- Kobayashi S and Nomizu K, 1969, *Foundations of Differential Geometry II*, Wiley InterScience, NY
- Lovelock D, 1971, *J Math Phys* **12**, 498
- Mignemi S and Stewart N R, 1993, *Phys Rev D* **47**, 5259
- Müller-Hoissen F, 1988, *Class Quantum Grav* **5**, L35
- Nanopoulos D B, 1997, *preprint*, hep-th/9711080
- Polchinski J 1998, *String Theory*, Cambridge University Press, Cambridge
- Padmanabhan T, 1989, *Int J Mod Phys A* **18**, 4735
- Schwartz J H, 1999, *Phys Rep* **315**, 107
- Whitt B, 1984, *Phys Lett B* **145**, 176

ANALYTICAL DESCRIPTION OF THE MOTION OF COMPACT BINARIES *

Gerhard Schäfer[†]

Theoretisch-Physikalisches Institut, Friedrich-Schiller-Universität, 07743 Jena, Germany

Abstract

In the theory of general relativity, the dynamics of compact binaries is explicitly known up to the third-and-a-half post-Newtonian order of approximation. For the conservative part of the dynamics, fully explicit analytical solutions for the motion are given in this contribution. Predictions for the location of the innermost stable circular orbit (ISCO) are made.

1. Introduction

The general relativistic problem of motion of compact binaries (neutron stars, black holes) has quite a long history. In 1938, Robertson derived an expression for the periastron advance appearing at the first post-Newtonian level of approximation (1PNA), i.e. order $1/c^2$, where c denotes the speed-of-light constant, based on the Einstein-Infeld-Hoffmann equations from 1938. It was only during the 1980s, when attempts were made to compute the next post-Newtonian correction to the periastron advance. In 1987, Damour & Schäfer succeeded in computing the periastron advance and orbital period expressions at 2PNA, relying on earlier works by Ohta et al (1974), Damour & Deruelle (1981), Damour (1982), and Damour & Schäfer (1985). Finally in the year 2000, motivated by the on-going efforts to detect gravitational waves, the periastron advance and orbital expressions at 3PNA were obtained by Damour et al (2000a) [see Damour et al (2001) for the unique determination of an ambiguous coefficient using dimensional regularization] relying on papers by Jaranowski & Schäfer (1998), (1999). Explicit solutions for the binary orbits were derived by Damour & Deruelle (1985) at 1PNA; by Damour & Schäfer (1988) and Schäfer & Wex (1993) at 2PNA; and by Memmesheimer et al (2004) at 3PNA. Further, the analytical description for the compact binary dynamics at 3PNA allowed Damour et al (2000b) and Blanchet (2002) to obtain estimates for the location of the innermost stable circular orbit (ISCO) at 3PNA.

*Presented at the Workshop on *Cosmology and Gravitational Physics*, 15-16 December 2005, Thessaloniki, Greece, *Editors*: N.K. Spyrou, N. Stergioulas and C.G. Tsagas.

[†]gos@tpi.uni-jena.de

2. Canonical approach to the dynamics of general relativity

The canonical formulation of general relativity by Arnowitt, Deser, and Misner (1962) provides a powerful tool for the calculation of the general relativistic dynamics of compact binaries. Within the ADM approach, the equations of motion of physical systems are obtained by solving the four constraint equations of general relativity. For point masses, the four constraint equations read

$$g^{1/2}R = \frac{1}{g^{1/2}} \left(\pi_j^i \pi_i^j - \frac{1}{2} \pi_i^i \pi_j^j \right) + \frac{16\pi G}{c^3} \sum_a \left(m_a^2 c^2 + g^{ij} p_{ai} p_{aj} \right)^{1/2} \delta_a , \quad (1)$$

$$-2\partial_j \pi_i^j + \pi^{kl} \partial_i g_{kl} = \frac{16\pi G}{c^3} \sum_a p_{ai} \delta_a , \quad (2)$$

where the first and second equations give the Hamiltonian and the momentum constraint, respectively. The determinant of the 3-metric g_{ij} , associated with spacelike hypersurfaces ($t = \text{constant}$), is denoted by g and the inverse metric g^{ij} is defined by $g^{il} g_{lj} = \delta_{ij}$. The canonical momentum conjugate to the 3-metric is proportional to $\pi^{ij} = -g^{1/2}(K^{ij} - g^{ij} K_l^l)$, where K_{ij} is the extrinsic curvature (second fundamental form) of the $t = \text{constant}$ slices, whose intrinsic curvature is denoted R . Lowering and raising of indices are performed with the 3-metric and its inverse. The mass parameter of a point mass, labeled a , is denoted m_a and its linear momentum and (coordinate) position vector are denoted by p_{ai} and x_a^i , respectively. By definition, $\delta_a = \delta(x^i - x_a^i)$ holds with $\int d^3x \delta = 1$, and as usual, G denotes the Newtonian gravitational constant.

Unique solutions of the constraint equations need four coordinate conditions. The following ADM coordinate conditions have proved very useful in analytical calculations,

$$\pi^{ii} = 0 , \quad g_{ij} = \psi^4 \delta_{ij} + h_{ij}^{\text{TT}} , \quad (3)$$

where h_{ij}^{TT} is a transverse and traceless tensor in flat 3-space. A related decomposition for π^{ij} takes the form $\pi^{ij} = \pi_{\text{LT}}^{ij} + \pi_{\text{TT}}^{ij}$, where π_{LT}^{ij} and π_{TT}^{ij} are longitudinal traceless and transverse traceless tensors, respectively. Notice that the coordinate conditions do not imply the often used maximal slicing condition $\pi_i^i = 2g^{1/2}K_i^i = 0$ but rather $\pi_i^i = \pi^{ij} h_{ij}^{\text{TT}}$ which is called asymptotically maximal slicing because of $\pi_i^i = O(1/r^3)$ at spacelike infinity.

The Hamiltonian functional which determines the equations of motion of the point masses and the evolution equations for the independent field degrees of freedom is given by

$$H_{\text{ADM}}[x_a^i, p_{ai}, h_{ij}^{\text{TT}}, \pi_{\text{TT}}^{ij}] = -\frac{c^4}{2\pi G} \int d^3x \Delta\psi . \quad (4)$$

The equations of motion for the point masses and the field equations read,

$$\dot{p}_{ai} = -\frac{\partial H_{\text{ADM}}}{\partial x_a^i} , \quad \dot{x}_a^i = \frac{\partial H_{\text{ADM}}}{\partial p_{ai}} , \quad (5)$$

$$\dot{\pi}_{\text{TT}}^{ij} = -\frac{\delta H_{\text{ADM}}}{\delta h_{ij}^{\text{TT}}}, \quad \dot{h}_{ij}^{\text{TT}} = \frac{\delta H_{\text{ADM}}}{\delta \pi_{\text{TT}}^{ij}}. \quad (6)$$

The transition to a Routh functional formulation simplifies the derivation of the conservative part of the dynamics. The associated Routh functional reads

$$R[x_a^i, p_{ai}, h_{ij}^{\text{TT}}, \dot{h}_{ij}^{\text{TT}}] = H_{\text{ADM}}[x_a^i, p_{ai}, h_{ij}^{\text{TT}}, \pi_{\text{TT}}^{ij}] - \frac{c^3}{16\pi G} \int d^3x \dot{h}_{ij}^{\text{TT}} \pi_{\text{TT}}^{ij}. \quad (7)$$

The resulting field equations

$$\frac{\delta R}{\delta h_{ij}^{\text{TT}}} - \partial_t \frac{\delta R}{\delta \dot{h}_{ij}^{\text{TT}}} = 0 \quad (8)$$

are solved by using the no-incoming radiation condition. When plugging the solution into R , a conservative Hamiltonian functional for the point masses is obtained,

$$H[x_a^i, p_{ai}] = R[x_a^i, p_{ai}, h_{ij}^{\text{TT}}[x_a^i, p_{ai}], \dot{h}_{ij}^{\text{TT}}[x_a^i, p_{ai}]]. \quad (9)$$

At 3PNA, the Hamiltonian has the following structure

$$H^{3\text{PN}}[x_a^i, p_{ai}] = H(x_a^i, p_{ai}, \dot{x}_a^i, \dot{p}_{ai}) \quad (10)$$

which implies prolonged equations of motion of the form

$$\dot{p}_{ai} = -\frac{\partial H^{3\text{PN}}}{\partial x_a^i} + \frac{d}{dt} \frac{\partial H^{3\text{PN}}}{\partial \dot{x}_a^i}, \quad \dot{x}_a^i = \frac{\partial H^{3\text{PN}}}{\partial p_{ai}} - \frac{d}{dt} \frac{\partial H^{3\text{PN}}}{\partial \dot{p}_{ai}}. \quad (11)$$

With the aid of a coordinate transformation in phase space, an ordinary Hamiltonian can be derived, $\bar{H}^{3\text{PN}}(\bar{x}_a^i, \bar{p}_{ai})$, see Damour et al (2000a). This Hamiltonian is straightforwardly obtained by setting

$$\bar{H}^{3\text{PN}}(x_a^i, p_{ai}) = H(x_a^i, p_{ai}, \dot{x}_a^i(x_b^i, p_{bi}), \dot{p}_{ai}(x_b^i, p_{bi})). \quad (12)$$

Notice the coordinate transformation which is implicit in Eq. (12).

The full dynamics of the binary system, including radiation reaction, results from the equations

$$\dot{p}_{ai} = -\frac{\partial R[x_a^i, p_{ai}, h_{ij}^{\text{TT}}, \dot{h}_{ij}^{\text{TT}}]}{\partial x_a^i}, \quad \dot{x}_a^i = \frac{\partial R[x_a^i, p_{ai}, h_{ij}^{\text{TT}}, \dot{h}_{ij}^{\text{TT}}]}{\partial p_{ai}}, \quad (13)$$

where after differentiation the functionals $h_{ij}^{\text{TT}}[x_a^i, p_{ai}]$ and $\dot{h}_{ij}^{\text{TT}}[x_a^i, p_{ai}]$ have to be substituted. The radiation reaction terms enter the dynamics, for the first time at 2.5PNA, and then at 3.5PNA.

3. Explicit Hamiltonian at 3PNA

The Hamiltonian for two point masses is explicitly known up to the 3.5PNA, i.e. to the order $1/c^7$. Its structure reads

$$H^{3.5PN}(t) = \bar{H}^{3PN} + \frac{1}{c^5} H_{[2.5PN]}(t) + \frac{1}{c^7} H_{[3.5PN]}(t), \quad (14)$$

where the (t) -argument indicates that the those Hamiltonians are not autonomous, i.e. they have to be treated as depending on h_{ij}^{TT} and \dot{h}_{ij}^{TT} . The non-conservative Hamiltonians result from Eq. (13). In the center-of-mass frame and in reduced variables, the conservative part of the total Hamiltonian reads

$$\hat{H}^{3PN} = \hat{H}_{[N]} + \frac{1}{c^2} \hat{H}_{[1PN]} + \frac{1}{c^4} \hat{H}_{[2PN]} + \frac{1}{c^6} \hat{H}_{[3PN]}, \quad (15)$$

where

$$\hat{H}_{[N]} = \frac{p^2}{2} - \frac{1}{r}, \quad (16)$$

$$\hat{H}_{[1PN]} = \frac{1}{8}(3\eta - 1)p^4 - \frac{1}{2} \left[(3 + \eta)p^2 + \eta p_r^2 \right] \frac{1}{r} + \frac{1}{2r^2}, \quad (17)$$

$$\begin{aligned} \hat{H}_{[2PN]} &= \frac{1}{16}(1 - 5\eta + 5\eta^2)p^6 \\ &+ \frac{1}{8} \left[(5 - 20\eta - 3\eta^2)p^4 - 2\eta^2 p_r^2 p^2 - 3\eta^2 p_r^4 \right] \frac{1}{r} \\ &+ \frac{1}{2} \left[(5 + 8\eta)p^2 + 3\eta p_r^2 \right] \frac{1}{r^2} - \frac{1}{4}(1 + 3\eta) \frac{1}{r^3}, \end{aligned} \quad (18)$$

$$\begin{aligned} \hat{H}_{[3PN]} &= \frac{1}{128}(-5 + 35\eta - 70\eta^2 + 35\eta^3)p^8 \\ &+ \frac{1}{16} \left[(-7 + 42\eta - 53\eta^2 - 5\eta^3)p^6 + (2 - 3\eta)\eta^2 p_r^2 p^4 \right. \\ &+ \left. 3(1 - \eta)\eta^2 p_r^4 p^2 - 5\eta^3 p_r^6 \right] \frac{1}{r} \\ &+ \left[\frac{1}{16}(-27 + 136\eta + 109\eta^2)p^4 + \frac{1}{16}(17 + 30\eta)\eta p_r^2 p^2 \right. \\ &+ \left. \frac{1}{12}(5 + 43\eta)\eta p_r^4 \right] \frac{1}{r^2} \\ &+ \left[\left(-\frac{25}{8} + \left(\frac{1}{64}\pi^2 - \frac{335}{48} \right) \eta - \frac{23}{8}\eta^2 \right) p^2 \right. \\ &+ \left. \left(-\frac{85}{16} - \frac{3}{64}\pi^2 - \frac{7}{4}\eta \right) \eta p_r^2 \right] \frac{1}{r^3} + \left[\frac{1}{8} + \left(\frac{109}{12} - \frac{21}{32}\pi^2 \right) \eta \right] \frac{1}{r^4}, \end{aligned} \quad (19)$$

and where the following definitions have been employed: $\hat{H}^{3PN} = (\bar{H}^{3PN} - Mc^2)/\mu$, $\mu = m_1 m_2 / M$, $M = m_1 + m_2$, $\eta = \mu / M$, $0 \leq \eta \leq \frac{1}{4}$, $\eta = 0$ (test-body case), $\eta = \frac{1}{4}$ (equal-mass case), $\mathbf{p}_1 + \mathbf{p}_2 = 0$ (center-of-mass condition), $\mathbf{p} \equiv \mathbf{p}_1 / \mu$, $p_r = (\mathbf{n} \cdot \mathbf{p})$, $\mathbf{r} \equiv (\mathbf{x}_1 - \mathbf{x}_2) / GM$, $\mathbf{n} = \mathbf{r} / |\mathbf{r}|$.

The Hamiltonian functions $H_{[2.5PN]}(t)$ and $H_{[3.5PN]}(t)$ were derived by Schäfer (1995) and Königsdörffer et al (2003), respectively, where the latter work is based on a paper by Jaranowski and Schäfer (1997). Parametric descriptions to the dynamics of compact binaries at 2.5PNA and 3.5PNA were obtained recently by Damour et al (2004) and Königsdörffer & Gopakumar (2006), respectively. In the following, we will only present a parametric prescription to describe the conservative compact binary dynamics at 3PNA [more details of the presented results may be found in Memmesheimer et al (2004)].

4. Stationary orbits at 3PNA

The invariance of \hat{H}^{3PN} under time translation and spatial rotations leads to the following conserved quantities: The 3PN reduced energy $E = \hat{H}^{3PN}$ and the reduced angular momentum $\hat{\mathbf{J}} = \mathbf{r} \times \mathbf{p}$ of the binary in the center-of-mass frame. The conservation of $\hat{\mathbf{J}}$ particularly implies that the motion is restricted to a plane and polar coordinates may be introduced such that $\mathbf{r} = r(\cos \phi, \sin \phi)$. The equations of motion for the velocity components read

$$\dot{r} = \left(\mathbf{n} \cdot \frac{\partial \hat{H}^{3PN}}{\partial \mathbf{p}} \right), \quad (20)$$

$$r^2 \dot{\phi} = \left| \mathbf{r} \times \frac{\partial \hat{H}^{3PN}}{\partial \mathbf{p}} \right|, \quad (21)$$

where $\dot{r} = dr/dt$, $\dot{\phi} = d\phi/dt$ and t denotes the coordinate time scaled by GM .

The 3PN-accurate orbital parameterization can be obtained by calculating the two non-zero positive roots, having finite limits as $\frac{1}{c} \rightarrow 0$, of the 3PN-accurate expression for \dot{r}^2 expressed in terms of E , $h = |\hat{\mathbf{J}}|$, η , and $s = 1/r$. These two 3PN-accurate roots, labeled s_- and s_+ , correspond to the turning points of the radial motion and hence to the periastron and the apastron of the post-Newtonian eccentric orbit. The radial motion is uniquely parametrized by using the ansatz

$$r = a_r(1 - e_r \cos u), \quad (22)$$

where a_r and e_r are some 3PN-accurate semi-major axis and radial eccentricity which may be expressed in terms of s_- and s_+ as

$$a_r = \frac{1}{2} \frac{s_- + s_+}{s_- s_+}, \quad e_r = \frac{s_- - s_+}{s_- + s_+}. \quad (23)$$

With the aid of the true anomaly v , parametrized as

$$v = 2 \arctan \left[\left(\frac{1 + e_\phi}{1 - e_\phi} \right)^{1/2} \tan \frac{u}{2} \right], \quad (24)$$

the 3PN-accurate generalized quasi-Keplerian parametrization for a compact binary moving in an eccentric orbit in ADM-type coordinates can be obtained in the form

$$\begin{aligned} l \equiv n(t - t_0) &= u - e_t \sin u + \left(\frac{g_{4t}}{c^4} + \frac{g_{6t}}{c^6} \right) (v - u) \\ &\quad + \left(\frac{f_{4t}}{c^4} + \frac{f_{6t}}{c^6} \right) \sin v + \frac{i_{6t}}{c^6} \sin 2v + \frac{h_{6t}}{c^6} \sin 3v, \end{aligned} \quad (25)$$

$$\begin{aligned} \frac{2\pi}{\Phi} (\phi - \phi_0) &= v + \left(\frac{f_{4\phi}}{c^4} + \frac{f_{6\phi}}{c^6} \right) \sin 2v + \left(\frac{g_{4\phi}}{c^4} + \frac{g_{6\phi}}{c^6} \right) \sin 3v \\ &\quad + \frac{i_{6\phi}}{c^6} \sin 4v + \frac{h_{6\phi}}{c^6} \sin 5v, \end{aligned} \quad (26)$$

where l is the mean anomaly, $P = 2\pi/n$ the orbital period, and Φ the angle of revolution in time P . The 3PN accurate expressions for the orbital elements $a_r, e_r^2, n, e_t^2, \Phi$, and e_ϕ^2 and the post-Newtonian orbital functions $g_{4t}, g_{6t}, f_{4t}, f_{6t}, i_{6t}, h_{6t}, f_{4\phi}, f_{6\phi}, g_{4\phi}, g_{6\phi}, i_{6\phi}$, and $h_{6\phi}$, in terms of E, h and η read

$$\begin{aligned} a_r &= \frac{1}{(-2E)} \left\{ 1 + \frac{(-2E)}{4c^2} (-7 + \eta) + \frac{(-2E)^2}{16c^4} \left[(1 + 10\eta + \eta^2) \right. \right. \\ &\quad \left. \left. + \frac{1}{(-2Eh^2)} (-68 + 44\eta) \right] + \frac{(-2E)^3}{192c^6} \left[3 - 9\eta - 6\eta^2 \right. \right. \\ &\quad \left. \left. + 3\eta^3 + \frac{1}{(-2Eh^2)} (864 + (-3\pi^2 - 2212)\eta + 432\eta^2) \right. \right. \\ &\quad \left. \left. + \frac{1}{(-2Eh^2)^2} (-6432 + (13488 - 240\pi^2)\eta - 768\eta^2) \right] \right\}, \end{aligned} \quad (27)$$

$$\begin{aligned} e_r^2 &= 1 + 2Eh^2 + \frac{(-2E)}{4c^2} \left\{ 24 - 4\eta + 5(-3 + \eta)(-2Eh^2) \right\} \\ &\quad + \frac{(-2E)^2}{8c^4} \left\{ 52 + 2\eta + 2\eta^2 - (80 - 55\eta + 4\eta^2)(-2Eh^2) \right. \\ &\quad \left. - \frac{8}{(-2Eh^2)} (-17 + 11\eta) \right\} + \frac{(-2E)^3}{192c^6} \left\{ -768 - 6\eta\pi^2 \right. \\ &\quad \left. - 344\eta - 216\eta^2 + 3(-2Eh^2) (-1488 + 1556\eta - 319\eta^2 \right. \\ &\quad \left. + 4\eta^3) - \frac{4}{(-2Eh^2)} (588 - 8212\eta + 177\eta\pi^2 + 480\eta^2) \right. \\ &\quad \left. + \frac{192}{(-2Eh^2)^2} (134 - 281\eta + 5\eta\pi^2 + 16\eta^2) \right\}, \end{aligned} \quad (28)$$

$$\begin{aligned}
n = & (-2E)^{3/2} \left\{ 1 + \frac{(-2E)}{8c^2} (-15 + \eta) + \frac{(-2E)^2}{128c^4} [555 + 30\eta \right. \\
& + 11\eta^2 + \frac{192}{\sqrt{(-2Eh^2)}} (-5 + 2\eta)] + \frac{(-2E)^3}{3072c^6} [-29385 \\
& - 4995\eta - 315\eta^2 + 135\eta^3 - \frac{16}{(-2Eh^2)^{3/2}} (10080 + 123\eta\pi^2 \\
& \left. - 13952\eta + 1440\eta^2) + \frac{5760}{\sqrt{(-2Eh^2)}} (17 - 9\eta + 2\eta^2)] \right\}, \quad (29)
\end{aligned}$$

$$\begin{aligned}
e_t^2 = & 1 + 2Eh^2 + \frac{(-2E)}{4c^2} \left\{ -8 + 8\eta - (-17 + 7\eta)(-2Eh^2) \right\} \\
& + \frac{(-2E)^2}{8c^4} \left\{ 8 + 4\eta + 20\eta^2 - (-2Eh^2)(112 - 47\eta + 16\eta^2) \right. \\
& - 24\sqrt{(-2Eh^2)}(-5 + 2\eta) + \frac{4}{(-2Eh^2)}(17 - 11\eta) \\
& \left. - \frac{24}{\sqrt{(-2Eh^2)}}(5 - 2\eta) \right\} \\
& + \frac{(-2E)^3}{192c^6} \left\{ 24(-2 + 5\eta)(-23 + 10\eta + 4\eta^2) - 15(-528 \right. \\
& + 200\eta - 77\eta^2 + 24\eta^3)(-2Eh^2) - 72(265 - 193\eta \\
& + 46\eta^2)\sqrt{(-2Eh^2)} - \frac{2}{(-2Eh^2)}(6732 + 117\eta\pi^2 - 12508\eta \\
& + 2004\eta^2) + \frac{2}{\sqrt{(-2Eh^2)}}(16380 - 19964\eta + 123\eta\pi^2 \\
& + 3240\eta^2) - \frac{2}{(-2Eh^2)^{3/2}}(10080 + 123\eta\pi^2 - 13952\eta \\
& \left. + 1440\eta^2) + \frac{96}{(-2Eh^2)^2}(134 - 281\eta + 5\eta\pi^2 + 16\eta^2) \right\}, \quad (30)
\end{aligned}$$

$$g_{4t} = \frac{3(-2E)^2}{2} \left\{ \frac{5 - 2\eta}{\sqrt{(-2Eh^2)}} \right\}, \quad (31)$$

$$\begin{aligned}
g_{6t} = & \frac{(-2E)^3}{192} \left\{ \frac{1}{(-2Eh^2)^{3/2}} (10080 + 123\eta\pi^2 - 13952\eta \right. \\
& \left. + 1440\eta^2) + \frac{1}{\sqrt{(-2Eh^2)}} (-3420 + 1980\eta - 648\eta^2) \right\}, \quad (32)
\end{aligned}$$

$$f_{4t} = -\frac{1}{8} \frac{(-2E)^2}{\sqrt{(-2Eh^2)}} \left\{ (4 + \eta)\eta\sqrt{(1 + 2Eh^2)} \right\}, \quad (33)$$

$$f_{6t} = \frac{(-2E)^3}{192} \left\{ \frac{1}{(-2Eh^2)^{3/2}} \frac{1}{\sqrt{1 + 2Eh^2}} (1728 - 4148\eta + 3\eta\pi^2 \right.$$

$$\begin{aligned}
& +600 \eta^2 + 33 \eta^3) + 3 \frac{\sqrt{(-2 E h^2)}}{\sqrt{(1 + 2 E h^2)}} \eta (-64 - 4 \eta + 23 \eta^2) \\
& + \frac{1}{\sqrt{(-2 E h^2)(1 + 2 E h^2)}} \left(-1728 + 4232 \eta - 3 \eta \pi^2 \right. \\
& \left. - 627 \eta^2 - 105 \eta^3 \right) \}, \tag{34}
\end{aligned}$$

$$i_{6t} = \frac{(-2 E)^3}{32} \eta \left\{ \frac{(1 + 2 E h^2)}{(-2 E h^2)^{3/2}} (23 + 12 \eta + 6 \eta^2) \right\}, \tag{35}$$

$$h_{6t} = \frac{13(-2 E)^3}{192} \eta^3 \left(\frac{1 + 2 E h^2}{-2 E h^2} \right)^{3/2}, \tag{36}$$

$$\begin{aligned}
\Phi & = 2 \pi \left\{ 1 + \frac{3}{c^2 h^2} + \frac{(-2 E)^2}{4 c^4} \left[\frac{3}{(-2 E h^2)} (-5 + 2 \eta) \right. \right. \\
& + \frac{15}{(-2 E h^2)^2} (7 - 2 \eta) \left. \right] + \frac{(-2 E)^3}{128 c^6} \left[\frac{24}{(-2 E h^2)} (5 - 5 \eta \right. \\
& + 4 \eta^2) - \frac{1}{(-2 E h^2)^2} (10080 - 13952 \eta + 123 \eta \pi^2 + 1440 \eta^2) \\
& \left. \left. + \frac{5}{(-2 E h^2)^3} (7392 - 8000 \eta + 123 \eta \pi^2 + 336 \eta^2) \right] \right\}, \tag{37}
\end{aligned}$$

$$f_{4\phi} = \frac{(-2 E)^2}{8} \frac{(1 + 2 E h^2)}{(-2 E h^2)^2} \eta (1 - 3 \eta), \tag{38}$$

$$\begin{aligned}
f_{6\phi} & = \frac{(-2 E)^3}{256} \left\{ \frac{4 \eta}{(-2 E h^2)} (-11 - 40 \eta + 24 \eta^2) \right. \\
& + \frac{1}{(-2 E h^2)^2} (-256 + 1192 \eta - 49 \eta \pi^2 + 336 \eta^2 - 80 \eta^3) \\
& \left. + \frac{1}{(-2 E h^2)^3} (256 + 49 \eta \pi^2 - 1076 \eta - 384 \eta^2 - 40 \eta^3) \right\}, \tag{39}
\end{aligned}$$

$$g_{4\phi} = -\frac{3(-2 E)^2}{32} \frac{\eta^2}{(-2 E h^2)^2} (1 + 2 E h^2)^{3/2}, \tag{40}$$

$$\begin{aligned}
g_{6\phi} & = \frac{(-2 E)^3}{768} \sqrt{(1 + 2 E h^2)} \left\{ -\frac{3}{(-2 E h^2)} \eta^2 (9 - 26 \eta) \right. \\
& - \frac{1}{(-2 E h^2)^2} \eta (220 + 3 \pi^2 + 312 \eta + 150 \eta^2) \\
& \left. + \frac{1}{(-2 E h^2)^3} \eta (220 + 3 \pi^2 + 96 \eta + 45 \eta^2) \right\}, \tag{41}
\end{aligned}$$

$$i_{6\phi} = \frac{(-2 E)^3}{128} \frac{(1 + 2 E h^2)^2}{(-2 E h^2)^3} \eta (5 + 28 \eta + 10 \eta^2), \tag{42}$$

$$h_{6\phi} = \frac{5(-2 E)^3}{256} \frac{\eta^3}{(-2 E h^2)^3} (1 + 2 E h^2)^{5/2}, \tag{43}$$

$$\begin{aligned}
e_\phi^2 = & 1 + 2 E h^2 + \frac{(-2 E)}{4 c^2} \left\{ 24 + (-15 + \eta) (-2 E h^2) \right\} \\
& + \frac{(-2 E)^2}{16 c^4} \left\{ -32 + 176 \eta + 18 \eta^2 - (-2 E h^2) (160 - 30 \eta \right. \\
& \left. + 3 \eta^2) + \frac{1}{(-2 E h^2)} (408 - 232 \eta - 15 \eta^2) \right. \\
& \left. + \frac{(-2 E)^3}{384 c^6} \left\{ -16032 + 2764 \eta + 3 \eta \pi^2 + 4536 \eta^2 + 234 \eta^3 \right. \right. \\
& \left. - 36 (248 - 80 \eta + 13 \eta^2 + \eta^3) (-2 E h^2) - \frac{6}{(-2 E h^2)} (2456 \right. \\
& \left. - 26860 \eta + 581 \eta \pi^2 + 2689 \eta^2 + 10 \eta^3) + \frac{3}{(-2 E h^2)^2} (27776 \right. \\
& \left. - 65436 \eta + 1325 \eta \pi^2 + 3440 \eta^2 - 70 \eta^3) \right\}. \tag{44}
\end{aligned}$$

We recall that it is also possible to obtain a similar looking parametric description in harmonic coordinates at 3PNA [see Memmesheimer et al (2004) for more details]. Recently, effects of leading order spin-orbit interactions were included into the above generalized quasi-Keplerian parametrization in Königsdörffer & Gopakumar (2005). In the next section, we briefly describe post-Newtonian based estimates for ISCO.

5. Estimates for the ISCO at 3PNA

In the case of circular motion, the only useful frequency is the sum of the radial and periastron frequencies. The orbital angular frequency is thus given by

$$\omega_{\text{circ}} = \omega_{\text{radial}} + \omega_{\text{periastron}} = 2\pi \frac{1+k}{P} = \frac{\Phi}{P}. \tag{45}$$

Defining

$$E^{3PN} \equiv \hat{H}_{[N]} + \hat{H}_{[1PN]} + \hat{H}_{[2PN]} + \hat{H}_{[3PN]}, \tag{46}$$

in terms of some orbital angular frequency, the energy at 3PNA takes the form

$$\begin{aligned}
\frac{E^{3PN}(x)}{c^2} = & -\frac{x}{2} + \left(\frac{3}{8} + \frac{1}{24} \eta \right) x^2 + \left(\frac{27}{16} - \frac{19}{16} \eta + \frac{1}{48} \eta^2 \right) x^3 \\
& + \left(\frac{675}{128} + \left(-\frac{34445}{1152} + \frac{205}{192} \pi^2 \right) \eta + \frac{155}{192} \eta^2 + \frac{35}{10368} \eta^3 \right) x^4, \tag{47}
\end{aligned}$$

where $x = \left(\frac{GM\omega_{\text{circ}}}{c^3} \right)^{2/3}$.

With the aid of the equation

$$\frac{dE^{3PN}(x)}{dx} = 0, \tag{48}$$

an approximate estimate for ISCO can be obtained, and its frequency and energy values, for equal-mass binaries, are $x^{3/2} = 0.13$ and $E^{3PN} = -0.08 c^2$ [see Blanchet (2002)]. A Padé-improved effective one-body approach puts the ISCO, also for equal-mass binaries, to $x^{3/2} = 0.09$ and $E^{3PN} = -0.07 c^2$ [see Damour et al (2000b)]. Various other estimates for the ISCO may be found in Faye et al (2004).

Acknowledgments.

Financial support by the Goethe-Institut Thessaloniki is thankfully acknowledged. The presented and cited results, published from 2003 on, have been supported by the SFB/TR7 Gravitational Wave Astronomy (DFG).

References

- Arnowitt, R., Deser, S., Misner, C.W., 1962, in *Gravitation: an introduction to current research*, L. Witten (ed.), John Wiley & Sons, 227; gr-qc/0405109
- Blanchet, L., 2002, Phys. Rev. D **65**, 124009
- Damour, T., 1982, C. R. Acad. Sci. Paris **294**, série II, 1355
- Damour, T., Deruelle, N., 1981, Phys. Lett. A **87**, 81
- Damour, T., Deruelle, N., 1985, Ann. Inst. Henri Poincaré (Phys. Théor.) **43**, 109
- Damour, T., Gopakumar, A., Iyer, B.R., 2004, Phys. Rev. D **70**, 064028
- Damour, T., Jaranowski, P., Schäfer, G., 2000a, Phys. Rev. D **62**, 044024
- Damour, T., Jaranowski, P., Schäfer, G., 2000b, Phys. Rev. D **62**, 084011
- Damour, T., Jaranowski, P., Schäfer, G., 2001, Phys. Lett. B **513**, 147
- Damour, T., Schäfer, G., 1985, Gen. Rel. Grav. **17**, 879
- Damour, T., Schäfer, G., 1987, C. R. Acad. Sci. Paris **305**, série II, 839
- Damour, T., Schäfer, G., 1988, Nuovo Cimento B **101**, 127
- Einstein, A., Infeld, L., Hoffmann, B., 1938, Ann. Math. **39**, 65
- Faye, G., Jaranowski, P., Schäfer, G., 2004, Phys. Rev. D **69**, 124029
- Jaranowski, P., Schäfer, G., 1997, Phys. Rev. D **55**, 4712
- Jaranowski, P., Schäfer, G., 1998, Phys. Rev. D **57**, 7274
- Jaranowski, P., Schäfer, G., 1999, Phys. Rev. D **60**, 124003
- Königsdörffer, C., Faye, G., Schäfer, G., 2003, Phys. Rev. D **65**, 044004
- Königsdörffer, C., Gopakumar, A., 2005, Phys. Rev. D **71**, 024039
- Königsdörffer, C., Gopakumar, A., 2006, Phys. Rev. D **73**, 124012
- Memmesheimer, R.-M., Gopakumar, A., Schäfer, G., 2004, Phys. Rev. D **70**, 104011
- Ohta, T., Okamura, H., Kimura, T., Hiida, K., 1974, Prog. Theor. Phys. **51**, 1598
- Robertson, H. P., 1938, Ann. Math. **39**, 101
- Schäfer, G., 1995, in *Symposia Gaussiana, Conf. A*, Behara/Fritsch/Lintz (eds.), Walter de Gruyter & Co., 667
- Schäfer, G., Wex, N., 1992, Phys. Lett. A **174**, 196; erratum **177**, 461

FUTURE SINGULARITIES AND COMPLETENESS IN COSMOLOGY *

Spiros Cotsakis[†]

University of the Aegean, Karlovassi 83200, Samos, Greece

Abstract

We review recent work on the existence and nature of cosmological singularities that can be formed during the evolution of generic as well as specific cosmological spacetimes in general relativity. We first discuss necessary and sufficient conditions for the existence of geodesically incomplete spacetimes based on a tensorial analysis of the geodesic equations. We then classify the possible singularities of isotropic globally hyperbolic universes using the Bel-Robinson slice energy that closely monitors the asymptotic properties of fields near the singularity. This classification includes all known forms of spacetime singularities in isotropic universes and also predicts new types.

1. Introduction

The general issue that we address in this paper is probably the most common one in cosmology:

Does the universe exist forever?

In other words, was there a finite proper time in the past common to whole space before which the universe did not exist? How about in the future? Commonly, if yes, we say the universe has past (resp. future) singularity, otherwise the universe is *complete*. Thus completeness is the negation of singularity and vice versa. In order to avoid endless philosophical debates for even the simplest issues, perhaps the first thing one should do in a subject of this sort is to have precise mathematical definitions and criteria.

The standard definition of spacetime completeness in general relativity is to say that spacetime is complete if it is geodesically complete that is every causal (i.e., timelike or null) geodesic defined in a finite subinterval can be extended to the whole real line. Otherwise, spacetime is singular that is geodesically incomplete, there is at least one incomplete geodesic.

*Presented at the Workshop on *Cosmology and Gravitational Physics*, 15-16 December 2005, Thessaloniki, Greece, *Editors*: N.K. Spyrou, N. Stergioulas and C.G. Tsagas.

[†]skot@aegean.gr

The traditional criteria (cf. Hawking and Ellis (1973)) provide sufficient conditions for a spacetime to be singular, that is geodesically incomplete. These conditions basically depend on the effect of spacetime curvature on a *congruence* of causal geodesics, in particular, they predict a blow up singularity in the expansion of the said congruence a finite parameter value after the congruence has started to converge, that is all geodesics will meet at a point conjugate to what can be called the *surface of last convergence*. All this follows from an analysis of the equation satisfied by the expansion of the bunch of geodesics called the Komar-Landau-Raychaudhuri equation.

A more analytic approach to the singularities of general relativity is to consider directly the equation satisfied not by a family of geodesics as above but by each individual geodesic, the geodesic equation. This is the approach taken in Choquet-Bruhat & Cotsakis (2002) wherein sufficient analytic conditions were found for geodesics to have infinite proper length. It is important to point out that in this approach the causal techniques, which are used in the traditional singularity theorems, are also used here, especially global hyperbolicity, however, the tensor-analytic technique is completely different.

The plan of this paper is as follows. In the next Section, we review the beginnings of the new approach to the singularity problem and state three theorems, the first giving conditions for the equivalence of global hyperbolicity to slice completeness, another giving sufficient conditions for a spacetime to be g-complete (theorem 3) and another (Theorem 2) offering a converse in the particular case of the so-called trivially sliced spaces. In Section 3, we state a new singularity theorem, that is *necessary* conditions for causal g-incompleteness, of particular relevance to cosmology which allows one to classify all possible FRW future singularities as being those with a non-integrable Hubble parameter. We also provide examples from the recent literature on sudden singularities and inflationary cosmology to illustrate our results. In Section 4, we introduce the Bel-Robinson energy as a new way towards a refined classification of the possible singularities in the isotropic category. This leads to many different types of singularities, for instance those in tachyonic cosmology. We provide examples which demonstrate the relevance of many of these new types. Lastly, we point out further consequences of our work and possible future extensions.

2. Geodesics and singularities: Necessary conditions

In this Section, we start with a very general situation. Consider a spacetime of the form (\mathcal{V}, g) with $\mathcal{V} = \mathcal{M} \times \mathcal{I}$, \mathcal{I} being an interval in \mathbb{R} (for simplicity we can take it to be the whole real line) and \mathcal{M} a smooth manifold of dimension n , in which the smooth, $(n + 1)$ -dimensional, Lorentzian metric g splits as follows:

$$g \equiv -N^2(\theta^0)^2 + g_{ij} \theta^i \theta^j, \quad \theta^0 = dt, \quad \theta^i \equiv dx^i + \beta^i dt. \quad (1)$$

Here $N = N(t, x^i)$ denotes the *lapse function*, $\beta^i(t, x^j)$ is the *shift function* and the spatial slices $\mathcal{M}_t (= \mathcal{M} \times \{t\})$ are spacelike submanifolds endowed with the time-

dependent spatial metric $g_t \equiv g_{ij}dx^i dx^j$. We call such a spacetime a *sliced space*, as in Cotsakis (2004). We shall assume that our sliced space (\mathcal{V}, g) is *regularly hyperbolic*, that is the lapse function is bounded, the shift is uniformly bounded and the spatial metric is itself uniformly bounded below. Under these conditions we can prove (cf. Choquet-Bruhat & Cotsakis (2002), Cotsakis (2004)):

Theorem 1 *Let (\mathcal{V}, g) be a regularly hyperbolic sliced space. Then the following are equivalent:*

1. (\mathcal{M}_0, g_0) is a g -complete Riemannian manifold
2. The spacetime (\mathcal{V}, g) is globally hyperbolic

This theorem shows that in a reasonable spacetime the basic causal notion of global hyperbolicity is in fact equivalent to the condition that each slice is a geodesically complete manifold.

Under what conditions is global hyperbolicity equivalent to geodesic completeness in the original spacetime (\mathcal{V}, g) ? What is the class of sliced spaces in which such an equivalence holds? In a sliced space belonging to this class, in view of the results of the previous Theorem, geodesic completeness of the spacetime would be guessed simply by looking at the completeness of a slice. Let us define a *trivially sliced space* to be a spacetime with constant lapse and shift and time-independent spatial metric. Then we can prove the following result (Cotsakis (2004)).

Theorem 2 *Let (\mathcal{V}, g) be a trivially sliced space. Then the following are equivalent:*

1. The spacetime (\mathcal{V}, g) is timelike and null geodesically complete
2. (\mathcal{M}_0, g_0) is a complete Riemannian manifold
3. The spacetime (\mathcal{V}, g) is globally hyperbolic.

We see that this theorem gives sufficient and necessary conditions for g -completeness in spacetimes of a particularly simple form, trivially sliced spaces. For more general situations, things can become very complicated and no general results offering sufficient and necessary conditions exist.

The first result giving *sufficient* conditions for a spacetime to be g -complete was proved in Choquet-Bruhat & Cotsakis (2002). The method of proof consisted of a tensor analytic argument using the geodesic equations. The tangent vector u to a geodesic in (\mathcal{V}, g) parametrized by arc length, or by the canonical parameter in the case of a null geodesic, with components dx^α/ds in the natural frame, satisfies in an arbitrary frame the differential equations,

$$u^\alpha \nabla_\alpha u^\beta \equiv u^\alpha \partial_\alpha u^\beta + \omega_{\alpha\gamma}^\beta u^\alpha u^\gamma = 0. \quad (2)$$

Since $u^0 \equiv dt/ds$, the zero component of the geodesic equations can be written in the form,

$$\frac{d}{dt} \left(\frac{dt}{ds} \right) + \frac{dt}{ds} (\omega_{00}^0 + 2\omega_{0i}^0 v^i + \omega_{ij}^0 v^i v^j) = 0, \quad (3)$$

where we have set,

$$v^i = \frac{dx^i}{dt} + \beta^i. \quad (4)$$

Setting $dt/ds = y$ and using the standard expressions for the connection coefficients, the geodesic equations yield

$$\log \frac{y(t)}{y(t_1)} = \int_{t_1}^t N^{-1} (-\partial_0 N - 2\partial_i N v^i + K_{ij} v^i v^j) dt, \quad (5)$$

or, using regular hyperbolicity,

$$\log \frac{y(t)}{y(t_1)} \leq 2 \log N_m^{-1} + N_m^{-1} \int_{t_1}^t (|\nabla N|_g N_M + |K|_g N_M^2) dt. \quad (6)$$

Since the length (or canonical parameter extension) of the curve C is

$$\int_{t_1}^{+\infty} \frac{ds}{dt} dt \quad (7)$$

and will be infinite if ds/dt is bounded away from zero i.e., if $y \equiv dt/ds$ is uniformly bounded, we arrive at the following consequence.

Theorem 3 *If the spacetime (\mathcal{V}, g) is globally and regularly hyperbolic and in addition the g -norms of the space gradient of the lapse, $|\nabla N|_g$, and of the extrinsic curvature, $|K|_g$, are integrable functions on the interval $[t_1, +\infty)$, then spacetime is future timelike and null geodesic complete.*

Note that in this theorem, the fact that the length of the geodesics is infinite is proved directly and not using the equation for the expansion of the geodesic congruence as one does to prove the usual singularity theorems.

3. Hubble rate and singularities

The completeness Theorem 2 of the previous Section gives sufficient conditions for timelike and null geodesic completeness and therefore implies that the negations of each one of its conditions are *necessary* conditions for the existence of singularities (while, the singularity theorems (cf. Hawking and Ellis (1973)) provide sufficient conditions for this purpose). Thus this theorem is precisely what is needed for applications to the analysis of the nature of specific cosmological models known from other reasons to have spacetime singularities. This is the line of thought followed in Cotsakis and Klaoudatou (2005).

Since for an FRW metric, $N = 1$ and $\beta = 0$, we see that regular hyperbolicity is satisfied provided the scale factor $a(t)$ is a bounded from below function of the proper time t on \mathcal{I} . The condition for the integrability of the spatial gradient of the lapse is trivially satisfied and this is again true in more general homogeneous cosmologies where the lapse function N depends only on the time and not on the

space variables. In all these cases the norm $|\nabla N|_g$ is zero. On the other hand, the condition on the norm of the extrinsic curvature is the only one which can create a problem.

For an isotropic universe $|K|_g^2 = 3(\dot{a}/a)^2 = 3H^2$, and so FRW universes in which the scale factor is bounded below can fail to be complete only when that norm is not integrable. This can happen in only one way: There is a finite time t_1 for which H fails to be integrable on the time interval $[t_1, \infty)$. Since this non-integrability of H can be implemented in different ways, we arrive at the following result for the types of future singularities that can occur in isotropic universes (cf. Cotsakis and Klaoudatou (2005)).

Theorem 4 *Necessary conditions for the existence of future singularities in globally hyperbolic, regularly hyperbolic FRW universes are:*

S1 *For each finite t , H is non-integrable on $[t_1, t]$, or*

S2 *H blows up in a finite time, or*

S3 *H is defined and integrable (that is bounded, finite) for only a finite proper time interval.*

When does Condition S1 hold? It is well known that a function $H(\tau)$ is integrable on an interval $[t_1, t]$ if $H(\tau)$ is defined on $[t_1, t]$, is continuous on (t_1, t) and the limits $\lim_{\tau \rightarrow t_1^+} H(\tau)$ and $\lim_{\tau \rightarrow t^-} H(\tau)$ exist. Therefore there are a number of different ways which can lead to a singularity of the type S1 and such singularities are in a sense more subtle than the usual ones predicted by the singularity theorems. For instance, they may correspond to the so-called *sudden*, or spontaneous, singularities (see Barrow (2004) for this terminology) located at the right end (say t_s) at which H is defined and finite but *the left limit*, $\lim_{\tau \rightarrow t_1^+} H(\tau)$, may fail to exist, thus making H non-integrable on $[t_1, t_s]$, for *any* finite t_s (which is of course arbitrary but fixed from the start).

In such a model, we have a solution of the Friedmann equations for a fluid source with unconnected density and pressure which, in a local neighborhood of the singularity located at the time $t = t_s$ ahead, reads

$$a(t) = 1 + \left(\frac{t}{a_s}\right)^q (a_s - 1) + \tau^n \Psi(\tau), \quad \tau = t_s - t. \quad (8)$$

Here we take $1 < n < 2$, $0 < q < 1$, $a(t_s) = a_s$ and $\Psi(\tau)$ is the so-called *logarithmic psi-series* which is assumed to be convergent, tending to zero as $\tau \rightarrow 0$. The form (8) exists as a *smooth* solution only on the interval $(0, t_s)$. Also a_s and $H_s \equiv H(t_s)$ are finite but \dot{a} blows up as $t \rightarrow 0$ making H continuous only on $(0, t_s)$. In addition, $a(0)$ is finite and we can extend H and define it to be finite also at 0, $H(0) \equiv H_0$, so that H is defined on $[0, t_s]$. However, since $\lim_{t \rightarrow 0^+} H(t) = \pm\infty$, we conclude that this model universe implements exactly Condition S1 of the previous Section and thus H is non-integrable on $[0, t_s]$, t_s arbitrary.

This then provides an example of a singularity characterized by the fact that as $t \rightarrow t_s$, $\ddot{a} \rightarrow -\infty$ while using the field equation we see that this is really a

divergence in the pressure, $p \rightarrow \infty$. In particular, we cannot have in this universe a family of privileged observers each having an infinite proper time and finite H . A further calculation shows that the product $E_{\alpha\beta}E^{\alpha\beta}$, $E_{\alpha\beta}$ being the Einstein tensor, is unbounded at t_s . Hence we find that this spacetime is future geodesically incomplete.

As another example consider a flat FRW model, $ds^2 = dt^2 - a^2(t)d\bar{x}^2$, and take all quantities along a null geodesic with affine parameter λ . Since this is conformally Minkowski we have $d\lambda \propto a(t)dt$, or, $d\lambda = a(t)dt/a(t_s)$, so that $d\lambda/dt = 1$ for $t = t_s$, where t_s is a finite value of time. Borde *et al* (2003) then define an averaged-out Hubble rate in this inflating spacetime by the equation

$$H_{av} = \frac{1}{\lambda(t_s) - \lambda(t_i)} \int_{\lambda(t_i)}^{\lambda(t_s)} H(\lambda)d\lambda, \quad (9)$$

and so if $H_{av} > 0$, as we would expect in a truly inflationary universe, we have, following Cotsakis and Klaoudatou (2005),

$$0 < H_{av} = \frac{1}{\lambda(t_s) - \lambda(t_i)} \int_{\lambda(t_i)}^{\lambda(t_s)} H(\lambda)d\lambda = \frac{1}{\lambda(t_s) - \lambda(t_i)} \int_{a(t_i)}^{a(t_s)} \frac{da}{a(t_s)} \leq \frac{1}{\lambda(t_s) - \lambda(t_i)}. \quad (10)$$

This shows that the affine parameter must take values only in a finite interval (otherwise we would get a vanishing H) which implies geodesic incompleteness. A similar proof is obtained for the case of a timelike geodesic. Notice that condition (10) holds if and only if H is integrable on only a finite interval of time, thus signalling incompleteness according to Theorem 4.

4. Bel-Robinson energy and the nature of singularities

Instead of starting from the geodesic equation, we take in this Section another path, a tensorial in spirit approach, and consider the Bel-Robinson energy (cf. Cotsakis and Klaoudatou (2006)). In a sliced space this can be defined as follows. We start with the 2-covariant spatial electric and magnetic tensors, defined by (cf. Choquet-Bruhat & York (2002))

$$\begin{aligned} E_{ij} &= R_{i0j}^0, \\ D_{ij} &= \frac{1}{4}\eta_{ihk}\eta_{jlm}R^{hklm}, \\ H_{ij} &= \frac{1}{2}N^{-1}\eta_{ihk}R_{0j}^{hk}, \\ B_{ji} &= \frac{1}{2}N^{-1}\eta_{ihk}R_{0j}^{hk}, \end{aligned}$$

where η_{ijk} is the volume element of the space metric g . The *Bel-Robinson energy* is then defined as the slice integral

$$\mathcal{B}(t) = \frac{1}{2} \int_{\mathcal{M}_t} (|E|^2 + |D|^2 + |B|^2 + |H|^2) d\mu_{\bar{g}_t}, \quad (11)$$

where by $|X|^2 = g^{ij}g^{kl}X_{ik}X_{jl}$ we denote the spatial norm of the 2-covariant tensor X . The Bel-Robinson energy is a kind of energy of the gravitational field *projected* in a sense to a slice in spacetime and as such it can be very useful in evolution studies of the Einstein equations. It was in fact used in Choquet-Bruhat & Moncrief (2002) to prove global existence results for cosmological spacetimes.

For an FRW universe filled with various forms of matter with metric given by $ds^2 = -dt^2 + a^2(t)d\sigma^2$, where $d\sigma^2$ denotes the usual time-independent metric on the 3-slices of constant curvature k , the norms of the magnetic parts, $|H|, |B|$, are identically zero while $|E|$ and $|D|$, the norms of the electric parts, reduce to

$$|E|^2 = 3(\ddot{a}/a)^2 \quad \text{and} \quad |D|^2 = 3\left((\dot{a}/a)^2 + k/a^2\right)^2. \quad (12)$$

Therefore the Bel-Robinson energy becomes

$$\mathcal{B}(t) = \frac{C}{2} (|E|^2 + |D|^2), \quad (13)$$

where C is the constant volume of (or *in* in the case of a non-closed space) the 3-dimensional slice at time t .

The approach to the singularity problem introduced in Cotsakis and Klaoudatou (2006) classifies the possible types of singularities that are formed in an FRW geometry during its cosmic evolution using the different possible combinations of the three main functions in the problem, namely, the scale factor a , the Hubble expansion rate H and the Bel Robinson energy \mathcal{B} . If we suppose that the model has a finite time singularity at $t = t_s$, then the possible behaviours of the functions in the triplet $(H, a, (|E|, |D|))$ in accordance with Theorem 4 are as follows:

S_1 H non-integrable on $[t_1, t]$ for every $t > t_1$

S_2 $H \rightarrow \infty$ at $t_s > t_1$

S_3 H otherwise pathological

N_1 $a \rightarrow 0$

N_2 $a \rightarrow a_s \neq 0$

N_3 $a \rightarrow \infty$

B_1 $|E| \rightarrow \infty, |D| \rightarrow \infty$

B_2 $|E| < \infty, |D| \rightarrow \infty$

B_3 $|E| \rightarrow \infty, |D| < \infty$

B_4 $|E| < \infty, |D| < \infty$.

The nature of a prescribed singularity is thus described completely by specifying the components in a triplet of the form (S_i, N_j, B_l) , with the indices i, j, l taking their respective values as above. Except some impossible cases (cf. Cotsakis and Klaoudatou (2006)), all other types of finite time singularities can in principle be formed during the evolution of FRW, matter-filled models, in general relativity or other metric theories of gravity. It is interesting to note that all the standard dust or radiation-filled big bang singularities fall under the *strongest* singularity type, namely, the type (S_1, N_1, B_1) . For example, in a flat universe filled with dust, at $t = 0$ we have

$$a(t) \propto t^{2/3} \rightarrow 0, \quad (N_1), \quad (14)$$

$$H \propto t^{-1} \rightarrow \infty, \quad (S_1), \quad (15)$$

$$|E|^2 = 3/4H^4 \rightarrow \infty, \quad |D|^2 = 3H^4 \rightarrow \infty, \quad (B_1). \quad (16)$$

Note that this scheme is organized in such a way that the character of the singularities (i.e., the behaviour of the defining functions) becomes milder as the indices of S , N and B increase (this applies to both collapse and rip-type singularities). Milder singularities in isotropic universes are thus expected to occur as one proceeds down the singularity list.

Further, we note that we can obtain a more detailed picture of the possible singularity formations by studying the relative asymptotic behaviours of the three functions that define the type of singularity. Using a standard notation that expresses the behaviour of two functions around the singularity at t_* , we introduce the notion of *relative strength* in the singularity classification. Let f, g be two functions. We say that

1. $f(t)$ is *much smaller* than $g(t)$, $f(t) \ll g(t)$, if and only if $\lim_{t \rightarrow t_*} f(t)/g(t) = 0$
2. $f(t)$ is *similar* to $g(t)$, $f(t) \sim g(t)$, if and only if $\lim_{t \rightarrow t_*} f(t)/g(t) < \infty$
3. $f(t)$ is *asymptotic* to $g(t)$, $f(t) \leftrightarrow g(t)$, if and only if $\lim_{t \rightarrow t_*} f(t)/g(t) = 1$.

Using these relations we find that for example, the standard radiation filled isotropic universes (with $k = 0, \pm 1$) have the asymptotic behaviours described by

$$a \ll H \ll (|E| \leftrightarrow |D|),$$

whereas the rest of the standard big bang singularities have

$$a \ll H \ll (|E| \sim |D|).$$

This shows the precise nature of these two specific types of singularities. Many more examples can be found in Cotsakis and Klaoudatou (2006) (see also Cotsakis and Klaoudatou (2006b)).

The Bel-Robinson energy can also be used to test g-completeness. For instance, consider the case of *tachyonic* cosmologies as in Cotsakis and Klaoudatou (2005b).

Tachyons, phantoms, Chaplygin gases etc, represent unobserved and unknown, tensile, negative energy and/or pressure density substances, violating some or all of the usual energy conditions. The chief purpose of such exotic types of matter is to cause cosmic acceleration and drive the late phases of the evolution of the universe. However, they are also bound to have a nontrivial effect on the singularity structure of such universes.

A question of interest to us is under what conditions are cosmological models sourced by such fields g-complete? Following Cotsakis and Klaoudatou (2005b), we consider again the Friedman model filled with a Chaplygin gas with equation of state given by $p = -\rho^{-\alpha}[C + (\rho^{1+\alpha} - C)^{\alpha/(1+\alpha)}]$, where $C = A/(1+w) - 1$ and subject to the condition $1 + \alpha = 1/(1+w)$. The scale factor is then given by the form $a(t) = (C_1 e^{-C_3 \tau} + C_2 e^{C_3 \tau})^{2/3}$, $\tau = t - t_0$, where C_1 , C_2 and C_3 are constants. Therefore we find that in the asymptotic limits $\tau \rightarrow 0$ and $\tau \rightarrow \infty$, H tends to suitable constants, that is it remains finite on $[t_0, \infty)$ and so by our theorems the model is geodesically complete. We can also arrive at the same conclusion using the Bel-Robinson energy of this universe which in this case can be shown that it tends to a constant value thereby signalling completeness.

However, this is by no means the only possible dynamical behaviour in phantom/tachyonic cosmologies. An example of g-incomplete universe is the so-called graduated inflationary models first considered in Barrow (1990). A more general class of models can be described by a flat space with a fluid having equation of state $p + \rho = \gamma \rho^\lambda$, $\gamma > 0$ and $\lambda < 1$. This family was further analyzed in Cotsakis and Klaoudatou (2006) using the Bel-Robinson energy. It was found that the exact behaviour of the model (which as we showed exhibits an $S2$ type singularity) described originally by Barrow (1990) has a more general significance and the Bel-Robinson energy diverges making this class of models g-incomplete.

5. Discussion

In this paper we have reviewed the recent introduction and application of two new methods to tackle the singularity problem in cosmology. The first method is based on a direct tensorial treatment of the geodesic equations that enables one to prove sufficient conditions for a spacetime to be g-complete, that is conditions under which geodesics have infinite length. This in conjunction with causal techniques allow one to show the equivalence of the deterministic concept of global hyperbolicity to the analytic concept of slice as well as general spacetime completeness. Also in the case of simple cosmological spacetimes one can prove necessary conditions for g-completeness, offering a converse to the completeness theorem. In this sense, a singular spacetime can then be tested directly as to how it becomes singular near a finite time singularity by checking which functions blow up and in what way at the finite time singularity.

This is in sharp contrast to the traditional method of showing geodesic incompleteness in general relativity where one considers the behaviour of a geodesic congruence and indirectly shows that the geodesics in the congruence must under certain

geometric conditions have finite length. The conditions reviewed in this paper allow, in the homogeneous and isotropic case, a complete analysis to be made for the finite time singularities by looking at the behaviour of the Hubble rate (extrinsic curvature). This leads to a classification of the relevant singularities in such models. In fact this approach results in an interesting demarcation and comparison of the singularity structures in different evolution cosmological models.

A further advance and refinement in this approach is possible with the consideration of the Bel-Robinson energy of the spacetime in addition to the Hubble rate and the scale factor in such universes. In this second analytic technique the Bel-Robinson energy monitors the asymptotic behaviour of the matter fields and is very sensitive even with slight changes in the matter content. This whole approach has led to a prediction of many different types of finite time singularities in cosmological models and their nature has become more amenable to an analytic treatment.

There are many deep, interesting and feasible open problems that remain in this field and a future synthesis of causal, tensor, dynamical as well as asymptotic methods will prove very useful in progressing towards the goal of discovering all different possibilities.

Acknowledgements

I am very grateful to Professor Spyrou and his group for the excellent organization and stimulating atmosphere of the Thessaloniki Meeting. This work was supported by the joint Greek Ministry of Education and European Union research grants ‘Pythagoras’ No. 1351 and ‘Heracleitus’ No. 1337.

References

- Barrow, J. D., *Sudden future singularities*, *Class. Quant. Grav.* 21 (2004) L79-L82 [arXiv: gr-qc/0403084].
- Barrow, J. D., *Graduated inflationary universes*, *Phys. Lett. B* 235 (1990) 40-43.
- Borde, A., & *et al*, *Inflationary spacetimes are not past-complete*, *Phys. Rev. Lett.* **90** (2003) 151301, [arXiv:gr-qc/0110012].
- Choquet-Bruhat, Y. and S. Cotsakis, *Global hyperbolicity and completeness*, *J. Geom. Phys.* 43 (2002) 345-350 (arXiv: gr-qc/0201057); see also, Y. Choquet-Bruhat, S. Cotsakis, *Completeness theorems in general relativity*, in *Recent Developments in Gravity*, Proceedings of the 10th Hellenic Relativity Conference, K. D. Kokkotas and N. Stergioulas eds., (World Scientific 2003), pp. 145-149.
- Choquet-Bruhat, Y. and V. Moncrief, *Non-linear Stability of an expanding universe with S^1 Isometry Group* (arXiv:gr-qc/0302021).
- Choquet-Bruhat, Y. and J. W. York, *Constraints and evolution in cosmology*, In: *Cosmological Crossroads*, S. Cotsakis and E. Papantonopoulos (eds.), LNP592, (Springer, 2002), pp. 29-58.
- Cotsakis, S., *Global hyperbolicity and completeness*, *Gen Rel. Grav.* 36 (2004) 1183-

1188.

- Cotsakis, S., and I. Klaoudatou, *Future singularities of isotropic cosmologies*, J. Geom. Phys. 55 (2005) 306-315.
- Cotsakis S., and I. Klaoudatou, (2005b) *Modern approaches to cosmological singularities*, In the Proceedings of the 11th Conference on Recent Developments in Gravity, S. Cotsakis and J. Miritzis (eds.), J. Phys. Conf. Series 8 (2005) 150-154.
- Cotsakis, S., and I. Klaoudatou, *Cosmological singularities and Bel-Robinson energy*, Samos Preprint RG-MPC/060405-1, [arXiv:gr-qc/0604029].
- Cotsakis, S., and I. Klaoudatou (2006b), *Singular isotropic cosmologies and Bel-Robinson energy*, to appear in the Proceedings of the A. Einstein Century International Conference, Paris, France, [arXiv:gr-qc/0603130].
- Hawking, S. W. and G. F. R. Ellis, *The large-scale structure of space-time*, Cambridge University Press, 1973.

REPULSIVE GRAVITY AND THE ACCELERATING UNIVERSE *

L. Perivolaropoulos †

University of Ioannina, Department of Physics, Ioannina, 451 10, Greece

Abstract

This is a pedagogical review of the recent observational data obtained from type Ia supernova (SnIa) surveys that support the accelerating expansion of the universe. The methods for the analysis of the data are reviewed and some of the theoretical implications obtained from their analysis are discussed. In particular, the existence of dark energy with negative pressure required by the data is demonstrated and the simplest type of dark energy (the cosmological constant) is shown to fit well the SnIa data. Dynamical forms of evolving dark energy are also shown at their best fit form to the data and their common features are discussed.

1. Introduction

Recent distance-redshift surveys (Astier *et al.* (2006), Riess *et al.* (2004), Riess *et al.* (1998), Tonry *et al.* (2003), Perlmutter *et al.* (1998)) of cosmologically distant Type Ia supernovae (SnIa) have indicated that the universe has recently (at redshift $z \simeq 0.5$) entered a phase of accelerating expansion. This expansion has been attributed to a dark energy (Huterer and Turner (2001)) component with negative pressure which can induce repulsive gravity and thus cause accelerated expansion. The evidence for dark energy has been indirectly verified by Cosmic Microwave Background (CMB) (Spergel *et al.* (2003)) and large scale structure observations.

The simplest and most obvious candidate for this dark energy is the cosmological constant with equation of state $w = \frac{p}{\rho} = -1$. The extremely fine tuned value of the cosmological constant required to induce the observed accelerated expansion has led to a variety of alternative models where the dark energy component varies with time. Many of these models make use of a homogeneous, time dependent minimally coupled scalar field ϕ (quintessence) (Caldwell, Dave and Steinhardt (1998)) whose dynamics is determined by a specially designed potential $V(\phi)$ inducing the appropriate time dependence of the field equation of state $w(z) = \frac{p(\phi)}{\rho(\phi)}$. Given the

*Presented at the Workshop on *Cosmology and Gravitational Physics*, 15-16 December 2005, Thessaloniki, Greece, *Editors*: N.K. Spyrou, N. Stergioulas and C.G. Tsagas.

†leandros@uoi.gr

observed $w(z)$, the quintessence potential can in principle be determined. Other physically motivated models predicting late accelerated expansion include modified gravity (Perrotta, Baccigalupi and Matarrese (2000), Torres (2002)), Chaplygin gas (Kamenshchik, Moschella and Pasquier (2001)), Cardassian cosmology (Freese and Lewis (2002)), theories with compactified extra dimensions (Perivolaropoulos (2003)), braneworld models (Sahni and Shtanov (2003)) etc. Such cosmological models predict specific forms of the Hubble parameter $H(z)$ as a function of redshift z . The observational determination of the recent expansion history $H(z)$ is therefore important for the identification of the viable cosmological models.

The most direct and reliable method to observationally determine the recent expansion history of the universe $H(z)$ is to measure the redshift z and the apparent luminosity of cosmological distant indicators (standard candles) whose absolute luminosity is known. The luminosity distance vs. redshift is thus obtained which in turn leads to the Hubble expansion history $H(z)$.

The goal of this review is to present the methods used to construct the recent expansion history $H(z)$ from SnIa data and discuss the most recent observational results and their theoretical implications. In the next section I summarize the method used to determine $H(z)$ from cosmological distance indicators and discuss the three cosmological puzzles that emerge from the observed expansion history $H(z)$ and other cosmological observations. In section 3 I show that the three puzzles may be resolved simultaneously by assuming that 70% of the energy content of the universe consists of a substance having negative pressure, the *dark energy*. The simplest form of dark energy, the *cosmological constant* is also discussed and its good fit to the SnIa data is demonstrated. Finally, in section 4 I discuss more general forms of dark energy whose energy density evolves dynamically with time. It is shown that these forms of dark energy can provide better fits to the observed expansion history $H(z)$.

2. Expansion History and Cosmological Puzzles

A particularly useful diagram which illustrates the expansion history of the Universe is the *Hubble diagram*. The x-axis of a Hubble diagram shows the redshift z of cosmological luminous objects while the y-axis shows the physical distance Δr to these objects. In the context of a cosmological setup the redshift z is connected to the scale factor $a(t)$ at the time of emission of radiation by $1 + z = \frac{a(t_0)}{a(t)}$ where t_0 is the present time. On the other hand, the distance to the luminous object is related to the time in the past t_{past} when the radiation emission was made. Therefore, the Hubble diagram contains information about the time dependence of the scale factor $a(t)$. The slope of this diagram at a given redshift denotes the inverse of the expansion rate $\dot{a}(z) \equiv H(z)$ ie $\Delta r = \frac{1}{H(z)}c z$. In an accelerating universe the expansion rate $H(z)$ was smaller in the past (high redshift) and therefore the slope H^{-1} of the Hubble diagram is larger at high redshift. Thus, at a given redshift, luminous objects appear to be further away (dimmer) compared to an empty universe expanding with a constant rate.

The luminous objects used in the construction of the Hubble diagram are objects

whose absolute luminosity is known and therefore their distance can be evaluated from their apparent luminosity along the lines discussed above. Such objects are known as *distance indicators* or *standard candles*. The best choice distance indicators for cosmology are SnIa not only because they are extremely luminous (at their peak they are as luminous as a bright galaxy) but also because their absolute magnitude can be determined at a high accuracy.

Our current knowledge of the expansion history of the universe can be summarized as follows: The universe originated at an initial state that was very close to a density singularity known as the Big Bang. Soon after that it entered a phase of superluminal accelerating expansion known as inflation. During inflation causally connected regions of the universe exited out of the horizon, the universe approached spatial flatness and the primordial fluctuations that gave rise to structure were generated. At the end of inflation the universe was initially dominated by radiation and later by matter whose attractive gravitational properties induced a decelerating expansion.

The SnIa data discussed in more detail below, strongly suggest that the universe has recently entered a phase of accelerating expansion at a redshift $z \simeq 0.5$. This accelerating expansion can not be supported by the attractive gravitational properties of regular matter. The obvious question to address is therefore 'What are the properties of the additional component required to support this acceleration?'

This is one of the three important cosmological puzzles that emerged during the past decade in the context of a matter dominated cosmology. The second puzzle can be summarized as follows: The location of the first peak of the Cosmic Microwave Background (CMB) angular spectrum corresponds to the size of the sound horizon at the last scattering surface and can therefore probe the geometry of the universe. Indeed, the angular scale at which we observe this peak is tied to the geometry of the universe since in a negatively (positively) curved universe, photon paths diverge (converge), leading to a larger (smaller) apparent angular size as compared to a flat universe. We can therefore relate the spatial curvature (determined by the total energy density of the universe ρ_{tot} to the observed peak in the CMB spectrum (Spergel *et al.*, (2003)). Using this method and the latest CMB data from WMAP it was found that the geometry of the universe is very nearly flat and therefore, in the context of General Relativity (GR) the total energy density ρ_{tot} is equal to the critical energy density ρ_{crit} required for flatness ie

$$\rho_{tot} = \rho_{crit} \tag{1}$$

On the other hand large scale structure observations based on dynamics of galaxies and clusters as well as on gravitational lensing of background galaxies and temperature profiles of the X-ray gas in clusters, indicate a smaller present energy density ρ_{0m} for matter. Observations converge towards

$$\rho_{0m} \simeq 0.3\rho_{crit} \tag{2}$$

instead of the expected value $\rho_{0m} \simeq \rho_{crit}$. This discrepancy raises the question: 'Where (and what) is the missing energy density which is not in the form of matter (or radiation)?'

The third cosmological puzzle is obtained by comparing the age of globular clusters (low metallicity old star populations) with the age of a flat matter dominated universe. By comparing a lower limit on the age of the oldest globular clusters in our galaxy estimated to be between $11Gyrs$ and $21Gyrs$ (Chaboyer (1995)) with the expansion age of a matter dominated universe ($\sim 10Gyrs$), determined by measurements of the Hubble constant $H_o \geq 60km/(sec \cdot Mpc)$, an apparent inconsistency arose: globular clusters appeared to be older than the Universe. This is known as 'the globular cluster age problem' or the 'age crisis of cosmology'.

3. Dark Energy and the Cosmological Constant

The simultaneous resolution to the above described three cosmological puzzles can come by assuming that 70% of the universe energy density consists of a substance called 'dark energy' which is characterized by 'negative pressure'.

As it is shown below, dark energy with negative pressure can induce repulsive gravity and thus cause accelerating expansion, it has positive energy and can therefore provide the missing mass required for flatness and can also lead to a larger age of the universe (with the same Hubble constant) thus resolving the cosmic age crisis. It can therefore resolve simultaneously the three cosmological puzzles described above.

To understand this resolution, we must consider the dynamical equation that determines the evolution of the scale factor $a(t)$. This equation is the Friedman equation which is obtained by combining General Relativity with the cosmological principle of homogeneity and isotropy of the universe. It may be written as

$$\frac{\ddot{a}}{a} = -\frac{4\pi G}{3} \sum_i (\rho_i + 3p_i) = -\frac{4\pi G}{3} [\rho_m + (\rho_X + 3p_X)] \quad (3)$$

where ρ_i and p_i are the densities and pressures of the contents of the universe assumed to behave as ideal fluids. The only directly detected fluids in the universe are matter ($\rho_m, p_m = 0$) and the subdominant radiation ($\rho_r, p_r = \rho_r/3$). Both of these fluids are unable to cancel the minus sign on the rhs of the Friedman equation and can therefore only lead to decelerating expansion. Accelerating expansion in the context of general relativity can only be obtained by assuming the existence of an additional component ($\rho_X, p_X = w\rho_X$) termed 'dark energy' which could potentially change the minus sign of eq. (3) and thus lead to accelerating expansion. Assuming a positive energy density for dark energy it becomes clear that negative pressure is required for accelerating expansion. In fact, writing the Friedman eq. (3) in terms of the dark energy equation of state parameter w as

$$\frac{\ddot{a}}{a} = -\frac{4\pi G}{3} [\rho_m + \rho_X(1 + 3w)] \quad (4)$$

it becomes clear that a $w < -\frac{1}{3}$ is required for accelerating expansion implying repulsive gravitational properties for dark energy for the resolution of the first cosmological puzzle. The second puzzle can be simply resolved by assuming that

$$\rho_{0m} + \rho_{0X} = \rho_{crit} \quad (5)$$

The third puzzle (the cosmic age crisis) is also resolved because a flat accelerating universe with the same present Hubble parameter as a flat decelerating matter dominated universe has a larger age (time since the Big Bang when $a(t) = 0$).

The redshift dependence of the dark energy can be easily connected to the equation of state parameter w by combining the energy conservation $d(\rho_X a^3) = -p_X d(a^3)$ with the equation of state $p_X = w\rho_X$ as

$$\rho_X \sim a^{-3(1+w)} = (1+z)^{3(1+w)} \quad (6)$$

This redshift dependence is related to the observable expansion history $H(z)$ through the Friedman equation

$$H(z)^2 = \frac{\dot{a}^2}{a^2} = \frac{8\pi G}{3} [\rho_{0m} (\frac{a_0}{a})^3 + \rho_X(a)] = H_0^2 [\Omega_{0m} (1+z)^3 + \Omega_X(z)] \quad (7)$$

where the density parameter $\Omega \equiv \frac{\rho}{\rho_{0crit}}$ for matter is constrained by large scale structure observations to a value (prior) $\Omega_{0m} \simeq 0.3$. Using this prior, the dark energy density parameter $\Omega_X(z) \equiv \frac{\rho_X(z)}{\rho_{0crit}}$ and the corresponding equation of state parameter w may be constrained from the observed $H(z)$.

In addition to $\Omega_X(z)$, the luminosity distance-redshift relation $d_L(z)$ obtained from SnIa observations can constrain other cosmological parameters. The only parameter however obtained directly from $d_L(z)$ is the Hubble parameter $H(z)$ which is related to $d_L(z)$ by

$$H(z) = c \left[\frac{d}{dz} \left(\frac{d_L(z)}{1+z} \right) \right]^{-1} \quad (8)$$

as indicated by the Hubble diagram.

A particularly interesting parameter from the theoretical point of view (apart from $H(z)$ itself) is the dark energy equation of state parameter $w(z)$ obtained from $H(z)$ as (Huterer and Turner (2001), Nesseris and Perivolaropoulos (2004))

$$w(z) = \frac{p_X(z)}{\rho_X(z)} = \frac{\frac{2}{3}(1+z) \frac{d \ln H}{dz} - 1}{1 - (\frac{H_0}{H})^2 \Omega_{0m} (1+z)^3} \quad (9)$$

This parameter probes directly the gravitational properties of dark energy which are predicted by theoretical models. The downside of it is that it requires two differentiations of the observable $d_L(z)$ to be obtained and is therefore very sensitive to observational errors.

The simplest form of dark energy corresponds to a time independent energy density obtained when $w = -1$ (see eq. (6)) and is known as the *cosmological constant*. Even though the cosmological constant may be physically motivated in the context of field theory and consistent with cosmological observation there are two important problems associated with it:

- *Why is it so incredibly small?* Observationally, the cosmological constant density is 120 orders of magnitude smaller than the energy density associated with the Planck scale - the obvious cut off. Furthermore, the standard model of cosmology posits that very early on the universe experienced a period of

inflation: A brief period of very rapid acceleration, during which the cosmological constant (and the Hubble parameter) was about 52 orders of magnitude larger than the value observed today. How could the cosmological constant have been so large then, and so small now? This is sometimes called *the cosmological constant problem*.

- *The ‘coincidence problem’*: Why is the energy density of matter nearly equal to the dark energy density today?

Despite the above problems and given that the cosmological constant is the simplest dark energy model, it is important to investigate the degree to which it is consistent with the SnIa data. I will now describe the main steps involved in this analysis. According to the Friedman equation the predicted Hubble expansion in a flat universe and in the presence of matter and a cosmological constant is

$$H(z)^2 = \frac{\dot{a}^2}{a^2} = \frac{8\pi G}{3}\rho_{0m}\left(\frac{a_0}{a}\right)^3 + \frac{\Lambda}{3} = H_0^2[\Omega_{0m}(1+z)^3 + \Omega_\Lambda] \quad (10)$$

where $\Omega_\Lambda = \frac{\rho_\Lambda}{\rho_{0crit}}$ and

$$\Omega_{0m} + \Omega_\Lambda = 1 \quad (11)$$

This is the LCDM (Λ +Cold Dark Matter) model which is currently the minimal standard model of cosmology. The predicted $H(z)$ has a single free parameter which we wish to constrain by fitting to the SnIa luminosity distance-redshift data.

Observations measure the apparent luminosity vs redshift ($l(z)$) or equivalently the apparent magnitude vs redshift ($m(z)$) which are related to the luminosity distance by

$$2.5\log_{10}\left(\frac{L}{l(z)}\right) = m(z) - M - 25 = 5\log_{10}\left(\frac{d_L(z)_{obs}}{Mpc}\right) \quad (12)$$

where M is the absolute magnitude assumed to be constant for standard candles like SnIa. From the theory point of view the predicted observable is the Hubble parameter (10) which is related to the theoretically predicted luminosity distance $d_L(z)$ by integrating eq. (8)

$$d_L(z; \Omega_{0m})_{th} = c(1+z) \int_0^z \frac{dz'}{H(z'; \Omega_{0m})} \quad (13)$$

Constraints on the parameter Ω_{0m} are obtained by the maximum likelihood method which involves the minimization of the $\chi^2(\Omega_{0m})$ defined as

$$\chi^2(\Omega_{0m}) = \sum_{i=1}^N \frac{[d_L(z)_{obs} - d_L(z; \Omega_{0m})_{th}]^2}{\sigma_i^2} \quad (14)$$

where N is the number of the observed SnIa luminosity distances and σ_i are the corresponding 1σ errors which include errors due to flux uncertainties, internal dispersion of SnIa absolute magnitude and peculiar velocity dispersion. If flatness is not imposed as a prior through eq. (11) then $d_L(z)_{th}$ depends on two parameters

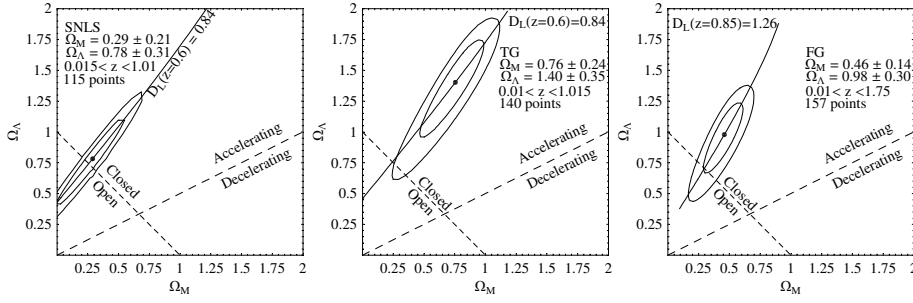


Figure 1: The 68% and 95% χ^2 contours in the $(\Omega_{0m}$ and $\Omega_{\Lambda})$ parameter space obtained using the SNLS, TG and FG datasets (from Nesseris and Perivolaropoulos (2005)).

$(\Omega_{0m}$ and $\Omega_{\Lambda})$ and the relation between $d_L(z; \Omega_{0m}, \Omega_{\Lambda})_{th}$ and $H(z; \Omega_{0m}, \Omega_{\Lambda})$ takes the form

$$d_L(z)_{th} = \frac{c(1+z)}{\sqrt{\Omega_{0m} + \Omega_{\Lambda} - 1}} \text{Sin}[\sqrt{\Omega_{0m} + \Omega_{\Lambda} - 1} \int_0^z dz' \frac{1}{H(z)}] \quad (15)$$

In this case the minimization of eq. (14) leads to constraints on both Ω_{0m} and Ω_{Λ} . This is the only direct and precise observational probe that can place constraints directly on Ω_{Λ} . Most other observational probes based on large scale structure observations place constraints on Ω_{0m} which are indirectly related to Ω_{Λ} in the context of a flatness prior.

The acceleration of the universe has been confirmed using the above maximum likelihood method since 1998 (Perlmutter et al, (1998), Riess *et al.*, (1998)). Even the early datasets of 1998 were able to rule out the flat matter dominated universe (SCDM: $\Omega_{0m} = 1$, $\Omega_{\Lambda} = 0$) at 99% confidence level. The latest datasets are the Gold dataset (Riess *et al.*, (2004)) ($N = 157$ in the redshift range $0 < z < 1.75$) and the first year SNLS (Astier *et al.* (2006)) (Supernova Legacy Survey) dataset which consists of 71 datapoints in the range $0 < z < 1$ plus 44 previously published closeby SniA. The 68% and 95% χ^2 contours in the $(\Omega_{0m}$ and $\Omega_{\Lambda})$ parameter space obtained using the maximum likelihood method are shown in Fig. 1 for the SNLS dataset, a truncated version of the Gold dataset (TG) with $0 < z < 1$ and the Full Gold (FG) dataset (Nesseris and Perivolaropoulos (2005)).

The following comments can be made on these plots:

- The two versions of the Gold dataset favor a closed universe instead of a flat universe ($\Omega_{tot}^{TG} = 2.16 \pm 0.59$, $\Omega_{tot}^{FG} = 1.44 \pm 0.44$). This trend is not realized by the SNLS dataset which gives $\Omega_{tot}^{SNLS} = 1.07 \pm 0.52$.
- The point corresponding to SCDM $(\Omega_{0m}, \Omega_{\Lambda}) = (1, 0)$ is ruled out by all datasets at a confidence level more than 10σ .
- If we use a prior constraint of flatness $\Omega_{0m} + \Omega_{\Lambda} = 1$ thus restricting on the corresponding dotted line of Fig. 1 and use the parametrization

$$H(z)^2 = H_0^2[\Omega_{0m}(1+z)^2 + (1 - \Omega_{0m})] \quad (16)$$

we find minimizing $\chi^2(\Omega_{0m})$ of eq (14)

$$\Omega_{0m}^{SNLS} = 0.26 \pm 0.04 \quad (17)$$

$$\Omega_{0m}^{TG} = 0.30 \pm 0.05 \quad (18)$$

$$\Omega_{0m}^{FG} = 0.31 \pm 0.04 \quad (19)$$

These values of Ω_{0m} are consistent with corresponding constraints from the CMB and large scale structure observations (Spergel *et al.*, (2003)).

5. Generalized Dark Energy Models

Even though LCDM is the simplest dark energy model and is currently consistent with all cosmological observations (especially with the SNLS dataset) the question that may still be addressed is the following: ‘Is it possible to get better fits (lowering χ^2 further) with different $H(z)$ parametrizations and if yes what are the common features of there better fits?’ The strategy towards addressing this question involves the following steps:

- Consider a physical model and extract the predicted recent expansion history $H(z; a_1, a_2, \dots, a_n)$ as a function of the model parameters a_1, a_2, \dots, a_n . Alternatively a model independent parametrization for $H(z; a_1, a_2, \dots, a_n)$ (or equivalently $w(z; a_1, a_2, \dots, a_n)$) may be constructed aiming at the best possible fit to the data with a small number of parameters (usually 3 or less).
- Use eq. (13) to obtain the theoretically predicted luminosity distance $d_L(z; a_1, a_2, \dots, a_n)_{th}$ as a function of z .
- Use the observed luminosity distances $d_L(z_i)_{obs}$ to construct χ^2 along the lines of eq. (14) and minimize it with respect to the parameters a_1, a_2, \dots, a_n .
- From the resulting best fit parameter values $\bar{a}_1, \bar{a}_2, \dots, \bar{a}_n$ (and their error bars) construct the best fit $H(z; \bar{a}_1, \bar{a}_2, \dots, \bar{a}_n)$, $d_L(z; \bar{a}_1, \bar{a}_2, \dots, \bar{a}_n)$ and $w(z; \bar{a}_1, \bar{a}_2, \dots, \bar{a}_n)$. The quality of fit is measured by the depth of the minimum of χ^2 ie $\chi^2_{min}(\bar{a}_1, \bar{a}_2, \dots, \bar{a}_n)$.

Most useful parametrizations reduce to LCDM of eq. (10) for specific parameter values giving a χ^2_{LCDM} for these parameter values. Let

$$\Delta\chi^2_{LCDM} \equiv \chi^2_{min}(\bar{a}_1, \bar{a}_2, \dots, \bar{a}_n) - \chi^2_{LCDM} \quad (20)$$

The value of $\Delta\chi^2_{LCDM}$ is usually negative since χ^2 is usually further reduced due to the larger number of parameters compared to LCDM. For a given number of parameters the value of $\Delta\chi^2_{LCDM}$ gives a measure of the probability of having LCDM physically realized in the context of a given parametrization. The smaller this probability is, the more ‘superior’ this parametrization is compared to LCDM. For example for a two parameter parametrization and $|\Delta\chi^2_{LCDM}| > 2.3$ the parameters of LCDM are more than 1σ away from the best fit parameter values of the given

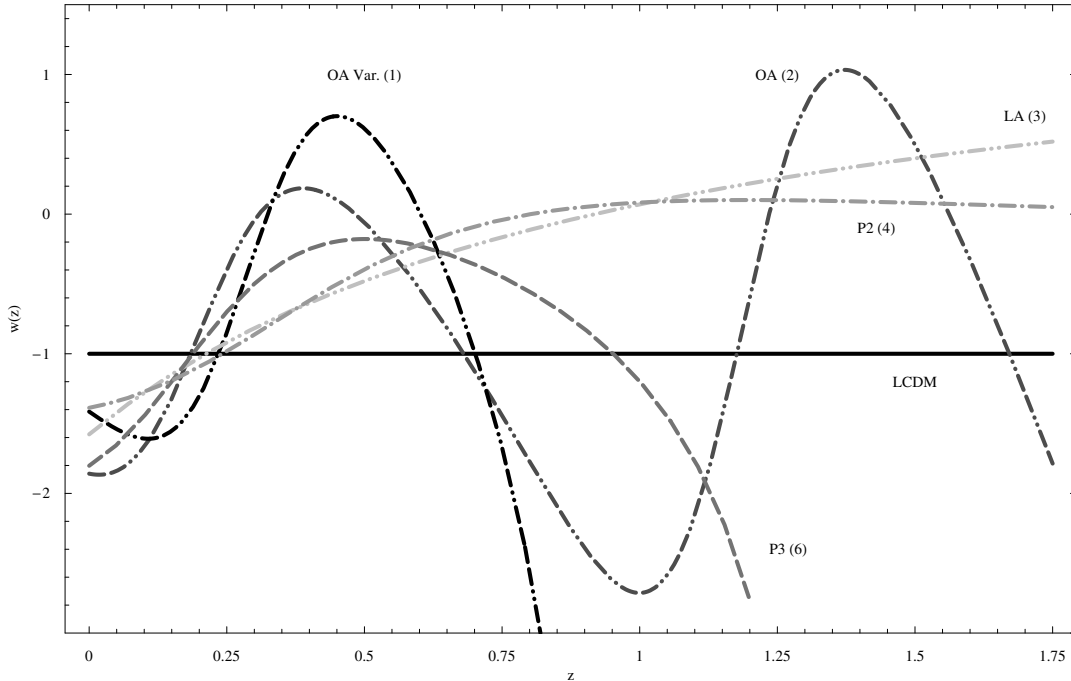


Figure 2: *The best fit forms of $w(z)$ obtained from a variety of parametrizations (Lazkoz, Nesseris and Perivolaropoulos (2005)) in the context of the Full Gold dataset. Notice that they all cross the line $w = -1$ also known as the Phantom Divide Line (PDL).*

parametrization. This statistical test has been quantified by Lazkoz, Nesseris and Perivolaropoulos (2005) and applied to several $H(z)$ parametrizations.

As an example let us consider the two parameter polynomial parametrization allowing for dark energy evolution

$$H(z)^2 = H_0^2[\Omega_{0m}(1+z)^3 + a_2(1+z)^2 + a_1(1+z) + (1 - a_2 - a_1 - \Omega_{0m})] \quad (21)$$

in the context of the Full Gold dataset. Applying the above described χ^2 minimization leads to the best fit parameter values $a_1 = 1.67 \pm 1.03$ and $a_2 = -4.16 \pm 2.53$. The corresponding $|\Delta\chi_{LCDM}^2|$ is found to be 2.9 which implies that the LCDM parameters values ($a_1 = a_2 = 0$) are in the range of $1\sigma - 2\sigma$ away from the best fit values.

The best fit forms of $w(z)$ obtained from a variety of parametrizations in the context of the Full Gold dataset are shown in Fig. 2.

Even though these best fit forms appear very different at redshifts $z > 0.5$ (mainly due to the two derivatives involved in obtaining $w(z)$ from $d_L(z)$), in the range $0 < z < 0.5$ they appear to have an interesting common feature: they all cross the line $w = -1$ also known as the Phantom Divide Line (PDL). This feature is difficult to reproduce (Vikman (2005), Perivolaropoulos (2005)) in most theoretical models based on minimally coupled scalar fields and therefore if it persisted in

other independent datasets it could be a very useful tool in discriminating among theoretical models.

For example the PDL can not be crossed in any model where the role of dark energy is played by a minimally coupled to gravity scalar field. Quintessence scalar fields (Caldwell, Dave and Steinhardt (1998)) with small positive kinetic term ($-1 < w < -\frac{1}{3}$) violate the strong energy condition ($\rho + 3p > 0$) but not the dominant energy condition $\rho + p > 0$. Their energy density scales down with the cosmic expansion and so does the cosmic acceleration rate. Phantom fields (Caldwell (2002)) with negative kinetic term ($w < -1$) violate the strong energy condition, the dominant energy condition and maybe physically unstable. However, they are also consistent with current cosmological data and according to recent studies (Alam, Sahni, Saini and Starobinsky (2004), Nesseris and Perivolaropoulos (2004), Lazkoz, Nesseris and Perivolaropoulos (2005)) they maybe favored over their quintessence counterparts.

Homogeneous quintessence or phantom scalar fields are described by Lagrangians of the form

$$\mathcal{L} = \pm \frac{1}{2} \dot{\phi}^2 - V(\phi) \quad (22)$$

where the upper (lower) sign corresponds to a quintessence (phantom) field in equation (22) and in what follows. The corresponding equation of state parameter is

$$w = \frac{p}{\rho} = \frac{\pm \frac{1}{2} \dot{\phi}^2 - V(\phi)}{\pm \frac{1}{2} \dot{\phi}^2 + V(\phi)} \quad (23)$$

For quintessence (phantom) models with $V(\phi) > 0$ ($V(\phi) < 0$) the parameter w remains in the range $-1 < w < 1$. For an arbitrary sign of $V(\phi)$ the above restriction does not apply but it is still impossible for w to cross the PDL $w = -1$ in a continuous manner. The reason is that for $w = -1$ a zero kinetic term $\pm \dot{\phi}^2$ is required and the continuous transition from $w < -1$ to $w > -1$ (or vice versa) would require a change of sign of the kinetic term. The sign of this term however is fixed in both quintessence and phantom models. This difficulty in crossing the PDL $w = -1$ could play an important role in identifying the correct model for dark energy in view of the fact that data favor $w \simeq -1$ and furthermore parametrizations of $w(z)$ where the PDL is crossed appear to be favored over the cosmological constant $w = -1$ according to the Gold dataset as shown in Fig. 2.

The recent SnIa data have opened new directions in cosmological research and have raised important questions related to the physical origin and dynamical properties of dark energy. In particular these questions can be structured as follows:

- Can the accelerating expansion be attributed to a dark energy ideal fluid with negative pressure or is it necessary to implement extensions of GR to understand the origin of the accelerating expansion?
- Is w evolving with redshift and crossing the PDL? If the crossing of the PDL by $w(z)$ is confirmed then it is quite likely that extensions of GR will be required to explain observations.

- Is the cosmological constant consistent with data? If it remains consistent with future more detailed data then the theoretical efforts should be focused on resolving the coincidence and the cosmological constant problems which may require anthropic principle arguments.

The main points of this brief review may be summarized as follows:

- *Dark energy* with *negative pressure* can explain SnIa cosmological data indicating accelerating expansion of the universe.
- The existence of a *cosmological constant* is consistent with SnIa data but other *evolving* forms of dark energy *crossing the $w = -1$* line may provide better fits to some of the recent data (Gold dataset).
- New *observational projects* are underway and are expected to lead to significant progress in the understanding of the properties of *dark energy*.

References

- Alam U., Sahni V., Saini T. and Starobinsky A., 2004, Mon. Not. Roy. Astron. Soc. **354**, 275
- Astier P. *et al.*, 2006, Astron. Astrophys. **447**, 31
- Caldwell R., 2002, Phys. Lett. B **545**, 23
- Caldwell R., Dave R. and Steinhardt P., 1998, Phys. Rev. Lett. **80**, 1582
- Chaboyer B., 1995, Astrophys. J. **444**, L9
- Freese K. and Lewis M., 2002, Phys. Lett. B **540**, 1
- Huterer D. and Turner M., 2001, Phys. Rev. D **64**, 123527
- Kamenshchik A., Moschella U. and Pasquier V., 2001, Phys. Lett. B **511**, 265
- Lazkoz R., Nesseris S. and Perivolaropoulos L., 2005, arXiv:astro-ph/0503230
- Nesseris S. and Perivolaropoulos L., 2004, Phys. Rev. D **70**, 043531
- Nesseris S. and Perivolaropoulos L., 2005, arXiv:astro-ph/0511040
- Perivolaropoulos L., 2003, Phys. Rev. D **67**, 123516
- Perivolaropoulos L., 2005, JCAP **0510**, 001
- S. Perlmutter *et al.*, 1998, Nature (London) **391**, 51
- Perrotta F., Baccigalupi C. and Matarrese S., 2000, Phys. Rev. D **61**, 023507
- Riess A *et al.*, 1998, Astron. J. **116** 1009
- Riess A *et al.*, 2004, Astrophys. J. **607**, 665
- Tonry, J L *et al.*, 2003, Astroph. J. **594** 1
- Sahni V. and Shtanov Y, 2003, JCAP **0311**, 014
- Spergel D. *et al.*, 2003, Astrophys.J.Suppl. **148** 175
- Torres D., 2002, Phys. Rev. D **66**, 043522
- Vikman A., 2005, Phys. Rev. D **71**, 023515
- Wang Y. and Mukherjee P., 2004, Astrophys. J. **606**, 654

MANIFESTATIONS OF STRONG GRAVITY IN COSMIC RAYS *

A. Nicolaidis^{1 †} and **N.G. Sanchez**^{2 ‡}

¹Department of Theoretical Physics, University of Thessaloniki,
54124 Thessaloniki, Greece

²Observatoire de Paris LERMA, UMR 8540, CNRS 61, Avenue de l'Observatoire,
75014 Paris, France

Abstract

In TeV scale unification models, gravity propagates in $4+\delta$ dimensions while gauge and matter fields are confined to a four dimensional brane, with gravity becoming strong at the TeV scale. For a such scenario, we study strong gravitational interactions in a effective Schwarzschild geometry. Two distinct regimes appear. For large impact parameters, the ratio $\rho \sim (R_s/r_0)^{1+\delta}$, (with R_s the Schwarzschild radius and r_0 the closest approach to the black hole), is small and the deflection angle χ is proportional to ρ (this is like Rutherford-type scattering). For small impact parameters, the deflection angle χ develops a logarithmic singularity and becomes infinite for $\rho = \rho_{crit} = 2/(3 + \delta)$. This singularity is reflected into a strong enhancement of the backward scattering (like a glory-type effect). We suggest as distinctive signature of black hole formation in particle collisions at TeV energies, the observation of backward scattering events and their associated diffractive effects.

The main motivation for introducing new physics comes from the need to provide a unified theory in which two disparate scales, ie the electroweak scale $M_W \sim 100$ GeV and the Planck scale $M_P \sim 10^{19}$ GeV, can coexist (hierarchy problem). A novel approach has been proposed for resolving the hierarchy problem [1]. Specifically, it has been suggested that our four dimensional world is embedded in a higher dimensional space with D dimensions, of which δ dimensions are compactified with a relatively large (of order of mm) radius. While the Standard Model (SM) fields live on the 4-dimensional world (brane), the graviton can propagate freely in the higher dimensional space (bulk).

The fundamental scale M_f of gravity in D dimensions is related to the observed 4-dimensional Newton constant G_N by

$$G_N = \frac{1}{V_\delta} \left(\frac{1}{M_f} \right)^{(2+\delta)} \quad (1)$$

*Presented at the Workshop on *Cosmology and Gravitational Physics*, 15-16 December 2005, Thessaloniki, Greece, *Editors*: N.K. Spyrou, N. Stergioulas and C.G. Tsagas.

[†]nicolaid@auth.gr

[‡]Norma.Sanchez@obspm.fr

where V_δ is the volume of the extra dimensional space. A sufficiently large V_δ can then reduce the fundamental scale of gravity M_f to TeV energies, which is not too different from M_W , thereby resolving the hierarchy problem.

The prospect of gravity becoming strong at TeV energies, opens the possibility of studying gravity in particle collisions at accessible energies (at present or in the near future). To that respect, salient features of the cosmic ray spectrum (the "knee") have been attributed to gravitational bremsstrahlung [2]. By reproducing the cosmic ray spectrum, the parameters of the low scale gravity can be inferred ($\delta \sim 4$ and $M_f \sim 8$ TeV).

In this letter, we would like to study the interactions among particles, mediated by low scale gravity. The optimum would be to address this issue within a complete quantum gravity theory. But we are lacking this framework. We could turn to perturbative quantum gravity. But we would miss all the essential features of strong gravity we are interested in. Furthermore, perturbative calculations are uncertain, since there is no definite method for summing up the Kaluza-Klein contributions [3]. We prefer to work within an effective approach in which gravity effects are treated classically but non-perturbatively. That is, the effect of particle collisions at TeV energy scale is considered as the scattering of a particle in the effective *curved* background produced by all the others. While our estimates would not be the exact answer, we anticipate that they would reflect the main characteristics of strong gravity effects. Several arguments support this approach. Particle collisions in string theory are, within the eikonal approximation, like the classical scattering of a particle in the effective gravitational shock wave background created by all the others [?],[?]. For large impact parameters, the shock wave profile is of Aichelburg-Sexl type (point particle source). For intermediate impact parameters, the shock wave profile is different, corresponding to a localized extended source [?]. The shock wave background description is only valid for large or intermediate impact parameters, namely weak gravity limit. The scattering phase shift in the Aichelburg-Sexl background just reproduces the phase shift of the newtonian gravitational tail. For small impact parameters (strong gravity effects) a full black hole background is necessary.

We consider a SM particle moving under the influence of a $(4+\delta)$ - dimensional black-hole. The effective metric is [4]

$$ds^2 = f(r)dt^2 - \frac{1}{f(r)} dr^2 - r^2(d\theta^2 + \sin^2 \theta d\varphi^2) \quad (2)$$

where

$$f(r) = 1 - \left(\frac{R_s}{r}\right)^{1+\delta} \quad (3)$$

$$R_s = \frac{1}{\sqrt{\pi}M_f} \left[\frac{M}{M_f} \frac{8\Gamma\left(\frac{\delta+3}{2}\right)}{\delta+2} \right]^{1/(\delta+1)} \quad (4)$$

$M_f \simeq$ TeV is related to G_N by eq (1). For particle collisions, $M = \sqrt{s}$, the center-of-mass energy. A particle impinging upon the black hole at impact parameter b

will approach the black hole at a closest distance r_0 , related by

$$b^2 = \frac{r_0^2}{1 - \rho} \quad (5)$$

with

$$\rho = \left(\frac{R_s}{r_0} \right)^{1+\delta} \quad (6)$$

The deflection angle χ of the particle is given by (details will be reported elsewhere)

$$\chi = 2\Phi_0 - \pi \quad (7)$$

$$\Phi_0 = \int_0^1 \frac{d\omega}{[1 - \omega^2 - \rho(1 - \omega^{3+\delta})]^{1/2}} \quad (8)$$

For large impact parameters, ρ acquires small values. A Taylor expansion in ρ provides then

$$\chi = I(\delta)\rho \quad (9)$$

where $I(\delta)$ is a constant depending solely on δ . Our result is in agreement with the results obtained within perturbative (classical or quantum) gravity. Furthermore, by setting $\delta = 0$ we find the traditional Rutherford formula, or the equivalent formula for perturbative Yang-Mills scattering in 4 dimensions.

Small b values give rise to larger values of ρ . We find that with decreasing b , χ increases and there is a critical ρ value where χ becomes infinite. A reasonable approximation of χ for all ρ values is the following

$$\chi = a \ln \left(\frac{1}{1 - \rho/\rho_{crit}} \right) \quad (10)$$

with

$$\rho_{crit} = \frac{2}{(3 + \delta)} \quad (11)$$

$$a = \rho_{crit} I(\delta) \quad (12)$$

The parameter ρ_{crit} has a clear physical meaning. It corresponds to the unstable circular orbit around the black hole. As ρ approaches ρ_{crit} , the particle starts orbiting around the black hole before escaping to infinity. At $\rho = \rho_{crit}$ the particle stays in circular orbit, implying an infinite value for χ . For $\rho < \rho_{crit}$ the particle is fully absorbed by the black hole.

Our findings, transformed into differential cross-section, provide

$$\frac{d\sigma_0}{d\Omega}(\chi) = CR_s^2 \frac{1}{\sin \chi} \frac{\exp(-\chi/a)}{[1 - \exp(-\chi/a)]^{\frac{(3+\delta)}{(1-\delta)}}} \quad (13)$$

where C is a δ -dependent constant. Notice that the one-to-one correspondence between the impact parameter b and the deflection angle χ is lost

$$\rho = \rho_{crit} - \rho_{crit} e^{-\chi/a} \quad (14)$$

Due to orbiting, different values of b give rise to the same χ . We have to sum over all $\chi_n = \chi + 2n\pi$ and the differential cross section becomes

$$\frac{d\sigma(\chi)}{d\Omega} = \sum_{n=0}^{\infty} \frac{d\sigma_0}{d\Omega}(\chi_n) \quad (15)$$

At small χ , the cross-section diverges like $(1/\chi)^\gamma$ with $\gamma = (4 + 2\delta)/(1 + \delta)$. (for $\delta = 0$, $\gamma = 4$). This is the well known focusing of forward scattering at $\chi = 0$ due to the large range (newtonian or coulombian) interaction at large distances. At large angles, the cross-section, although is relatively suppressed, it diverges again at $\chi = \pi$, like $\frac{1}{(\chi-\pi)}$ for any δ . This focusing at backward scattering is due to the strong attractive black hole potential at short distances (it is not present in less attractive gravitational fields, nor in Rutherford scattering).

Imagine then collisions of cosmic rays particles in the atmosphere. At very high energies, approaching the fundamental scale of gravity M_f , gravitational interactions become important and it is expected that in some events, backward scattering will occur. Experimental devices like EUSO [5], OWL [6], will register the development of a shower changing direction suddenly. We suggest that this type of events should be seen as evidence for black hole formation in cosmic rays interactions, mediated by TeV scale gravity. Similar situations may arise in detecting high energy neutrinos by a neutrino telescope [7]. The induced energetic muon might spiral and the emitted Cherenkov light will form a luminous halo rather than a forward cone. Again, these events should be classified as black hole formation. Experiments to be carried out in the near future would test the reality of gravity becoming strong at TeV energies.

There is an extensive literature on black hole formation in particle collisions, within the framework of low scale gravity [8],[9]. In these works, the detection of the emitted Hawking radiation has been proposed as signal for black hole production. Hawking radiation corresponds to particles just escaping the horizon and in a realistic situation one should include the radiation emitted in the whole scattering process. Furthermore a black-body spectrum for emitted particles is not synonymous of Hawking radiation. In hadronic collisions at high energies the emitted particles follow thermal spectra, without even implying thermal equilibrium [10]. The relevant calculations [8],[9], presuppose also the validity of the parton model. However the formation of a black hole corresponds to the strong gravity regime, with multiple gravitons being exchanged, and the hypothesis of individual "free" partons is not justified.

Our calculation reveals another generic feature known as duality [11]. Gravity at large distances behaves like perturbative Yang-Mills fields at short distances, both providing power-law behaviours. On the other hand, gravity at short distances is described by exponential cutoffs, very similar to soft QCD phenomena at large distances. Clearly, this issue deserves further study.

References

- [1] I. Antoniadis, Phys. Lett. **B 246**, 377 (1990);
N. Arkani-Hamed, S. Dimopoulos, and G. Dvali, Phys. Lett. **B 429**, 263 (1998)
I. Antoniadis, N. Arkani-Hamed, S. Dimopoulos and G. Dvali, Phys. Lett. **B 436**, 257 (1998)
- [2] D. Kazanas and A. Nicolaidis, Gen. Rel. Grav. **35**, 1117 (2003)
- [3] G. Giudice and A. Strumia, hep-ph/0301232 preprint.
- [4] R. Myers and M. Perry, Ann. Phys. **172**,304 (1986)
- [5] L.Scarsi, EUSO : Using high energy cosmic rays and neutrinos as messengers from the unknown universe, in Proc. "Venice 2001, Neutrino telescopes, vol. 2" p. 545-568.
- [6] J. Krizmanic et al., in Proc. of the 26th International Cosmic Ray Conference (ICRC 99), Salt Lake City, 1999, Cosmic Ray, Vol. 2, p. 388-391.
- [7] The AMANDA collaboration, Astropart. Phys. **13**, 1 (2000)
The NESTOR collaboration, Nucl. Phys. **Proc. Suppl. 87**, 448 (2000)
The ANTARES collaboration, Nucl. Phys. **Proc. Suppl. 81**, 174 (2000)
- [8] S. Dimopoulos and G. Landsberg, Phys. Rev. Lett. **87**, 161602 (2001)
- [9] A partial list on black hole formation at TeV energies includes
S. Giddings and S. Thomas, Phys. Rev D**65**, 056010 (2002)
J. Feng and A. Shapere, Phys. Rev. Lett. **88**, 021303 (2002)
G. Landsberg, Phys. Rev. Lett. **88**, 181801 (2002)
L. Anchordoqui and H. Goldberg, Phys. Rev. D **65**, 047502 (2002)
L. Anchordoqui, J. Feng, H. Goldberg and A. Shapere, Phys. Rev. D **65**, 124027 (2002)
Y. Uehara, Prog. Theor. Phys. **107**,621 (2002)
R. Emparan, M. Masip and R. Rattazzi, Phys. Rev. D **65**, 064023 (2002)
J. Alvarez-Muniz, J. Feng, F. Halzen, T. Han and D. Hooper, Phys. Rev. D **65**, 124015 (2002)
K. Cheung, Phys. Rev. Lett. **88**,221602 (2002)
A. Ringwald and H. Tu, Phys. Lett. B **525**, 135 (2002)
M. Kowalski, A. Ringwald and H. Tu, Phys. Lett. B **529**,1 (2002)
M. Bleicher, S. Hofmann, S. Hossenfelder and H. Stocker, Phys. Lett. B **548**, 73 (2002)
S. Dutta, M. Reno and I. Sarcevic, Phys. Rev. D **66**,033002 (2002)
K. Cheung, Phys. Rev. D **66**, 036007 (2002)
A. Chamblin and G. Nayak, Phys. Rev D **66**, 091901 (2002)
L.Anchordoqui and H. Goldberg, Phys. Rev. D **67**, 064010 (2003)
M. Cavaglia, Int. J. Mod. Phys. A **18**,1843 (2003)
P. Kanti and J. March-Russell, Phys. Rev. D **67**, 104019 (2003)

I. Mocioiu, Y. Nara and I. Sarcevic, Phys. Lett. B **557**, 87 (2003)
V. Cardoso, J.P.S. Lemos, Phys. Lett. B **538**, 1 (2002)
T. Banks, W. Fishler, hep-th/9906038

- [10] T. Chou, C. Yang and E. Yen, Phys. Rev. Lett. **54**, 510 (1985).
T. Chou and C. Yang, Phys. Rev D **32**, 1692 (1985)

- [11] See for example G. Veneziano, “A new approach to semiclassical gravitational scattering”, in “Second Paris Cosmology Colloquium”, H.J. de Vega and N. Sanchez Editors, WSPC, (1995), pp 322-326.

MODERN SOLAR SYSTEM DYNAMICS AND THE HISTORY OF THE SOLAR SYSTEM *

H. Varvoglis †

University of Thessaloniki, Department of Physics, Thessaloniki, GR-541 24, Greece

Abstract

Until recently, through the pioneering work on gravitation of astronomers of the 17th and 18th century such as Newton, Laplace and Lagrange, it was believed that the celestial bodies of the solar system are moving on almost periodic orbits. The last decades, however, it became more and more evident that chaotic behavior is rather the rule than the exception in the solar system and that in some cases non-gravitational forces are non-negligible, at least in what concerns the motion of minor bodies, such as asteroids. The net result of these two effects is that the solar system is not the clockwork quasi-periodic system envisioned by Newton, but rather a system evolving in time. Moreover collisions are still frequent in astronomical time scales, a fact that has important consequences for the life in our planet. The work of the Solar System Dynamics Group on chaotic diffusion of ensembles of solar system bodies, on the effects of non-gravitational forces and on N -body simulations gives important information on the past history of the solar system and on its future evolution.

1. Newton's Celestial Mechanics

The proof by Newton that his theory of Gravitation, in connection with his second law of motion, was able to interpret all three Kepler's laws set the foundations of Celestial Mechanics, the branch of Dynamical Astronomy which deals with dynamics in the solar system. According to *classical* Celestial Mechanics, all bodies of the solar system are moving on almost periodic orbits, which are ellipses in the zero-th order approximation of the two-body problem. The next step of generalization, however, namely the three-body problem, proved to be very hard to attack. As it was proven later by Poincaré, it is not possible to find analytical solutions of the three-body problem, but astronomers were able to find *perturbative solutions* of the two-body problem. In this way they developed the so-called *secular theory*, which describes the actual motions of all planets, asteroids and comets in remarkable accuracy. In

*Presented at the Workshop on *Cosmology and Gravitational Physics*, 15-16 December 2005, Thessaloniki, Greece, *Editors*: N.K. Spyrou, N. Stergioulas and C.G. Tsagas.

†varvogli@physics.auth.gr

the secular theory the orbits of planets are ellipses, which are *modulated* slowly in time.

The secular theory¹ is most conveniently presented in a special set of canonical action-angle variables, the so-called *modified Delaunay variables* Λ, Γ and Z , which take advantage of the specific symmetries of the problem and the actual physics (many small bodies revolving about a dominant one). For small values of eccentricity and inclination, as it is the case for most bodies of the solar system, Λ, Γ and Z are related to the elements of the trajectory through the relations $\Lambda \sim \sqrt{a}, \Gamma \sim e^2, Z \sim \sin^2 i$. Therefore for all practical purposes we can think of the semi-major axis, the eccentricity and the inclination of an orbit as the three “actions” of an action-angle co-ordinate system. In the framework of the linear secular theory, the semi-major axis is constant and the other two elements, eccentricity and inclination, are varying periodically about constant values, with amplitudes e_P and i_P , which are called *proper eccentricity* and *proper inclination*. The proper elements, together with the (constant) semi-major axis, characterize fully the orbital properties of solar system bodies.

2. Shortcomings of the classical theory

In the last decade it became apparent that the “classical” secular theory cannot tackle two aspects of solar system dynamics, that were recognized very recently. The first is that the solar system, as a whole, is chaotic, with a Lyapunov time ~ 100 Myrs.² But some bodies have Lyapunov times of the order ~ 100 yrs, which means that there is a component of the solar system that changes within the life span of an astronomer! In other words, one might say that, in the solar system, chaos is the rule, rather than the exception. This is in direct disagreement with the Newtonian point of view, which is reflected in the secular theory, namely that the solar system is evolving in a quasi-periodic way. The second aspect is that non-gravitational forces (mainly of electromagnetic origin) are non-negligible for the motion of minor bodies, especially those with diameters, as a rule, less than 10 km. As a result, the traditional approach, through the “classical” secular theory, fails, since

- Numerically integrated solutions are useless, beyond the Lyapunov time
- Chaotic orbits cannot be described by the analytical functions of the secular theory
- Electromagnetic forces have to be included to the secular theory in a consistent way.

The last years new ideas have emerged, which help us to tackle problems that cannot be addressed by classic Celestial Mechanics. The fact that the computa-

¹A modern presentation of the secular theory can be found in Morbidelli (2002); see also Vargolis (2006).

²The Lyapunov time is the inverse of the Lyapunov Characteristic Number (LCN), which is a measure of the exponential divergence of nearby trajectories. Positive LCNs indicate chaos.

tion of individual trajectories is useless beyond the Lyapunov time, on one hand, can be circumvented through a statistical approach, by studying ensembles of initial conditions. This can be done either theoretically, by solving an appropriate *diffusion equation*, or numerically, by running simulations in powerful computers. The importance of non-gravitational forces, on the other hand, is addressed by the recent development of a theory, which takes into account the most important electromagnetic force in the solar system, the *Yarkovsky effect*, as a non-conservative perturbation of the (purely gravitational) secular solutions of the equations of motion. In what follows we summarize each one of the above three approaches and present typical applications developed by our group.

3. Diffusive approach

Let's assume that a chaotic trajectory of a one-degree-of-freedom dynamical system is hovering *stochastically* in phase space. For conservative systems this is certainly not true, but a chaotic dynamical system, under certain conditions, may be approximated in this way. Then the evolution of an ensemble of initial conditions in the *action space*, I , of the system is described by the Fokker-Planck equation, which, for conservative systems, takes the form

$$\frac{\partial P}{\partial t} = \frac{\partial}{\partial I} \left(\frac{D}{2} \frac{\partial P}{\partial I} \right)$$

In the above equation $P(x, t)$ is the probability density function and D is the *diffusion coefficient*.

This result may be generalized for conservative dynamical system with more than one degrees of freedom. Our group has proposed since 1996 (Varvoglis and Anastasiadis, 1996; Tsiganis *et al.*, 2003a; Varvoglis, 2004) the use of the Fokker-Planck equation for the study of the evolution of chaotic solar system bodies. Here we give one recent application of the “diffusive approach”, introduced above, to the solution of an actual problem of asteroid dynamics, namely the estimation of the age of the *Veritas family*.

We know that collisions played a crucial role in the evolution of the asteroid belt. A collision between two asteroids gives rise to a bunch of fragments, which follow orbits with similar proper elements. This property enables us to recognize asteroids originating from collisionally disrupted parent bodies, by looking for local groupings in the space of proper elements. These groupings are referred to as *asteroid families*. An important information concerning asteroid families is their age, since from that we may estimate the rate of collisions in the history of the asteroid belt. We were able to estimate, by applying our diffusive approach, the age of the Veritas family. Recently Nesvorný *et al.* (2003) integrated backwards the trajectories of a subgroup of this family, whose members follow ordered trajectories, and they found that the trajectories converged 8.3 Myrs in the past. Therefore the age of the family should be 8.3 Myrs, unless of course that the subgroup, used by these authors, was created by a secondary breakup. In order to confirm their estimate, we applied our diffusive

approach to another subgroup of the same family, whose members follow chaotic trajectories. Our method is summarized as follows.

First we calculated the diffusion coefficient, D , of the asteroid trajectories belonging to the chaotic subgroup. This is done by first numerically integrating the trajectories of many fictitious asteroids with initial conditions in the same phase space region where chaotic asteroids lie. Then we plot the variance of e , $\langle [e(t) - \langle e(t) \rangle]^2 \rangle$, as a function of time and we fit a least square straight line. The slope of this line is the diffusion coefficient. Now we know that, for an initial distribution $f_0(e) = \delta(e - e_0)$, the solution of the diffusion equation, $P(e, t)$, is a Gaussian with mean $\mu = e_0$ and a variance increasing linearly in time, $\sigma^2 = Dt$. Therefore we fit a Gaussian to the present day distribution, $P(e, t_0) = f(e)$ of the observed chaotic members of the Veritas family and we find $t_0 = \frac{\sigma^2}{D} = 8.7 \pm 1.7$ Myrs, a result that nicely corroborates the one found by Nesvorný *et al.*

4. Yarkovsky effect

The Yarkovsky effect is a force applied to a body by the anisotropic emission of thermal photons. On a rotating body (e.g. an asteroid) illuminated by the Sun, the surface is warmer in the afternoon and early night, than in the morning and late night (the same happens in Earth, as well). The result is that more heat is radiated on the “dusk” side than the “dawn” side, leading to a back reaction force in the opposite “dawn” direction. For prograde rotators, this is in the direction of motion on their orbit, produces work and causes their semi-major axis to steadily increase. The semi-major axis of retrograde rotators decreases.

The Yarkovsky effect is the only known process that may “break” the adiabatic invariance of the semi-major axis of an asteroid and, therefore, may force a net radial “drift”, either towards the Sun or away from it, depending on the sense of rotation of the body. We have used this idea to propose an interpretation for the existence of 50 asteroids in the 7:3 Kirkwood gap (semi-major axis $a \approx 2.956$ AU) with diameters in the range $2 \text{ km} < D < 12 \text{ km}$ (Tsiganis *et al.*, 2003b). We know that the 7:3 resonance is a highly unstable region of the main asteroid belt, since the mean dynamical lifetime of objects initially placed in the resonance is ~ 20 Myr. Given this short time scale, the probability that the currently observed resonant objects are on their primordial orbits is effectively null. The question then is where do these bodies originate from. The clue to the answer of this question was the bimodal distribution of the resonant asteroids in proper inclination, with two peaks at $i = 2^\circ$ and $i = 10^\circ$. We know that on either side of the 7:3 gap lie two of the most populated families of the asteroid belt, the Koronis family with $i = 2^\circ$ and the Eos family with $i = 10^\circ$. Therefore we suggested that what we see today is a dynamical equilibrium between two processes: the escape of asteroids from the 7:3 gap and the “injection” of asteroids into the gap through a drift in semi-major axis, caused by the Yarkovsky force. In order to check this conjecture, we calculated the mean life-time of 7:3 resonant asteroids with inclinations equal to 2° and 10° and we found $T_{2^\circ}^{escape} = 52.8$ Myrs and $T_{10^\circ}^{escape} = 12.4$ Myrs. From these numbers we calculate,

on the one hand, the present “outward” flux of asteroids from the 7:3 gap through the relation $F = \frac{N_{observed}}{T_{escape}}$ and we find $F_{2^\circ} = 0.48$ bodies/Myr and $F_{2^\circ, 10^\circ} = 0.30$ bodies/Myr. On the other hand we know that the mean drift rate of the semi-major axis of an asteroid, due to the Yarkovsky effect, is $\frac{\langle \Delta a \rangle}{t} = \tau^{-1} = \frac{2.7 \times 10^{-4} \cos^2 \theta}{D}$ AU/Myr, where θ is the obliquity of the asteroid. The mean time, required for an asteroid to drift in semi-major axis by δa , is $T_{drift} = \delta a \cdot \tau$ Myr. Denoting by $N(\delta a)$ the number of bodies within a distance δa from the border of the resonance, the mean flux into the resonance is $F_{\pm} = \frac{N(\delta a)}{2T_{drift}}$, where the factor 2 in the denominator is due to the fact that asteroids can drift towards smaller or larger values of a with the same probability. Since we ask for the steady state solution, we impose $F_{\pm} = F_{2^\circ, 10^\circ}$ and solve for $N(\delta a)$. The result is that, to explain the observed resonant group at $i = 2^\circ$, 19 – 24 bodies per 0.002 AU should be currently observed in the Koronis family. Similarly, for the $i = 10^\circ$ group, we should be observing 45 – 57 bodies per 0.002 AU in the Eos family. The lower bounds of these estimates correspond to θ being either 0° or 180° , while the upper bounds are computed for randomized values of θ . By binning the observed distribution in the same way, we find the observed number density to be ~ 22 and ~ 50 bodies per 0.002 A.U. respectively. As we can see, the agreement between the number density of observed asteroids away from the location of the resonance a_{res} , on the one hand, and the number density calculated by assuming the action of the Yarkovsky force, on the other, is very good. This work was one of the first cases, in which the importance of the Yarkovsky effect in the dynamics of the solar system was shown.

5. Simulations

The two approaches of studying the evolution of our planetary system under the influence of only gravitational forces (*secular theory* for ordered trajectories or *statistical description* for chaotic ones) are only two “extreme” cases. For all “intermediate” cases a satisfactory appropriate theory does not exist today and, therefore, these cases have to be studied numerically. Indeed, the motion of a large number of bodies can be studied consistently, including the “hard to model” collisions and/or close encounters, provided that one has the appropriate computer power to follow their evolution for time intervals of the order of the age of the solar system. The last years this approach has gained momentum, through the continuous increase of speed and memory of “classical” computers or the use of dedicated machines.

An interesting example of this new approach is the triggering of planetary formation, through the interaction of planetesimals of a protoplanetary disk with a close approaching star (Varvoglis *et al.*, 2006). The corresponding simulation was performed using a GRAPE machine, a dedicated computer accelerator which calculates the gravitational forces between N -bodies at a speed of 1 Tflop. We have shown that parabolic encounters between gas-free protoplanetary disks result into

- (i) the exchange of material between the disks, and

- (ii) the restructuring of the initial disk, into a “core” of nearly circular and co-planar orbits and an extended 3-D cloud of eccentric and inclined bodies.

These processes may prove to be particularly important for the formation of planets and small-body belts around the Sun or other stars, where the planet formation process resulted in the creation of planetary systems.

6. Conclusions

Statistical approach gives information for the past and the future of chaotic bodies of the Solar System. The Yarkovsky effect may explain secular changes in the mean distance of small solar system objects from the Sun. N-body simulations reveal the formation processes of planetary systems.

Acknowledgements.

This work was supported by the research program EPEAEK-II / Pythagoras-I of the Greek Ministry of Education. I would like to thank Empeirikio Foundation of Greece and Aristotle University of Thessaloniki for funding the purchase of the Grape-6/Pro8 system and Dr. K. Tsiganis for reading the first draft of this article.

References

- Morbidelli, A., 2002, *Modern Celestial Mechanics, Aspects of Solar System Dynamics*, Taylor & Francis, London
- Nesvorný, D., Bottke, W.F., Levison, H.F., and Dones, L., 2003, *Astrophys. J.* 591, 486
- Tsiganis, K., Knežević, Z., and Varvoglis, H., 2006, *Icarus*, in press
- Tsiganis, K., Varvoglis, H., and Anastasiadis, A., 2003a, in *Modern Celestial Mechanics: from Theory to Applications*, A. Celletti, S. Ferraz-Mello, and J. Henrard (eds.), Kluwer, Dordrecht, p. 451
- Tsiganis, K., Varvoglis, H., and Morbidelli, A., 2003b, *Icarus*, 166, 131
- Varvoglis, H., 2004, in *Proceedings IAU Colloquium No. 197, Dynamics of Populations of Planetary Systems*, Z. Knežević and A. Milani (eds.), Cambridge Univ. Press, p. 157
- Varvoglis, H., 2006, in *Recent Advances in Astronomy and Astrophysics, 7th International Conference of the Hellenic Astronomical Society*, N. Solomos (ed.), AIP Conference Proceedings Vol. 848, p. 613
- Varvoglis, H., and Anastasiadis, A., 1996, *Astron. J.* 111, 1718
- Varvoglis, H., Tsiganis, K., and Vozikis, Ch., 2006, in *International Workshop: Rotation of Celestial Bodies*, A. Lemaître (ed.), in press

ROTATIONAL INSTABILITIES IN SUPERMASSIVE STARS: A NEW WAY TO FORM SUPERMASSIVE BLACK HOLES *

Burkhard Zink^{1,4†}, Nikolaos Stergioulas^{2‡}, Ian Hawke^{3§}, Christian D. Ott^{4¶},
Erik Schnetter^{1||} and Ewald Müller^{5**}

¹Center for Computation and Technology, Louisiana State University,
Baton Rouge, LA 70803, USA

²Department of Physics, Aristotle University of Thessaloniki,
Thessaloniki 54124, Greece

³School of Mathematics, University of Southampton,
Southampton SO17 1BJ, UK

⁴Max-Planck-Institut für Gravitationsphysik, Albert-Einstein-Institut,
14476 Golm, Germany

⁵Max-Planck-Institut für Astrophysik,
Karl-Schwarzschild-Str. 1, 85741 Garching bei München, Germany

Abstract

We investigate new paths to black hole formation by considering the general relativistic evolution of a differentially rotating polytrope with toroidal shape. We find that this polytrope is unstable to nonaxisymmetric modes, which leads to a fragmentation into self-gravitating, collapsing components. In the case of one such fragment, we apply a simplified adaptive mesh refinement technique to follow the evolution to the formation of an apparent horizon centered on the fragment. This is the first study of the one-armed instability in full general relativity.

1. Introduction

*Presented at the Workshop on *Cosmology and Gravitational Physics*, 15-16 December 2005, Thessaloniki, Greece, *Editors*: N.K. Spyrou, N. Stergioulas and C.G. Tsagas.

†bzink@cct.lsu.edu

‡niksterg@astro.auth.gr

§I.Hawke@soton.ac.uk

¶cott@aei.mpg.de

||schnetter@cct.lsu.edu

**ewald@mpa-garching.mpg.de

The formation of black holes from neutron stars, iron cores or supermassive stars is expected to be associated with a characteristic gravitational wave signal which may give information about the collapse dynamics and the physical environment of such objects. Therefore, and given that gravitational wave detectors are already taking data or are coming online, it is of prime importance to understand the dynamical features of the gravitational collapse of hydrodynamical systems.

The prototypical model of stellar collapse is an equilibrium polytrope subject to a radial or quasi-radial perturbation growing on a dynamical timescale. In spherical symmetry, every general relativistic polytrope with index $N = 3$ is unstable to radial oscillations (Chandrasekhar 1964) – in turn, there exists a critical $N_c < 3$ for which the star is marginally stable. Without spherical symmetry, rotation can increase this critical value again, Fowler (1966). The black hole formation from the collapse of uniformly and differentially rotating polytropes induced by this instability is a well-investigated phenomenon, either with restriction to axisymmetry (Nakamura & Sato 1981; Stark & Piran 1985; Shibata 2000;2003;2003b; Shibata & Shapiro 2002; Sekiguchi & Shibata 2004) or without (Shibata, Baumgarte & Shapiro 2000; Duez, Shapiro & Yo 2004; Baiotti et al. 2005, Baiotti et al. 2005b). In the gauge choices usually employed, the dynamical behaviour of the system shows a radial contraction of the star, accompanied by the formation of an apparent horizon at late times.

Black hole formation from a dynamically unstable *nonaxisymmetric* mode, however, has not been modelled so far. In Newtonian theory, instabilities and fragmentation have received considerable attention, specifically in the context of binary formation from protostellar disks (e.g. Durisen et al. 1986, Tohline 1990; Bonnell & Bate 1994; Pickett, Durisen & Davies 1996; Banerjee, Pudritz & Holmes 2004 and references therein) and compact object production in stellar core collapse (e.g. Bonnell & Pringle 1995; Davies et al. 2002; Shibata & Sekiguchi 2004 and references therein).

The cooling evolution of supermassive stars can be approximately described by the $N = 3$ mass-shedding sequence when the angular momentum transport timescales are short compared to the cooling timescale, Baumgarte & Shapiro (1999), so that uniform rotation is enforced. This sequence has a turning point for the onset of a quasi-radial instability, and numerical experiments confirm that the collapse remains axisymmetric (Saijo et al. 2002). If the star is differentially rotating, the cooling sequence is less constrained and might end in a transition to nonaxisymmetric instability (Bodenheimer & Ostriker 1973; New & Shapiro 2001a,b). The canonical expectation that a supermassive star produces one central black hole with a low-mass accretion disk might thus not be appropriate for differentially rotating configurations.

In Zink et al. (2006) we have considered the production of a black hole through the fragmentation of a general relativistic polytrope. We focus on $N = 3$ polytropes, which are associated with pre-collapse cores of massive stars or supermassive stars. To represent this process accurately on a grid, we make use of an adaptive mesh refinement technique, since a possibly highly deformed apparent horizon needs to be located in some region of the domain which is unknown in advance.

2. Numerical Simulations

The recent investigation of the collapse of differentially rotating supermassive stars by Saijo (2004) was based on a sequence of relativistic $N = 3$ polytropes with a parameterized rotation law of the commonly used form $j(\Omega) = A^2(\Omega_c - \Omega)$, where Ω_c is the angular velocity at the center, and the parameter A specifies the degree of differential rotation ($A \rightarrow \infty$ is uniform rotation). The sequence selected was constrained by a constant central density $\rho_c = 3.38 \times 10^{-6}$ in units $K = G = c = 1$, and the choice $A/r_e = 1/3$, where r_e denotes the equatorial coordinate radius.

To examine the indirect collapse by fragmentation of a polytrope with toroidal shape, we choose a model with the same central density as in the Saijo (2004) models, but with a ratio of polar to equatorial coordinate radius $r_p/r_e = 0.24$. The ratio of rotational kinetic energy to gravitational binding energy is $T/|W| = 0.227$. While the critical limit for the dynamical f-mode instability in uniform density, uniformly rotating Maclaurin spheroids is $(T/|W|)_{\text{dyn}} = 0.2738$ (e.g. Tassoul 1978), recent investigations of the stability of soft ($N \sim 3$) differentially rotating polytropes in Newtonian gravity Centrella et al. 2001; Shibata, Karino & Eriguchi 2002;2003; Saijo 2003) have shown that the Maclaurin approximation is inappropriate for such systems, and generally find the critical $(T/|W|)_{\text{dyn}}$ to be below the Maclaurin value. Consequently, the toroid-like star considered in this study might be unstable to nonaxisymmetric perturbations. Here we present the first investigation of this instability in full general relativity, showing that relativistic effects are significant for the final outcome, as we observe that black holes can be produced.

All simulations have been performed in full general relativity. The only assumption on symmetry is a reflection invariance with respect to the equatorial plane of the star. The gauge freedom is fixed by the generalized 1+log slicing condition for the lapse function (Bona et al. 1995) with $f(\alpha) = 2/\alpha$, and by the hyperbolic-type condition suggested in Shibata (2003b) for the shift vector.

The computational framework is the *Cactus* code (www.cactuscode.org), which also provides a module to solve the geometric part of the field equations in the well-known BSSN form (Nakamura, Oohara & Kojima 1987, Shibata & Nakamura 1995, Baumgarte & Shapiro 1999). In addition, the *Carpet* driver (Schnetter, Hawley & Hawke 2004) is used for mesh refinement in *Cactus*. The hydrodynamics part of the field equations is evolved using the high-resolution shock-capturing PPM-Marquina implementation in the *Whisky* module (Baiotti et al. 2005), and a gamma law equation of state ($P = \rho\epsilon/N$).

To numerically construct the axisymmetric initial model described in the introduction, we use the *RNS* initial data solver (Stergioulas & Friedman 1995) with a radial resolution of 601 and an angular resolution of 301 points. With the parameters described above, the model has toroid-like structure, with an off-center density maximum, but a non-zero central density. After mapping the model to the hierarchy of Cartesian grids provided by *Carpet*, a small perturbation of the form

$$\rho(x) \rightarrow \rho(x) \left[1 + \frac{1}{\lambda r_e} \sum_{m=1}^4 \lambda_m B r \sin(m\phi) \right]$$

is applied with $\lambda_m = 0, 1$ and $\lambda = \sum_i \lambda_i$. In addition, the polytropic constant K is reduced by 0.1% to induce collapse if the model is radially unstable. After perturbing the model, the constraint equations are not solved again, since the amplitude B is chosen such that the violation of the constraints by the initial perturbation is about an order of magnitude smaller than that caused by the systematic error induced by the $m = 4$ symmetry of the Cartesian grid.

For most simulations, a fixed *box-in-box* mesh refinement with 5 levels is used to accurately resolve the central high-density ring. The three innermost grids cover the star, while the two outermost ones push the outer boundaries to $6.4r_e$. The typical resolution used was $65 \times 65 \times 33$ per grid patch, leading to a central resolution of $\delta_x \approx 10^{-2}r_e$. To determine the amplitude of a specific mode in the equatorial plane, we perform a projection onto Fourier modes at certain coordinate radii (New, Centrella & Tohline 2000; De Villiers & Hawley 2002).

Examining the amplitude of the Fourier modes during the evolution, it is evident that, initially, the $m = 4$ component induced by our Cartesian grid is dominant. However, the star is unstable to $m = 1$ and $m = 2$, and these modes consequently grow into the nonlinear regime, their e-folding times being rather close.

The rest mass is conserved numerically within 1.8%. An approximate measurement of the e-folding times and mode frequencies can be obtained within an error of 5 – 10% related to ambiguities in defining the interval of extraction. All setups show consistent results within this uncertainty. In units of the dynamical timescale, which is defined here as $t_D = r_e \sqrt{r_e/M}$, the e-folding times are $\approx 0.93t_D$ for $m = 1$, and $\approx 0.84t_D$ for $m = 2$, respectively. Mode frequencies are $\approx 3.05/t_D$ for $m = 1$ and $\approx 3.31/t_D$ for $m = 2$, respectively.

To establish whether a black hole is formed by a fragment it is necessary to cover the fragment with significantly more resolution than affordable by fixed mesh refinement. Hence we have implemented a simplified adaptive mesh refinement scheme to follow the system to black hole formation: In this scheme, a tracking function, here provided by the location of a density maximum, is used to construct a locally fixed hierarchy of grids moving with the fragment. Additional refinement levels are switched on during contraction, until an apparent horizon is found.

Since the e-folding times for $m = 1$ and $m = 2$ turn out to be close, the number and interaction behaviour of the fragments in the non-linear regime depend sensitively on the initial perturbation. The time evolution of the equatorial plane density for setup is shown in Fig 1. While the initial model is axisymmetric, it has already developed a strong $m = 1$ type deviation from axisymmetry at $t = 6.43t_D$, which consequently evolves into a collapsing off-center fragment. At $t = 7.45t_D$, we find an apparent horizon, using the numerical code described in Thornburg (2004). The horizon is centered on the collapsing fragment at a coordinate radius of $r_{AH} \approx 0.16r_e$, and has an irreducible mass of $M_{AH} \approx 0.24M_{star}$. Its coordinate representation is significantly deformed: its shape is close to ellipsoidal, with an axes ratio of $\sim 2 : 1.1 : 1$. The apparent horizon is covered by three refinement levels and 50 to 100 grid points along each axis.

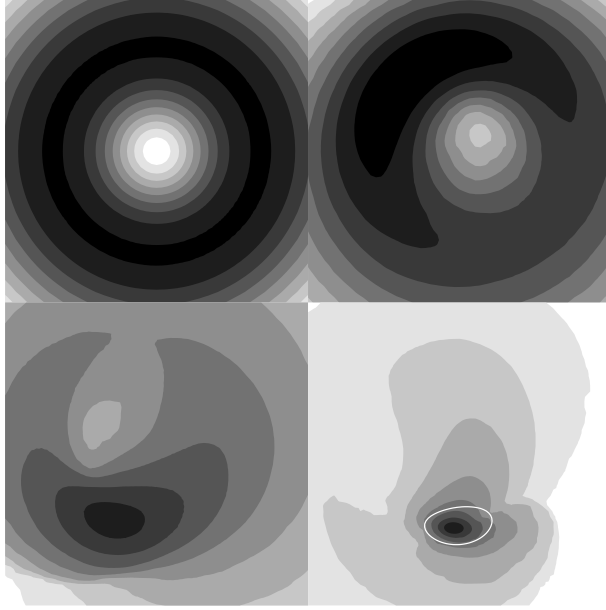


Figure 1: Time evolution of the equatorial plane density. Shown are isocontours of the logarithm of the rest-mass density. The four snapshots extend to $0.37r_e$ and are taken at $t/t_D = 0, 6.43, 7.14,$ and 7.45 , respectively. They show the formation and collapse of the fragment produced by the $m = 1$ instability. The last slice contains an apparent horizon demarked by the thick white line.

3. Discussion

The dynamics of a nonaxisymmetric single-star collapse of this type is significantly different from that of the quasi-radial cases usually investigated. From the often considered case of quasi-radial collapse, to bar formation and subsequent collapse, to fragmentation and fragment inspiral we have a range of possible dynamical scenarios, which may be connected to discernable observable features in their gravitational wave signature. In that sense, the evolution presented here can be considered as an example of such processes. For an extensive discussion of this work, see Zink et al. (2006b).

4. Acknowledgements

This work has been supported in part by the DFG SFB-TR7 on Gravitational Wave Astronomy, the IKYDA 2006/7 program and the ILIAS network.

References

Baiotti, L., Hawke, I., Montero, P., Löffler, F., Rezzolla, L., Stergioulas, N., Font, J.A., Seidel, E., 2005, Phys. Rev. D, 71, 024035

Baiotti, L., Hawke, I., Rezzolla, L., Schnetter, E., 2005b, *Phys. Rev. Lett.*, 94, 131101

Banerjee, R., Pudritz, R., Holmes, L., 2004, *MNRAS*, 355, 248

Baumgarte, T., Shapiro, S.L., 1999, *ApJ*, 526, 941

Baumgarte, T., Shapiro, S.L., 1999b, *Phys. Rev. D*, 59, 024007

Bodenheimer, P., Ostriker, J., 1973, *ApJ*, 180, 159

Bona, C., Massó, J., Seidel, E., Stela, J., 1995, *Phys. Rev. Lett.*, 75, 600

Bonnell, I., Bate, M., 1994, *MNRAS*, 271, 999

Bonnell, I., Pringle, J., 1995, *MNRAS*, 273, L12

Centrella, J., New, K., Nowe, L., Brown, D., 2001, *ApJ*, 550, L193

Chandrasekhar, S., 1964, *ApJ*, 140, 417

Davies, M., King, A., Rosswog, S., Wynn, G., 2002, *ApJ*, 579, L63

De Villiers, J., Hawley, J., 2002, *ApJ*, 577, 866

Duez, M., Shapiro, S., Yo, H., 2004, *Phys. Rev. D*, 69, 104016

Durisen, R., Gingold, R., Tohline, J., Boss, A., 1986, *ApJ*, 305, 281

Fowler, W., 1966, *ApJ*, 144, 180

Nakamura, T., Oohara, K., Kojima, Y., 1987, *Progr. Theoret. Phys. Suppl.*, 90, 1

Nakamura, T., Sato, H., 1981, *Progr. Theoret. Phys.*, 66, 2038

New, K., Centrella, J., Tohline, J., 2003, *Phys. Rev. D*, 62, 064019

New, K., Shapiro, S., 2001, *ApJ*, 548, 493

New, K., Shapiro, S., 2001b, *CQG*, 18, 3965

Pickett, B., Duisen, R., Davies, G., 1996, *ApJ*, 458, 714

Saijo, M., 2003, *ApJ*, 595, 352

Saijo, M., 2004, *ApJ*, 615, 866

Saijo, M., Baumgarte, T., Shapiro, S., Shibata, M., 2002, *ApJ*, 569, 349

Schnetter, E., Hawley, S., Hawke, I., 2004, *CQG*, 21, 1465

Sekiguchi, Y., Shibata, M., 2004, *Phys. Rev. D*, 70, 084005

Shibata, M., 2000, *Progr. Theoret. Phys.*, 104, 325

Shibata, M., 2003, *Phys. Rev. D*, 67, 024033

Shibata, M., 2003b, *ApJ*, 595, 992

Shibata, M., Baumgarte, T., and Shapiro, S.L., 2003, *Phys. Rev. D*, 61, 044012

Shibata, M., Karino, S., Eriguchi, Y., 2002, *MNRAS*, 334, L27

Shibata, M., Karino, S., Eriguchi, E., 2003, *MNRAS*, 343, 619

Shibata, M., Nakamura, T., 1995, *Phys. Rev. D*, 52, 5428

Shibata, M., Sekiguchi, Y., 2005, *Phys. Rev. D*, 71, 024014

Shibata, M., Shapiro, S.L., 2002, *ApJ*, 573, L39

Stark, R., Piran, T., 1985, *Phys. Rev. Lett.*, 55, 891

Stergioulas, N., Friedman, J.L., 1995, *ApJ*, 444, 306

Tassoul, J., 1978, *Theory of Rotating Stars*, Princeton Univ. Press

Thornburg, J., 2004, *CQG*, 21, 743

Tohline, J., 1990, *ApJ*, 361, 394

Zink, B., Stergioulas, N., Hawke, I., Ott, C., Schnetter, E., Müller, E., 2006, *Phys. Rev. Lett.*, 96, 161101

Zink, B., Stergioulas, N., Hawke, I., Ott, C., Schnetter, E., Müller, E., 2006b, *astro-ph/0611601*

GRAVITATIONAL WAVES FROM FIRST ORDER DIFFERENTIALLY ROTATING COMPACT STARS *

A. Passamonti¹ †, M. Bruni^{2,3}, L. Gualtieri⁴, A. Nagar⁵ and C. F. Sopuerta⁶

¹Department of Physics, Aristotle University of Thessaloniki,
Thessaloniki 54124, Greece

²Institute of Cosmology and Gravitation, University of Portsmouth,
Portsmouth PO1 2EG, UK

³Dipartimento di Fisica, Università degli Studi di Roma “Tor Vergata”,
00133 Roma, Italy

⁴Dipartimento di Fisica “G. Marconi”, Università di Roma “La Sapienza”,
00185 Roma, Italy

⁵Dipartimento di Fisica, Politecnico di Torino, Corso Duca degli Abruzzi 24,
10129 Torino, Italy

⁶Center for Gravitational Wave Physics, Penn State University,
University Park PA 16802, USA

Abstract

This is a report on the study of nonlinear effects arising from the coupling between radial and non-radial oscillations of static spherically-symmetric neutron stars. We focus on the case where the initial configuration is such that the linear axial perturbations are described by a harmonic component of a differentially rotating neutron star. We have set up a gauge-invariant formalism based on a multi-parameter perturbative framework and developed a computational scheme to evolve, in the time domain, the non-linear perturbations describing the coupling. The spectrum of the gravitational wave signal exhibits, due to the non-linear coupling, the same features as the one of the linear radial normal modes. In addition, we have observed the appearance of amplifications in the signal when one of the frequencies associated with the radial pulsations is close to the axial w -mode frequencies of the star.

1. Introduction

*Presented at the Workshop on *Cosmology and Gravitational Physics*, 15-16 December 2005, Thessaloniki, Greece, *Editors*: N.K. Spyrou, N. Stergioulas and C.G. Tsagas.

†passamonti@astro.auth.gr

Neutron stars can undergo oscillating phases during the dynamical evolution of various astrophysical scenarios, such as in a binary system due to the tidal force exerted by the companion during the coalescence, or in a protoneutron star after the core bounce due either to the bounce dynamics or to the fall-back accretion of material, which has not been expelled by the supernova shock. Gravitational radiation is one of the dissipative processes that damp the stellar oscillations carrying away important information about the physical properties of the sources. Several works have been dedicated to the understanding of the spectral properties and wave forms of gravitational waves emitted by neutron stars, e.g. [1, 2, 3, 4]. Stellar oscillations of compact stars generate high frequency gravitational waves, above 500 – 600 Hz, where the sensitivity curves of Earth-based laser interferometers (LIGO, VIRGO, GEO600 and TAMA [5]) are dominated by the laser shot noise. In order to increase the chances of detection, it is necessary to increase our theoretical understanding of the sources and provide more accurate templates of the gravitational wave signals.

Although strong non-linearities requires a fully numerical relativistic approach, the development of a nonlinear perturbative theory may help us to describe and interpret phenomena in mildly nonlinear regimes. To this end, we are investigating the coupling between radial and nonradial perturbations of compact stars, where for simplicity, the equilibrium configuration is taken to be a perfect-fluid spherically-symmetric star. Radial and nonradial oscillations are expected to be excited after a core bounce. Even though the quadrupole component provides the dominant contribution to the gravitational wave signal, the radial pulsations may store a considerable amount of kinetic energy and transfer a part of it, due to non-linear effects, to nonradial perturbations. As a result, this non-linear interaction may produce a damping of the radial pulsations and hence, an interesting gravitational wave signal. The strength of this signal naturally depends on the efficiency of the coupling, which is the effect we want to explore. To that end, we have developed a gauge-invariant perturbative formalism to study, in the time domain, the coupling between the radial pulsations and both polar [6] and axial [7] nonradial oscillations. We have used a relativistic multi-parameter perturbative scheme [9] that allows us to address consistently the gauge issues associated with nonlinear perturbations.

In what follows we outline the main results of our numerical simulations for the axial sector, where the linear axial perturbations describe a differentially rotating star (see [7, 8] for a complete description). Simulations for the polar sector are currently under way and their results will be presented in a forthcoming paper.

2. The Perturbative Framework

The structure of perturbative schemes uses to be hierarchical in the sense that the perturbations at a given order depend on the lower-order ones. In this section, we briefly describe the main ingredients of our framework, from the background configuration to the non-linear perturbations describing the coupling.

The equilibrium configuration of the star consist of a relativistic perfect-fluid spherically-symmetric matter distribution, which is determined by solving the Tolman–Oppenheimer–Volkoff equations for a polytropic equation of state $p = K\rho^\Gamma$, with

adiabatic index $\Gamma = 2$ and $k = 100 \text{ km}^2$. For a central mass energy density $\rho_c = 3 \times 10^{15} \text{ g cm}^{-3}$ one obtains $M = 1.26 M_\odot$ and $R = 8.862 \text{ km}$.

At first perturbative order, we have two independent classes of oscillations: i) the radial pulsations, which correspond to the $l = 0$ harmonic index and, ii) the axial nonradial perturbations with $l \geq 2$. The *radial* oscillations are completely described by two metric and two fluid perturbations subject to a set of three first-order evolution equations and two constraints, as there is a single radial degree of freedom. This structure allows us to set up a hyperbolic-elliptic formulation, where the Hamiltonian constraint is solved at any time step to obtain one of the metric perturbations. Our description of the *axial non-radial* oscillations consists of two equations: the axial master wave equation and a conservation equation. The former governs the dynamics of the only gauge-invariant metric variable of the axial sector Ψ^{NR} , which has the gravitational-wave content, while the latter governs the axial velocity perturbation β^{NR} . At first order, the stationary character of the axial velocity perturbation has allowed us to study separately the spacetime dynamical degree of freedom from the stationary part. In particular, the stationary solution describes the differential rotation induced on the background star by the l harmonic component of the velocity perturbation, and the related metric perturbation describes the dragging of the inertial frames.

The *axial* non-linear perturbations associated with the coupling are again described by a gauge-invariant metric perturbation Ψ^C and an axial velocity perturbation β^C . The difference with the linear case is that, in the stellar interior, they are governed by inhomogeneous equations, whose homogeneous part is the same as in the linear case, and the *source* terms are made out of products of first-order radial and axial non-radial perturbations. In the exterior we do not have matter fields and hence, the dynamics is described by Regge-Wheeler-type equations. Interior and exterior communicate through the junction conditions at the surface of the star.

In this setup we can study two differentiated initial configurations: i) a differentially rotating and radially pulsating star, ii) the scattering of a gravitational wave by a radially pulsating star. We will focus here on the former configuration since its dynamics exhibits more interesting features as the second one (see [8] for a detailed description of the two cases).

2.1 The Initial Data

The initial configuration for the radial pulsations consists of a selection of specific radial eigenmodes. We have chosen an origin of time such that the radial eigenmodes are described only by the eigenfunctions associated with the radial velocity perturbation, γ^R . To this end, we have first transformed the wave equation for this variable into a standard Sturm-Liouville problem. Then, we have solved the associated eigenvalue problem, by using a numerical code based on the relaxation method, so that the eigenfrequencies of the radial modes are determined with an accuracy better than 0.2 percent with respect to the values given in the literature. Our numerical evolutions of any initial radial eigenmode satisfy with high accuracy the Hamiltonian constraint and are long-term stable. The spectrum of the radial

perturbations, obtained from a Fast Fourier Transformation of the time evolution, reproduce the results in the literature with an accuracy to better than 0.2 percent.

The way we deal with the axial differential rotation is by expanding in vector harmonics the velocity perturbations and using the relativistic *j-constant* rotation law. Then, we just take the first component, $l = 3$, the one associated with the gravitational-wave emission. The initial profile for the axial velocity perturbations has two specifiable parameters: the *differential* parameter A and the angular velocity at the rotation axis Ω_c . The value for A has been chosen in order to have a smooth profile and a relatively high degree of differential rotation, as for high A the rotation tends to be uniform and then the $l = 3$ component vanishes. We have chosen an angular velocity that corresponds to a 10 *ms* rotation period at the axis of the star. For other values of the angular velocity, the linearity of the perturbative equations allows us to get the respective gravitational signal just by a re-scaling. In order to study the effects of the coupling between the linear perturbations we have prescribed vanishing initial data for the coupling non-linear perturbations.

3. Numerical results

Our numerical evolutions of a radially pulsating and differentially rotating star have shown an interesting new effect on the gravitational wave signal. The wave forms have the following properties: i) an excitation of the first w -mode at the early stage of the evolution. ii) A periodic signal which is driven by the radial pulsations through the source terms (see Fig. 2). This picture is confirmed by the spectra, where we have noticed that the radial normal modes are precisely mirrored in the gravitational signal at the non-linear perturbative order. On the other hand, the excitation of the w -mode at the early stages of the numerical simulations is an unphysical response of the system to the initial violation of the axial constraint equations for the coupling perturbations.

In Fig. 2, the wave forms of the axial master metric function Ψ^C exhibit an interesting amplification when the radial oscillations pulsate at frequencies close to the $l = 3$ axial spacetime w -mode, $\nu_w = 16.092$ kHz. For the stellar model under consideration this effect appears at the third and fourth radial overtones, whose frequencies are 13.545 kHz and 16.706 kHz respectively. It is worth emphasizing that this effect takes place despite the energy of the radial modes and the maximum radial displacement of the surface decrease proportionally to the magnitude of the radial oscillations (see Table 1). We can interpret this amplification as a resonance effect between the radial frequencies of the source, which behave as the forcing agent, and the natural frequencies of the axial master wave-like equation.

Our perturbative approach does not include backreaction, that is, it does not account for the damping of the radial oscillations or the slowing down of the stellar rotation due to contribution of the non-linear coupling to the energy loss in gravitational waves. Backreaction could be studied by looking at higher perturbative orders, which may be computationally demanding. However, we can provide a rough estimate of the damping time of the radial pulsations by assuming that the energy

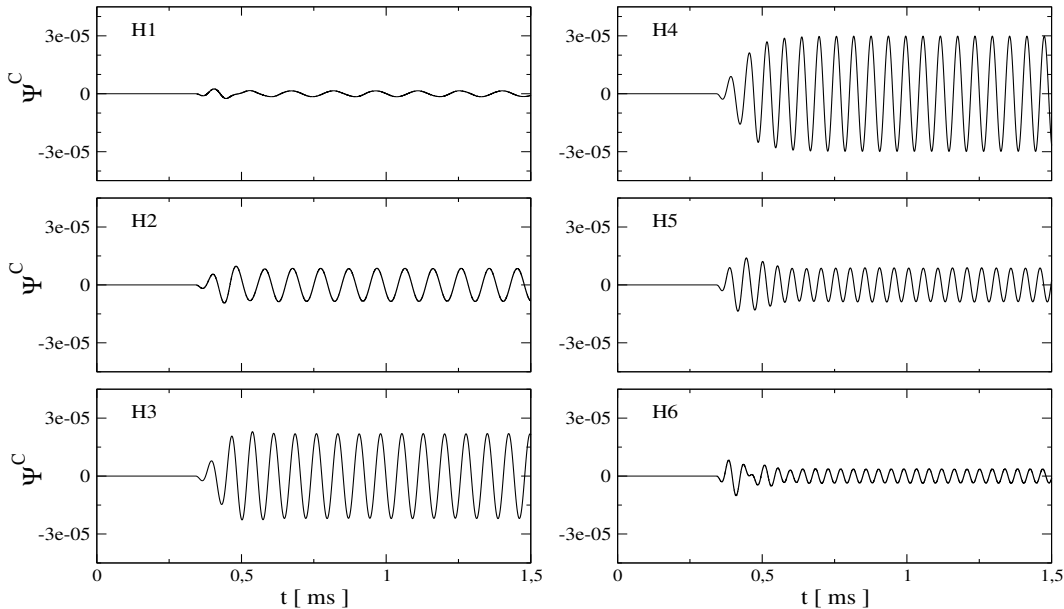


Figure 2: Comparison of six Ψ^C waveforms, in km , for the $l = 3$ multipole. The radial pulsations considered correspond to single-mode oscillations from the H1 to the H6 overtone. These plots show that a resonance effect takes place in Ψ^C . See the text for a discussion.

emitted is completely supplied by the first-order radial oscillations, and that the power radiated in gravitational waves is constant in time. In this way, the damping time is given by the following expression:

$$\tau_{lm}^C \equiv \frac{E_n^R}{\langle \dot{E}_{lm}^C \rangle}, \quad (1)$$

where E_n^R is the energy of a radial eigenmode (see Table 1), and $\langle \dot{E}_{lm}^C \rangle$ is the averaged value of the non-linear coupling contribution to the power emitted. The results for τ_{30}^C are shown in Table 1. Moreover, in the last row of Table 1 we give an estimation of the damping of the radial pulsations associated with a certain radial eigenmode in terms of the number of oscillation cycles:

$$N_{\text{osc}} = \frac{\tau_{lm}^C}{T_n}, \quad (2)$$

where $T_n = \nu_n^{-1}$, with ν_n being the eigenfrequency of the radial eigenmode. It is interesting to mention that the number of oscillations required for the damping of the H4 mode is only 12, and hence it would already affect the H4-waveform shown in Figure 2. This is not surprising, and shows that the coupling near resonances is a very effective mechanism for extracting energy from the radial oscillations.

In this sense, it is important to remark that a possible detection of such gravitational-wave signals may provide new information about the parameters that determine the stellar structure, since the second-order gravitational-wave spectrum reproduce the

Radial Mode	Frequency [kHz]	E_n^R [10^{-8} km]	ξ_{sf}^R [m]	$\langle \dot{E}_{30}^C \rangle$ [10^{-14}]	τ_{30}^C [ms]	N_{osc}
F	2.138	35.9	12.65	1.54×10^{-6}	7.78×10^{10}	1.67×10^{11}
H1	6.862	4.2	4.02	5.69×10^{-2}	24.59×10^4	1.69×10^6
H2	10.302	1.37	2.66	4.04	11.29×10^2	1.16×10^4
H3	13.545	0.62	2.02	46.69	44.28	5.99×10^2
H4	16.706	0.34	1.64	130.84	8.64	1.44×10^2
H5	19.823	0.21	1.38	15.90	44.04	8.73×10^2
H6	22.914	0.14	1.19	3.71	126.12	2.89×10^3

Table 1: Quantities associated with radial normal modes and their coupling to the first-order axial differential rotation: Energy, E_n^R , and maximum stellar surface displacement ξ_{sf}^R of the radial eigenmodes for initial conditions (Sec.) with velocity amplitude 0.001; average power, $\langle \dot{E}_{30}^C \rangle$, emitted in gravitational waves to infinity from the coupling between the radial eigenmode and the axial differential rotation; estimated values of the damping times, τ_{30}^C ; and number of oscillation periods, N_{osc} , that takes for the non-linear oscillations to radiate the total energy initially contained in the radial modes.

properties of the radial modes of a non-rotating star, which can be easily determined for a large class of equations of state.

Acknowledgements.

A.P. work is supported by a ‘‘VESF’’ grant. M.B. work was partially funded by MIUR (Italy). C.F.S. acknowledges the support of the Center for Gravitational Wave Physics funded by the National Science Foundation under Cooperative Agreement No. PHY-0114375, and partial support from NSF Grant No. PHY-0244788 to Penn State University.

References

- [1] Andersson, N., 2003, *Class. Quant. Grav.*,
- [2] Kokkotas, K. D.Schmidt, B. G, 1999, *Living Rev. Rel.*, 2, 2.
- [3] Stergioulas, N., 2003, *Living Rev. Rel.*, 6, 3.
- [4] Font, J. A., 2003, *Living Rev. Rel.*, 6, 4. 20, R105.
- [5] www.ligo.caltech.edu, www.virgo.infn.it, www.geo600.uni-hannover.de, tamago.mtk.nao.ac.jp, igec.lnl.infn.it.
- [6] Passamonti, A., Bruni, M., Gualtieri, L., Sopuerta, C. F., 2005, *Phys. Rev. D*, 71, 024022.

- [7] Passamonti, A., Bruni, M., Gualtieri, L., Nagar, A., Sopena, C. F., 2006, Phys. Rev. D, 73, 084010.
- [8] Passamonti, A., 2006, PhD Thesis, ICG, Portsmouth University.
- [9] Sopena, C. F., Bruni, M., Gualtieri, L., 2004, Phys. Rev. D, 70, 064002.

GRAVITATIONAL WAVES FROM INTERACTIONS BETWEEN WHITE DWARFS AND BLACK HOLES *

A. Stavridis¹ †C. Casalvieri² ‡& V. Ferrari² §

¹ Section of Astronomy and Astrophysics,
Department of Physics, Aristotle University of Thessaloniki,
54 124, Thessaloniki, Greece

² Dipartimento di Fisica “G.Marconi”,
Università di Roma “La Sapienza” and Sezione INFN ROMA1, piazzale Aldo Moro 2,
I-00185 Roma, Italy

Abstract

In this contribution we present a computation of the gravitational signal emitted when a white dwarf moves around a black hole on a closed or open orbit using the affine model approach. We compare the orbital and the tidal contributions to the signal, assuming that the star moves in a safe region where, although very close to the black hole, the strength of the tidal interaction is insufficient to provoke the stellar disruption. We show that for all considered orbits the tidal signal presents sharp peaks corresponding to the excitation of the star non radial oscillation modes, the amplitude of which depends on how deep the star penetrates the black hole tidal radius and on the type of orbit. Further structure is added to the emitted signal by the coupling between the orbital and the tidal motion.

1. Introduction

Recent astronomical observations have shown evidence of interactive processes in action between stars and black holes. The ESO Very Large Telescope (VLT) has observed stars that move on very elliptic orbits around the supermassive black hole at the center of our Galaxy (Schodel et al. 2004), and X-ray satellite CHANDRA has monitored the event of a star disrupted and swollen by the giant black hole at the center of the galaxy RXJ1242-11 (Komossa et al. 2004). These and similar phenomena that take place around black holes generate gravitational waves essentially because of two mechanisms: one related to the time variation of the quadrupole moment of the system star-black hole due to the orbital motion, the second to the quadrupole moment of the star which changes in time because the star is deformed by the tidal

*Presented at the Workshop on *Cosmology and Gravitational Physics*, 15-16 December 2005, Thessaloniki, Greece, *Editors*: N.K. Spyrou, N. Stergioulas and C.G. Tsagas.

†astavrid@astro.auth.gr

‡casalvie@roma1.infn.it

§valeria@roma1.infn.it

interaction with the black hole. The orbital contribution has been computed using the Post-Newtonian formalisms (see for instance Blanchet, 2002 and references therein). We focused on the second mechanism: we considered a white dwarf (WD) moving on assigned orbits around a black hole (BH), we computed how the stellar shape and structure change along its motion and the gravitational wave (GW) signal emitted due to this time-varying deformation.

The problem of tidal deformation has been widely investigated both in newtonian gravity and in general relativity, using different approaches.

In 1977 Press and Teukolsky studied the formation of binary systems by two-body tidal capture using a perturbative approach and provided estimates of the amount of orbital energy absorbed in the encounter (Press & Teukolsky, 1977).

In the early eighties a formalism was developed (Carter & Luminet, 1982; 1983; 1985) that allows to compute the tidal deformation by integrating a set of equations which describe the motion of an element of stellar fluid due to the effect of the tidal tensor of the other massive body, on the assumption that while deforming the star maintains an ellipsoidal form (affine model). This approach, initially developed in the framework of Newtonian gravity, was subsequently generalized to general relativity when one of the interacting bodies is a Schwarzschild or a Kerr black hole (Marck, 1983; Luminet & Marck, 1985). The affine model has been used in several papers addressing some relevant astrophysical problems: in Luminet & Carter (1986), Luminet & Pichon (1989), Bicknell & Gingold (1983), the authors investigated whether, in the interaction with a massive companion, a main sequence (MS) star can be compressed to such an extent that the temperature increase in the core can ignite a detonation of the nuclear fuel (a process which may occur in active galactic nuclei having a central massive black hole); the tidal capture of a main sequence star and its disruption have been investigated in Carter (1992) and in Kochanek (1992), respectively; tidal processes occurring in neutron star-neutron star coalescing binaries before contact has been investigated in Kochanek (1992), where the phase shift induced on the emitted gravitational signal has also been computed; the chemical and mechanical behaviour of a WD passing inside the tidal radius of a black hole has been studied in Luminet & Pichon (1989) furthermore, the affine model has also been used in Kosovichev & Novikov (1992) and in Diener et al. (1997) to study the tidal capture and interaction of a star and a massive BH.

Tidal effects in close compact binaries have also been studied using different formalisms; for instance, by integrating the hydrodynamical equations in 3D, in a form adapted to express the evolution of the star principal axes and of other relevant quantities, and including radiation reaction and viscous dissipation Lai, Rasio & Shapiro (1993; 1994a,b), Lai & Shapiro (1995), Rasio & Shapiro (1995). An alternative approach to the integration of the 3D-hydrodynamical equations has been used in Frolov et al. (1984), to study disruptive and non disruptive encounters between white dwarfs and black holes, focusing on the determination of the periastron distance, time delay, relativistic precession and tidal forces.

Further studies on tidal interactions in close binaries are in Evans & Kochanek (1989), Novikov, Pethick & Polnarev (1992), Laguna et al. (1993), Khokhlov, Novikov & Pethick (1993a,b), Gualtieri et al. (2002), Ivanov & Novikov (2001), Marck, Lioure & Bonazzola (1996), Pons et al. (2002), Shibata & Uryu (2001), Ferrari, D'Andrea & Berti (2000), Fryer et al. (1999), Gomboc & Cadez (2005), Ivanov, Chernyakova & Novikov (2003), Diener et al. (1997) Berti & Ferrari (2001), Ogawaguchi & Kojima (1996).

In this work we used the Carter-Luminet approach to study the tidal interaction of a white

dwarf and a black hole, with the purpose of computing the gravitational signal emitted in this process. We integrated the Carter-Luminet equations for open and closed orbits choosing a white dwarf mass $M_* = 1 M_\odot$ and a black hole mass $M_{BH} = 10 M_\odot$. The WD was modeled using a polytropic equation of state (EOS) with adiabatic index $\gamma = 5/3$. The gravitational radiation was computed by using the quadrupole approach and the orbital and the tidal contributions were compared. We further discussed how the results changed for higher values of the black hole mass.

Our study is based on several simplifying assumptions:

- The WD mass is assumed to be much smaller than the black hole mass.
- The black hole does not rotate and the equations of motion of the star, its internal structure and the black hole tidal tensor are computed using the equations of newtonian gravity; thus, we call “black hole” an object which is basically a point mass star. We plan to extend our calculations to general relativity and to rotating black holes in the near future.
- We neglect tidal effects on the orbital motion.
- We neglect viscous effects, an hypothesis which appears to be justified in the case of WD-BH binaries (Wiggins & Lai, 2000).

2. The model equations

As mentioned in the introduction, the equations we use to describe the tidal deformation of the star are fully Newtonian, and are fully described in Casalvieri et. al. 2006. The gravitational wave signal emitted by the system will be computed by using the quadrupole formalism in the TT-gauge. We give in Table 1 the limiting values of the penetration factor β .

Table 1: The limiting value of β above which the tidal interaction between the white dwarf and the black hole becomes disruptive is given for the orbits considered in this paper.

Orbit	e	β_{crit}
Circular	0	0.78
Parabolic	1	1.05
Elliptic	0.25	0.78
	0.75	0.97
	0.95	1.03

3. Results

3.1 Circular orbits

When the orbit is circular, the orbital contribution to the gravitational signal is

$$h_+^{orb}(t) = ih_\times^{orb}(t) = A \frac{\cos(2\omega_{orb}t)}{r}, \quad (1)$$

where $\omega_{orb} = \left(\frac{GM}{D^3}\right)^{1/2}$ is the Keplerian angular velocity, D being the separation between the two bodies, r is the radial distance from the source, and

$$A = \frac{4G^2 M \mu}{c^4}, \quad (2)$$

where $M = M_* + M_{BH}$ is the total mass and $\mu = \frac{M_* M_{BH}}{M}$ is the reduced mass of the system. Thus, radiation is emitted in a single spectral line at a frequency $\nu_{orb} = \frac{\omega_{orb}}{2\pi}$, i.e.

$$h_+^{orb}(\nu) = \frac{1}{r} \frac{A}{4\pi} [\delta(\nu - 2\nu_{orb}) - \delta(\nu + 2\nu_{orb})]. \quad (3)$$

Due to gravitational emission the orbit decays; thus the signal we compute using eqs. (1) may not be correct, unless the changes induced on the orbit by the energy lost in GW occur on a timescale much longer than the orbital period, so that we can neglect radiation reaction effects. To check whether this is the case for the orbits we consider, we have computed the adiabatic timescale τ

$$\tau \sim \frac{E_{orb}}{L_{GW}}, \quad (4)$$

where $E_{orb} = -\frac{1}{2} \frac{GM\mu}{D}$ is the system orbital energy, and $L_{GW} \equiv \frac{dE_{GW}}{dt}$ is the GW-luminosity due to the time variation of the orbital quadrupole moment

$$L_{GW} = \frac{32 G^4 \mu^2 M^3}{5 c^5 D^5}.$$

The results of our calculations on the tidal interaction are summarized in figure 1.

In the left panel of figure 1 we plot the Fourier transform of the tidal signal $h_+^{def}(\nu)$ for $\beta = 0.4$. The plot shows a number of very sharp peaks. The first is at $\nu = 2\nu_{orb}$, and it is a signature of the orbital motion on the tidal deformation of the star. The highest peak is at a frequency $\nu_f = 0.146$ Hz, which is the frequency of the fundamental mode of the non radial oscillations of the star in the unperturbed configuration (i.e. when it has a spherical form). This peak is surrounded by equally spaced peaks, at frequencies $\nu = \nu_f \pm 2n\nu_{orb}$, $n = 1, 2, \dots$, due to the coupling of the orbital motion to the deformation. In addition, we also see smaller peaks at the frequencies of the first pressure mode, $\nu_{p1} = 0.316$, and further harmonics $\nu = \nu_{p1} \pm 2n\nu_{orb}$. This picture clearly shows that the non radial modes of oscillations of the star are excited in the tidal interaction and their signature appears in the gravitational wave spectrum.

The plot for $h_\times^{def}(\nu)$ is entirely similar and will not be shown.

In the right panel of figure 1 we show $h_+^{def}(\nu)$ for increasing values of β (i.e. for decreasing orbital radii); we see that, as β increases and the orbit shrinks, the $2\nu_{orb}$ -peak shifts toward higher frequencies, but the peaks corresponding to the excitation of the **f**- and **p**-modes, of course, do not move. Moreover, due to the change of ν_{orb} the spacing between the harmonics changes as well.

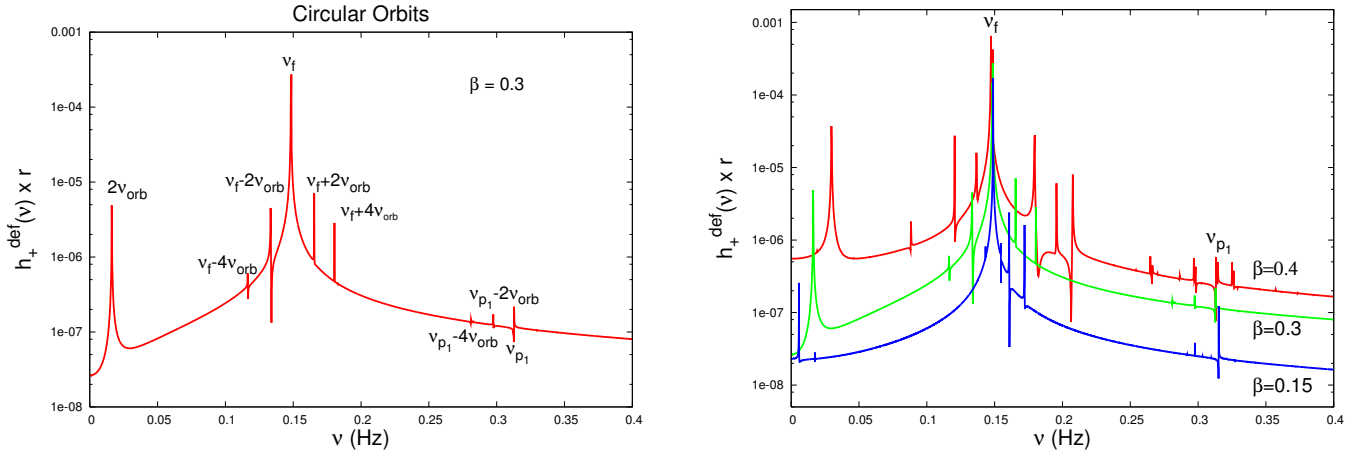


Figure 1: The Fourier transform of the GW signal associated to the tidal interaction between a $1 M_{\odot}$ WD and a $10 M_{\odot}$ BH is plotted as a function of frequency for a circular orbit with $\beta = 0.3$ (up) and for different values of β (down). The main peak at $\nu_f = 0.146$ Hz corresponds to the frequency of the fundamental mode of the non radial oscillations of the star, a smaller peak at $\nu = 0.316$ Hz indicates the excitation of the first **p**-mode. The remaining harmonics are due to the coupling between orbital and tidal motion (see text).

3.2 Elliptic orbits

Whereas for a circular orbit radiation is emitted in a single spectral line at twice the orbital frequency, when the orbit is eccentric waves are emitted at frequencies multiple of ν_{orb} , and the number of equally spaced spectral lines increases with the eccentricity. In the left panel of figure 2 we compare the orbital (up) and the tidal (down) signal emitted on an orbit with $\beta = 0.4$ and $e = 0.75$.

As in the circular case, the excitation of the **f**- and **p**₁-modes is manifested by the sharp peaks at the corresponding frequencies, and it is interesting to see that the coupling between the orbital and tidal motion introduces a large number of harmonics. Note also that the maximum of the orbital signal is much larger than the **f**-mode peak in tidal signal.

In the right panel of figure 2 we show how the structure of the tidal signal changes due to eccentricity, plotting $h_+^{def}(\nu)$ for $\beta = 0.4$ and for two values of e , (upper panel): as expected, we see that lower eccentricities correspond to a smaller number of spectral lines due to the orbital-tidal coupling. In the same figure (lower panel) we compare the tidal signal emitted on orbits with the same eccentricity ($e = 0.75$) and different values of β , showing how the mode excitation is sensitive to the penetration parameter.

3.3 Parabolic orbits

The interesting example of parabolic orbits is when the star penetrates deeply into the black hole tidal radius, $\beta > 1$, but lower than the tidal disruption limit. In this case the star is highly deformed and assumes a “cigar” like shape. This cigar also oscillates and it’s eigenfrequencies

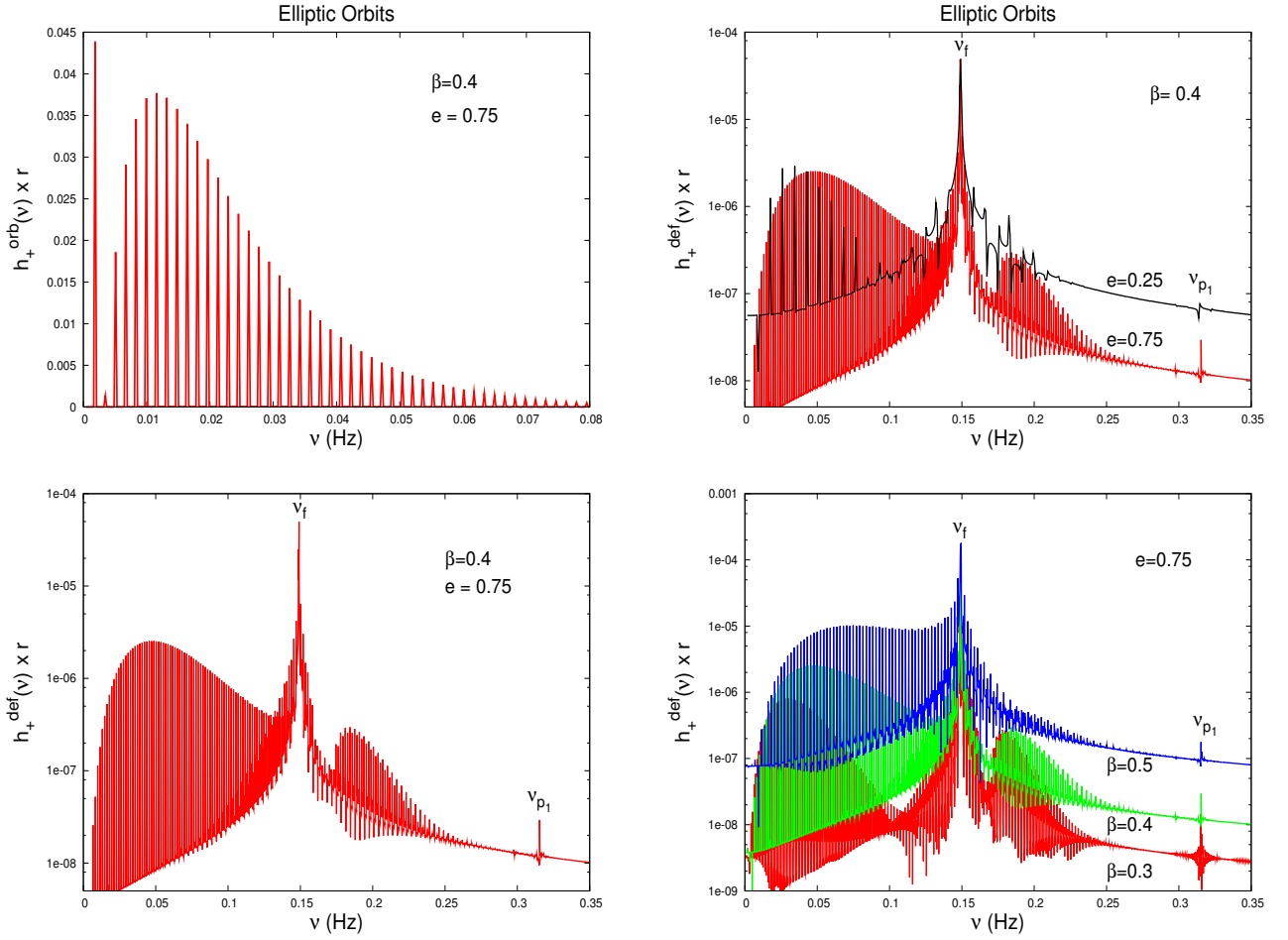


Figure 2: In the left panel we plot the Fourier transform of the orbital signal (up) and of the tidal signal (down) emitted by the WD-BH binary studied in this paper when the orbit is an ellipse with $\beta = 0.4$ and $e = 0.75$. As in the circular case, the main peak in h_+^{def} corresponds to the excitation of the **f**-mode, but its amplitude is much lower than that of the maximum in h_+^{orb} . In the right panel we show the tidal signal for elliptical orbits with β assigned and varying e (up), and with e assigned and varying β (down).

scale as the inverse of its length, for a fixed mass. In figure 3 we show the signal for e different $\beta = 1, 1.03, 1.05$.

Indeed the tidal signal presents a very interesting structure shown in figure 3. In the three panels on the left we show $h_+^{def}(\nu)$ for $\beta = 1, 1.03, 1.05$. We see that there is a dominant peak which corresponds to the excitation of the fundamental mode of the cigar; indeed, as expected, when β increases the tidal interaction is stronger, the star assumes a more elongated cigar shape and the frequency of the main peak decreases. The spectrum also shows several equally spaced spectral lines and their origin can be understood by looking at the right panel of figure 3, where we plot the principal axes of the star as functions of time. When the star approaches the black hole, one of the axes on the equatorial plane - let us name it 'a' - grows much more than the other two, 'b' and 'c'. In the figure the axes are normalized to their initial values, therefore at large distance (large negative time) they are all equal to 1 since the star is spherical. Analysing

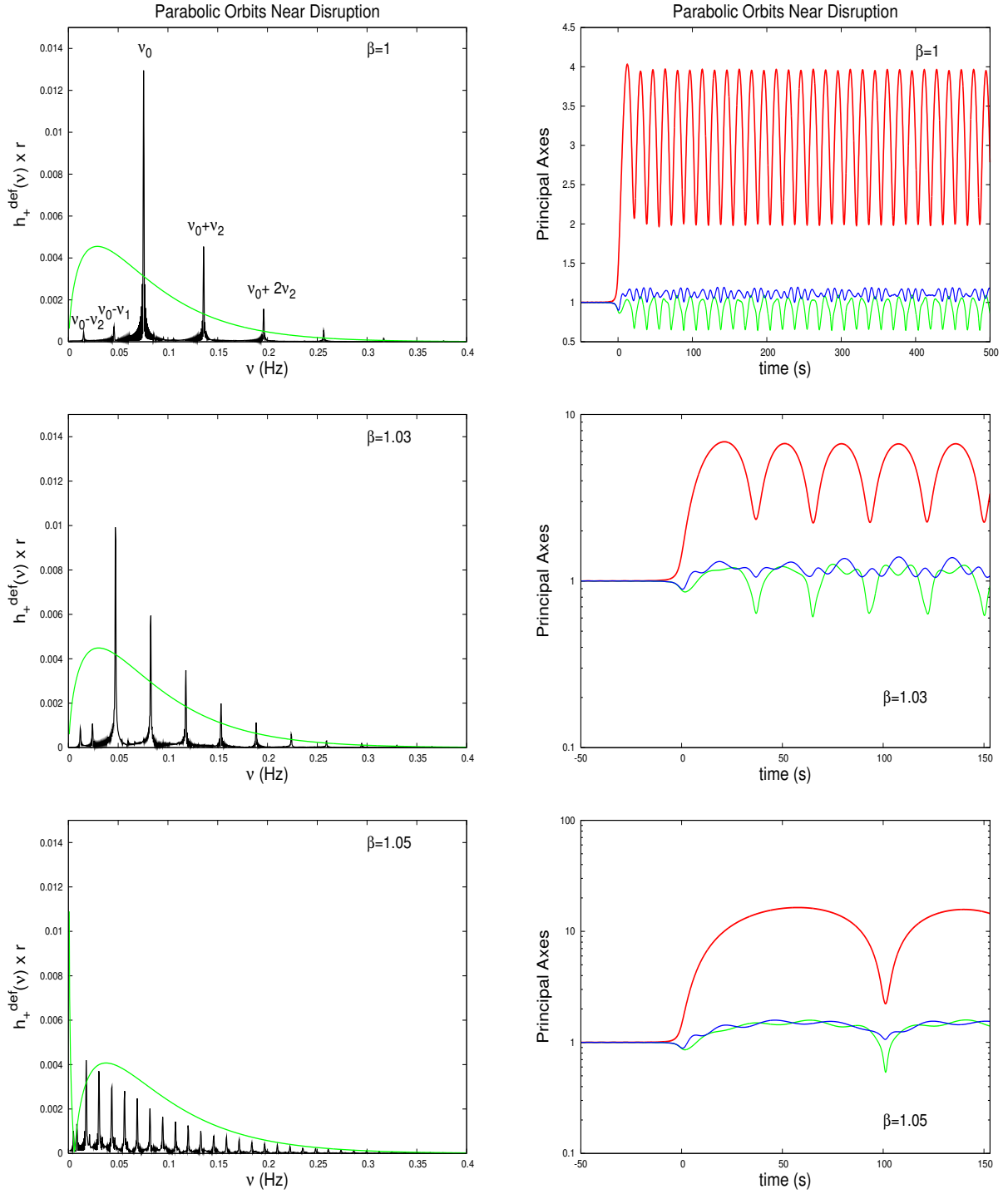


Figure 3: The tidal signal emitted in a parabolic orbit is plotted for three values of β approaching the critical value (left panel). The green continuous line is the orbital signal, plotted for comparison. On the right panel we show the behaviour of the principal axes of the star as a function of time, when the star passes through the periastron. The relation between the axes behaviour and the emitted signal, and the origin of different peaks in h^{def} are explained in the text.

the axes behaviour, we can identify two characteristic frequencies: one, ν_1 , which corresponds to the first oscillation, when the a-axis starts to grow, reaches the maximum elongation, and then decreases to the value about which it will oscillate in the new, approximately Riemannian, stationary configuration; the second one, ν_2 , corresponds to the oscillation of the a-axis about the new configuration.

4 Conclusions

We have computed the gravitational signal emitted when a white dwarf moves around a black hole on a closed or open orbit. We have computed both the orbital and the tidal contributions and compared the two, assuming that the star is close to the black hole, but in a region safe enough to prevent its tidal disruption. In all cases, the non radial oscillation modes of the star are excited (in our approach we do not include the dynamical behaviour of the black hole) to an extent which depends on how deep in the tidal radius the star penetrates and on the type of orbit. The orbital, h^{orb} , and the tidal, h^{def} , contributions are emitted at different frequencies: smaller for h^{orb} , higher for h^{def} .

The system we have analyzed in detail is composed of a $1 M_\odot$ white dwarf and a $10 M_\odot$ black hole. In this case we find that for circular orbits up to the critical one, the amplitude of the single spectral line in h^{orb} is always smaller than that of the **f**-mode peak in h^{def} ; however if the black hole mass is larger, the situation reverses, since h^{def} is nearly independent of M_{BH} , while h^{orb} is proportional to it. It is interesting to note that h^{def} contains several peaks that shows the coupling between the orbital and tidal motion.

When the orbit is elliptic, h^{orb} shows several spectral lines emitted at multiples of the orbital frequency; h^{def} has again a main peak at the **f**-mode frequency, and in addition a number of peaks due to the orbital-tidal interaction, that contain a signature of the nature of the orbit. The amplitude of the **f**-mode peak of course increases with the penetration factor β and also, for a fixed β , with the eccentricity; for the system we have considered this amplitude tends to that of the maximum of h^{orb} for very elongated orbits ($e > 0.95$). Again changing the black hole mass to a higher value the orbital contribution increases with respect to the tidal one.

For parabolic orbits the situation is very interesting, since the star can penetrate more deeply into the tidal radius, allowing for larger values of β . As β tends to the critical value the star assumes a very elongated, cigar-like shape, deviating considerably by its initial spherical structure. Thus the main peak in h^{def} shifts toward lower frequencies, since the **f**-mode frequency scales as the inverse of the length of the principal axis. The harmonics which appear in the tidal signal correspond to the oscillation frequencies of the principal axis of the ‘cigar’, and the larger is β the higher will be the number of excited harmonics. A comparison with the behaviour of the orbital signal (see figure 3) shows that if $\beta < 1.03$ the tidal signal is considerably higher than h^{orb} if $M_{BH} = 10 M_\odot$, but again the situation reverses if the black hole mass is sufficiently higher.

The results of our study show that the tidal signals emitted by a close encounter between a white dwarf and a black hole lay in a frequency region which is intermediate between the sensitivity region of LISA ($10^{-4} - 10^{-1}$ Hz) and that of ground-based interferometers VIRGO, LIGO, GEO, TAMA, sensitive above ~ 10 Hz. Detectors that fill this gap have recently been proposed, like the Big Bang Observatory, thought as follow on mission to LISA (Bender et

al. 2005), and DECIGO, proposed by (Seto, Kawamura & Nakamura, 2001) they should both be extremely sensitive in the decihertz region $10^{-1} - 1$ Hz, and would be the appropriate instruments to detect the tidal signals we have studied and to shed light on the dynamics of dense stellar clusters where these processes are more likely to occur.

Acknowledgements.

We would like to thank L. Rezzolla for introducing us to the literature on the subject, and L. Gualtieri for useful conversations and fruitful insights in various aspects of the work.

References

- C. Casalvieri, V. Ferrari, A. Stavridis, 2006, MNRAS, 365, 929
Bender P.L., Armitage P.J., Begelman M.C., Perna R., iper submitted to the NASA SEU Roadmap Committee
Berti E., Ferrari V., 2001, Phys. Rev. D, 63, 064031
Bicknell G.V., Gingold R.A., 1983, ApJ, 273, 749
Blanchet, L., Living Reviews of Relativity, lrr-2002-3, (<http://www.livingreviews.org/>) 2002
Carter B., 1992, ApJ, 391, L67
Carter B., Luminet J.P., 1982, Nature, 296, 211
Carter B., Luminet J.P., 1983, A&A, 121, 97
Carter B., Luminet J.P., 1985, MNRAS, 212, 23
Diener P., Kosovichev A.G., Kotok E.V., Novikov I.D., Pethick C.J., 1995, MNRAS, 275, 498
Diener P., Frolov V.P., Khokhlov A.M., Novikov I.D., Pethick C.J., 1997, ApJ, 479, 164
Evans C.R., Kochanek C.S., 1989, ApJ, 346, 13
Ferrari V., D'Andrea M., Berti E., 2000, Int. J. Mod. Phys. D, 9 n. 5, 495
Frolov V.P., Khokhlov A.M., Novikov I.D., Pethick C.J., 1984, ApJ, 432, 680
Fryer C.L., Woosley S.E., Herant M., Davies M.B., 1999, ApJ, 520, issue 2, 650
Gomboc A., Cadez A., 2005, ApJ, 625, 278
Gualtieri L., Berti E., Pons J.A., Miniutti G., Ferrari V., 2002, Phys. Rev. D, 64, 104007
Ivanov P.B., Novikov I.D., 2001, ApJ, 549, 467
Ivanov P.B., Chernyakova M.A., Novikov I.D., 2003, MNRAS, 338, 147
Khokhlov A., Novikov I.D., Pethick C.J., 1993a, ApJ, 418, 163
Khokhlov A., Novikov I.D., Pethick C.J., 1993b, ApJ, 418, 181
Kochanek C.S., 1992, ApJ, 385, 604
Kochanek C.S., 1992, ApJ, 398, 234
Komossa S., Halpern J., Schartel N., Hasinger G., Santos-Lleo M., Predehl P., 2004, ApJ, 603, L17
Kosovichev A.G., Novikov I.D., 1992, MNRAS, 258, 715
Laguna P., Miller W.A., Zurek W.H., Davies M.B., 1993, ApJ, 410, 83
Lai D., Rasio F.A., Shapiro S.L., 1993, ApJ Suppl., 88, 205
Lai D., Rasio F.A., Shapiro S.L., 1994a, ApJ, 423, 344
Lai D., Rasio F.A., Shapiro S.L., 1994b, ApJ, 437, 742

Lai D., Shapiro S.L., 1995, ApJ, 443, 701
Luminet J.P., Marck J.-A., 1985, MNRAS, 212, 57
Luminet J.P., Carter B., 1986, ApJ, 61, 219
Luminet J.P., Pichon B., 1989, A&A, 209, 85
Luminet J.P., Pichon B., 1989, A&A, 209, 103
Marck J.-A., 1983, Proc. R. Soc. of London, 385, 431
Marck J.-A., Lioure A., Bonazzola S., 1996, A&A, 306, 666
Novikov I.D., Pethick C.J., Polnarev A.G., 1992, MNRAS, 255, 27
Ogawaguchi W., Kojima Y., 1996, Prog. Theor. Phys., 96, 901
Peters P.C., Mathews J., 1963, Phys. Rev. 131, 435
Pons J.A., Berti E., Gualtieri L., Miniutti G., Ferrari V., 2002, Phys. Rev. D, 65, 104021
Press W.H., Teukolsky S.A., 1977, ApJ, 213, 183
Rasio F.A., Shapiro S.L., 1995, ApJ, 438, 887
Schodel R., Ott T., Genzel R., Hofmann R., Lehnert M., Eckart A., Mouawad N., Alexander
T., Reid M.J., Lenzen R., Hartung M., Lacombe F., Rouan D., Gendron E., Rousset G.,
Lagrange A.M., Brandner W., Ageorges N., Lidman C., Moorwood A.F.M., Spyromillio J.,
Hubin N., Menten K.M., 2002, Nature, 419, 694
Shibata M., Uryu K., 2001, Phys. Rev. D, 64, 104017
Seto N., Kawamura S., Nakamura T., 2001, Phys. Rev. Lett, 87, 221103
Wiggins P., Lai D., 2000, ApJ, 532, 530

WELL-POSED CONSTRAINED EVOLUTION OF 3+1 FORMULATIONS OF GENERAL RELATIVITY *

V. Paschalidis

[†]Department of Astronomy and Astrophysics, The University of Chicago,
5640 S Ellis Ave., Chicago IL 60637, U.S.A.

Abstract

In this work we present an analysis of well-posedness of constrained evolution of 3+1 formulations of GR. In this analysis we explicitly take into account the energy and momentum constraints as well as possible algebraic constraints on the evolution of high-frequency perturbations of solutions of Einstein's equations. Our study reveals the existence of subsets of the linearized Einstein's equations that control the well-posedness of constrained evolution. We argue that the posedness of the Einstein equations depends entirely on the properties of the gauge. For certain classes of gauges we formulate conditions for well-posedness of constrained evolution.

1. Introduction

A long-standing problem in numerical relativity is the achievement of long-term stable numerical integration of Einstein's equations. At present, this is possible for rather short times or for special symmetric cases. Complex problems of GR, such as general collision or internal structure of black holes (BH) cannot not be solved, possibly due to ill-posedness or intrinsic instability of existing 3+1 formulations, Shibata & Nakamura (1995), Baumgarte & Shapiro (1999), Laguna (1999), Kidder, Scheel & Teukolsky (2001), Yoneda & Shinkai (2003).

Well-posedness, Heinz-O. Kreiss & Jenz Lorenz (1989), of free evolution of 3+1 formulations has been analysed in Alcubierre et. al. (2000) and Yoneda & Shinkai (2003). Ill-posedness of free evolution precludes stable numerical integration. There has been a number of attempts to overcome this problem. However, numerical experiments show that in general three-dimensional problems of GR the constraint equations are eventually violated and this terminates computations.

The concept of well-posedness is related to the evolution of high frequency fourier modes. In a high-frequency perturbation analysis of a free evolution it is possible

*Presented at the Workshop on *Cosmology and Gravitational Physics*, 15-16 December 2005, Thessaloniki, Greece, *Editors*: N.K. Spyrou, N. Stergioulas and C.G. Tsagas.

[†]vpaschal@uchicago.edu

to separate perturbations in three classes: (1) space-time perturbations, (2) coordinate perturbations and (3) perturbations describing deviations from constraints. If the behavior of space-time is future independent, we must associate ill-posedness with coordinate and constraint-violating modes of perturbations. To achieve stable numerical integration, we must (A) use a gauge that does not lead to ill-posedness, and (B) eliminate or suppress ill-posedness caused by constraint violating modes.

Recently, attempts have been made to stabilize numerical integration by enforcing the constraint equations after every integration time step of a hyperbolic free evolution Anderson & Matzner (2003), Holst et. al. (2004). Analysis of well-posedness of a constrained evolution for a hyperbolic 3+1 formulation, densitized lapse, zero shift, and flat Minkowski space-time is given in Matzner (2005). A general theory for the study of well-posedness of constrained evolution is given in Paschalidis et. al. (2005).

An alternative to enforcement of constraints after a free evolution time step may be the construction of numerical schemes for constrained evolution in which growing constraint-violating modes are explicitly removed. In order to achieve this goal we must understand the nature of evolution of perturbations which satisfy constraints.

In this work we present a general analysis of constraint-satisfying perturbations and address the issue of well-posedness of constrained evolution of 3+1 formulations of GR with various gauges. We explicitly take into consideration the constraints of GR on the evolution of high-frequency perturbations of solutions of the Einstein equations. Our study reveals the existence of subsets of the linearized Einstein equations that control well-posedness of constrained evolution. We argue that the well-posedness of the Einstein equations depends entirely on the properties of the gauge. For certain classes of gauges we formulate conditions for well-posedness.

2. ADM 3+1 formulation and Gauges

A general form of the ADM 3+1 formulation Arnowitt et. al. (1962) consists of the evolutionary part

$$\frac{\partial \gamma_{ij}}{\partial t} = -2\alpha K_{ij} + \nabla_i \beta_j + \nabla_j \beta_i, \quad (1)$$

$$\begin{aligned} \frac{\partial K_{ij}}{\partial t} = & \alpha \left({}^{(3)}R_{ij} + K K_{ij} - 2\gamma^{mn} K_{im} K_{jn} \right) - \nabla_i \nabla_j \alpha \\ & + (\nabla_i \beta^m) K_{mj} + (\nabla_j \beta^m) K_{mi} + \beta^m \nabla_m K_{ij}, \end{aligned} \quad (2)$$

and the energy and momentum constraints which we will call the kinematic constraints,

$$\mathcal{H} : \quad {}^{(3)}R + K^2 - K_{mn} K^{mn} = 0, \quad (3)$$

$$\mathcal{M} : \quad \nabla_m K^m_i - \nabla_i K = 0, \quad i = 1, 2, 3, \quad (4)$$

where $K = \gamma^{mn} K_{mn}$, γ_{ij} and K_{ij} are the three-dimensional metric of a space-like hypersurface and the extrinsic curvature respectively, α is the lapse function, β^i is

the shift vector (these are gauge functions), and ${}^{(3)}R_{ij}$ is the three-dimensional Ricci tensor, ${}^{(3)}R = \gamma^{ij}{}^{(3)}R_{ij}$. We must add a specification of gauge (lapse and shift) in order to close the system (1), (2).

For the classification of gauges we follow Khokhlov & Novikov (2002), but instead of the dual shift vector β_k , here we work with the shift vector $\beta^k = \gamma^{kj}\beta_j$ and we distinguish three types of gauges.

1. *Fixed gauges* for which both the lapse and shift are functions of coordinates $t = x^0$ and $x^i, i = 1, \dots, 3$ only,

$$\alpha = \alpha(t, x^i), \quad \beta^k = \beta^k(t, x^i), \quad i, k = 1, 2, 3. \quad (5)$$

2. *Algebraic gauges* for which both the lapse and shift can be expressed as algebraic functions of coordinates and local values of γ_{ij} and its derivatives,

$$\alpha = \alpha \left(x^a, \gamma_{ij}, \frac{\partial \gamma_{ij}}{\partial x^b}, \dots \right), \quad \beta^k = \beta^k \left(x^a, \gamma_{ij}, \frac{\partial \gamma_{ij}}{\partial x^b}, \dots \right). \quad (6)$$

3. *Differential gauges* which are defined by a set of partial differential equations and which cannot be reduced to an algebraic form. Algebraic gauges are a subset of differential gauges.

For fixed and algebraic gauges, the total number of partial differential equations of the ADM formulation does not increase compared to (1)- (4). For differential gauges, a complete ADM formulation will consist of (1) - (4) plus differential equations describing the gauge.

3. Analysis of well-posedness

We begin with a brief description of our approach to analyze well-posedness of constrained sets of partial differential equations (PDE). Let

$$\partial_t \vec{u} = \mathcal{M}^\ell(\vec{u}) \partial_\ell \vec{u} + \mathcal{M}^o(\vec{u}), \quad \ell = 1, 2, 3 \quad (7)$$

be a set of n first order quasi linear partial differential equations, where \vec{u} is the column vector of the n unknown variables, \mathcal{M}^ℓ are $n \times n$ matrices and \mathcal{M}^o is an $n \times 1$ column vector. The dynamical variables satisfy a set of $m < n$ quasi linear constraint equations of the form

$$\mathcal{C}^\ell(\vec{u}) \partial_\ell \vec{u} + \mathcal{C}^o(\vec{u}) = 0, \quad \ell = 1, 2, 3 \quad (8)$$

where \mathcal{C}^ℓ are $m \times n$ matrices and \mathcal{C}^o is an $m \times 1$ column vector. Solutions of equations (7) satisfy constraints. If evolution starts with constraint satisfying data it should satisfy the constraints at all times.

Next consider high frequency planar perturbations on the dynamical variables along a line locally specified by a unit vector \vec{v} and parameterized by λ so that only

the principal part of equations (7) and (8) is important. Linearization of equations (7) yields:

$$\partial_t \delta \vec{u} = \mathcal{M}^\ell v_\ell \frac{\partial \delta \vec{u}}{\partial \lambda} \equiv \mathcal{M} \frac{\partial \delta \vec{u}}{\partial \lambda}, \quad (9)$$

where v_i is the dual vector to v^i , given by $v_i = \gamma_{ij} v^j$ and γ_{ij} is the 3-metric of a spacelike hypersurface embedded in the manifold carrying the background solution \vec{u} about which we perturb, and $\delta \vec{u}$ are perturbations of \vec{u} . Perturbations of \vec{u} must satisfy the linearized constraint equations (8)

$$\mathcal{C}^\ell v_\ell \frac{\partial \delta \vec{u}}{\partial \lambda} \equiv \mathcal{C} \frac{\partial \delta \vec{u}}{\partial \lambda} = 0, \quad (10)$$

where \mathcal{M} and \mathcal{C} are the principal matrices of equations (7) and (8) respectively. System (10) is a set of m equations for the spatial derivatives of the n unknown variables, which in general can be solved for m of the n spatial derivatives of variables \vec{u} . Substitution of (10) in equations (9), leads to a set of $q = n - m$ linear partial differential equations for q of the initial n variables. This is schematically given by

$$\frac{\partial \vec{a}_q}{\partial t} = \hat{A}(\vec{u}, v_i) \frac{\partial \vec{a}_q}{\partial \lambda}, \quad (11)$$

where \hat{A} is a $(q \times q)$ matrix. We will refer to (11) as the minimal set. The solution of (11) completely determines the solution of the entire linearized system (9). Therefore, the well-posedness of the minimal set determines the well-posedness of the entire system.

4. Analysis of the Well-Posedness of the Einstein Equations

In this section we present the results of analysis of well-posedness of the constrained evolution (as outlined in the previous section) of the Einstein equations with different gauge choices. After eliminating the degrees of freedom that correspond to the constraint equations, we are left with gauge degrees of freedom and the degrees of freedom which correspond to the two polarization modes of gravitational waves. Therefore, in a high frequency perturbation analysis of GR, there are two subsets of equations. A subset which describes propagation of gravitational waves and is well-posed, and a subset which describes the coordinate degrees of freedom which we call the gauge subset. This means that the well-posedness of the entire system depends only on the properties of the gauge.

We note here that our method concerns the constraint satisfying modes only. Those are present in free evolution schemes, too. Therefore, a bad choice of gauge, which we define as one that produces ill-posed constrained evolutions, is bad for a free evolution, as well. However, a good choice of gauge for a constrained evolution scheme cannot in principle guarantee the well-posedness of a free evolution with the same gauge, due to the existence of constraint violating modes.

The ADM formulation: After reducing the ADM formulation to first order our study, Paschalidis et. al. (2005), shows that the minimal set of ADM in conjunction with fixed gauges has gauge subsets that are only weakly hyperbolic and therefore the entire constrained evolution is ill-posed. The physical interpretation of the ill-posedness associated with fixed gauges is the well known fact that these gauges form coordinate singularities.

ADM with algebraic gauges of the form $\alpha = \alpha(t, x^k, \gamma_{ik})$, $\beta^i = \beta^i(t, x^k)$ and $\alpha = \alpha(t, x^k, \gamma_{ik})$, $\beta_i = \beta_i(t, x^k)$, result in a well-posed Cauchy problem provided that they satisfy the following conditions

$$\left(\frac{\partial\alpha^2}{\partial\gamma_{ij}}\right)v_iv_j > 0 \quad \text{and} \quad \left(\frac{\partial\alpha^2}{\partial\gamma_{ij}} + \beta^i\beta^j\right)v_iv_j > 0 \quad (12)$$

respectively. Here v_i is a unit one form.

Our analysis can be applied to ADM with either elliptic or parabolic as well as hyperbolic differential gauges. An example of an elliptic differential gauge is the widely used maximal slicing condition $K = 0$ Smarr & York (1978). Here K is the trace of the extrinsic curvature. Our study shows that there is a fundamental difference between the algebraic condition $K = 0$ and the differential equation by which maximal slicing is implemented

$$\gamma^{ij}\nabla_i\nabla_j\alpha - \alpha K_{ij}K^{ij} = 0 \quad \text{or} \quad \gamma^{ij}\nabla_i\nabla_j\alpha - \alpha R = 0. \quad (13)$$

In particular, if in addition to (13) one imposes the $K = 0$ constraint at every time step, then the constrained evolution is well posed and coordinate singularity free, as it is theoretically expected to be. However, if one uses only (13), then the resulting constrained evolution is ill-posed because the $K = 0$ condition may be violated.

The parabolic extension of maximal slicing Baumgarte & Shapiro (2003)

$$\frac{\partial\alpha}{\partial t} = \frac{1}{\epsilon} (\gamma^{ij}D_iD_j\alpha - K_{ij}K^{ij}\alpha - cK), \quad (14)$$

where ϵ is a positive constant, was introduced as another potential gauge which has the desired property of coordinate singularity avoidance. However, application of the constrained perturbation analysis of the ADM equations with this gauge shows that the resulting initial value problem is ill-posed.

As an example of a hyperbolic gauge, we consider the Bona-Maso family conditions Bona et. al. (1995)

$$\partial_t \ln \alpha = \beta^i \partial_i \alpha - \alpha f(\alpha)(K - K_o), \quad (15)$$

where $f(a)$ is a strictly positive function of the lapse, K is the trace of the extrinsic curvature and $K_o = K(t = t_o)$. The Cauchy problem of ADM with the Bona Maso family of gauges is well-posed.

The KST and BSSN formulations: The constrained perturbation approach can be applied to other first order formulations of GR. As an example we consider

the KST formulation Kidder et. al. (2001) and the BSSN formulation Nakamura et. al. (1987), Shibata & Nakamura (1995) and Baumgarte & Shapiro (1999).

The KST formulation is derived from ADM by addition of combination of constraints to the right hand side (RHS) of the ADM formulation. Since our approach explicitly enforces the constraints, the well-posedness of a constrained evolution with KST is the same as that of the ADM formulation. So, all our previous results apply to the KST formulation and in general to the class of formulations that are derived from ADM by addition of combinations of constraints to the RHS of ADM and linear transformation of the ADM dynamical variables.

The BSSN formulation involves a conformal decomposition of the three-metric and introduction of 5 new dynamical variables. Paschalidis et. al. (2005) showed that the well-posedness properties of BSSN with fixed and algebraic gauges is the same as that of the ADM formulation.

Acknowledgements.

The author would like to thank A. Khokhlov, I. Novikov and J. Hansen for helpful discussions.

References

- R. Arnowitt, S. Deser, and C. W. Misner, *Gravitation: An Introduction to Current research* (Wiley, New York, 1962), p. 227-265, gr-qc/0405109;
- T. Nakamura, K. Oohara, and Y. Kojima, Prog. Theor. Phys. Suppl. **90**, 1 (1987);
- M. Shibata and T. Nakamura, Phys. Rev. D **52**, 5428 - 5444 (1995)
- V. Paschalidis, A. Khokhlov, and I. Novikov gr-qc/0511075, (2005).
- T. W. Baumgarte and S. L. Shapiro, Phys. Rev. D **59**, 024007 (1999).
- P. Laguna, Phys. Rev. D **60**, 084012 (1999).
- L. E. Kidder, M. A. Scheel, and S. A. Teukolsky, Phys. Rev. D **64**, 064017 (2001).
- Gen Yoneda and Hisa-aki Shinkai, Class. Quant. Grav. **18**, 441-462 (2001).
- Matthew Anderson and Richard A. Matzner, gr-qc/0307055 (2003).
- M. Holst, L. Lindblom, R. Owen, H. P. Pfeiffer, M. A. Scheel, and L. E. Kidder, Phys. Rev. D **70**, 084017 (2004).
- Hisa-aki Shinkai and Gen Yoneda, *Recent Progress in Astronomy and Astrophysics* (Nova Science Publ., New York, 2003), gr-qc/0209111.
- Richard A. Matzner, Phys. Rev. D **71**, 024011 (2005).
- A. M. Khokhlov and I. D. Novikov. Class. Quantum Grav. **19**, 827–846 (2002).
- L. Smarr and J. W. York Jr., Phys. Rev. D **17**, 10, 2529 (1978).
- C. Bona, J. Massó, E. Seidel, and J. Stela, Phys. Rev. Lett. **75**, 600 (1995), gr-qc/9412071.
- T. W. Baumgarte and S. L. Shapiro. Phys. Reports **376**, 41-131 (2003).
- Heinz-O. Kreiss and Jenz Lorenz, *Initial-Boundary Value Problems and the Navier-Stokes Equations*, (Academic Press Inc., 1989).

An Epilogue

In the context of this Workshop, during two full working days, we had the opportunity to hear many interesting talks and exchange useful ideas on a variety of current, hot cosmological problems from the theoretical, numerical, and observational points of view.

If a conclusion is to be derived at the end, this, certainly, is that, in our community here, there is an intense and productive interest in the above subjects. The contribution has to be stressed especially of the younger participants, who constitute our scientific future.

I wish to remind to all the speakers that the organizers will expect, by the end of next May 2006, their contributions to be included in the proceedings volume of the workshop. All of you will shortly receive a relevant note from the organizers.

Once more I wish to express our warm thanks to all our sponsors.

Finally, on behalf of the organizers, I thank you all for participating in the Workshop, I believe that you had a pleasant stay in Thessaloniki, and I look forward to seeing you in the closing dinner tonight, and, hopefully, meeting you again in the near future.

On behalf of the Editors

Nikolaos K. Spyrou